R/V Gaia Blu Cruise report n.1

PIONEER: Processes in the IONian Sea: Exploring, Experimenting, Researching

Marzia Rovere

Federico Falcini, Alina Polonia, Katrin Schroeder

Andrea Argnani, Malek Belgacem, Elisa Camatti, Simone Colella, Lorenzo Consorti, Valtere Evangelista, Francesco Falcieri, Valentina Ferrante, Emanuela Frapiccini, Andrea Gallerani, Donatella Insinga, Florian Kokoszka, Giovanni La Forgia, Giuseppe Lo Mauro, Luca Gasperini, Giulia Lisi, Alessandra Mercorella, Sara Meschiari, Emanuele Organelli, Camilla Palmiotto, Chiara Pambianco, Danilo Pavone, Claudio Pellegrini, Jaime Pitarch Portero, Simone Redolfi Bristol, Alessandro Remia, Stefania Romano, Fabio Savelli, Giuseppe Suaria, Vittorio Tulli, Marina Vingiani, Gianluca Volpe

Catania 18 November 2023 - Crotone 9 December 2023

Report Tecnico dell'Istituto di Scienze Marine del CNR
ISSN 2611-4070

Operational Assessment and Scientific Report of the PIONEER Cruise

1. Introduction

1.1. Background and Purpose

In March 2022, the CNR received the donation of the 84 meters long ocean vessel Falkor from the Schmidt Ocean Institute and renamed her Gaia Blu. This new fundamental CNR infrastructure will allow the Italian marine scientific community to carry out the new era of oceanographic research in the open and deep sea.

For this purpose, the Gaia Blu vessel has been equipped over the last year with new instrumentation suitable for the acoustic investigation of the seabed, the subseafloor, the water column and for their sampling. The use of this new instrumentation in the context of future oceanographic campaigns requires a careful operational test phase in order to verify and analyze any possible issue on the field, especially in deep waters, where the technical and technological challenges are greater.

The Institute of Marine Sciences (ISMAR) - which represents the largest CNR marine scientific community including physical, geological, chemical and biological oceanographers - was tasked to propose an oceanographic campaign that could combine the need to test the ship and at the same time achieve scientific objectives. The proposed oceanographic cruise 'PIONEER: Processes in the IONian Sea: Exploring, Experimenting, Researching' had therefore the dual purpose of testing the new equipment instruments of the ship and to conduct interdisciplinary and exploratory research on complex oceanic circulation of the Ionian Sea, its climatic and environmental implications; subseafloor geological and sedimentary processes along the seabed and how they impact the transport and dispersion of contaminants, sediments and biodiversity.

1.2. Scope of the report

The scope of the report is to provide a comprehensive assessment of the RV Gaia Blu oceanographic cruise, focusing on its operational aspects. This includes an analysis of various measurements, surveys, and sampling activities conducted by the CNR marine institutes. The report aims to identify both the strengths and challenges encountered during the campaign, offering constructive insights into the effectiveness of different operations. Additionally, it seeks to generate practical recommendations for improvement in specific areas, such as CTD operations, wet and dry lab functionality, control room efficiency, seawater sampling, on-deck activities, and various specialized measurements. The scope extends to suggestions for refining methodologies, setting future campaign objectives, optimizing equipment usage, and exploring potential collaborations or integrations with other projects or institutions. The ultimate

goal is to contribute to the enhancement of overall operational efficiency and the success of future oceanographic endeavors conducted aboard the RV Gaia Blu.

1.3. Scientific objectives of the oceanographic campaign

The main scientific objectives of the PIONEER cruise are:

a) **Dynamics of the intermediate and deep waters in the Ionian Sea**. The ocean circulation of the Ionian Sea is extremely complex with thermohaline characteristics dictated by delicate ventilation processes connected to the formation of dense waters in neighboring basins and to circulation patterns that can undergo significant changes, with strong impacts on the Mediterranean climate and on weather-climatic events, even extremes, in adjacent regions. The results of the PIONEER campaign, by integrating existing time series, can contribute to improving the knowledge of the Ionian circulation and analyze the origin, transport, mixing and climatic feedback of the different water masses, and the relative impact on the dynamics of biogeochemical cycles.

b) **Interactions between intermediate circulation and seabed morphology**. The analysis of transects of sediment cores together with L-ADCP measurements during the PIONEER campaign can improve the reconstruction of ocean circulation over the geological time scale by studying the internal geometry, sedimentary characteristics and chronostratigraphic framework of contouritic sedimentary bodies.

c) **Geo-biodiversity of sites of deep fluid circulation**. These sites represent extreme life environments controlled by delicate geochemical and microbial balances that are still unevenly studied in the Mediterranean Sea. The genesis of these sites is closely connected to the geological context and to the presence of faults, including at the lithospheric scale, canyons, subduction processes. The objectives of the PIONEER campaign are to understand the interplay between the geological and chemical-physical characteristics and the biological diversity of both the benthic and deep-sea pelagic communities.

d) **Anthropogenic impact in the deep sea**. The Ionian Sea is surrounded by coastal sites characterized by intense anthropic signature (e.g. Sites of National Interest such as Taranto, and Crotone) which represent important sources of contamination almost unknown in terms of their impact onto the deep sea. The results of the PIONEER campaign address the study of contamination (chemical, biological, plastics, including persistent and emerging classes) in relation to coastal-offshore sediment transport, oceanographic dispersal dynamics and atmospheric deposition with a final aim to define background values in the deep-sea environment.

1.4. Background on the Study Area

- *Tectonic and Geological Background*

The Ionian Sea straddles the Eurasia–Africa plate boundary and hosts remains of the Tethyan ocean, the oldest in situ oceanic crust in the world (Catalano et al., 2001; Speranza et al., 2012; Dellong et al., 2018; Dannowski et al., 2019; Tugend et al., 2019). It has been described as the last remaining segment of oceanic crust

subduction in the central Mediterranean (de Voogd et al., 1992; Faccenna et al., 2004; D' Agostino et al., 2008) and has recorded a long history of sedimentation, erosion, vertical movements and tectonic activity.

Consumption of the oceanic lithosphere has caused the emplacement of the Calabrian Arc (CA, Figure 1), a narrow and arcuate subduction system related to plate convergence, and to the southeastward retreat of the subducting slab (Malinverno and Ryan, 1986; Cernobori et al., 1996; Doglioni et al., 1999; Argnani and Bonazzi, 2005; Minelli and Faccenna, 2010; Polonia et al., 2011; Gutscher et al., 2015). Slab tearing plays a major role in producing a deep fragmentation of the subduction system (Polonia et al., 2016), asthenospheric upwelling, dynamic topography and magmatism (Govers and Wortel, 2005; Faccenna et al., 2011; Rosenbaum et al., 2008; Schellart, 2010; Polonia et al., 2017).

The migrating Calabria trench drives the entire subduction complex outward, but different boundary conditions on the plate interface lead to arc-orthogonal segmentation along lithospheric faults (Doglioni et al., 2012; Polonia et al., 2016; Gutscher et al., 2015; Argnani, 2020) that were the source of major earthquakes in the Calabrian Arc (Argnani et al., 2012; 2023; Polonia et al., 2013; Billi et al., 2020) and drives dewatering from below and the formation of mud volcanoes.

Mud volcanism, or sedimentary volcanism, represents one of the most intriguing phenomena of the Earth's crust, with important implications in energy resource exploration, seismicity, geo-hazard and atmospheric budget of greenhouse gases. Evidence of mud volcanoes and allochthonous material emplacement was reported in many regions of the Ionian Sea (Praeg et al., 2009; Panieri et al., 2013; Ceramicola et al., 2014; Gutscher et al., 2017; Loher et al., 2018) where they are manifestations of plate convergence and underthrusting of unconsolidated sediments and can be considered as markers of overpressure-related geofluid circulation, efflux, and ascent.

Mud volcanoes are geological structures that can release large amounts of gas (e.g., CO_2, CH_4, and N) and result from the upward migration of mobilized subsurface sediments, gas, and water by focused fluid flow and the extrusion of a mixture of these components, referred to as mud breccia (Camerlenghi et al., 1992; Cita et al., 1981; Mazzini and Etiope, 2017; Pape et al., 2010). The onset of mud volcanism can be related to seismic activity, with many examples of earthquakes affecting or triggering onshore and offshore mud volcanoes (MVs) (Hensen et al., 2019 and references therein). However, mud volcanism and seepage at large (pockmarks, mud diapirs, mud pools) can occur in different tectonic and sedimentary settings, related or unrelated to fault controlled mechanisms (e.g. Rovere et al., 2014; 2020; 2022) and characterized by a complex suite of emitted gas which are the result of different and interacting processes along the plumbing system (thermo-metamorphism, methanogenesis, anaerobic oxidation of methane) (Franchi et al., 2017). Mud volcanoes and seepage systems (cold seeps) are well studied on land but on the

seafloor, where they are much more common, the volumes of released sediments and methane are poorly known.

Previous surveys across the CA have documented numerous cold seeps encompassing different tectonic settings, from extensional on the upper slope to compressional on the accretionary wedge (Praeg et al., 2009; Panieri et al., 2013; Bohrmann et al., 2015; Ceramicola et al., 2014; Loher et al., 2018a,b; Cuffaro et al., 2019; Doll et al., 2023; Argnani et al., submitted). Several structures have been reported to show signs of recent mud breccia extrusion (Ceramicola et al., 2014; Foucher et al., 2009; Panieri et al., 2013; Praeg et al., 2009) or fluid seepage (Foucher et al., 2009). Most extrusive features occur along structural lineaments related to compressional, transpressive or transtensive tectonics of the CA (Polonia et al., 2011; Ceramicola et al., 2014b; Gutscher et al., 2017; Panieri et al., 2013; Praeg et al., 2009). The onset of mud volcanism on the CA is inferred to have originated >3 Ma ago (Late Pliocene; Praeg et al., 2009) and the study of mud breccia and microfossil assemblages indicated source materials as old as the Late Cretaceous for some of the piercing features (Morlotti et al., 1982; Panieri et al., 2013; Praeg et al., 2009). The ecosystems associated with these deep vent sites (e.g. tubeworms growing on authigenic carbonate hardgrounds) have been studied for few case studies (Loher et al., 2018b), while the majority remain unexplored.

In the western part of the CA, geophysical data reveal a number of sub-circular magnetic bodies beneath the seafloor intruding the accretionary wedge. Indirect evidences (seismic reflection profiles, multibeam, potential field and geochemical data) suggest that these diapirs may be made of inherited Mesozoic Tethyan serpentinites, which rise along transtensive faults controlling rifting processes perpendicular to the subduction arc (Polonia et al., 2017). Sampling the sedimentary cover on top the diapirs might provide important information on the age and nature of the Tethyan basement, and on the connection with deep fluid circulation and how this can open a window into the deep Earth and deep microbial life sustained by serpentinitic and thermogenic processes (IODP pre-proposal P968, Polonia et al., 2019).

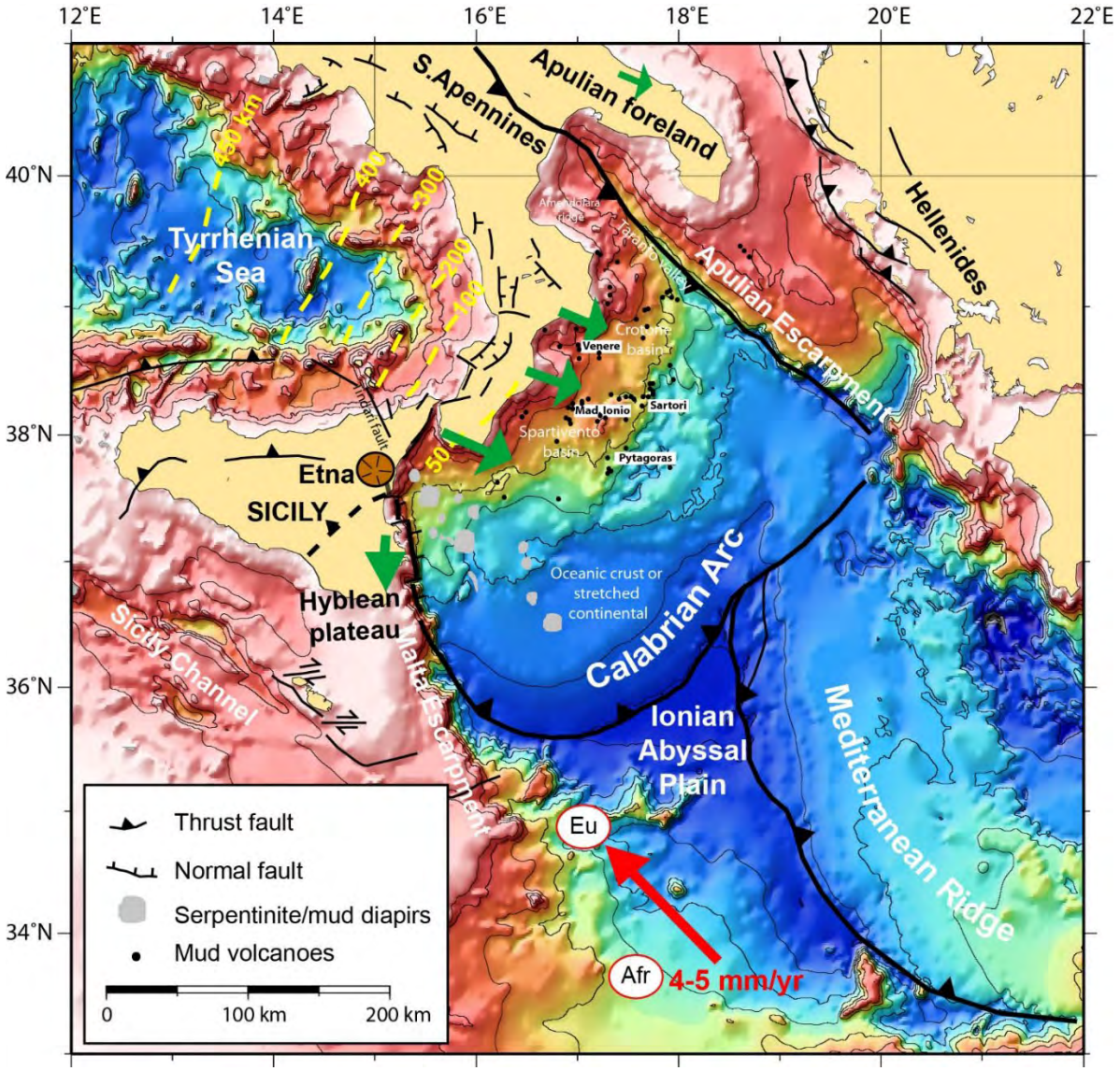

Figure 1.4.1. Geodynamic setting of the study area. Slip vector in the African reference frame is indicated by a red arrow. In green GPS vectors in the Apulian fixed reference frame in which the motion of Calabria is parallel to the slip vector suggesting active crustal compression as a result of subduction of the Ionian lithosphere beneath the Calabrian Arc (D'Agostino et al., 2008). The NWward dipping subducting slab of the African plate is represented by the yellow contours spacing from 100 to 450 km in the Tyrrhenian Sea (Selvaggi and Chiarabba, 1995). Eu: Europe, Afr: Africa. Black dots: mud volcanoes in the Calabrian Arc accretionary wedge from Rovere et al. (2017). Grey areas: serpentinite/mud diapirs as proposed by Polonia et al. (2017).

- *Oceanographic Background*

Deep-water exchanges between the western and the eastern Mediterranean basins occur within the shallow Sicily Channel (Figure 2), which makes the deep-water circulation of the two sub-basins rather independent from each other (Sparnocchia et al., 1999; Napolitano et al., 2003; Béranger et al., 2004; Schroeder et al., 2006). In the eastern basin, the Eastern Mediterranean Deep Water (EMDW) is formed, alternately, in separate regions of the Eastern Mediterranean Sea, i.e., the southern Adriatic Sea and the Aegean Sea (Gačić et al., 2010). This cold and high salinity winter water, after deep convection, flows into the Ionian Sea (Wüst, 1961; Roether and Schlitzer, 1991; Schlitzer et al., 1991; Roether et al., 1996; Bensi et al., 2013a; Bensi et al., 2013b; Bellacicco et al., 2016), i.e., the deepest sub-basin of the Mediterranean Sea, which has a maximum depth close to the mean depth of the global ocean. Such a thermohaline circulation is, therefore, characterized by a superposition of intermediate and deep, zonal and meridional overturning cells (Bergamasco and Malanotte-Rizzoli, 2010).

The Ionian Sea is crossed by the open thermohaline cell of the Mediterranean, where the main water masses circulate from east to west: the Atlantic Water (AW) and the Intermediate Water (IW, which can originate from the Levantine and/or Cretan Sea). It also receives in its deep basin the dense water formed in the Eastern Mediterranean (the Eastern Mediterranean Deep Water, or EMDW): until the late 80s, the Adriatic Sea was the main source of deep water, but then a significant climatic change occurred, known as the Eastern Mediterranean Transient (EMT), which activated a new source of dense water in the Aegean Sea. The Aegean water was warmer, saltier and denser than the one previously formed in the Adriatic Sea, so it occupied the deepest layers of the Ionian (Roether et al., 1996). Around 1995, the Aegean source declined and the Adriatic became an active source again, producing new water with higher temperature and salinity than before the EMT (Theocharis et al., 2002; Roether et al., 2007).

The oceanographic studies in the last decade have concentrated on the Adriatic–Ionian bimodal oscillating system (BiOS), i.e. the sea surface circulation in the Ionian, at decadal timescales, switches from a cyclonic basin-wide gyre occupying the entire northern area to anticyclonic meandering (Civitarese et al., 2010). During the cyclonic circulation mode, the Ionian and Adriatic seas are invaded by highly saline Levantine Intermediate Water (LIW). Conversely, during anticyclonic circulation, the two basins are affected by low-salinity surface Atlantic Water coming from the western Mediterranean, with profound impacts on circulation pattern and nutrients availability. The deep-water circulation is characterized by significant spatial and variability which has been addressed in few studies based on deep mooring stations.

For the Ionian Sea, boundary currents show intense downwelling due to their interaction with the topographic constraints while the deepest part of the basin is characterized by extremely weak stratification (Holte and Straneo, 2017; Send and Testor, 2017; Waldman et al., 2018). Moreover, the Ionian Sea shows a semi-diurnal lunar tidal (M2) and a dominant motion that is around the inertial frequency, mainly as freely propagating internal waves (Gerkema and Zimmerman, 2008; van Haren and Gostiaux, 2011). For this particular reason, the Ionian Sea constitutes a unique example for studying the fundamental dynamics and processes of the abyssal layers in the Mediterranean basin, also in the light of turbulent and diapycnal mixing due to internal-wave breaking (Rubino et al., 2012; Artale et al., 2018).

In particular, Artale et al. (2018), by analyzing water column characteristics of the Ionian Sea, observed during the last three decades, focused on the hydrological processes occurring at the bottom layer. They found that the ocean circulation in this abyssal plain is strongly affected by an interplay between advection and diffusion. The progressive warming and salinification of this sub-basin produced warmer near-bottom waters, causing an anomalous heat storage of ~1.6 W/m^2, i.e., a value three times larger than the equivalent climate trend occurring in the same period at global scale (Bindoff et al., 2007). The analysis of Artale et al. (2018) investigated the triggering of a diapycnal mixing due to rough bathymetry. In particular, to explore topographic-induced mixing, these authors estimated dissipation rates from the "CTD strain-based" parameterization (Kunze et al., 2006), showing the role of sea bottom in enhancing isopycnal vertical strain.

Finally, The Ionian Sea is directly impacted by several coastal settlements and industrial activities (i.e., Taranto, Crotone, Augusta), as well as river runoffs, representing important sources of contamination for the intermediate and deep waters. In particular, the peculiar cost-to-sea Taranto system of inter-connected land-locked basins (formed by the Mar Piccolo, Mar Grande, Gulf of Taranto and Mar Ionio) remains poorly investigated (Liubartseva et al., 2021).

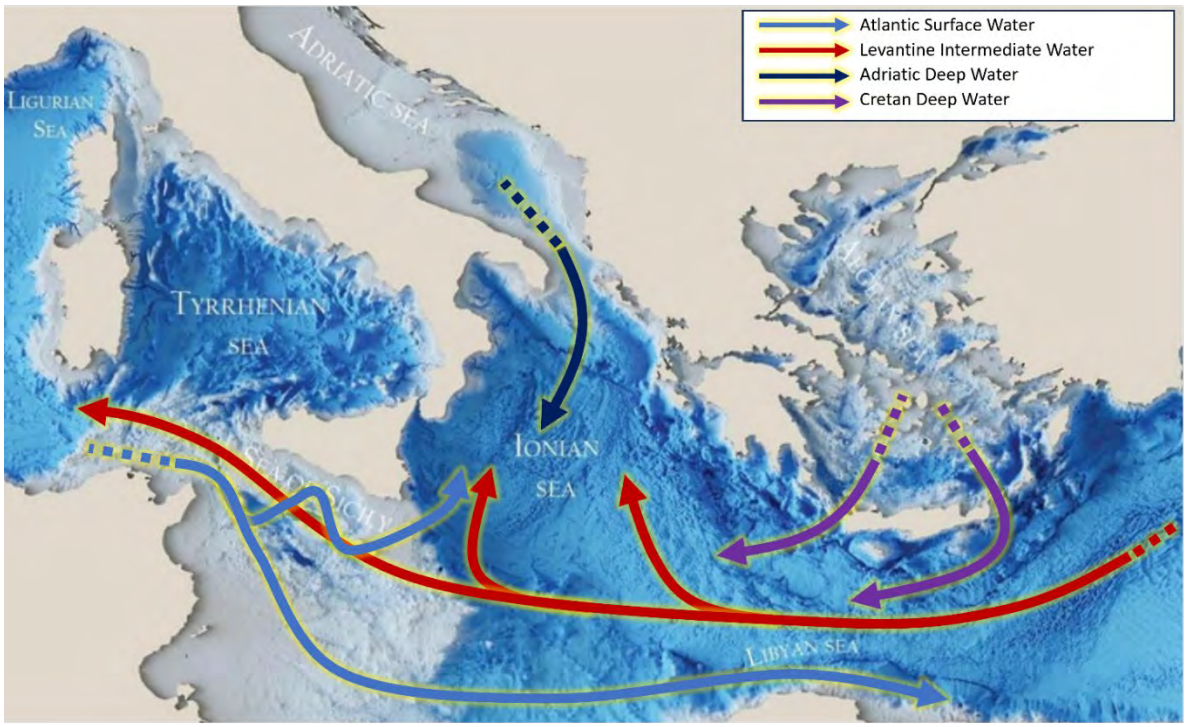

Figure 1.4.2. Sketch representing the general circulation of the Central and Eastern Mediterranean Sea, with a focus on the Ionian Sea.

- *Morphotectonics, oceanography and sedimentation*

The Ionian Sea is characterized by a complex morphology reflecting the combined effect of tectonic, sedimentary, oceanographic and biological processes (Marani et al., 1993; Argnani et al., 1993, 2001; Micallef et al., 2022). Active tectonics, sediment supply, oceanography and vertical movement reshape the seafloor forming unstable steep slopes, canyon systems, sedimentary basins and controlling current sediment paths, deposition, and geometry (Savini and Corselli, 2010; Ceramicola et al., 2014a; Zecchin et al., 2020).

The Ionian Basin sedimentary processes are affected by gravitational sediment transport. Frequent slope instability processes, triggered by tectonic activity (Merlini et al., 2000; Argnani et al., 2001), seismic shaking and tsunami propagation (Polonia et al., 2021), allow sediment transport from the continental shelf into the deep basin (Marani et al., 1993; Zecchin et al., 2020). Other sedimentary processes and deposits include drifts and large sediment waves along the Malta and Apulian Escarpments (Marani et al., 1993; Rebesco et al., 2021). These features have been associated with the flow of bottom currents, mainly the Levantine Intermediate Water (LIW) and the Adriatic Deep Water (ADW) (e.g. Marani et al., 1993; Pepe et al., 2018; Rebesco et al., 2021). At the base of the Malta Escarpment, sediment waves have been steadily growing and migrating since about 500 ka due to variation in sediment input resulting from the tectonic uplift in NE Sicily and Calabria and the onset of a bottom current regime (Rebesco et al., 2021).

Despite these recent investigations and the study of large contourite systems in the adjoining area of the Sicily Channel (Gauchery et al., 2021 a,b), the areal extent,

internal geometry, and volume of active drift deposits in the Ionian Sea remain poorly constrained, mainly due to the lack of a systematic grid of high-resolution seismic profiles acquired at the regional scale and calibrated throughout sediment cores.

The unique oceanographic and geological characteristics, including the strategic position of the Central Mediterranean swept by westerlies, allowed the deposition and preservation of key sedimentary horizons (e.g. tephra layers), which contain excellent proxies for constraining the chronological and stratigraphic framework of sedimentary records (Narcisi & Vezzoli, 1999; Insinga et al., 2014).

Furthermore, Quaternary sediments of the Mediterranean Sea are characterized by the occurrence of organic carbon-rich sapropels (Total Organic Carbon, TOC >2%), deposited during wet climate periods in the Mediterranean region (Vigliotti et al., 2011). Sapropels are useful for paleoclimate and paleoceanographic reconstructions of the entire Mediterranean and its connection with the Atlantic Ocean. In the Ionian Sea and Gulf of Taranto, few studies have covered their occurrence (e.g. Negri et al., 1999; Emeis et al., 2003; Goudeau et al., 2013), showing significant differences in TOC, magnetic content and thus redox conditions in which deposited, that need to be better understood.

- *Biogeochemical cycles*

The Ionian Sea is an oligotrophic basin characterized by low productivity (D'Ortenzio and Ribera d'Alcalà, 2009), without reaching the lowest values of the Levantine Basin. Surface phytoplankton blooms are occasional and limited in space, often linked to mesoscale instabilities in the flow due to the interaction with the bathymetry in the phase of nutricline uplift due to the general circulation (e.g., D'Ortenzio at al., 2003).

As in other oligotrophic areas the microbial food web based on bacteria dominates, even though picoeukaryotes and, in some cases diatoms, play a role (Civitarese et al., 1996; Boldrin et al., 2002; Casotti et al., 2003; Placenti et al., 2018). Stocks of dissolved and particulate matter in the Ionian basin are also known to be influenced by water circulation properties (Malanotte-Rizzoli et al., 1999). The influence of the Adriatic water is mostly evident in the north-western part of the basin in the form of higher phytoplankton biomass, particularly diatoms, while water of Atlantic origin makes up its southern part, with the exception of the whole eastern side bordering the coasts, when oligotrophic water from the Cretan Sea (Casotti et al., 2003) or the anticyclonic phase of the BIOS drive the surface circulation.

Winter mixing does not reach the nutricline basin wide thus hampering injection of nutrients into the surface layer (Civitarese and Gacic, 2001; D'Ortenzio and Ribera d'Alcalà, 2009). On the other hand particulate export is not neglible (Boldrin et al., 2003), which highlights the importance of atmospheric inputs (Ribera d'Alcalà et al., 2003; Powley et al., 2017). The latter, together with nutrients may also carry pollutants which makes the characterization of vertical fluxes in the open Ionian sea an important

issue. Mesoscale features such as small eddies and coastal filaments may also support photosynthetic capacity locally (e.g. Casotti et al., 2003).

One important biogeochemical event affecting the deep layers occurred at the time of the EMT with the subduction of water presumably rich in respirable carbon, which remarkably increased deep respiration and oxygen utilization rate (Klein et al., 2003, La Ferla et al., 2003, Zaccone et al., 2003). Considering the recent alternation in newly formed dense water supply to Ionian deep waters, the previous observation raises the question on the extent to which exogenic substances conveyed to the sea along the coastlines may reach the bottom. In addition, the anomalous higher temperature in the deep layers of the basin, if compared to oceanic deep layers, increasing metabolic rates may have favoured specific adaptations of bacteria connected with the rise in temperature (Zaccone et al., 2010).

Current knowledge of the spatial and temporal variations in the microbial activities involved in the carbon cycles occurring in the Ionian Sea revealed an increase in bacterial growth efficiency. This could be dependent on the occurrence of higher temperature in the deep layer of the Ionian Sea, recently observed by Artale et al. (2018). Taken all things together, also the deep pelagial of the Ionian sea constitutes an important area of investigation which confronts with a poor past sampling of that layer, especially for what concerns unicellular and metazoan plankton.

1.5. Summary

The first scientific campaign of the CNR oceanographic vessel, Gaia Blu, ended on 9 December 2023 in the port of Crotone. The scientific campaign was divided into two "legs" and involved more than 50 people including researchers, technologists, technicians from the CNR institutes ISMAR, IRBIM, ISP, IBF with the remote support of IAS and IGG. The campaign was also an opportunity for training-on-the-job new researchers and technologists hired on PNRR projects and doctoral students from Italian and European universities. During the second "leg", two technicians from CNR-ISPC and the CNR-URS were present on board to film the campaign and provide multimedia support for the video conference connection with some middle schools, as part of a project of scientific dissemination coordinated by the Communication and Education Office of the CNR Area of Tor Vergata, virtually bringing very young students for a day on board the ship.

The activities that took place were numerous and made use of all the ship's infrastructural equipment. This stress-test highlighted all the ship's potential but also its critical issues, on which all the participants expressed their views which were collected in a report that has been delivered to the ship's coordination and management office for the necessary improvement actions.

During the 22 days of navigation, despite the unfavorable weather conditions typical of the late autumn season, 3600 nautical miles were explored in an area of approximately 130,000 square km, up to 4000 meters below sea level. Here, bathymetric and reflectivity data of the seabed and the water column and seismo-acoustic profiles were acquired. The seabed and the sub seabed was sampled through 15 sediment cores with gravity and piston gears to

reconstruct the paleoceanography and paleoclimate of the Mediterranean in the last tens of thousands of years and the deep circulation of interstitial fluids of both mantle and biogenic origin in seepage sites. To analyze the superficial and undisturbed portion of the seabed, 19 box coring stations were performed. The sediments thus recovered were sampled for sedimentology and stratigraphy analyses, for the measurement of classic and emerging contaminants and the estimate of the microplastic content, to define the microbiological and meiofauna characteristics and make eDNA extractions.

36 CTD/Rosette casts were performed to investigate the chemical-physical properties of the water column and define its stratification. During profiling, the following parameters were measured: temperature, salinity, dissolved oxygen, fluorescence, inherent optical properties; Water samples will be analyzed for alkalinity, pH, inorganic carbon and dissolved organic matter. Furthermore, environmental DNA analyses with eDNA metabarcoding will be carried out on bacteria and metazoans, phytoplankton and zooplankton, especially in correspondence with the box cores where a comparison will be attempted between demersal and benthic environments. To sample pelagic organisms and characterize them from both a morphological and molecular point of view, a WP2 net was used up to a depth of 500 m. A turbulence profiler was used to characterize the mutual interaction between different water masses and understand how their mixing may impact circulation and pelagic communities.

Radiometers and instruments were used to measure the optical properties of the first 100 m of the water column. Furthermore, to increase the density of data, a continuous surface water analysis system was put into operation through a pumping and filtering system, measuring the water parameters with the same instruments used in profiling mode. In addition to scientific use, these optical data are fundamental for the calibration of the algorithms used in the processing of satellite images that the CNR produces for the marine operational service of the European Copernicus programme.

During the first days of the cruise, a BGC-Argo float of the CNR-ISMAR fleet (contributing to EURO-ARGO ERIC and to the Italian node Argo-Italy) was deployed in the middle of the Ionian Sea. The float was equipped with sensors to autonomously measure 0-2000 dbar profiles of the following Essential Ocean, Climate and Biological Variables (EOVs, ECVs and EBVs) temperature, salinity, pressure, oxygen, chlorophyll, optical backscatter, dissolved organic matter, downwelling irradiance, particle size distribution and zooplankton taxonomy. During the cruise, the sampling strategy adopted for the BGC-Argo float was to profile every day, thus providing a spatio-temporal coverage of the measured EOVs, ECVs, and EBVs that complemented cruise activities within the investigated region.

During navigation, observation transects of macro plastics were carried out, useful for training on Artificial Intelligence (AI) algorithms for the automatic recognition of these pollutants floating on the sea surface. Furthermore, an experiment of transmission-listening of acoustic signals was carried out on one of the stations that make up the INFN's "cubic kilometer" (KM3NeT) submarine telescope for cosmic neutrinos, which in addition to measuring the flux of cosmic muons at abyssal depths, monitors the physical and acoustic properties of this stretch of Ionian Sea a few tens of kilometers deep off the coast of Capo Passero.

1.6. Areas, scientific parties and investigation periods

The oceanographic campaign aboard the RV Gaia Blu was primarily focused on the exploration of the Ionian Sea and the Gulf of Taranto. The investigation periods spanned from November to December 2023. The cruise was organized into 2 legs, the first focused on the deeper Ionian domain, south of 38°N, the latter on the Gulf of Taranto (delimited by the line connecting Santa Maria di Leuca and Punta Alice) and the northern Ionian Sea.

1° LEG CATANIA 18 NOVEMBER - CROTONE 28 NOVEMBER			
Name	**Duty**	**Role**	**Affiliation**
Marzia Rovere	Party Chief	Researcher	ISMAR-CNR
Simone Colella	CTD-Rosette/radiometry/IOP	Researcher	ISMAR-CNR
Malek Belgacem	CTD-Rosette/O2, salinity, nutrients/LADCP	Post doc researcher	ISMAR-CNR
Florian Kokoszka	CTD-Rosette/ salinity/LADCP	Technologist PNRR	ISMAR-CNR
Valtere Evangelista	CTD-Rosette/DOM	Technician	IBF-CNR
Gianluca Volpe	Flow through/radiometry/IOP	Researcher	ISMAR-CNR
Jaime Pitarch Portero	Radiometry/IOP/Secchi	Researcher PNRR	ISMAR-CNR
Francesco Falcieri	Microstructure probe	Researcher	ISMAR-CNR
Emanuele Organelli	BGC Argo	Researcher	ISMAR-CNR
Giovanni La Forgia	BGC Argo	Technologist PNRR	ISMAR-CNR
Elisa Camatti	Net sampling/DNA metabarcoding	Researcher	ISMAR-CNR
Simone Redolfi Bristol	Net sampling/DNA metabarcoding	Technologist PNRR	ISMAR-CNR
Luca Gasperini	Coring/box coring	Researcher	ISMAR-CNR
Donatella Insinga	Coring/box coring	Researcher	ISMAR-CNR
Giuseppe Suaria	Box coring/microplastics/marine litter	Researcher	ISMAR-CNR
Marina Vingiani	Microbiology/DNA metabarcoding	PhD student	UNIGALWAY
Valentina Ferrante	Surveyor	Researcher	ISMAR-CNR
Camilla Palmiotto	Surveyor	Researcher	ISMAR-CNR
Giuseppe Lo Mauro	Surveyor/coring	PhD student	UNIBARI
Sara Meschiari	Surveyor	Post doc researcher	ISMAR-CNR

Table 1.4.1. List of personnel involved in Leg 1 of the PIONEER 2023 cruise.

Figure 1.4.1. Scientific party of Leg 1.

The planning of activities during Leg 1 was contained in the latest version of the cruise proposal and station coordinates were prepared for clearing and permitting processes.

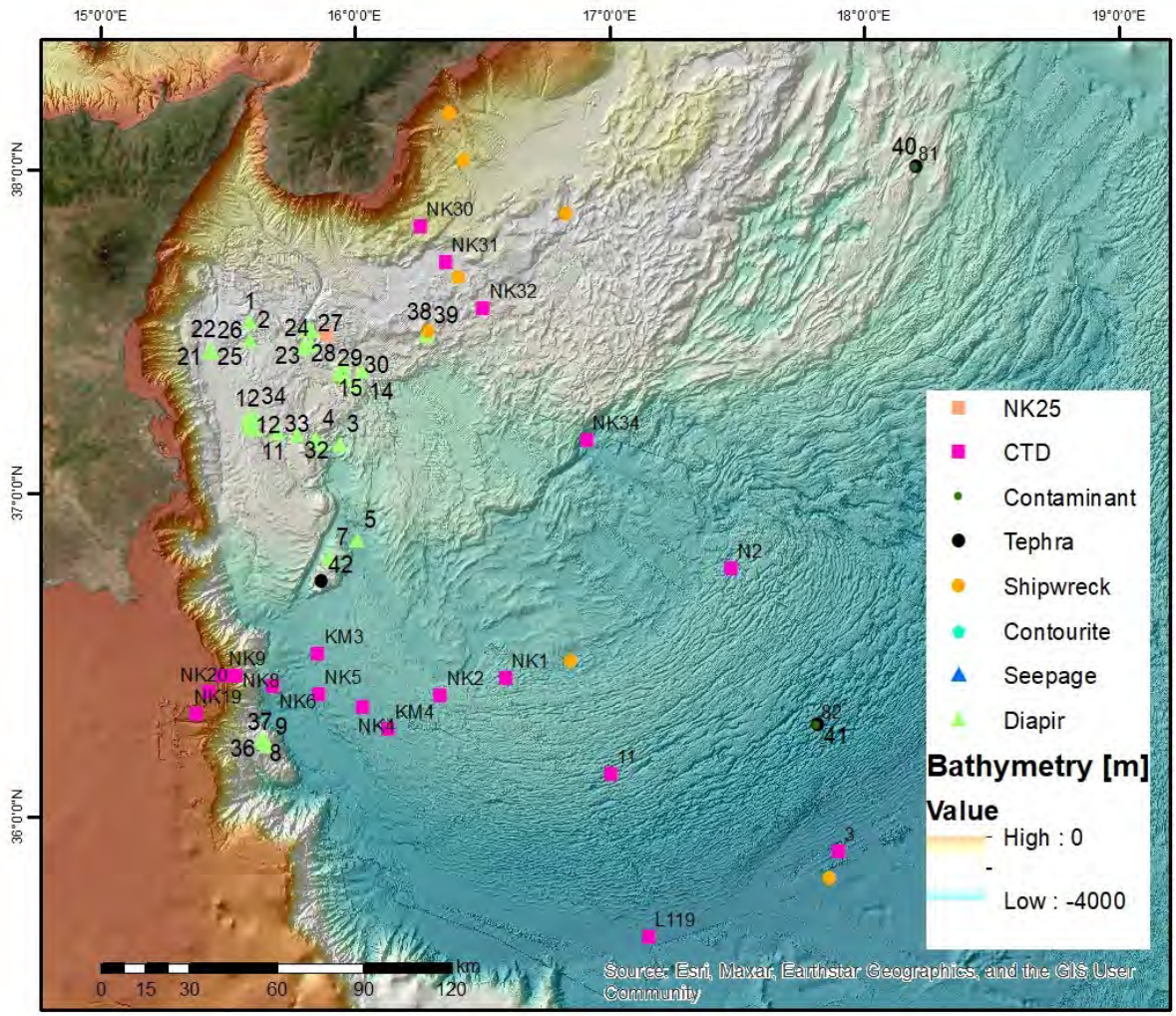

Figure 1.4.2. Plan of activities during Leg 1 of the PIONEER 2023 cruise.

The actual survey carried out during Leg 1 can be summarized as follows:

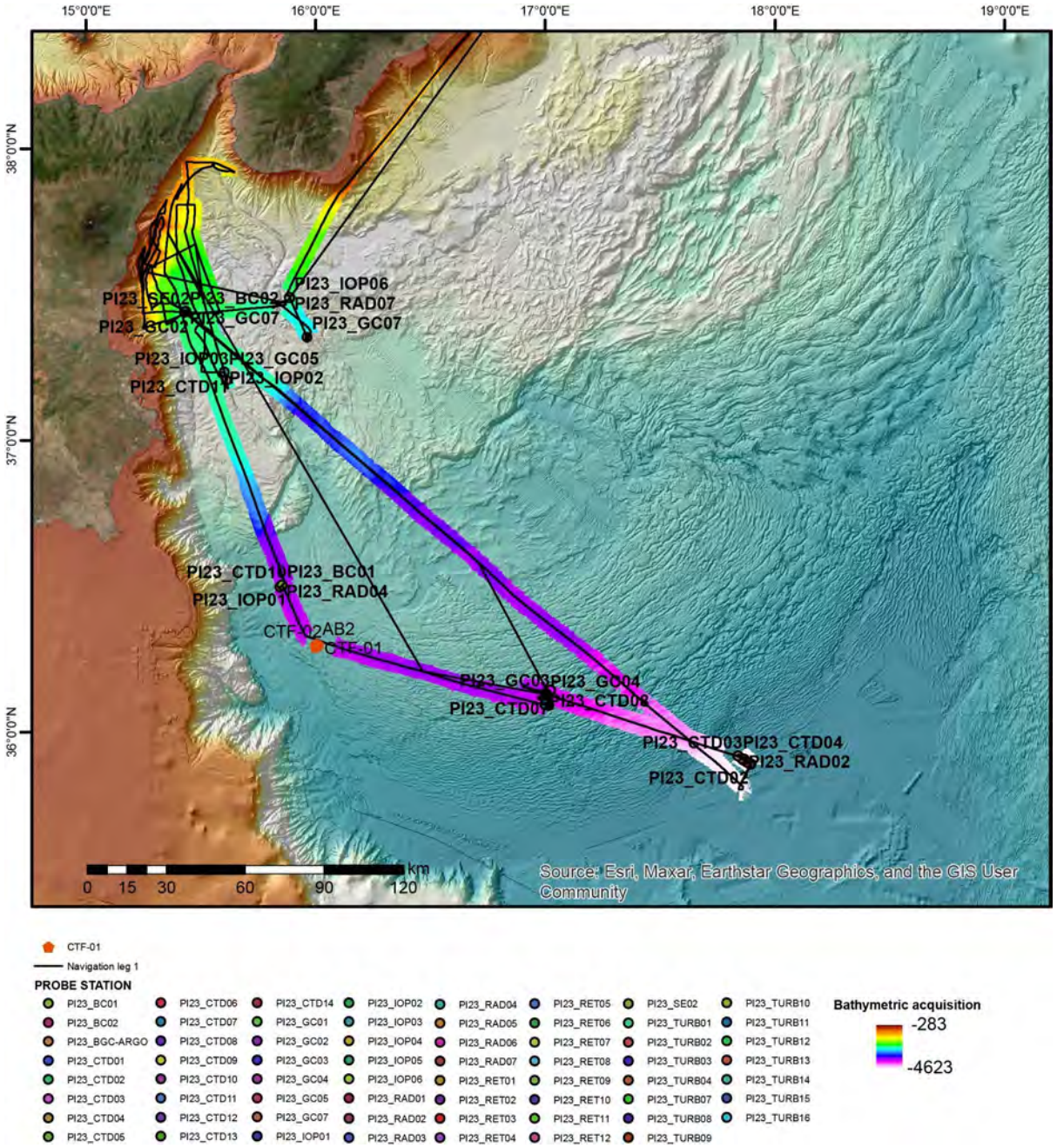

Figure 1.4.3. Effective survey carried out during Leg 1 of the PIONEER 2023 cruise.

LONG-WGS84	LAT-WGS84	UNIQUE STATION	PROBE STATION	DATE	UTC
15.4252840	37.4397183	22	PI23_GC01	11/19/2023	10:15
15.4257995	37.4397298	22	PI23_CTD01	11/19/2023	12:44
15.4253333	37.4399500	22	PI23_RAD01	11/19/2023	13:05
15.4240883	37.4376900	25	PI23_GC02	11/19/2023	14:54
17.8034764	35.8592846	3	PI23_CTD02	11/20/2023	11:00
17.7735288	35.8754639	3	PI23_RAD02	11/20/2023	12:34
17.8016820	35.8571664	3	PI23_BGC-ARGO	11/20/2023	14:39
17.7978333	35.8567833	3	PI23_TURB01	11/20/2023	14:50
17.7859000	35.8645100	3	PI23_TURB02	11/20/2023	15:25
17.7710300	35.8725402	3	PI23_TURB03	11/20/2023	16:06
17.7641266	35.8771676	3	PI23_TURB04	11/20/2023	16:27
17.7486668	35.8863064	3	PI23_CTD03	11/20/2023	17:39
17.7486965	35.8863386	3	PI23_CTD04	11/20/2023	18:17
16.9446415	36.1161806	11	PI23_CTD05	11/21/2023	4:20
16.9449421	36.1160480	11	PI23_RET01	11/21/2023	6:03
16.9449315	36.1160306	11	PI23_RET02	11/21/2023	6:35
16.9450260	36.1159937	11	PI23_RET03	11/21/2023	7:26
16.9448458	36.1160290	11	PI23_CTD06	11/21/2023	8:14
16.9449696	36.1159728	11	PI23_RAD03	11/21/2023	8:44
16.9396549	36.1149227	11	PI23_CTD07	11/21/2023	9:39
16.9396885	36.1149011	11	PI23_CTD08	11/21/2023	10:00
16.9393776	36.1149245	11	PI23_GC03	11/21/2023	12:00
16.9445414	36.1108402	11	PI23_GC04	11/21/2023	14:30
16.9464504	36.1064620	11	PI23_TURB07	11/21/2023	16:18
16.9381524	36.1026309	11	PI23_TURB08	11/21/2023	16:42
16.9570202	36.0748000	11	PI23_TURB09	11/21/2023	19:40
16.9482654	36.0762982	11	PI23_TURB10	11/21/2023	20:08
16.9397572	36.0786545	11	PI23_TURB11	11/21/2023	20:35

15.8334819	36.5002579	KM3	PI23_CTD09	11/22/2023	5:37
15.8338188	36.5002732	KM3	PI23_RET04	11/22/2023	7:16
15.8337545	36.5003168	KM3	PI23_RET05	11/22/2023	7:38
15.8338615	36.5002524	KM3	PI23_RET06	11/22/2023	8:16
15.8338336	36.5002567	KM3	PI23_IOP01	11/22/2023	8:32
15.8321477	36.4991427	KM3	PI23_RAD04	11/22/2023	9:20
15.8318793	36.4990038	KM3	PI23_CTD10	11/22/2023	9:43
15.8280957	36.4963960	KM3	PI23_TURB12	11/22/2023	10:46
15.8238109	36.4936041	KM3	PI23_TURB13	11/22/2023	11:24
15.8338440	36.5005226	KM3	PI23_BC01	11/22/2023	13:15
15.6025775	37.2045969	34	PI23_RAD05	11/24/2023	11:31
15.5928171	37.2320770	34	PI23_GC05	11/24/2023	13:05
15.5927596	37.2320119	34	PI23_CTD11	11/24/2023	14:58
15.5930278	37.2316963	34	PI23_IOP02	11/24/2023	15:35
15.5931002	37.2317115	34	PI23_IOP03	11/24/2023	15:57
15.4249793	37.4387192	26	PI23_GC06	11/26/2023	12:29
15.4248333	37.4386667	26	PI23_RAD06	11/26/2023	12:31
15.4252438	37.4386143	26	PI23_SE02	11/26/2023	13:03
15.4251650	37.4384617	26	PI23_RET07	11/26/2023	13:35
15.4252287	37.4384806	26	PI23_RET08	11/26/2023	13:46
15.4252434	37.4384797	26	PI23_RET09	11/26/2023	14:06
15.4258523	37.4404940	26	PI23_BC02	11/26/2023	15:17
15.4261495	37.4407131	26	PI23_CTD12	11/26/2023	16:45
15.4258605	37.4408505	26	PI23_IOP04	11/26/2023	17:40
15.4258580	37.4408479	26	PI23_IOP05	11/26/2023	17:43
15.4261143	37.4408321	26	PI23_CTD13	11/26/2023	18:10
15.4260412	37.4409386	26	PI23_TURB14	11/26/2023	18:27
15.4282686	37.4413426	26	PI23_TURB15	11/26/2023	19:25
15.4254045	37.4410531	26	PI23_TURB16	11/26/2023	20:18
15.9502332	37.3504892	29	PI23_GC07	11/27/2023	6:57
15.8769211	37.4855426	NK25	PI23_CTD14	11/27/2023	9:33

15.8766667	37.4855000	NK25	PI23_RET10	11/27/2023	10:21
15.8766667	37.4855000	NK25	PI23_RET11	11/27/2023	10:31
15.8771574	37.4854581	NK25	PI23_RET12	11/27/2023	10:53
15.8772470	37.4855452	NK25	PI23_RAD07	11/27/2023	11:39
15.8756117	37.4866414	NK25	PI23_IOP06	11/27/2023	12:18

Table 1.4.2. Effective measurement stations performed during Leg 1 of the PIONEER cruise 2023 with multiple platforms and probes. For correct depth of deployment of single probes and devices refer to the tables describing each activity. BC = box corer; GC = gravity corer; RAD = radiometer; IOP = Integrated (Optical) Observing System; RET = plankton net; CTD = CTD/Rosette; TURB = microstructure probe; SE = Secchi measurement; BGC-ARGO = deployment of drifting buoy. PI23 is the short name for PIONEER 2023. The unique station refers to the number of the station in the planning and permitting phase.

The Logbook of activities carried out during PIONEER 2023 is attached as Annex 1.

Activities in the first leg concentrated, among others, on the investigation of the Ionian deep water circulation, dissipation mechanisms at boundary layers, zooplankton biodiversity, optical properties of the upper water column, sediment sampling for deep-fluid (mantle) circulation and paleotephras. As side activities of national interest, multibeam bathymetric surveys were carried out over suggested locations of shipwrecks upon the request of the Ministry of Environment and Energy Security (MASE). Furthermore, a transit over the CTF-01 station was carried out with the pinging of 12 kHz signals transmitted by the hull-mounted CHIRP echosounder to be recorded by the hydrophones of the mooring station.

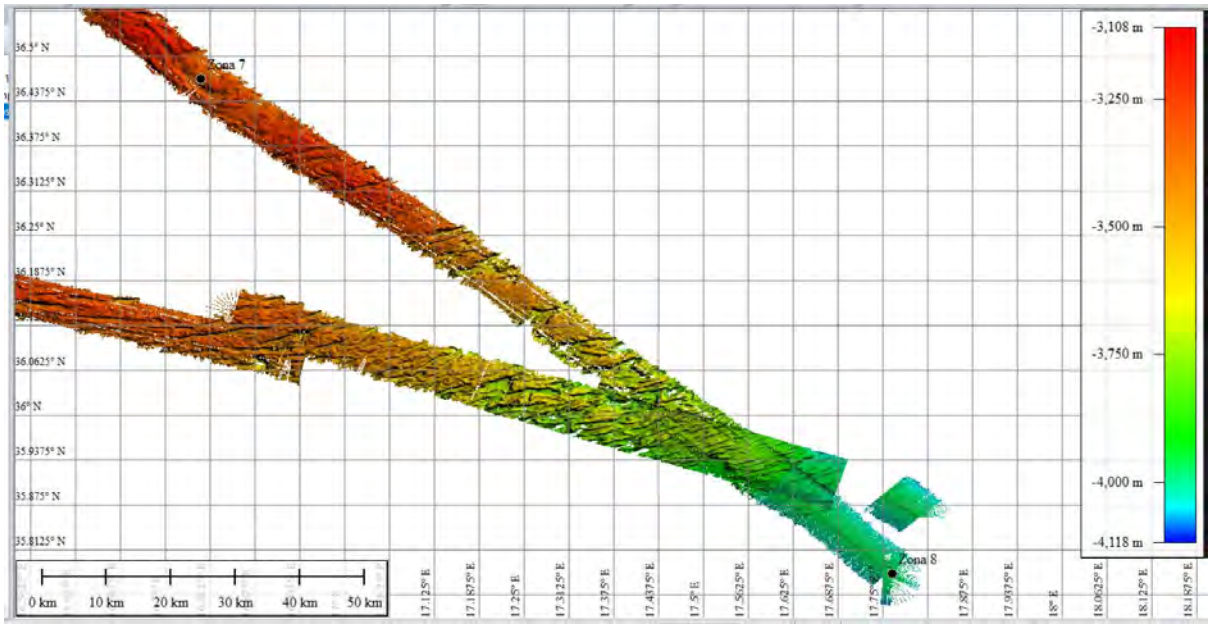

Figure 1.4.4. Transit over 2 shipwreck targets indicated by MASE.

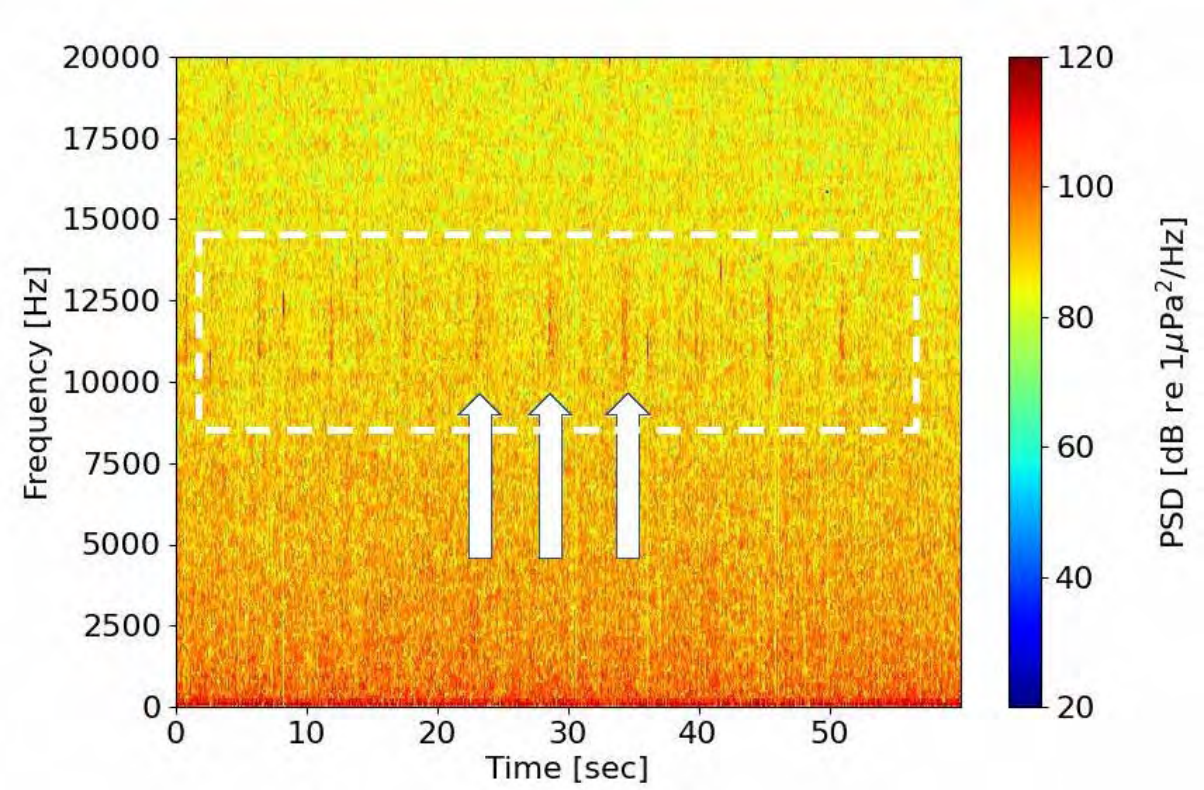

Figure 1.4.5. Spectrogram recorded by station CTF01 of the "cubic kilometre" (KM3NeT) submarine telescope for cosmic neutrinos. Arrows indicate the Gaia Blu's signals received by the hidrophones installed on the submarine observatory. The signal is sampled at 195300 Hz and the analysis is performed over 2048 FFT points and aHamming window with 50% overlap.

2° LEG CROTONE 28 NOVEMBER - CROTONE 9 DECEMBER			
Marzia Rovere	Party Chief	Researcher	ISMAR-CNR
Malek Belgacem	CTD-Rosette/O2, salinity, nutrients/LADCP	Post doc researcher	ISMAR-CNR
Florian Kokoszka	CTD-Rosette/nutrients, salinity/LADCP	Technologist PNRR	ISMAR-CNR
Lorenzo Consorti	CTD-Rosette/Carbon	Researcher	ISMAR-CNR
Jaime Pitarch Portero	Flow through	Researcher PNRR	ISMAR-CNR
Andrea Gallerani	Coring/box coring	Technician	ISMAR-CNR
Fabio Savelli	Coring/box coring	Technician	ISMAR-CNR
Claudio Pellegrini	Coring/box coring/sedimentology	Researcher	ISMAR-CNR
Stefania Romano	Box coring/contaminants	Researcher	ISMAR-CNR
Emanuela Frapiccini	Box coring/bisphenolA/IPA	Researcher	IRBIM-CNR
Marina Vingiani	Microbiology/DNA metabarcoding	PhD student	UNIGALWAY
Giuseppe Suaria	Box coring/microplastics/marine litter	Researcher	ISMAR-CNR
Chiara Pambianco	Box coring/organic matter	Post doc researcher	UNIVENEZIA
Alessandra Mercorella	Surveyor	Technician	ISMAR-CNR
Giulia Lisi	Surveyor	PhD student	UNIBOLOGNA
Alessandro Remia	Surveyor	Technologist	ISMAR-CNR
Andrea Argnani	Surveyor	Researcher	ISMAR-CNR
Vittorio Tulli	Video-maker, Photographer	Technician	URS-CNR
Danilo Pavone	Video-maker, Photographer	Technician	DSU-CNR

Table 1.4.3. List of personnel involved in Leg 2 of the PIONEER 2023 cruise.

Figure 1.4.5. Scientific party of Leg 2.

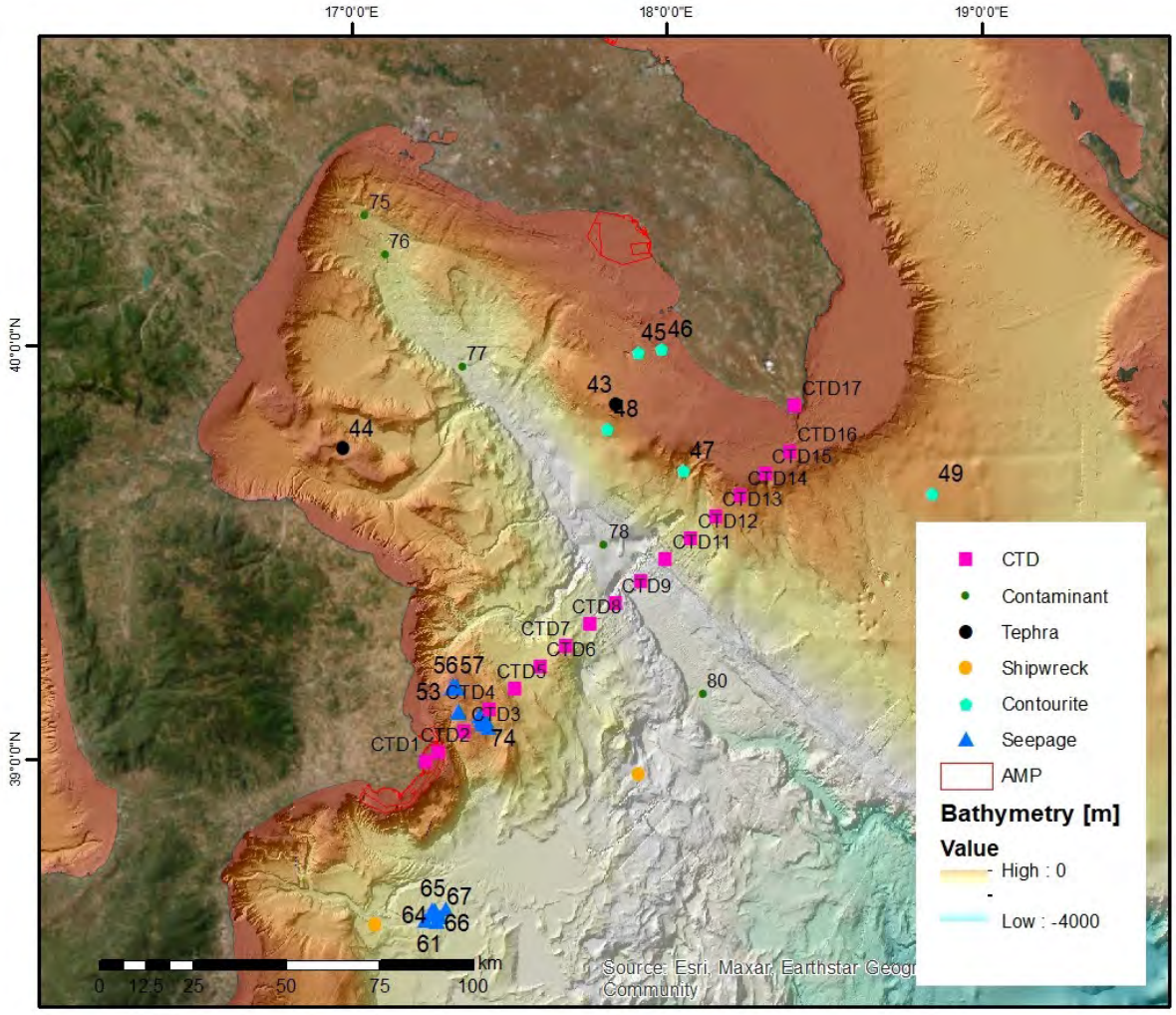

Figure 1.4.6. Plan of activities during Leg 1 of the PIONEER 2023 cruise.

The actual survey carried out during Leg 2 can be summarized as follows:

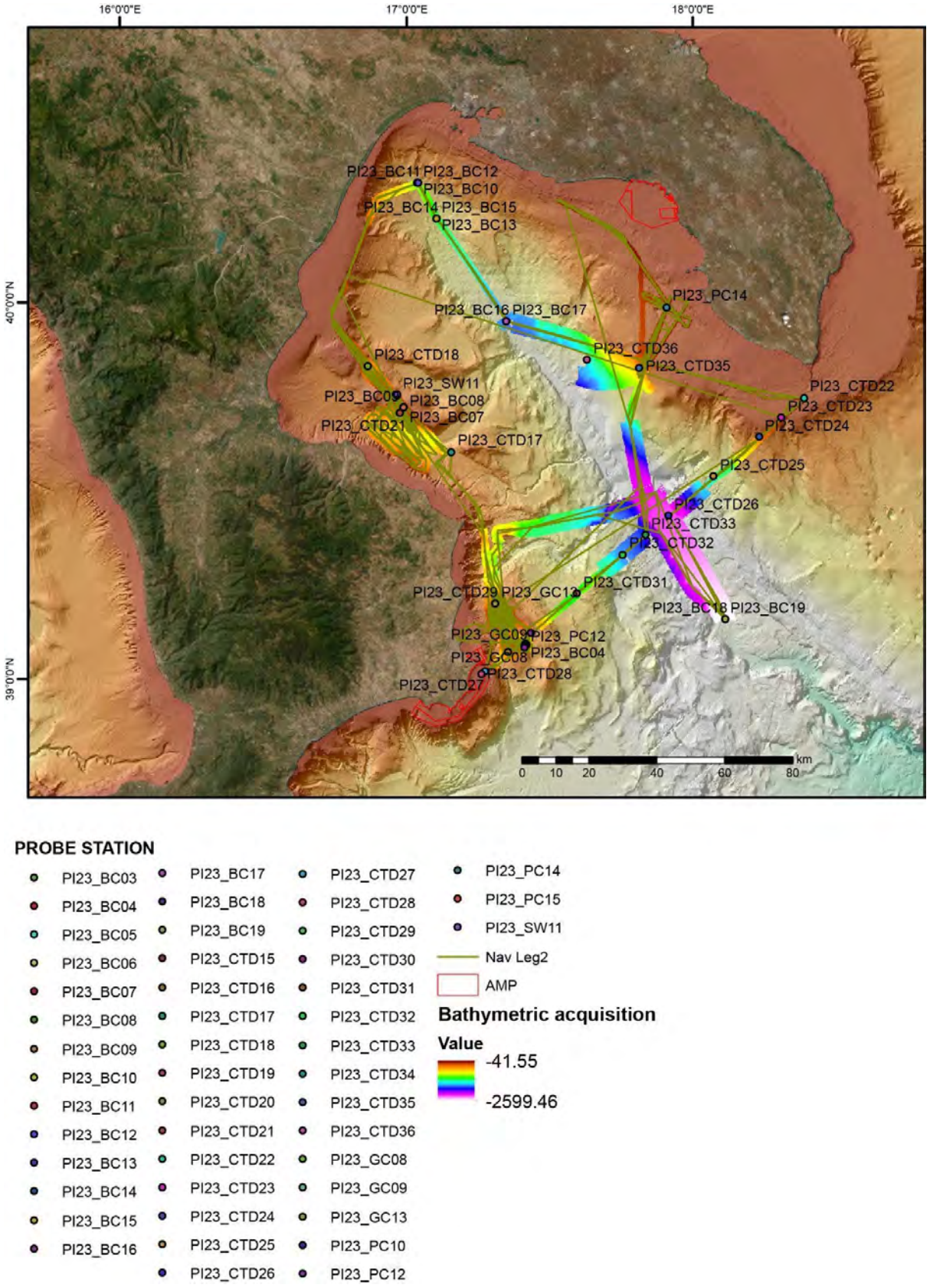

Figure 1.4.7. Effective survey carried out during Leg 2 of the PIONEER 2023 cruise.

LONG-WGS84	LAT-WGS84	UNIQUE STATION	PROBE STATION	DEPTH (m)	DATE	UTC
17.3630983	39.0684617	50	PI23_CTD15	607	29/11/2023	9:25
17.2997867	39.0498400	CTD3	PI23_CTD16	416	30/11/2023	5:53
17.3592333	39,0700900	50	PI23_BC03	609	30/11/2023	7:43
17.3594300	39.0702967	50	PI23_GC08	607	30/11/2023	8:56
17.3572492	39.0646017	69	PI23_BC04	615	30/11/2023	10:32
17.3575523	39.,0654860	69	PI23_GC09	612	30/11/2023	12:46
17.1228167	39.5851842	44	PI23_CTD17	676	01/12/2023	11:12
16.8430087	39.8172263	44	PI23_CTD18	420	01/12/2023	22:13
16.9401796	39.7400423	44	PI23_PC10	370	02/12/2023	9:35
16.9402860	39.7399369	44	PI23_CTD19	370	02/12/2023	10:27
16.9405970	39.7395868	44	PI23_BC05	368	02/12/2023	12:05
16.9408583	39.7396773	44	PI23_BC06	368	02/12/2023	12:40
16,9613782	39.7060328	44	PI23_CTD20	287	03/12/2023	8:23
16.9610417	39.7060017	44	PI23_BC07	281	03/12/2023	8:55
16.9610785	39.7061703	44	PI23_BC08	281	03/12/2023	9:47
16.9610541	39.7061235	44	PI23_BC09	281	03/12/2023	10:51
16.9400483	39.7400000	44	PI23_SW11	369	03/12/2023	13:28
16.9472033	39.6928333	44	PI23_CTD21	387	03/12/2023	14:49
17.0276062	40.3010565	75	PI23_BC10	1008	04/12/2023	6:16
17.0279018	40.3010382	75	PI23_BC11	1007	04/12/2023	6:58
17.0279755	40.3009762	75	PI23_BC12	1008	04/12/2023	7:47
17.0888153	40.2052608	76	PI23_BC13	1209	12/4/2023	9:30
17.0888453	40.2052503	76	PI23_BC14	1208	12/4/2023	10:30
17.0888267	40.2053195	76	PI23_BC15	1205	12/4/2023	11:23
17.3230827	39.9283483	77	PI23_BC16	1708	12/4/2023	14:28
17.3231142	39.9284625	77	PI23_BC17	1708	12/4/2023	15:38
18.3397578	39.7000908	CTD16	PI23_CTD22	121	12/4/2023	21:43
18.2596927	39.6501930	CTD15	PI23_CTD23	196	12/4/2023	23:02

18.1799657	39.6003575	CTD14	PI23_CTD24	412	12/5/2023	0:13
18.0198747	39.5000712	CTD12	PI23_CTD25	1356	12/5/2023	2:16
17.8602032	39.4003308	CTD10	PI23_CTD26	2274	12/5/2023	4:46
18.0418263	39.1212138	80	PI23_BC18	2594	12/5/2023	8:01
18.0419523	39.1211730	80	PI23_BC19	2592	12/5/2023	9:10
17.2201800	38.9998968	CTD02	PI23_CTD27	62	12/6/2023	6:54
17.2074262	38.9928310	CTD01	PI23_CTD28	40	12/6/2023	7:29
17.3565582	39.0614055	69bis	PI23_PC12	590	12/6/2023	9:38
17.2591450	39.1800333	Biocostruzioni	PI23_CTD29	160	12/6/2023	12:02
17.2593233	39.1796972	Biocostruzioni	PI23_GC13	160	12/6/2023	12:46
17.3801570	39.1001835	CTD04	PI23_CTD30	588	12/6/2023	14:33
17.5399743	39.2000775	CTD06	PI23_CTD31	1129	12/6/2023	16:44
17.7003868	39.3002415	CTD08	PI23_CTD32	1662	12/6/2023	19:19
17.7795797	39.3502480	CTD09	PI23_CTD33	1893	12/6/2023	21:26
17.8772493	39.9536830	45	PI23_PC14	200	12/7/2023	9:14
39.7702262	17.7727548	48	PI23_CTD34	710	12/8/2023	10:54
39.7705110	17.7727482	48	PI23_PC15	712	12/8/2023	12:23
17.7770233	39.7953937	possible cascading point	PI23_CTD35	538	12/8/2023	17:06
17.5974290	39.8204475	along slope	PI23_CTD36	1492	12/8/2023	20:09

Table 1.4.5. Effective measurement stations performed during Leg 2 of the PIONEER cruise 2023 with multiple platforms and probes. For correct depth of deployment of single probes and devices refer to the tables describing each activity. BC = box corer; GC = gravity corer; PC = Piston corer; SW = SeaWater; CTD = CTD/Rosette. PI23 is the short name for PIONEER 2023. The unique station refers to the number of the station in the planning and permitting phase.

Activities in the second leg concentrated, among others, on the investigation of the Earth System Cycles along an external transect of the Gulf of Taranto, pelagic and benthic biodiversity, sediment and water sampling for the comprehensive study of seepage systems, paleoceanographic reconstructions and contamination in deep sea sediments.

1.7. Activities, methodologies and tools

The PIONEER oceanographic campaign aboard RV Gaia Blu involved a diverse range of activities and methodologies and focused on various aspects of marine research, covering physical, chemical, geological and biological parameters. Specific activities included CTD measurements and L-ADCP, seawater sampling with Niskin bottles, the deployment of microstructure profiler, plankton net, coring and box coring sediment sampling devices, the operation of specialized geophysical equipment such as multibeam, CHIRP, ADCP. The wet and dry labs provided essential spaces for conducting experiments and analyses. The control room facilitated coordination and communication during operations. The following paragraphs provide a detailed assessment of the operations carried out.

2. CTD and LADCP Operations

2.1. Insights

CTD profiles (Conductivity, Temperature and Depth) were carried out with a Seabird SBE-911+ mounted on a 12-bottle Rosette sampler, with all sensors calibrated yearly. About the Rosette, two casts were released to provide a proper water sampling of the water column for the deepest stations (e.g. 12 bottles in the deep layers, below 1000 m depth, and then 12 others in the superior layers, from 1000m to the surface). Additional casts were performed on demand to carry the IOP instrumentation (fixed on the Rosette structure) to measure the optic properties and radiometry of the water column (see the Section IOP/Radiometry). Regarding the CTD measurements, the raw 24 Hz profiles were processed using the standard Seabird software SBE data Processing (Version 7.26.7) to obtain bin-averaged data on a 1-m regular vertical grid.

The main variables measured are temperature (ºC), seawater conductivity (mS/cm), and pressure (decibar). Salinity (PSU) is inferred by the Seabird software on the fly from conductivity and temperature, using the TEOS equation. Values are recalculated later during the data processing using the Gibbs Sea Water (GSW) Oceanographic Toolbox. Observations presented thereafter are preliminary results that were obtained before the re-calibration process.

To acquire a full depth-ocean velocity, two Lowered ADCPs are mounted on the CTD carousel. The system is composed of two workhorse LADCPs (WH 300). One upward-looking and one downward-looking. While in the water, the Lowered ADCPs (LADCPs) utilize acoustic pings to gather short-range velocity profiles (approximately 100 m) relative to the moving instruments. To obtain absolute velocities in the Earth's frame of reference, these short profiles are combined, and the effects of instrument motion are corrected using additional constraints.

The system consisted of two RD instrument Workhorse ADCPs (WH 300) operating at a frequency of 300 kHz. One ADCP looked upward (Slave s/n 1805), while the other looked downward (Master s/n 1465). The downward-looking ADCP allowed for tracking instrument velocity over the seabed, providing a constraint for LADCP profiles near the seabed. LADCP measurements were conducted at 25 CTD stations and processed using the LDEO Matlab LADCP-processing system based on the velocity-inversion method initially developed by Visbeck (2002).

This software utilized the raw LADCP data, processed CTD data to generate vertical profiles of the u- and -v velocity components (Figure 2.1.4).

Leg	CTD	Filename	Cast type	Date, time (UTC)	Lon. (dd)	Lat. (dd)	Depth max (m)	Bottom depth (m)
1	CTD01	PI23_CTD01	Full column	2023-11-19 12:40:30	15.425	37.439	202	220
1	CTD02	PI23_CTD02_st3deep	Full column	2023-11-20 09:01:30	17.803	35.857	3896	3950
1	CTD03	PI23_CTD03_st3iop1	Carrying IOP	2023-11-20 17:28:02	17.748	35.886	99	3950
1	CTD04	PI23_CTD04_st3sup	Sup 0-1000m	2023-11-20 17:59:24	17.748	35.886	1001	3950
1	CTD05	PI23_CTD05_st11deep	Full column	2023-11-21 03:23:20	16.944	36.116	3382	3414
1	CTD06	PI23_CTD06_st11sup	Sup 0-500m	2023-11-21 08:05:03	16.944	36.115	505	3414
1	CTD07	PI23_CTD07_st11iop01	Carrying IOP	2023-11-21 09:29:37	16.939	36.114	98	3601
1	CTD08	PI23_CTD08_st11iop02	Carrying IOP	2023-11-21 09:49:19	16.939	36.114	98	3601
1	CTD09	PI23_CTD09_stKM3deep	Full column	2023-11-22 04:41:28	15.833	36.500	3273	3304
1	CTD10	PI23_CTD10_stKM3sup	Sup 0-400m	2023-11-22 09:26:53	15.831	36.498	402	3304
1	CTD11	PI23_CTD11_st34	Full column	2023-11-24 14:18:36	15.592	37.232	2152	2200
1	CTD12	PI23_CTD12_st26	Full column	2023-11-26 16:10:20	15.426	37.440	1971	1989
1	CTD13	PI23_CTD13_st26_bis	Sup 0-60m	2023-11-26 18:07:42	15.426	37.441	72	1989
1	CTD14	PI23_CTD14_stNK25	Full column	2023-11-27 08:55:01	15.876	37.485	2206	2227
2	CTD15	PI23_CTD15_st50	Full column	2023-11-29 09:13:46	17.361	39.069	569	
2	CTD16	PI23_CTD16_stctd03	Full column	2023-11-30 05:19:22	17.299	39.050	394	
2	CTD17	PI23_CTD17	Full column	2023-12-01 11:00:07	17.122	39.585	645	
2	CTD18	PI23_CTD18	Full column	2023-12-01 22:04:19	16.843	39.817	395	
2	CTD34	PI23_CTD34_st48	Full column	2023-12-02 10:19:39	16.940	39.740	349	
2	CTD19	PI23_CTD19_st44	Full column	2023-12-02 10:19:39	16.940	39.740	273	

2	CTD20	PI23_CTD20	Full column	2023-12-03 08:16:37	16.961	39.705	368	
2	CTD21	PI23_CTD21	Full column	2023-12-03 14:41:34	16.946	39.692	122	
2	CTD22	PI23_CTD22_stctd16	Full column	2023-12-04 21:39:04	18.340	39.700	181	
2	CTD23	PI23_CTD23_stctd15	Full column	2023-12-04 22:58:42	18.260	39.650	401	
2	CTD24	PI23_CTD24_stctd14	Full column	2023-12-05 00:05:02	18.180	39.600	1337	
2	CTD25	PI23_CTD25_stctd12	Full column	2023-12-05 01:53:25	18.020	39.500	2256	
2	CTD26	PI23_CTD26_stctd10	Full column	2023-12-05 04:08:57	17.859	39.400	52	
2	CTD27	PI23_CTD27_stctd02	Full column	2023-12-06 06:52:07	17.220	38.999	30	
2	CTD28	PI23_CTD28_stctd01	Full column	2023-12-06 07:27:33	17.207	38.992	135	
2	CTD29	PI23_CTD29_stGCbiogeo	Full column	2023-12-06 11:58:21	17.259	39.179	569	
2	CTD30	PI23_CTD30_stctd04	Full column	2023-12-06 14:23:22	17.380	39.100	1113	
2	CTD31	PI23_CTD31_stctd06	Full column	2023-12-06 16:24:18	17.539	39.199	1646	
2	CTD32	PI23_CTD32_stctd08	Full column	2023-12-06 18:51:26	17.700	39.300	1877	
2	CTD33	PI23_CTD33_stctd09	Full column	2023-12-06 20:55:21	17.780	39.350	697	
2	CTD35	PI23_CTD35	Full column	2023-12-08 16:55:23	17.777	39.795	533	
2	CTD36	PI23_CTD36	Full column	2023-12-08 19:45:08	17.597	39.820	1477	

Table 2.2.1. General metadata information of each CTD casts (*Deep*: full-column depth coverage, from surface to bottom; *Sup*: superior depth range coverage, from surface up to 1000m, to complete the water sampling; *IOP*: downcast performed up to 100m deep to carry IOP's instrumentations).

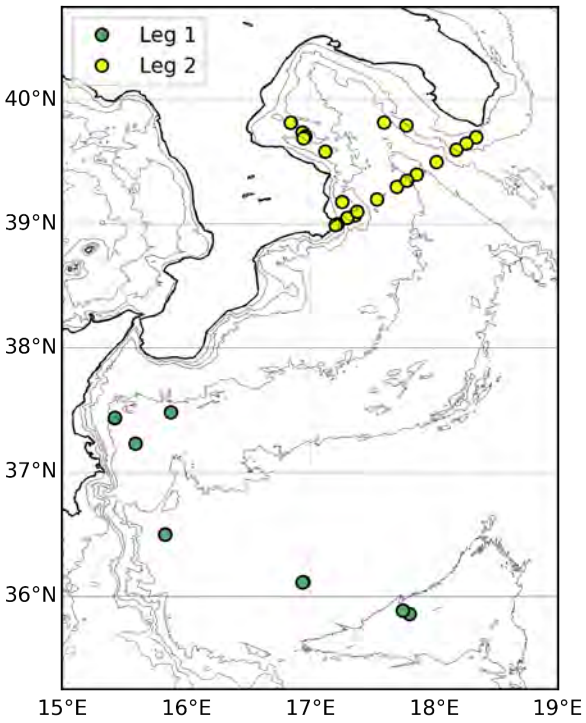

Figure 2.1.1. Geographical position of the CTD casts over the Ionian sea bathy-morphology (GEBCO, 2020; isobaths: -100m,-500m,-1000m,-2000m,-3000m,-4000m). In green: Leg 1; yellow: Leg 2.

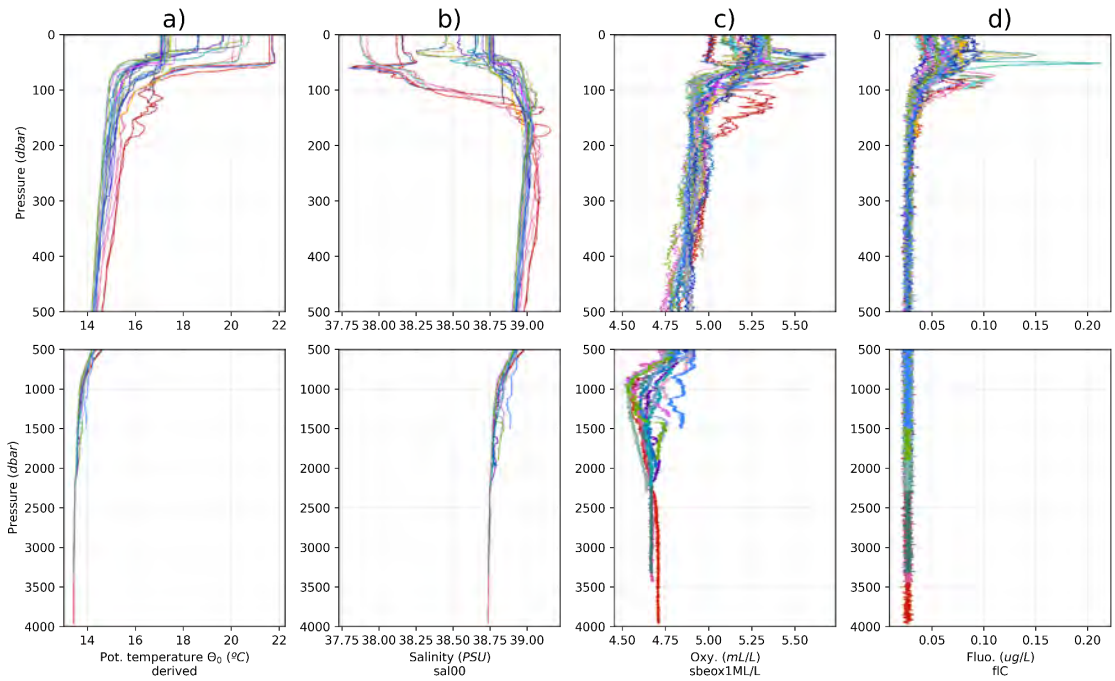

Figure 2.1.2. Overview of the vertical profiles obtained from the CTD sensor. a) Temperature; b): salinity; c) oxygen; d) fluorescence. The water-column is splitted with two panels to present the upper (Top: 0-500m) and the deep layers (Bottom: 500m-bottom).

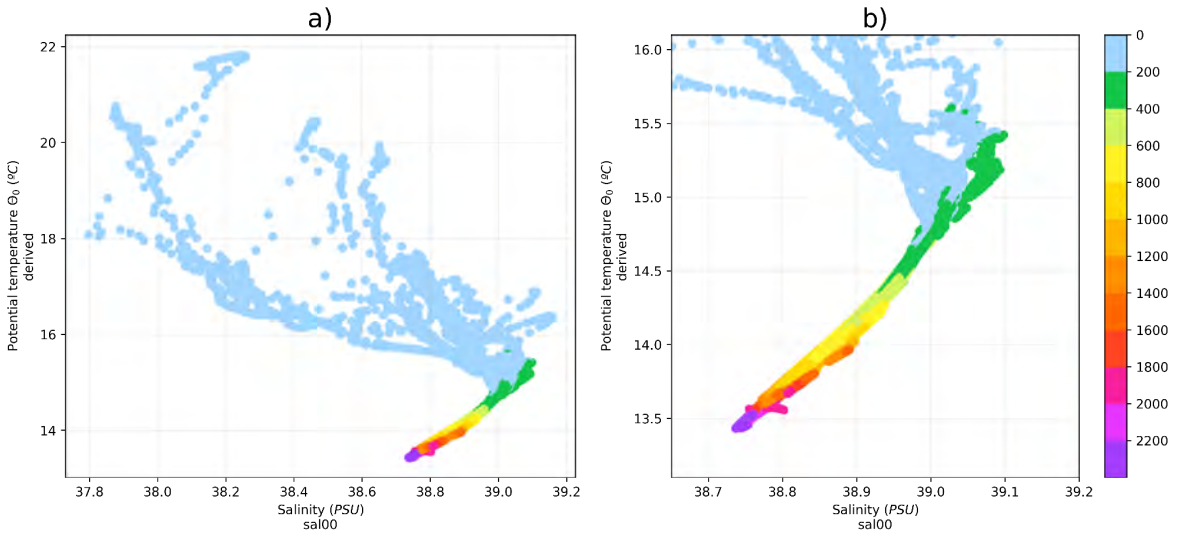

Figure 2.1.3. General temperature-salinity diagrams. In colour: pressure ranges of measurements (in decibar) Left: all values; Right: zoom over intermediate layers.

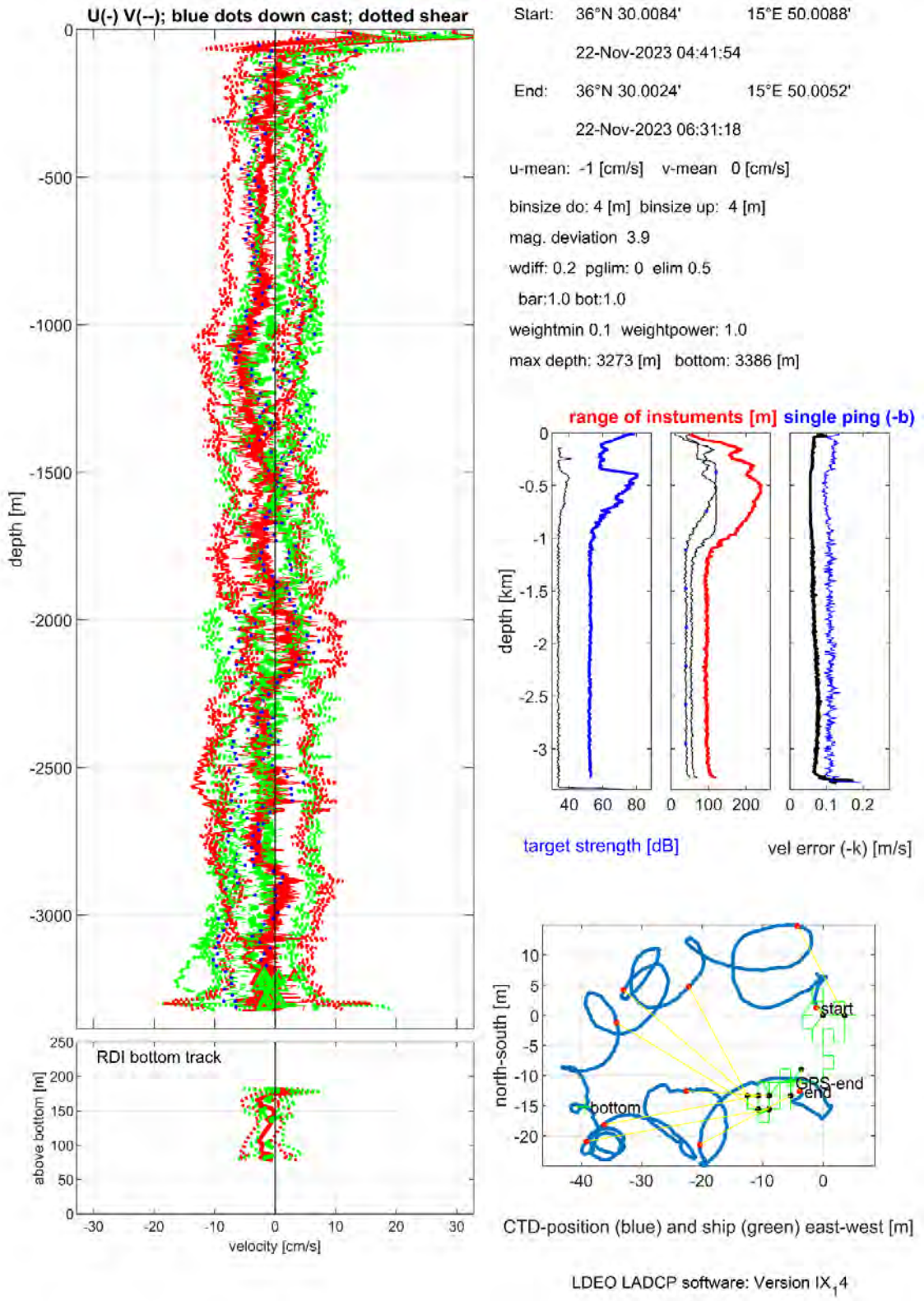

Figure 2.1.4. Overview plot of station CTD09. Main panel: eastward (in red) and northward (in green) velocities: full solution with error bars, down and upcast solutions, shear solution, bottom track. bottom-left panel: bottom track velocities. Bottom-right panel: ship and instrument drift during cast. Center-right panels: target-strength, range and error profiles. Top-right text: metadata and velocity referencing constraints used for processing.

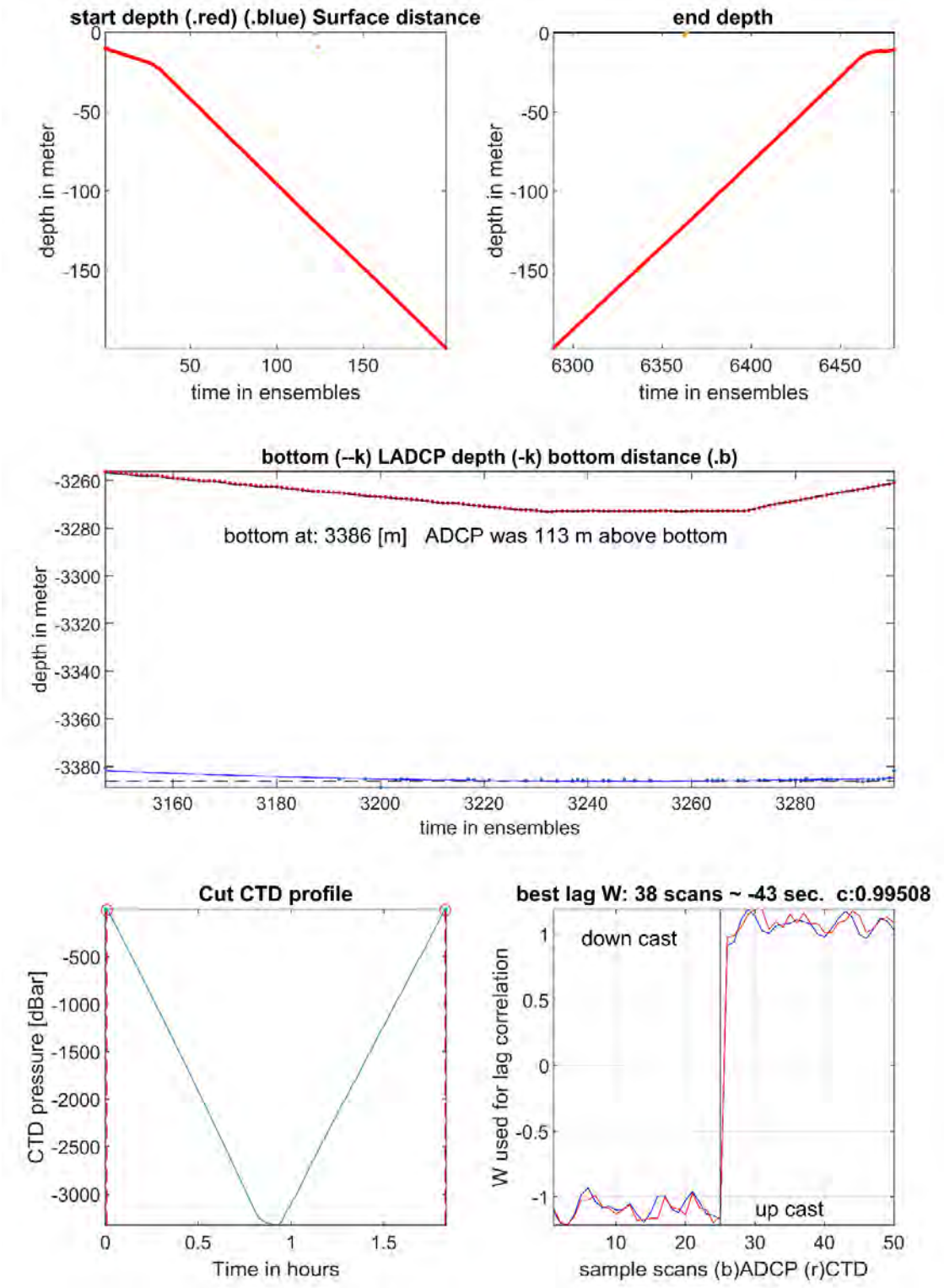

Figure 2.1.5. Surface/ seabed detection and CTD/LADCP times series match (example from station CTD09). upper panels: start and end of the cast (in red), and the detected sea-surface (in yellow). central panel: bottom depth of the cast (from CTD depth in black, from LADCP in red) with the detected sea-bed (in blue). Bottom right panel: CTD/LADCP times series match (downcast: left, upcast: right).Bottom-left panel: time range of CTD cast (dashed red lines).

2.2. Challenges

The CTD acquisition took place as expected and, after pre-processing, the quality of the data appears good and meets the expected standards.

However, there is discrepancy between the cable length indicated by the winch system and the actual depth of the CTD, even at shallow depths (e.g. for 50 m displayed by the CTD, the winch underestimates at 48 m). The CTD depth inferred from the pressure sensor is reliable, while the cable length, digitally calculated from the winch parameters, proved to be unreliable. Repeated observations have shown that this difference increases with depth (about 5 m difference at 100 m depth, 50 m at 1000 m and up to 300 m at 3000 m). An example of this behavior can be seen in the following image.

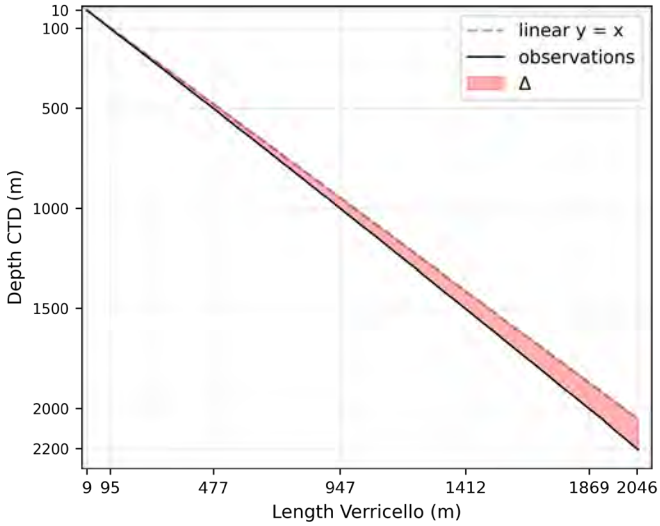

Figure 2.2.1. Differences noted between CTD probe depth and winch length. This difference increases with depth. Taking into consideration a payout strictly equal to the depth of the CTD (y=x), there would be high risk of touch down.

In addition, during profile PI23_CTD02 problems occurred to the pulley that led the operator to stop the descent several times to adjust the winch settings. When the probe was lifted, the 0 of the CTD (at the sea surface) corresponded to a value of 30 m on the winch, which could be stopped in time by the intervention of the operator. Subsequently, for the other profiles, this difference could be observed and documented and operations could continue in complete safety.

2.3. Recommendations

The main recommendation that emerged during the practice on board concerns the use of the winch and checking the difference between the unrolled length and the CTD depth. Once the definitive correspondence between the cable length and the CTD depth has been established, a simple procedure can be used, during the implementation for each profile:

Example of protocol:

1- check the local depth using the multibeam (e.g. 677 m).

2- round down to the nearest decade (e.g. if 677 m consider 670 m).

3- subtract a safety distance (e.g. 40 m, corresponding to the altimeter range): 670m - 40m = 630 m.

4- consider this depth value, and find its correspondence with the length of the cable (e.g. according to our observations, 630m of depth corresponds to 600 m of cable).

5- report the payout value of 600 in the payout, and not the depth of 630 m, in order to limit the maximum depth of the descent to a reasonable safety distance from the bottom.

6- start the profile (slowly, at 20 m/min, then faster, 40 m/min, up to 60 m/min = 1 m/s) and continue to check the CTD value and its difference with the winch during the downhill.

7- once the descent has been completed and the probe has reached the bottom area (e.g. payout cable value 600, CTD depth of approximately 630 m and beam depth of the seabed of approximately 670 m), increase the payout (e.g. payout value of 620 to the square of payout 600 m) then slowly continue the descent (20 m/min) to finish the last metres of the profile, up to a proximity of 15-20 m from the bottom, checking the distance from the bottom using the altimeter.

Furthermore, as a general recommendation it would be necessary to train more people in the use of the winch to ensure the possibility of carrying out measurements during all work shifts 24 hours a day.

3. Seawater Sampling

3.1. Insights

Seawater sampling was carried out using a Carousel 32 twelve positions for Niskin. This is a rosette sampler that can hold up to 12 Niskin bottles of 12 liters each. It allows the collection of water samples at different depths and locations. The sampler is triggered by a remote control. The Niskin plastic bottles have a spring-loaded mechanism that closes the bottle when the command is given. They can collect water samples from any depth. Water samples were collected and analyzed for different parameters as follows.

- *Dissolved oxygen sampling*

Besides the CTD SBE43 oxygen profiles, 24 discrete oxygen samples were collected during 5 CTD casts from Niskin bottles to calibrate the CTD oxygen sensors and correct for any drift. Seawater samples were collected at different depth levels to cover the full range of dissolved oxygen (DO) in the water column.

Samples were immediately fixed with ½ ml of manganous chloride ($MnCl_2$) and ½ sodium hydroxide solution (NaOH/NaI). Samples were shaken and taken back to the onboard lab and stored in the dark normally for three to four hours of sample collection to allow the precipitate formation. After adding the reagents Mn^{2+} is oxidized by the molecule of oxygen in the seawater sample, to the point that it precipitates as $Mn(OH)_2$ at the bottom of the bottle.

- *Salinity sampling*

During 6 CTD stations, probes at 7 depth levels were sampled for salinity analysis. samples were collected in 250ml flasks and stored at least 12 hours prior analysis.

- Inorganic nutrient sampling

Seawater samples for inorganic nutrients were collected during the CTD upcast at standard depths using 50 ml flasks. Samples were immediately stored at -20°C.

- eDNA sampling

During Leg 1, deep and surface seawater for eDNA analysis was sampled at 5 CTD stations collecting several liters of water (maximum 10 liters) from Niskin bottles and filtering in the wet lab shortly afterwards. During Leg 1, at each selected station, seawater for eDNA analysis was collected at 6 or 7 different depth levels (Table 3.1.1). Thus, filters were stored at -80°C for further molecular analysis.

Then, deep seawater for eDNA analysis was sampled at all the CTD stations during Leg 2; 10 litres collected from each Niskin rosette deployment and filtered in the wet lab shortly afterwards (Fig. 3.1.1). Thus, filters were stored at -80°C for further molecular analysis.

A. **B.**

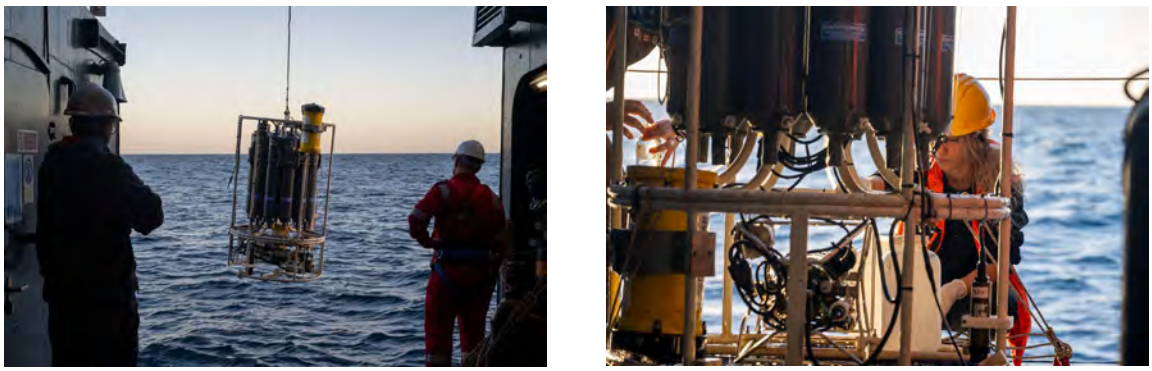

Figure 3.1.1. A. Deployment of the Niskin Rosette system. B. Operations of rinsing the plastic tanks with Niskin water before sampling 10 liters.

Date	Station	Depth (m)	Sample name
20/11/2023	3	4081	PI23_CTD02_st3_eDNA_1
20/11/2023	3	3250	PI23_CTD02_st3_eDNA_5
20/11/2023	3	1500	PI23_CTD02_st3_eDNA_12
20/11/2023	3	750	PI23_CTD04_st3_eDNA_3
20/11/2023	3	400	PI23_CTD04_st3_eDNA_5
20/11/2023	3	100	PI23_CTD04_st3_eDNA_8

20/11/2023	3	5	PI23_CTD04_st3_eDNA_12
21/11/2023	11	3377	PI23_CTD05_st11_eDNA_1
21/11/2023	11	2600	PI23_CTD05_st11_eDNA_5
21/11/2023	11	1000	PI23_CTD05_st11_eDNA_12
21/11/2023	11	500	PI23_CTD06_st11_eDNA_1
21/11/2023	11	80	PI23_CTD06_st11_eDNA_7/8/9
21/11/2023	11	5	PI23_CTD06_st11_eDNA_12
22/11/2023	KM3	3272	PI23_CTD09_KM3_eDNA_1
22/11/2023	KM3	2600	PI23_CTD09_KM3_eDNA_4
22/11/2023	KM3	2000	PI23_CTD09_KM3_eDNA_7
22/11/2023	KM3	900	PI23_CTD09_KM3_eDNA_11
22/11/2023	KM3	110	PI23_CTD10_KM3_eDNA_3
22/11/2023	KM3	35	PI23_CTD10_KM3_eDNA_6
22/11/2023	KM3	5	PI23_CTD10_KM3_eDNA_11
26/11/2023	26	1971	PI23_CTD12_st26_eDNA_1
26/11/2023	26	1100	PI23_CTD12_st26_eDNA_3
26/11/2023	26	150	PI23_CTD12_st26_eDNA_7
26/11/2023	26	60	PI23_CTD12_st26_eDNA_8
26/11/2023	26	40	PI23_CTD12_st26_eDNA_10
26/11/2023	26	5	PI23_CTD12_st26_eDNA_11
27/11/2023	NK25	2200	PI23_CTD14_NK25_eDNA_1
27/11/2023	NK25	1500	PI23_CTD14_NK25_eDNA_3A PI23_CTD14_NK25_eDNA_3B
27/11/2023	NK25	675	PI23_CTD14_NK25_eDNA_5
27/11/2023	NK25	150	PI23_CTD14_NK25_eDNA_8A PI23_CTD14_NK25_eDNA_8B
27/11/2023	NK25	50	PI23_CTD14_NK25_eDNA_10
27/11/2023	NK25	5	PI23_CTD14_NK25_eDNA_12

Table 3.1.1. Samples collected at each station and each depth level for eDNA analysis during Leg 1.

- Enzymatic activity (EEA) and nutrients analysis samplings

Deep and surface seawater for enzymatic activity and nutrients analysis was sampled at the CTD stations collecting respectively 100 ml and 15 ml from Niskin bottles. Thus, sampled water was stored at +4°C and -20°C respectively for enzymatic activity analysis and nutrients analysis. During Leg 1, water for enzymatic analysis and nutrient analysis was collected in 5 stations at different depth levels (Tab. 3.1.2, 3.1.3).

Date	Station	Depth (m)	EEA sample name
20/11/23	3	4081	PI23_CTD02_st3_EEA_1
20/11/23	3	3900	PI23_CTD02_st3_EEA_2
20/11/23	3	3800	PI23_CTD02_st3_EEA_3
20/11/23	3	3500	PI23_CTD02_st3_EEA_4
20/11/23	3	3250	PI23_CTD02_st3_EEA_5

20/11/23	3	3000	PI23_CTD02_st3_EEA_6
20/11/23	3	2750	PI23_CTD02_st3_EEA_7
20/11/23	3	2500	PI23_CTD02_st3_EEA_8
20/11/23	3	2250	PI23_CTD02_st3_EEA_9
20/11/23	3	1750	PI23_CTD02_st3_EEA_11
20/11/23	3	1500	PI23_CTD02_st3_EEA_12
20/11/23	3	1250	PI23_CTD04_st3_EEA_1
20/11/23	3	1000	PI23_CTD04_st3_EEA_2
20/11/23	3	750	PI23_CTD04_st3_EEA_3
20/11/23	3	500	PI23_CTD04_st3_EEA_4
20/11/23	3	400	PI23_CTD04_st3_EEA_5
20/11/23	3	200	PI23_CTD04_st3_EEA_7
20/11/23	3	100	PI23_CTD04_st3_EEA_8
20/11/23	3	25	PI23_CTD04_st3_EEA_11
20/11/23	3	5	PI23_CTD04_st3_EEA_12
21/11/23	11	3377	PI23_CTD05_st11_EEA_1
21/11/23	11	3250	PI23_CTD05_st11_EEA_2
21/11/23	11	3000	PI23_CTD05_st11_EEA_3
21/11/23	11	2800	PI23_CTD05_st11_EEA_4
21/11/23	11	2600	PI23_CTD05_st11_EEA_5
21/11/23	11	2400	PI23_CTD05_st11_EEA_6
21/11/23	11	2200	PI23_CTD05_st11_EEA_7
21/11/23	11	1750	PI23_CTD05_st11_EEA_9
21/11/23	11	1500	PI23_CTD05_st11_EEA_10
21/11/23	11	1250	PI23_CTD05_st11_EEA_11
21/11/23	11	1000	PI23_CTD05_st11_EEA_12
21/11/23	11	500	PI23_CTD06_st11_EEA_1
21/11/23	11	400	PI23_CTD06_st11_EEA_2
21/11/23	11	300	PI23_CTD06_st11_EEA_3
21/11/23	11	200	PI23_CTD06_st11_EEA_4
21/11/23	11	150	PI23_CTD06_st11_EEA_5
21/11/23	11	100	PI23_CTD06_st11_EEA_6
21/11/23	11	80	PI23_CTD06_st11_EEA_7/8/9
21/11/23	11	50	PI23_CTD06_st11_EEA_10
21/11/23	11	25	PI23_CTD06_st11_EEA_11
21/11/23	11	5	PI23_CTD06_st11_EEA_12
22/11/23	KM3	3272	PI23_CTD09_KM3_EEA_1
22/11/23	KM3	3100	PI23_CTD09_KM3_EEA_2
22/11/23	KM3	3000	PI23_CTD09_KM3_EEA_3
22/11/23	KM3	2600	PI23_CTD09_KM3_EEA_4
22/11/23	KM3	2400	PI23_CTD09_KM3_EEA_5
22/11/23	KM3	2200	PI23_CTD09_KM3_EEA_6

22/11/23	KM3	2000	PI23_CTD09_KM3_EEA_7
22/11/23	KM3	1800	PI23_CTD09_KM3_EEA_8
22/11/23	KM3	1500	PI23_CTD09_KM3_EEA_9
22/11/23	KM3	1250	PI23_CTD09_KM3_EEA_10
22/11/23	KM3	900	PI23_CTD09_KM3_EEA_11
22/11/23	KM3	500	PI23_CTD09_KM3_EEA_12
22/11/23	KM3	300	PI23_CTD10_KM3_EEA_1
22/11/23	KM3	110	PI23_CTD10_KM3_EEA_3
22/11/23	KM3	60	PI23_CTD10_KM3_EEA_4
22/11/23	KM3	35	PI23_CTD10_KM3_EEA_6
22/11/23	KM3	20	PI23_CTD10_KM3_EEA_9
22/11/23	KM3	5	PI23_CTD10_KM3_EEA_11
26/11/23	26	1971	PI23_CTD12_st26_EEA_1
26/11/23	26	1750	PI23_CTD12_st26_EEA_2
26/11/23	26	1100	PI23_CTD12_st26_EEA_3
26/11/23	26	800	PI23_CTD12_st26_EEA_4
26/11/23	26	400	PI23_CTD12_st26_EEA_5
26/11/23	26	150	PI23_CTD12_st26_EEA_7
26/11/23	26	60	PI23_CTD12_st26_EEA_8
26/11/23	26	40	PI23_CTD12_st26_EEA_10
26/11/23	26	5	PI23_CTD12_st26_EEA_11
27/11/23	NK25	2200	PI23_CTD14_NK25_EEA_1
27/11/23	NK25	1750	PI23_CTD14_NK25_EEA_2
27/11/23	NK25	1500	PI23_CTD14_NK25_EEA_3
27/11/23	NK25	1100	PI23_CTD14_NK25_EEA_4
27/11/23	NK25	675	PI23_CTD14_NK25_EEA_5
27/11/23	NK25	400	PI23_CTD14_NK25_EEA_6
27/11/23	NK25	150	PI23_CTD14_NK25_EEA_7
27/11/23	NK25	50	PI23_CTD14_NK25_EEA_10

Table 3.1.2. Samples collected at each station and each depth level for enzymatic activity analysis during Leg 1.

Date	Station	Depth (m)	Nutrients sample name
20/11/23	3	4081	PI23_CTD02_st3_NUT_1
20/11/23	3	3500	PI23_CTD02_st3_NUT_4
20/11/23	3	3000	PI23_CTD02_st3_NUT_6
20/11/23	3	2500	PI23_CTD02_st3_NUT_8
20/11/23	3	1500	PI23_CTD02_st3_NUT_12
20/11/23	3	1250	PI23_CTD04_st3_NUT_1
20/11/23	3	500	PI23_CTD04_st3_NUT_4
20/11/23	3	100	PI23_CTD04_st3_NUT_8

20/11/23	3	5	PI23_CTD04_st3_NUT_12
21/11/23	11	3377	PI23_CTD05_st11_NUT_1
21/11/23	11	3000	PI23_CTD05_st11_NUT_3
21/11/23	11	2600	PI23_CTD05_st11_NUT_5
21/11/23	11	1000	PI23_CTD05_st11_NUT_12
21/11/23	11	500	PI23_CTD06_st11_NUT_1
21/11/23	11	100	PI23_CTD06_st11_NUT_6
21/11/23	11	80	PI23_CTD06_st11_NUT_7/8/9
21/11/23	11	50	PI23_CTD06_st11_NUT_10
21/11/23	11	25	PI23_CTD06_st11_NUT_11
21/11/23	11	5	PI23_CTD06_st11_NUT_12
22/11/23	KM3	3272	PI23_CTD09_KM3_NUT_1
22/11/23	KM3	2600	PI23_CTD09_KM3_NUT_4
22/11/23	KM3	2000	PI23_CTD09_KM3_NUT_7
22/11/23	KM3	1500	PI23_CTD09_KM3_NUT_9
22/11/23	KM3	900	PI23_CTD09_KM3_NUT_11
22/11/23	KM3	500	PI23_CTD09_KM3_NUT_12
22/11/23	KM3	300	PI23_CTD10_KM3_NUT_1
22/11/23	KM3	110	PI23_CTD10_KM3_NUT_3
22/11/23	KM3	60	PI23_CTD10_KM3_NUT_4
22/11/23	KM3	35	PI23_CTD10_KM3_NUT_6
22/11/23	KM3	20	PI23_CTD10_KM3_NUT_9
22/11/23	KM3	5	PI23_CTD10_KM3_NUT_11
26/11/23	26	1971	PI23_CTD12_st26_NUT_1
26/11/23	26	1100	PI23_CTD12_st26_NUT_3
26/11/23	26	150	PI23_CTD12_st26_NUT_7
26/11/23	26	60	PI23_CTD12_st26_NUT_8
26/11/23	26	40	PI23_CTD12_st26_NUT_10
26/11/23	26	5	PI23_CTD12_st26_NUT_11
27/11/23	NK25	2200	PI23_CTD14_NK25_NUT_1
27/11/23	NK25	1500	PI23_CTD14_NK25_NUT_3
27/11/23	NK25	675	PI23_CTD14_NK25_NUT_5
27/11/23	NK25	400	PI23_CTD14_NK25_NUT_6
27/11/23	NK25	50	PI23_CTD14_NK25_NUT_10
27/11/23	NK25	5	PI23_CTD14_NK25_NUT_12

Table 3.1.3. Samples collected at each station and each depth level for nutrients analysis during Leg 1.

- DOC and CDOM samplings

Samples for dissolved organic matter (DOM) were collected directly from the Niskin bottles in 250 ml polycarbonate acid-washed bottles after 3 rinsing and immediately filtered with a

peristaltic pump through a 0.22 µm Sterivex-GV filter. Samples were collected at the following CTD stations: CTD_02, CTD_04, CTD_05, CTD_06, CTD_09, CTD_10, CTD_12, CTD_14 at all the depths, except some depths due to problems with sampling bottles. The filtered subsamples for dissolved organic carbon (DOC) and for chromophoric DOM (CDOM) were collected into 200 ml dark glass bottles and stored at 4°C until analysis. The measurements will be carried out in the laboratories of the Biophysics Institute of CNR in Pisa.

3.2. Challenges

Since the used Rosette system is vintage, the operation and closing of the bottles have been progressively improved. It was possible to replace the drainage neck of bottle 8, as well as the rubber bands of bottles 2, 5 and 11. The quality of sampling was not affected by these substitutions.

The altimeter mounted at the base of the Rosette allowed the detection of the seabed at approximately 40 m above it. This short distance highlights the importance of ensuring a good match between the winch length and the depth inferred by the CTD probe pressure sensor.

3.3. Recommendations

A new carousel system is under purchase as part of the resident equipment of the R/V Gaia Blu, it is the same brand and has the same dimensions of the system previously used on board the R/V Falkor. Concerns exist on the space availability in the Baltic Room of the vessel, dedicated to the launch and recovery of the DTC/Rosette system and maneuverability and safety of the operations in such a small space, especially during water sampling.

4. **Wet Lab**

4.1. Insights

- *Dissolved oxygen analysis*

In the wet-lab, oxygen samples were analyzed by automated Winkler titration (Fig. 3.1.1) with thiosulfate solution $Na_2S_2O_3$, this is done using a computer controlled potentiometric end-point titration procedure. To do so, an acid solution (Sulfuric acid) was added gradually to the sample to reduce the Manganese in Mn^{2+}. Once the titration finished, the thiosulfate volume was recorded.

A. **B.**

Figure 3.1.1. A. Dissolved oxygen samples (after 2-3 hours storage) and B. the Metrohm Winkler titration instrument used on board for the analysis.

- *Salinity analysis*

Samples were analyzed on board using the Guideline Portsal Salinometer (Fig. 3.1.2A). The salinometer was standardized prior to analysis using the IAPSO standard seawater. The batch number was P167 of the standard seawater samples with a K15 factor of 0.99988 and practical salinity of 34.995. Figure 3.1.2B shows an example of the salinity measurements from the CTD bottle file and the corresponding salinity values analyzed on board in red circles).

Figure 3.1.2B shows a vertical profile of salinity from the CTD derived bottle files (blue: primary sensor and green: secondary sensor), and the corresponding salinity water samples measured onboard (red circles).

A. **B.**

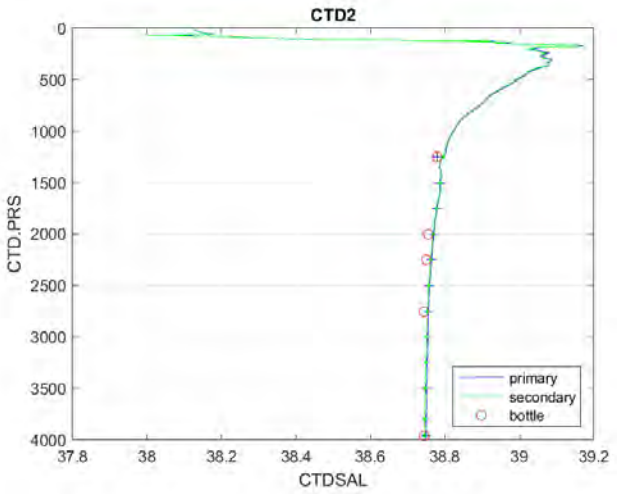

Figure 3.1.2. A. Portasal Salinometer on RV Gaia Blu, B. comparison between salinity values from the CTD sensors (primary in Blu and secondary in green) and the salinometer (in red circles).

A slope of 0.9997 was calculated and applied the CTD data to correct the bias in both sensors. The mean difference between precalibrated CTD-Salinity and BTL-Salinity was 0.0124 (primary sensor) and 0.0098 (secondary sensor). By applying the new slope, the average mean improved to be 0.0056 (primary sensor) and 0.0057(secondary sensor). The results are shown in the following plots.

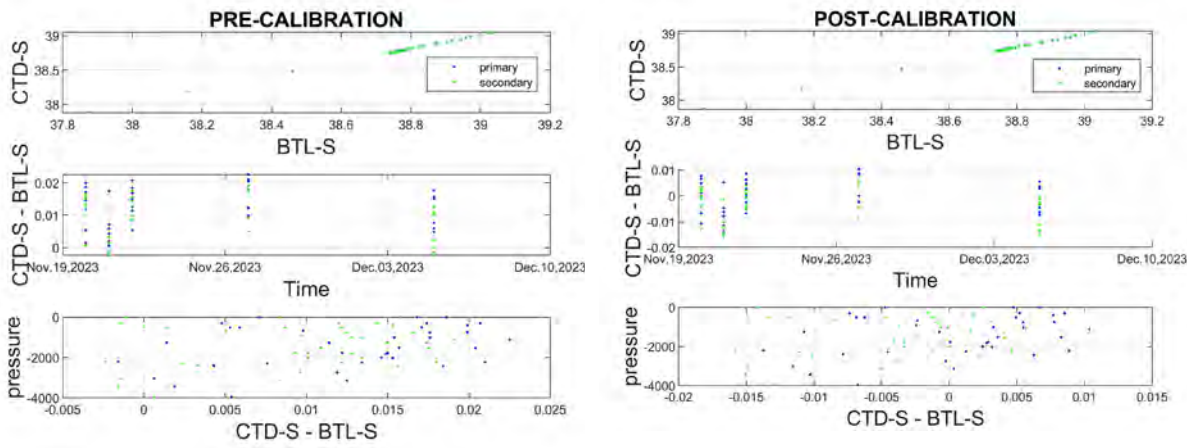

Figure 3.1.3. Scatter plot of CTD salinity and bottle salinity relation and vertical distribution of the difference between CTD salinity and Bottle salinity before calibration.

- *Water filtering for eDNA analysis*

During Leg 1, for each selected depth levels, several litres of seawater (maximum 10 litres) sampled via Niskin bottles at the CTD stations were filtered at the wet lab using a peristaltic pump. Sterivex filters with 0.22 µm pore size membrane were used. Thus, filters retaining environmental DNA were dried employing silica beads and stored at -80°C for further eDNA molecular analysis.

10 liters deep seawater sampled via Niskin bottles at the CTD stations (leg II) were filtered in the wet lab using a peristaltic pump equipped with a specific filter holder. Nitrocellulose (NC) filters with 0.45 um pore size membrane and 47mm diameter were used. Thus, filters retaining environmental DNA were dried employing silica beads and stored at -80°C for further eDNA molecular analysis. One water negative control (PI23_CTD_NC) was performed by fulfilling

one Niskin bottle with MilliQ water and collecting it using the same workflow used for seawater sampling downstream.

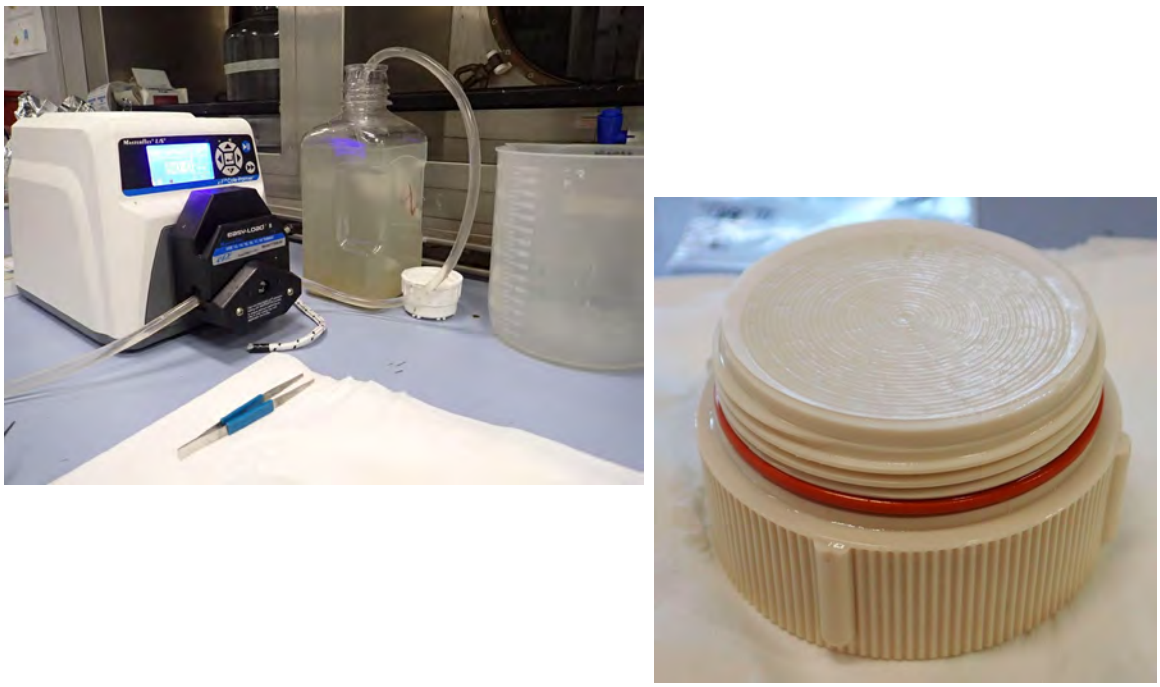

Figure 3.1.4. A. Filtration set-up. B. NC filter on the holder after 10L flow ready to be packed and stored at -80°C.

- *pH, Total Alkali (TA) and Dissolved Inorganic Carbon (DIC) sampling*

Water samples for pH and TA were taken from Niskin bottles at selected depths throughout the CTD transect during leg 2. Each aliquot has been collected within a 300 ml glass bottle with 50% overflow. 1 ml of $HgCl_2$ has been added in each bottle for fixation. Bottles have been then secured and stored in a box, shipped back to the laboratory and then analyzed in Trieste (ref. Carolina Cantoni).

DIC samples were taken from Niskin bottles at each depth for CTD stations 12 and 14 during leg 2. Each aliquot has been collected within a 50 ml glass bottle with 50% overflow. 0.25 ml of $HgCl_2$ has been added in each bottle for fixation. Bottles have been then secured and stored in a box, shipped back to the laboratory and then analysed.

- *Analytical protocols for DOM, CDOM, FDOM*

Dissolved Organic Carbon concentration will be measured by the Shimadzu Total Organic Carbon analyzer (TOC-L) by high temperature catalytic oxidation by following Santinelli et al. (2015, 2021). Samples will be acidified with HCl 2N and sparged for 3 minutes with CO2-free pure air, in order to remove inorganic carbon. Samples (150 µL) will be injected in the furnace (680°C) after rinsing with the sample three times. From 3 to 5 replicate injections will be performed until the analytical precision is lower than 1% (± 1µM). A five-point calibration curve will be done by injecting standard solutions of potassium hydrogen phthalate in the expected concentration range of the samples. At the beginning and end of each analytical day the

system blank will be measured using Milli-Q water and the reliability of measurements will be controlled by comparison of data with a DOC reference (CRM) seawater (Hansell, 2005).

Absorbance spectra of chromophoric DOM (CDOM) will be measured throughout the UV and visible spectral domains (230–700 nm) using a spectrophotometer UV-visible (Shimadzu UV-2600i), with a 10 cm quartz cell following Retelletti Brogi et al. (2022). For each sample 3 spectra will be measured. The absorption spectrum of Milli-Q water will be used as blank and subtracted from each sample spectrum. After the subtraction, the absorption coefficient at 254 nm (a_{254}) and the spectral slope between 275 and 295 nm ($S_{275–295}$) will be calculated by using the ASFit software (Omanović et al., 2019). a_{254} can be used to have semi-quantitative information on CDOM, whereas, the $S_{275–295}$ will be calculated in order to obtain indirect information on the average molecular weight and aromaticity of the CDOM pool. In addition, the absorption coefficient at all the wavelengths (between 230 and 600 nm), the indexes and the spectral slopes in different ranges can be calculated. These data can be also useful for satellite validation.

Excitation Emission Matrixes (EEMs) for the analysis of Fluorescent Dissolved Organic Matter (FDOM) will be obtained by using the Aqualog spectrofluorometer (HORIBA Jobin Yvon) with a 10 x 10-mm quartz cuvette following Bachi et al. (2023). This instrument uses a charge-coupled device to detect the signal, guaranteeing a high acquisition velocity and reduced photobleaching. The characteristics of the lamp improve the sensibility of data acquisition at low excitation wavelengths (250-350 nm) allowing a better identification of the protein-like fluorescence. Emission will be registered between 212 and 620 nm every 3.27 nm (8 pixels) with an integration time of 10 s. Excitation will range between 250 and 450 nm at 5 nm increment. EEMs will be corrected for instrumental bias. Rayleigh and Raman scatter peaks will be removed by using monotone cubic interpolation. The EEMs will be elaborated using the TreatEEM software (Omanovic Dario, TreatEEM-program for treatment of fluorescence EEMs, http://sites.google.com/site/daromasoft/home/treateem).

The EEMs will be normalized dividing the fluorescence intensity by the Raman band of Milli-Q water integrated between 371 and 428 nm (λEx = 350 nm). Fluorescence will be therefore reported in Raman Units (Lawaetz and Stedmon 2009).

PArallel FACtor (PARAFAC) analysis will be applied to EEMs measured by using the drEEM (decomposition routines for Excitation Emission Matrices) toolbox for MATLAB software (Murphy et al. 2013). The OpenFluor online database, a database of environmental fluorescence spectra, will be used as a validation tool to characterize the validated components (Murphy et al. 2014).

- *Phytoplankton pigments and particulate absorption*

For each measurement station, in-situ data for the determination of phytoplankton pigment concentration and algal and non-algal absorption coefficients (aphy and aNAP, respectively) were collected at several depths, based on fluorescence vertical profiles.

Sampling was performed by Niskin bottles mounted on a rosette sampler. Seawater was pre-filtered by a planktonic net with a mesh of 250 µm to eliminate the zooplankton component. Different water volumes, dependent on the water optical properties, were vacuum filtered

through Whatmann GF/F glass microfiber filter (nominal porosity 0.7 μm). Lastly, samples were stored in liquid nitrogen.

Regarding instruments and analysis methods, pigment concentrations (Chla and several accessory pigments commonly used to estimate phytoplankton size classes and functional types) will be estimated by High Performance Liquid Chromatography following standard protocols (Van Heukelem and Thomas, 2001) after a few weeks from sampling. Particulate absorption measurements will be carried out by a dual beam Spectrophotometer equipped with an integrative sphere, following reference protocols for Satellite Ocean Colour Sensor Validation (IOCCG, 2018) at the ISMAR laboratories in Rome.

Figure 3.1.5. Filtration apparatus for phytoplankton pigment concentration in the wet lab of the R/V Gaia Blu.

4.2. Challenges

Identified issues related to wet lab space and equipment are related to the difficulty of maintaining the temperature of the wet lab constant for the salinity analysis that requires a constant temperature for at least 12 hours prior to sample analysis using the portsal.

4.3. Recommendations

We strongly encourage the installation of at least one MilliQ water system, crucial for most if not all WetLab activities. All electrical plugs should be reconverted to a European (not American) standard (Schuko?).

For a full laboratory operability it is imperative that the laboratory must be left empty and clean after any use; this should be appropriately monitored by the ship crew.

It would be appreciated if the central bench would be equipped with drawers (10 to 15 cm high) allowing a better functionality of the table and still leaving enough space underneath the bench to place boxes and other bulky material.

All benches should be equipped with an easy-to-use system to ensure the instrumentation and the scientific equipment during navigation or rough sea conditions.

The installation of a second Wet Lab is strongly encouraged, to allow different activities to be carried out at the same time by a number of technicians and scientists, for example sediment treatment on one side and clean water analysis on the other. It is important that the second Wet Lab is equipped with a chemical fume hood, other than fresh and clean sea water outlets (from the ship bow). One possible location could be the hangar on the other side of the corridor right opposite the existent Wet Lab.

The doors should allow access to the laboratories without the need of using handles, as most of the time hands are used to carry samples and other equipment in and out of the Labs.

5. Dry Lab

5.1. Insights

The effective utilization of dry lab space and equipment concerned the Imaging Flow Cytobot, which can identify and count different species and groups of plankton using machine learning algorithms, some working stations and the pore water extraction, therefore currently this space should be re-thinked in terms of use and destination.

5.2. Challenges

The dry lab is currently an empty space that could be better organized with a division between electronic devices and other operations. When not in use for scientific activities, the dry lab desks can be used to provide suitable workstations to researchers onboard and therefore more chairs are needed.

5.3. Recommendations

The purchase of some additional chairs is recommended.

6. BioGeoChemical-Argo float deployment

6.1. Insights

During the PIONEER2023 cruise, the first BGC-Argo autonomous float (WMO 2903797) of CNR ISMAR has been successfully deployed from the winch astern of the R/V Gaia Blu (Figure 5.1.1). The float model was a JUMBO PROVOR CTS5 (NKE Instruments, France) equipped with sensors: CTD (Seabird SBE41-CP) for Temperature, Salinity and Pressure; Dissolved Oxygen (Aandera Optode 4330); Phytoplankton chlorophyll, optical backscattering at 700 nm and CDOM - coloured dissolved organic matter (Seabird/WetLABS ECO3); Downwelling irradiance at 4 bands (Seabird/Satlantic OCR-504); Zooplankton communities and particle size distribution within the range 50-2580 □m (Hydroptic UVP-6). This float is a

contribution to the ARGO-Italy program and the European Research Infrastructure EURO-ARGO ERIC.

Figure 5.1.1. Deployment of the CNR ISMAR BGC-Argo float from the R/V Gaia Blu. Photo credits: Simone Ridolfi Bristol (CNR ISMAR).

The float was deployed in the Ionian Sea at Station 3 (35.86°N, 17.80°E) on November 20th, 14:40 UTC. The float mission was set to passivily drift at a parking depth of 1000 dbar and to profile between 0-2000 dbar every 18h on the first two days from deployment, and then every 24h with surface time around local noon. Deployment location, float trajectory and the first 4 profiling sampling stations are shown in Figure 5.1.2.

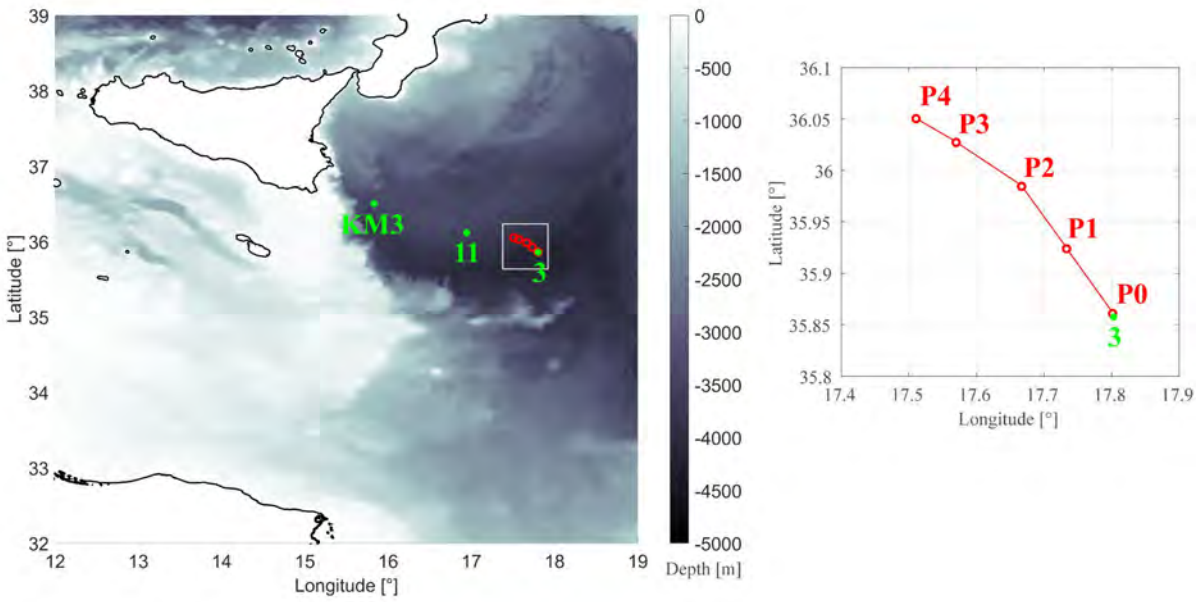

Figure 5.1.2. BGC-Argo deployment location and trajectory. P0 indicates the deployment site; P1-P4 indicates the four stations where the float acquired 0-2000 dbar profiles. Left panel: hydrological stations 3, 11, and KM3 are reported.

The float successfully transmitted, via iridium satellite communication, the data acquired. Examples of T-S plots, profiles of biogeochemical variables and Particle Size Distributions obtained at profiling stations P1-P4 are reported in Figure 5.1.3, 5.1.4, 5.1.5 respectively.

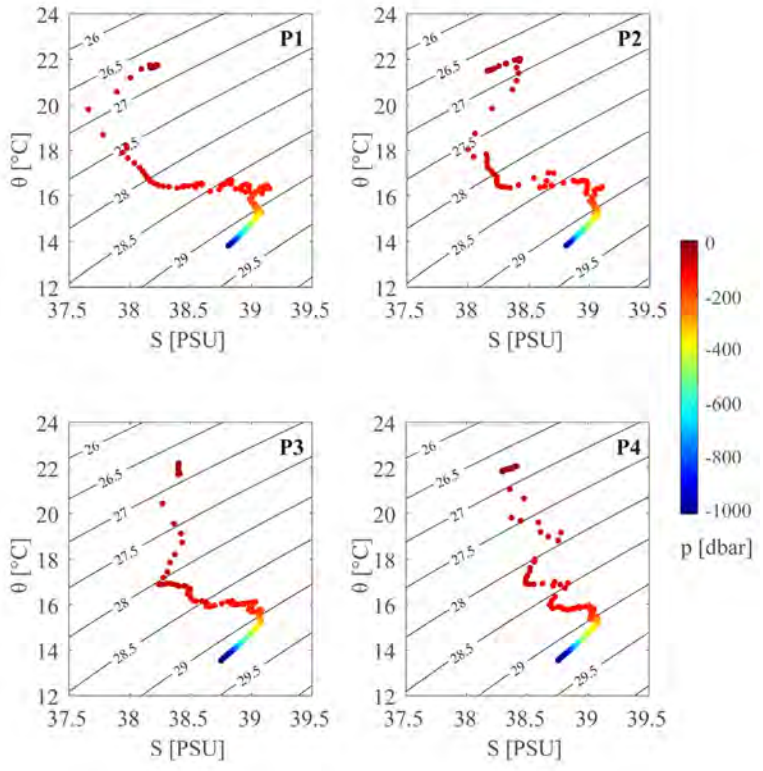

Figure 5.1.3. T-S plots acquired by the BGC-Argo float at P1-P4 profiling stations (21-24/11/2023).

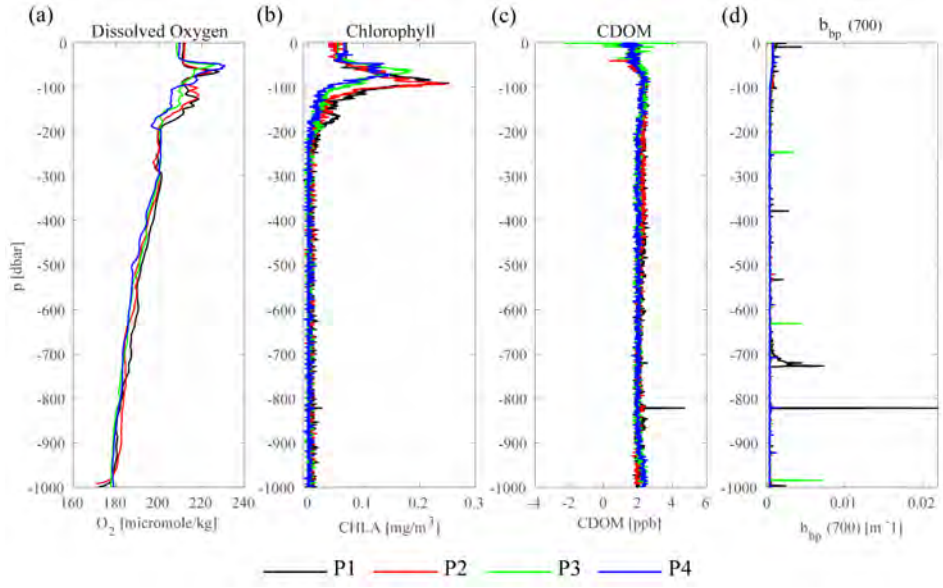

Figure 5.1.4. 0-1000 dbar profiles of dissolved oxygen, phytoplankton chlorophyll, CDOM and optical backscattering acquired by the BGC-Argo float at P1-P4 profiling stations (21-24/11/2023).

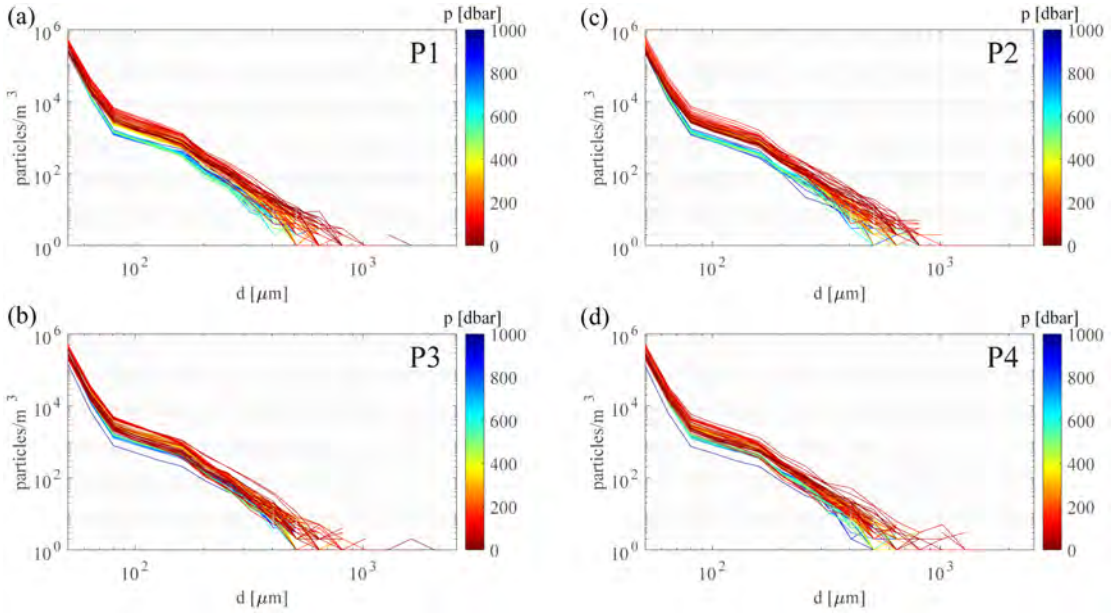

Figure 5.1.5. 0-1000 dbar Particle Size Distributions acquired by the BGC-Argo float at P1-P4 profiling stations (21-24/11/2023).

The float trajectory and collected data can be monitored at https://fleetmonitoring.euro-argo.eu/float/2903797. Data are distributed in open access.

6.2. Challenges

None. The R/V Gaia Blu is fully suitable for the deployment of BGC-Argo floats in open seas.

6.3. Recommendations

The R/V Gaia Blu needs to be tested for BGC-Argo float recovery in the near future.

7. Microstructure Profiler Operations

7.1. Insights

A modified version of the MSS090L (serial number No. 069, operated by CNR-ISMAR) produced by Sea & Sun Technology GmbH was used to collect microstructure observations during the PIONEER 2023 cruise. A detailed description of the MSS90L general characteristics, features and operational modes can be found in Prandke et al. (2000). A microstructure profiler is essentially a CTD probe equipped with two shear sensors, a fast thermistor and 3 optical sensors (oxygen, chlorophyll and turbidity). The probe is designed to reach 3000 m but the oxygen sensor operational depth is up to 2000. The deployments during PIONEER 2023 were further limited by a winch cable length of 1300 m.

The probe was installed on the aft deck with a bracket built on board and secured to the deck using two bolts (Fig. 6.1.1) . The set was very stable and efficient.

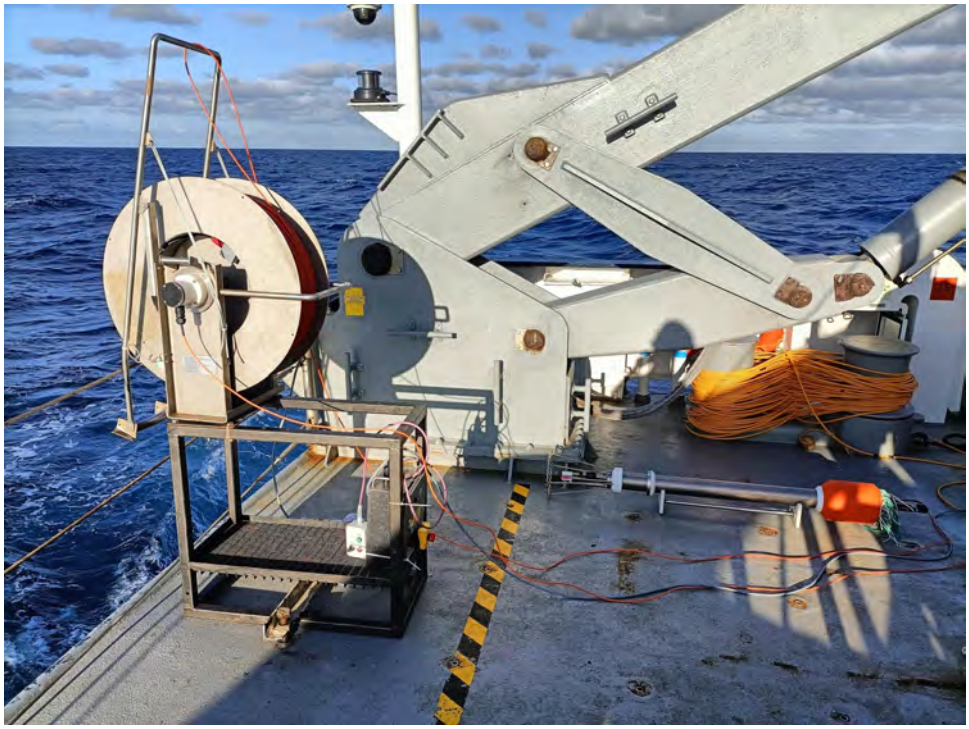

Figure 6.1.1. Microstructure profiler installed on the aft deck of the R/V Gaia Blu.

7.2. Challenges

During deployment the ship should drift away at the slowest possible speed to move away from the free sinking cable. Out of 13 casts just in three cases the ship was able to move slower than 1nm. Even if this is mostly due to the weather conditions (wind and waves) a ship this size should be able to move less than 1nm in operational conditions.

Moreover the lighting of the aft deck is not sufficient, especially when the A-Frame is retracted over the deck at night; in this configuration the water behind the ship is completely dark. We had to use a torchlight to be able to see the free sinking cable.

7.3. Recommendations

Review the lighting plan for the aft deck.

8. **Plankton Net and eDNA Operations**

8.1. Insights

During the PIONEER2023 cruise, a WP2 Closing Net, which is a vertical plankton net with a mesh size of 200 µm and a messenger-operated closing mechanism, was successfully deployed from the winch "astern-left" of the R/V Gaia Blu (Fig. 7.1.1).

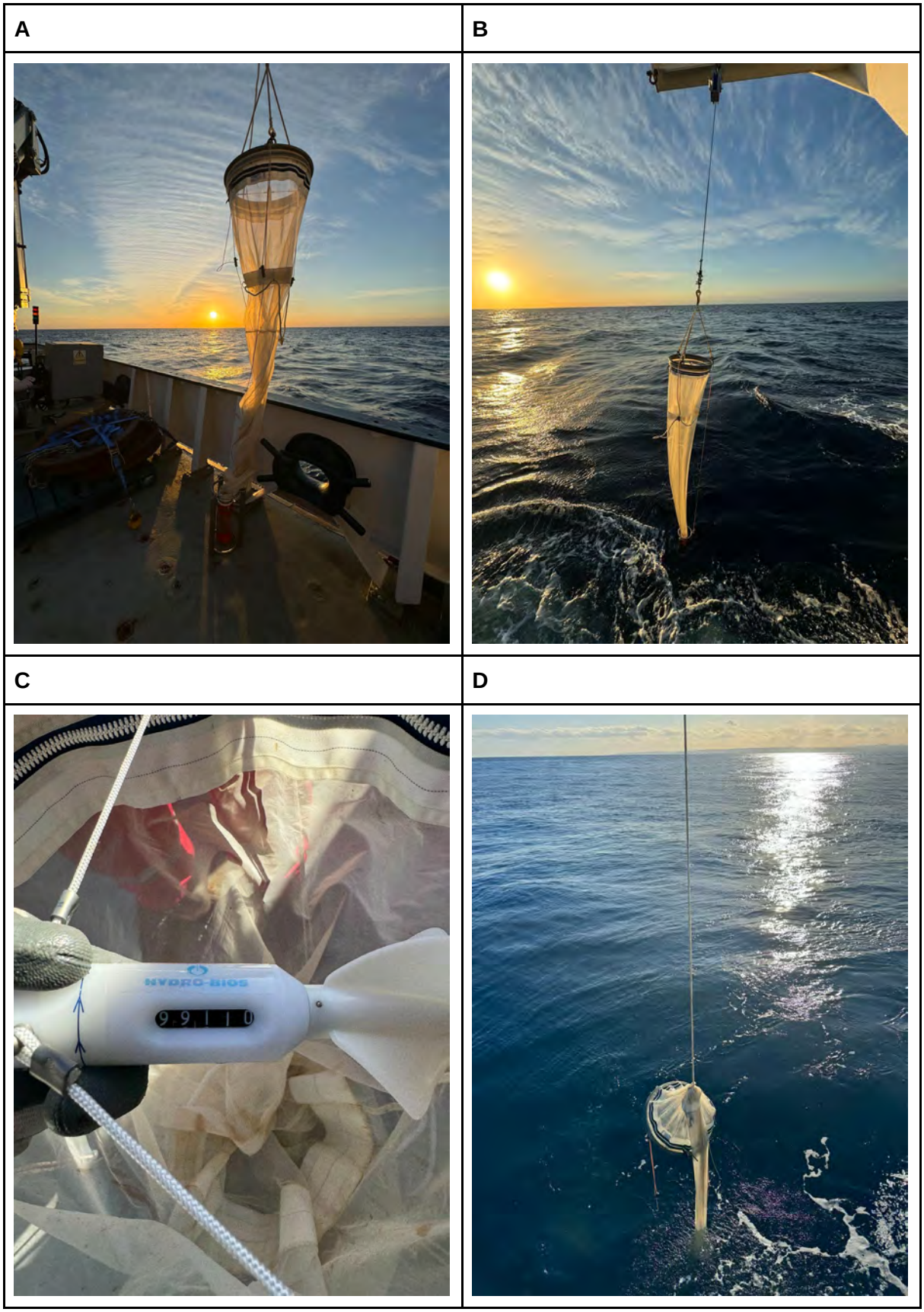

Figure 7.1.1. A-B. WP2 Closing Net sampling. C. Mechanical Flow Meter. D. Strangled Net in order to sample defined depth layers.

The purpose was to investigate the processes of physical-zooplankton-carbon dynamics interactions with links to the deep sea and connectivity. The net samples will be used for morphological microscopy identification and molecular identification via bulk-sample metabarcoding, which will be compared to traditional analysis of samples using a microscope.

The open net was taken to the greatest scheduled depth of 500 m. During the ascent, the net has been closed at intended depths by strangling the net bag below the net ring (Fig 9.1). This enabled the sampling of defined depth layers (see Table 9.1). The WP2 lock screen was used in conjunction with a Mechanical Flow Meter with a back-run stop to measure the filtered water volume (Fig. 7.1.1). At the end, the sample was divided into two halves, one for molecular analyses (metabarcoding), the other for classic taxonomic analyses (morphological) (Fig. 7.1.1, Tab. 7.1.1). WP2 Closing Net was used in 4 sampling stations during Leg 1 (Fig. 7.2.2).

Date	Station	Depth range (m)	Metabarcoding analyses	Morphological analyses
21/11/2023	11	0-100	*	*
21/11/2023	11	100-300	*	*
21/11/2023	11	300-500	*	*
22/11/2023	KM3	0-130	*	*
22/11/2023	KM3	130-200	*	*
22/11/2023	KM3	200-500	*	*
26/11/2023	26	0-100	*	*
26/11/2023	26	100-200	*	*
26/11/2023	26	200-500	*	*
27/11/2023	NK25	0-100	*	*
27/11/2023	NK25	100-300	*	*
27/11/2023	NK25	300-500	*	*

Table 7.1.1. Samples collected at each station using WP2 Closing Net during Leg 1.

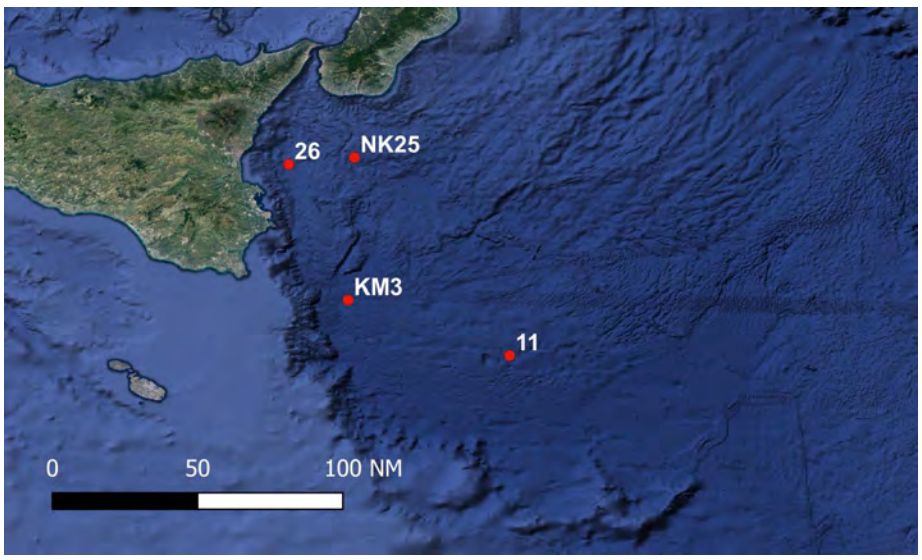

Figure 7.2.2. Sampling station explored with WP2 Closing Net during Leg 1.

At the same sampling stations, water samples have been collected at discrete depths using the CTD-Rosette, as reported in paragraph 3.1. These water samples will be used for molecular identification via eDNA metabarcoding and will target groups such as bacteria, phytoplankton, microzooplankton, and large metazoans.
These studies, which combine various traditional and modern techniques, serve as prototypes for a global integrated approach and demonstrate that the oceanographic and biological research community, but also geological one, can work together. By combining nets with images obtained from the Underwater Vision Profiler (UVP6), data from turbulence profiles, and eDNA analysis, we can gain innovative insights into zooplankton community structure at finer scales over larger distances and investigate vertical small-scale physical processes related to zooplankton vertical migration.

8.2. Challenges

The deployment system of the instrument may be suitable, and the operations proceeded smoothly. However, it is noted that the winch and portal are poorly positioned as they are located near the stationary propeller. This causes the disruption of the water column in the first few meters (which may alter the water column structure) and the presence of air bubbles.

The meteo-marine conditions did not allow sampling with the net in station 3 (20/11/2023) and in station 26 (26/11/2023) the second CTD lowering was carried out at too great a time distance compared to the first.

8.3. Recommendations

It is suggested to have greater maneuverability on the starboard side by using the CTD winch to deploy other instruments, with the need for enlarging the designated area. The addition of a seawater and freshwater inlet in the CTD compartment will be necessary.

Winch: A meter pulley and precise speed adjustment are required for the winch. It should be operable from both the stern and the control room. A cable with a minimum length of 3000 m is needed.

Stern deployment: For deployments from the stern, a controlled cable of at least 3000 m is necessary.

9. **Sediment Sampling Operations**

9.1. Insights

Sediment sampling was completed using a: i. oceanic box-corer lowered from aft using the multi-purpose winch, ii. a gravity/piston corer lowered from the side using the dedicated winch; iii. a SeaWater corer lowered from stern using the multipurpose winch.

The box corer is designed to collect undisturbed sediment samples from marine seafloor. The oceanic box corer used during this cruise had a cylindrical sampler with a diameter of 32 cm and cylinder height of 52 cm (sampling area of 804.2 cm2 and sampling volume of 42 liters). The corer consists of a sample box mounted on gimbals, and a spade assembly. The box corer is lowered onto the seabed on a wire at a controlled rate until its frame rests on the bottom. The sample bucket is forced into the sediment by the weight of the corer. As the corer

is slowly pulled out of the sediment, a mechanism allows two spades to swing below the sample box sealing in the sediment. Simultaneously, spring-loaded flaps above the sample box are closed to prevent the sample from being disturbed during recovery.

A	B
	
C	**D**
	

Figure 8.1.1. A. Equipment of the box corer on the aft deck of the RV Gaia Blu. B. Triggering of the release mechanism. C. Launch of the box corer. D. Lowering overboard of the box-corer.

Gravity and triggered piston cores used the same system on board Gaia Blu (Figure 8.1.2), which is basically composed of: 1. a coring head providing the necessary momentum to the

device for penetration. 2. Steering yellow fins designed to maintain the vertical position of the device during free fall. 3. A stainless-steel 5 m long barrel, several sections (85 kg) can be used to compose a 5 to 15 m (potentially 25 m) barrel. 4. A PVC 100 mm diameter liner placed inside the barrel to collect the sediment core. The lowermost part of the barrel is reinforced by a core nose, which ends with a cutter shoe, designed to ease core penetration and includes a core catcher, designed to hold the sediment into the liner when the core is pulled out of the seabed. To reduce friction, a cutting shoe in ertalyte is also provided for advanced coring operations. In very soft muddy sediment, this tool gives high recovery and minimum disturbance of the sample.

The core barrel is mounted on a truss system (white framework), which extends over one meter from the starboard side of the vessel, the coring head is hosted in a cradle system. The launching operation is carried out by means of the combination of a winch and a crane, which allows the framework to be rotated 90° degrees before lowering in the water. This is a very complex system, designed and adapted in narrow spaces that required some important refitting of the original structure of the ship.

A	B
	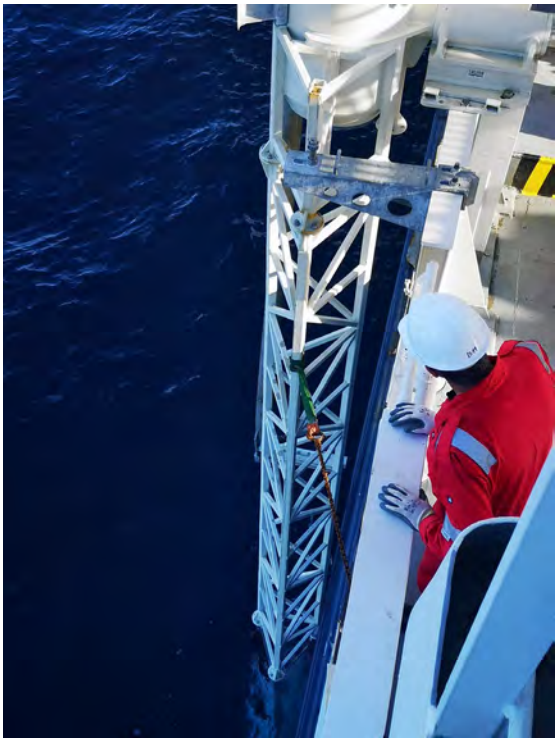
C	D

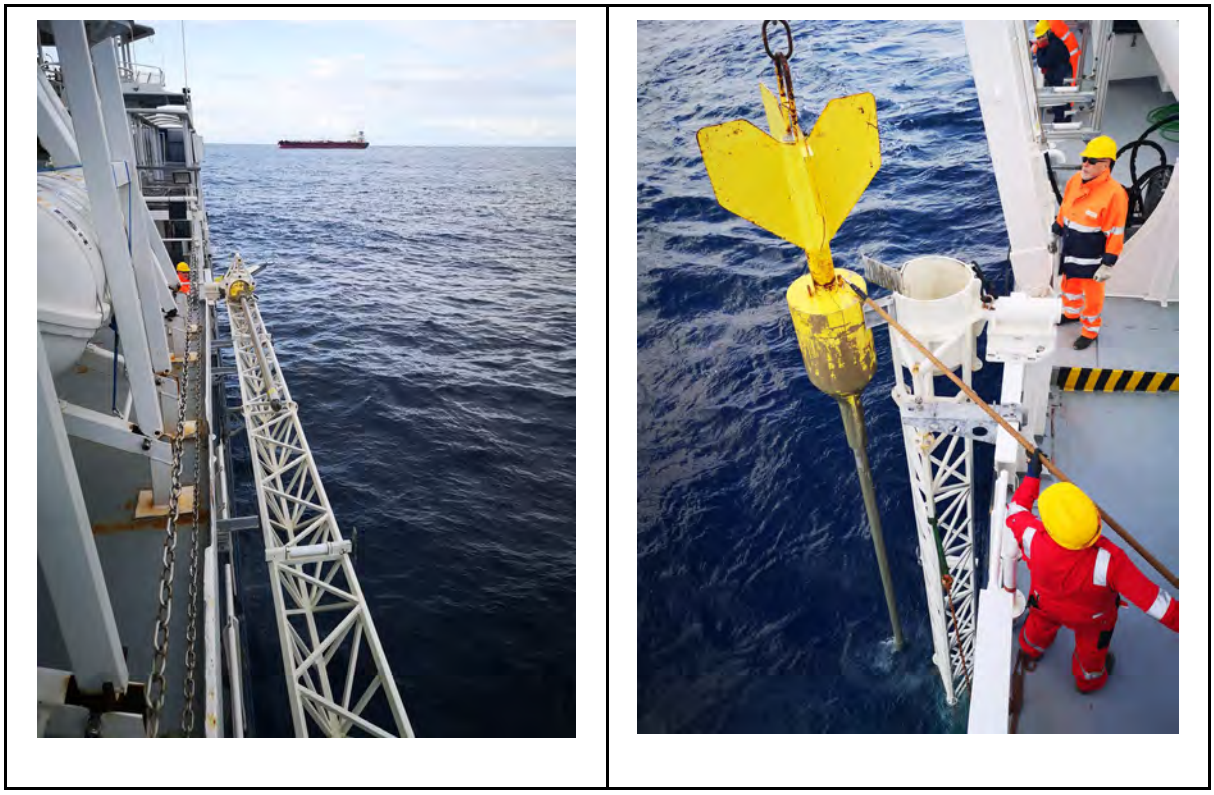

Figure 8.1.2. Details of the sediment coring system mounted on board the R/V Gaia Blu. A. close view of the coring head and the cradle. B. The framework displayed in its vertical position ready to be lowered in the water. C. The framework in its horizontal position during navigation and sampling of the core. D. Recovery of the core barrel.

The Triggered Piston Corer can be set on variable lengths, total weight and piston configuration, according to the predicted lithology of the target site. In addition to the specifications of the gravity corer, the piston has few options: 1. The piston which is meant to remain steady relative to the downgoing core barrel creates a suction that helps the penetration of sediment into the liner. To be more effective, the piston, which has adjustable plastic o-rings on its outside, contains 16 adjustable pressure valves that control the water flow through it and therefore limit the rate of suction avoiding the implosion of the liner. 2. The triggering mechanism is constituted by a 100-cm iron releaser, adjustable releaser weights (17 kg each, up to a total weight of 122 kg) and trigger iron cables of different lengths, adjustable on the base of the barrel length and the chosen free-fall height from the seabed.

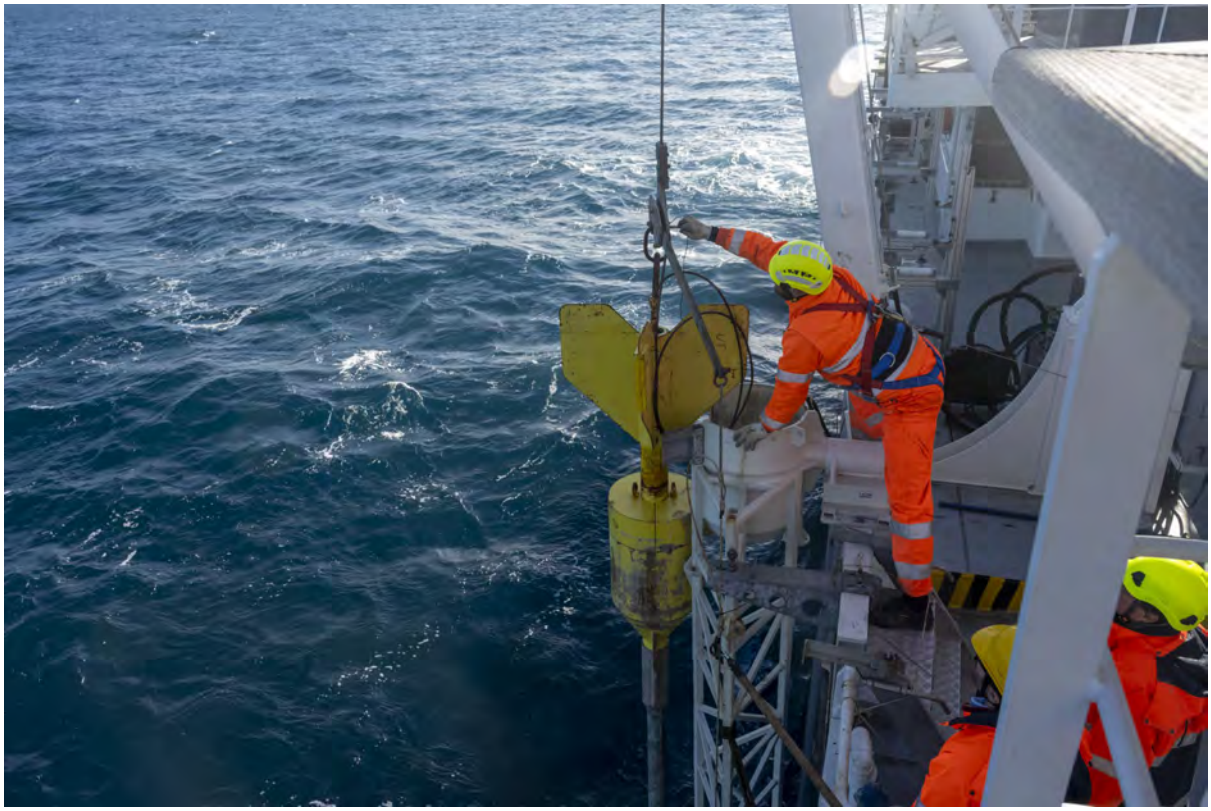

Figure 8.1.3. Triggering of the release mechanism of the piston coring system. This procedure will be soon changed with a safer activation from the deck.

The SW-104 is a light corer, 100 kg maximum, designed with the purpose of recovering cores of clayey or slightly sandy sediments with maximum reduction of disturbance of the core, in particular on top and recovery ratio of the penetration close to 100%. The Core Tube is made up of a thin tube of stainless-steel ø 114.3 mm, 1.5 mm thick, long 2008 mm (maximum length), 1354 mm or 654 mm (minimum length). It supports a transparent liner (110 mm diameter, 3 mm thick) that contains the sediment core and bottom water sample by way of a lower barrier in the form of a duck closing device and an upper water-containment valve. The load-bearing lattice, one with the core tube, consists of the arming, closure and recovery mechanisms; in addition it supports the dead weight made up of masses from 17 kg to 100 kg. The gravity corer SW-104 is equipped with an aluminum service tripod: a variable-tilt carrier can hold the corer in a vertical position or at different angles to optimize on-board operations on the corer itself or on the recovered sample. The best technique is using gravity speed controlled/reduced by a winch.

A

B

Figure 8.1.4. A. Preparation of the SW-104 corer on the aft deck of the R/V Gaia Blu. B. Equipment of the release mechanism of the SW-104.

During Leg 1, 2 box-cores (1 failed) and 7 gravity cores (2 failed) have been lowered at depths ranging from ca. 2000 m to 3500 m bsl. During Leg 2, 17 box-cores (4 failed), 3 gravity cores, 4 piston cores and 1 SW core have been retrieved. Each sample has been subsampled according to different objectives and analysis to be carried out at onshore laboratories. Most of the sediment cores, collected on inferred extreme environments, have been sampled for biological purposes at their bottom and at the top of each section before being closed. Pore water has been extracted onboard on two cores (PI23_GC08 and PI23_GC09).

Sediment cores PI23_GC03, PI23_GC04 (Station 11) and PI23_PC10 (Station 44), targeting paleoclimatic studies, have been collected at 3434 m bsf, 3492 m bsf and 370 m bsf in the Ionian basin and the Gulf of Taranto, respectively. They have been half splitted and measured for petrophysical and chemical properties (magnetic susceptibility, resistivity, natural gamma ray, P-wave velocity, colour, XRF) in the laboratories of ISMAR-Napoli. Gravity cores GC03 and 04 recovered ca. 1.35 m and 5.15 m of sediments and their lithology is mostly represented by hemipelagic muds, frequently interrupted by turbidites and tephra layers. A dark-gray thick deposit, likely interpreted as sapropel S1, also occurs in both records. The PI23_PC10 record is 8.29 m long and it is mostly characterized by olive gray homogenous mud with rare visible sedimentary structures. These successions will be sampled at 1 cm- step and analyzed with an integrated stratigraphic approach including sedimentology, micropaleontology, tephrochronology, organic and isotope geochemistry.

Figure 8.1.5. Photo of the PI23_GC04 sediment core, collected in the deep Ionian Basin, is characterized by the alternation of turbidites, tephra layers and hemipelagic deposits.

All remaining cores have been scanned for X-Ray Fluorescence (Avaatech XRF core scanner major and trace element countings) and magnetic susceptibility, opened, processed and sub-sampled in the laboratories of ISMAR-Bologna according to their specific scientific objectives.

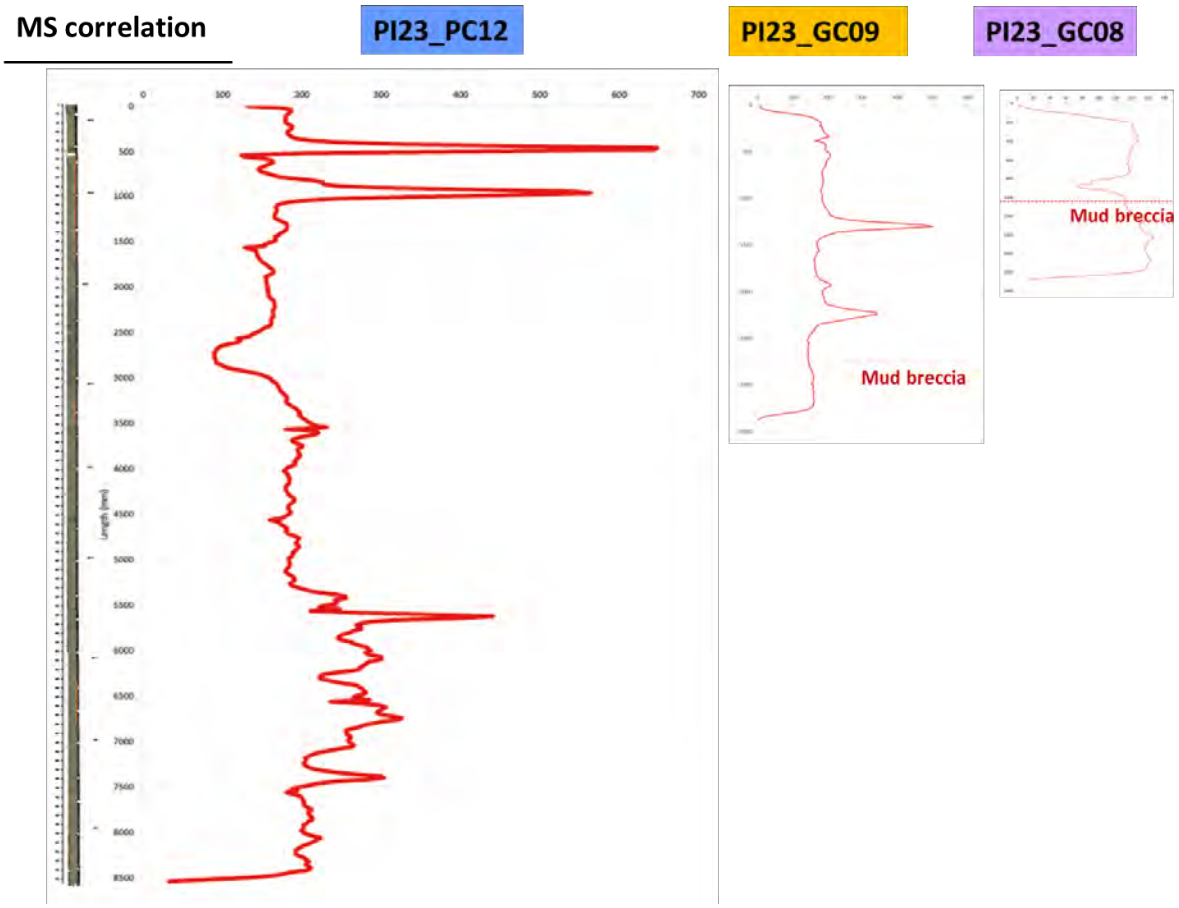

Figure 8.1.6. Example of magnetic susceptibility measured on three sediment cores (PI23_GC08-09-PC12) collected along and outside a seepage structure in the northern Ionian Sea at the boundary with Gulf of Taranto. Tephra layers are present in the upper sedimentary sequence.

- *Pore water analysis*

The sampling of porewater consists of extracting small quantities of interstitial water present in core samples. During the PIONEER cruise, several aliquots of pore water were extracted from the core sections, specifically from samples PI23_GC08 and PI23_GC09. Pore water sampling was conducted using rhizons and syringes, positioned approximately every 20 cm along the core sediment. These aliquots are used for the determination of some sulfates, sulfides, Cl, Br, DIC. Additionally, two aliquots (top and bottom of the PI23_GC08 core sediments) were collected in the glass vials, and immediately crimped, for the analysis of methane in the head-space.

Figure 8.1.6. Pore water sampling performed in the dry lab on board R/V Gaia Blu.

The box-corers have been sampled for several purposes such as stratigraphy, chronology, biology, microplastic, bisphenol, organic and inorganic contaminants and foraminifera (Tab. zz). Particularly, Taranto Valley stations were sampled for replicate samples.

Leg	Coring sequence	Gear Type	Station	Site	Depth (m)	Penetration (m)	Recovery (m)	Fall (m/min)	Pull (t)	Subsampling/notes
1	PI23_GC01	Gravity, 5 m	22	Diapir	1980	4	3.25	60	4	Biology on top and bottom each section
1	PI23_GC02	Gravity, 5 m	25	Diapir	2070	2	0	60	4	Incorrect placement of core nose
1	PI23_GC03	Gravity, 10 m	11	Paleo	3508	1.7	1.7	60	NN	Biology on top and bottom each section
1	PI23_GC04	Gravity, 10 m	11	Paleo	3523	10	5	60	5.7	Biology on core nose/catcher
1	PI23_GC05	Gravity, 10 m	34	Diapir	2200	10	3.7	60	NN	Biology on top and bottom each section
1	PI23_GC06	Gravity, 5 m	26	Diapir	2050	1	1	120	NN	Barrel damaged due to hard bottom, bad target
1	PI23_GC07	Gravity, 5 m	29	Diapir	2448	> 5	5	60	4.2	Biology on top and bottom each section
2	PI23_GC08	Gravity, 5 m	50	Seepage	607	4.5	1.9	30	2.7	Biology on top and bottom each section

2	PI23_GC09	Gravity, 5 m	69	Seepage	612	5.4	3.3	60	3.2	Biology on top and bottom each section
2	PI23_PC10	Triggered piston, 10 m	44	Paleo	370	10.5	8.3	20	NN	Biology on core nose/catcher, top section
2	PI23_SW11	SW104, 1 m	44	Paleo	369	1	1	20	NN	Biology on core top section
2	PI23_PC12	Triggered piston, 10 m	69 bis	Seepage	590	11	8.5	60	3.8	Biology on core nose/catcher, top section
2	PI23_GC13	Gravity, 5 m	biocostriuzioni	Bioconstruction	160	3	2.8	60	3.9	Biology on core nose/catcher, outer barrel
2	PI23_PC14	Triggered piston, 10 m	45	Contourite	200	11	8.5	60	4.07	Biology on core nose and loose top
2	PI23_PC15	Triggered piston, 10 m	48	Contourite	712	11	8.5	60	3.78	Biology on core nose and loose top

Table 8.1.1. List of gravity and piston core samples during the entire duration of the PIONEER cruise.

Leg	**BC sequence**	**Station**	**Site**	**Depth (m)**	**Height BC (m)**	**Subsamples (stratigraphy, m)**	**Subsamples (chronology, m)**	**Subsamples (biology)**	**Susamples (microplastics)**	**Subsamples (bisphenol - IPA)**	**Subsamples (inorganic elements)**	**Subsamples (organic contaminants)**	**Subsamples (foraminifera surface 0-0.5 cm)**
1	PI23_BC01	KM3	Water	3330		1 core	1 core	0-3 cm 6 falcon, 3 meio cores	0-3 cm remaining surface	from microplastics sample			
1	PI23_BC02	26	Diapir	1990	0 failed possibly for incorrect activation or slope seabed								
2	PI23_BC03	50	Mud pool central	609	0.40	1 core (0.40)	1 core (0.40)	0-3 cm 6 falcon, 3 meio cores	0-3 cm remaining surface	0-0.5 cm (1 falcon BpA)			
2	PI23_BC04	69	Mud pool border	613	0.40	1 core (0.40)	1 core (0.40)	0-3 cm 6 falcon, 3 meio cores	0-3 cm remaining surface	0-0.5 cm (1 falcon BpA)			
2	PI23_BC05	44	Reference point outside Taranto Valley	368	0.40	1 core (0.40)		0-3 cm 6 falcon, 3 meio cores	0-3 cm remaining surface,	0-0.5 cm (1 falcon BpA)	0-3 cm	0-3 cm	
2	PI23_BC06	44	Reference point outside	368	0.40		1 core (0.40)		1 stainless steel core (0.40 m)	0-0,5 cm (2 falcon)	1 core (0.40 m)	1 core (0.30 m)	15 ml falcon

			Taranto Valley										
2	PI23_BC07	44new	pockmark Amendolara	281	> 0.55 failed								50 ml falcon
2	PI23_BC08	44new	pockmark Amendolara	281	> 0.55 failed								
2	PI23_BC09	44new	pockmark Amendolara	281	0.40 - 0.45	1 core (0.342)	1 core (0.38)	0-3 cm 6 falcon, 3 meio cores	0-3 cm	0-0.5 cm (2 falcon)			
2	PI23_BC10	75	Taranto Valley	1008	< 0 failed possibly for incorrect activation								
2	PI23_BC11	75	Taranto Valley	1008	0.37			0-3 cm 6 falcon, 3 meio cores	0-3 cm	0-0.5 cm (2 falcon)	0-2 cm	0-2 cm	
2	PI23_BC12	75	Taranto Valley	1008	0.47	1 core (0.395)	1 core (0.47)				1 core (0.435)	1 core (0.445)	50 ml falcon
2	PI23_BC13	76	Taranto Valley	1208	0.30				0-3 cm	0-0.5 cm (2 falcon)	0-2 cm	0-2 cm	
2	PI23_BC14	76	Taranto Valley	1208	< 0 failed possibly for incorrect activation								
2	PI23_BC15	76	Taranto Valley	1207	0.355	1 core (0.32)		0-3 cm 6 falcon, 3 meio cores				1 core (0.35 m) + 0-2 cm (lpa)	15 ml falcon + 15 ml falcon
2	PI23_BC16	77	Taranto Valley	1708	0.36	1 core (0.356)		0-3 cm 6 falcon, 3 meio cores				1 core (0.34.5 m)	50 ml falcon
2	PI23_BC17	77	Taranto Valley	1708	0.377				0 - 3cm	0-0.5 cm (2 falcon)	0 - 2cm	0-2 cm	
2	PI23_BC18	80	Taranto Valley	2592	0.43				0 - 3cm	0-0.5 cm (2 falcon)	0 - 2cm	0-2 cm	
2	PI23_BC19	80	Taranto Valley	2592	0.355	1 core (0.353)		0-3 cm 6 falcon, 3 meio cores				1 core (0. 357)	50 ml falcon

Table 8.1.2. List of box-corer samples and their use.

- *Box-corer subsampling strategy*

A	B
	
C	**D**
	

Figure 8.1.7. A. Box corer ready for operations. B. Collection of sediment from outside the cylinder of the box corer for experiments to be conducted on the bulk component. C. Precautionary protection of the sediment from atmospheric input (e.g. microplastics) before sub-sampling D. Box-coring team.

- *Water filtering and sediment collection for eDNA analysis*

Two liters of seawater were first collected from the bottom water on the top of box corer and filtered in the wet lab using a peristaltic pump equipped with a specific filter holder. To retain the environmental DNA, 0.45 um pore size nitrocellulose (NC) membrane filters of 47 mm diameter were employed then dried in silica beads and stored at -80°C for eDNA analysis.

Figure 8.1.8. A. Seawater collection from the box corer and B. falcon tubes filled with sediment.

Moreover, six 50 ml tubes were filled up with 0-3 cm layer sediments and stored at -80°C for further environmental DNA molecular analysis to couple with water genetic information.

- *Core sampling for Chronology and Stratigraphy*

Two plastic liners with diameter of 9 cm have been used to collect the sediment thickness with the care of minimizing the sediment compaction and deformations of the sub-surface stratification. Successively, liners were closed with plastic stoppers and stored in the fridge at 4°C. A total of 9 and 4 stations were collected for stratigraphy and chronology purposes, respectively (see Table 8.1.2).

Figure 8.1.9. Liner for stratigraphy and 3 small cores for meiofauna sampling.

- *Core sampling for meiofauna analysis*

Three rigid plastic pipes with a diameter of 3.6 cm have been randomly inserted to collect sediment cores replicates. The extrusion followed: sediment was gently pushed out from the tubes to save in jars the upper layer (0-3 cm) and covered with 40 ml of 70% ethanol tainted with Bengal Rose.

A	B
	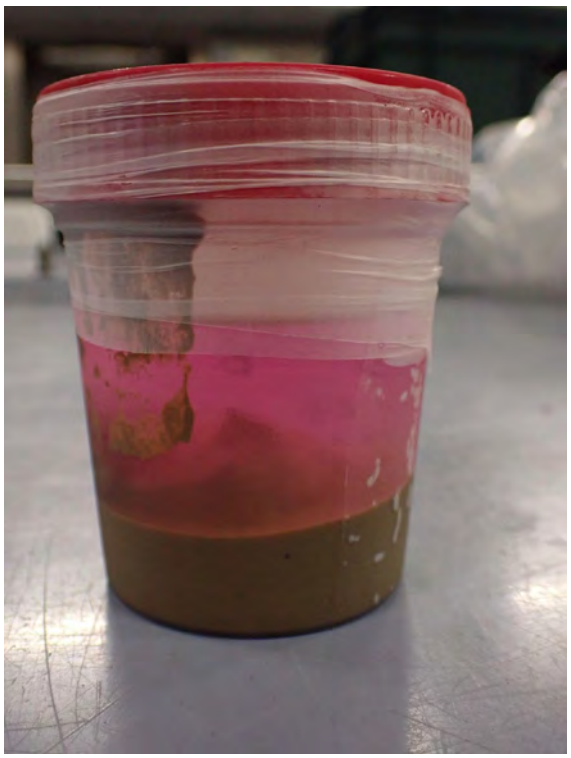

Figure 8.1.10. A. sediments with liner. B. Meiofauna sample.

- *Microplastics sampling*

Aliquots of superficial sediment (0-3 cm) were sampled from the box corer for microplastic extraction, analysis and quantification. Once on board the box corer sample was immediately covered with aluminium foil to prevent external contamination. Aerial controls to measure external contamination levels were performed by exposing a clean filter to the open air during sampling procedures on deck. Varying aliquots of superficial sediment (½, ⅓, ¼ of sampling surface) were collected using a ruler and a metal spoon. The samples were immediately transferred in aluminium containers and stored frozen at -20 °C. In total, 9 surface sediment samples were collected during the PIONEER cruise and transported to the microplastic laboratory of ISMAR Lerici for subsequent processing and microplastic analysis (particle extraction through density separation, organic matter digestion and µFTIR analysis for polymer identification). One sediment blank (PI23_BC05) was collected from the deepest part of the box-corer (in pre-industrial era sediments) using the same procedure used for sampling surface sediments. Station 44 (PI23_BC06) was sampled using a 0,4 m stainless steel liner (inner diameter 8,5 cm). The core was sliced in 48 samples. The first 10 cm of the core were

sliced every 0,5 cm, then one slice per cm was collected in a separate aluminum container until the end of the core. Lastly, 5x10L buckets were filled with sediments collected from samples PI23_BC03, PI23_BC04, PI23_BC05, PI23_BC07, PI23_BC08. These samples were kept oxygenated with an aquarium air pump and stored in the fridge. Sediments will be used in the laboratory to conduct experiments for the projects PRIN 2022 MICROBEEF (MICROplastic effects on marine Benthic Ecosystem Functioning) and DeepDeg (Development of a reliable system to assess biodegradation of different materials in the European deep sea).

- *Contaminants sampling*

Aliquots of superficial sediment (0-0.5 cm) were sampled from the box-corer for bisphenol and PAHs analysis. The samples were collected with a metal spoon in a glass tube and immediately stored frozen at -20°C. In total, 9 bisphenol and 6 PAH samples were collected during the cruise and transported to the laboratory of IRBIM Ancona for processing (extraction and UHPLC-FLD-DAD analysis).

Aliquots of surficial sediment (0-2 cm) were sampled in selected locations (4 stations) for inorganic and organic contaminants (see Table 8.1.2). Surficial sediments were collected with a plastic spoon and storage in PTE jars previously decontaminated and weighted. Successively samples were stored frozen at -20°C.

Selected locations (see Table 8.1.2) were sampled with plastic liner. In total 2 stations for inorganic contaminants and 5 stations for organic contaminants. Cores were closed with decontaminated plastic stoppers and stored in the fridge at 4°C for successive analysis.

Figure 8.1.11. Sampling of sediments for contaminants.

- *Foraminifera sampling*

Aliquots of superficial sediment (0-0.5 cm) were sampled by using a spoon from the box-corer in order to extract its foraminiferal content, including both living and dead assemblage. The aliquot is collected into a 50 ml or 15 ml falcon with addition of 10 to 20 ml of 70% ethanol stained with Bengal Rose. The samples will be washed and sieved at 64 microns, and microfauna picked up under an optical microscope.

9.2. Challenges

The main challenge faced for sediment coring operations during the first Leg of the cruise concerned the limited experience of the operation team on deck in managing the coring system, as it requires a remarkable technical expertise and body strength and agility considering that the coring system is mounted on a cradle-pylon system which is hanging some half a meter overboard. For this reason, piston cores were not carried out during the first part of the cruise, reducing the chance of collecting long sedimentary records. Moreover, due to its shape, the core barrel can only enter the cradle in one direction: it is not possible to rotate 180° according to its axis of symmetry. This caused major problems during an event of pipe bending, which forced a series of time-consuming maneuvers to recover the barrel and the framework in its horizontal position. This particular issue has been already managed and the coring head has been modified soon after the end of the cruise.

No particular issues were encountered during box corer deployment and retrieval operations, apart from a technical failure of the IBERCISA multipurpose winch at stern that prevented the completion of the all foreseen box coring stations. Indeed, on 05/12/2023 at 10.30 local time, during box corer recovery operations from a depth of 2500 m, unusual and loud noise from the winch motor was heard. For safety, it was decided to complete the recovery of the box corer at a minimum speed of 25 m/min. Checks were immediately carried out which, however, did not lead to any particular anomalies being found by the chief engineer. On 06/12/2023, in the morning, a meeting between the on-board technician, the Captain, IBERCISA and the project manager highlighted the following points: inability for IBERCISA to understand the problem and to give any indications on possible breakages of the mechanical parts and IBERCISA concluded that, in the absence of a clear picture, the winch should have been put into disuse until new and conclusive checks are carried out.

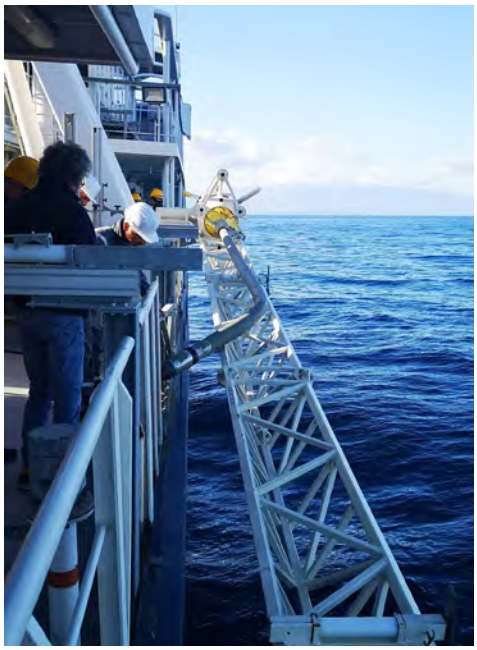

Figure 8.1.11. Difficult recovery of a bended core barrel due to the impossibility of rotating the coring head inside the cradle with the risk of damages to the ships' hull and important postponement of sea operations.

9.3. Recommendations

Limited storage space is available on-board for samples and this should be addressed by a separate action such as providing a refrigerated container on deck. Training courses for technicians/technologists/researchers available to acquire expertise on the coring system are required.

10. **Floating macro litter survey**

10.1. Insights

A visual survey of floating macro litter (FML) was conducted during the cruise. Observations were made during regular navigation of the ship between sampling stations at a speed of about 9-10 knots. The observations were made by a dedicated observer who scanned the sea surface from the bow of the vessel and registered UTC time, GPS coordinates, size, type, color and perpendicular distance of all floating macro-debris (>2 cm) items sighted on one side of the ship, chosen according to wind direction and sun position. Sightings were all performed during daylight hours, by naked eye and under good weather conditions only. 7x50 binoculars were used to better identify more distant objects. Recorded item were allocated to one of two major type categories: Anthropogenic Marine Debris (AMD) and Natural Marine Debris (NMD). The survey effort was split into 30-min transects in order to standardize fatigue for the observer, enhance the number of replicates and better account for the patchy distribution of debris at sea. Litter concentrations will be computed using standard strip-transect techniques. During the cruise, a total of 30 visual transects were performed (total survey length: 223.27 km, total survey time: 14.03 hours). During the visual survey, a GoPro camera was also installed on a bulwark located on the upper deck (monkey island). The camera recorded georeferenced time lapses of the sea surface in parallel with the observer. The acquired footage will be analyzed using a newly developed object-detection algorithm, which will be trained, ground-thruted and validated using the survey results.

Transect	Date	Start			Stop			Duration (min)	Distance (km)
		Time	Lat	Lon	Time	Lat	Lon		
1	19/11/23	08:20	37,452570	15,174407	08:50	37,446734	15,282321	30	9,60
2	20/11/23	08:45	35,791059	17,756333	09:15	35,852529	17,799031	30	7,83
3	22/11/23	15:52	36,566219	15,819702	16:13	36,622897	15,792366	21	6,78
4	24/11/23	08:52	37,272882	15,539105	09:22	37,312207	15,518558	30	4,76
5	25/11/23	09:17	37,637902	15,289722	09:47	37,687838	15,312124	30	6,00
6	25/11/23	10:39	37,763190	15,321530	11:09	37,704367	15,292129	30	7,32
7	25/11/23	12:14	37,598988	15,278255	12:26	37,606684	15,251636	12	2,55
8	25/11/23	12:31	37,613748	15,256070	13:01	37,666202	15,275178	30	6,20
9	25/11/23	14:13	37,777468	15,329570	14:42	37,824797	15,348953	28	6,07
10	25/11/23	16:12	37,633589	15,259194	16:41	37,565554	15,231275	28	8,01
11	27/11/23	08:53	37,372555	15,937409	09:23	37,443882	15,898562	30	8,65
12	27/11/23	14:13	37,538799	15,888182	14:43	37,622471	15,944344	30	10,53
13	27/11/23	15:04	37,681302	15,983508	15:34	37,765635	16,037285	30	10,47
14	27/11/23	15:57	37,822281	16,078712	16:27	37,888704	16,147671	30	9,56

15	29/11/23	08:45	39,127279	17,189378	09:15	39,094939	17,291058	30	9,50
16	04/12/23	09:27	40,282733	17,042464	09:57	40,220674	17,080700	30	7,61
17	04/11/23	13:06	40,183667	17,110852	13:36	40,108807	17,176446	30	10,01
18	04/12/23	14:06	40,032842	17,241190	14:36	39,955815	17,303622	30	10,07
19	05/12/23	07:36	39,234779	17,976604	08:06	39,155848	18,027334	30	9,85
20	05/12/23	11:33	39,157395	18,004122	12:03	39,215759	17,928012	30	9,25
21	05/12/23	12:49	39,326720	17,851887	13:06	39,368192	17,825125	17	5,18
22	05/12/23	13:53	39,449126	17,819843	13:59	39,464610	17,818843	6	1,71
23	05/12/23	14:26	39,431887	17,740843	14:56	39,410887	17,630200	30	9,86
24	05/12/23	15:56	39,382110	17,407637	16:26	39,377977	17,326100	30	7,01
25	06/12/23	08:57	39,004368	17,233588	09:27	39,039511	17,307824	30	7,52
26	06/12/23	11:40	39,088403	17,333088	12:10	39,138942	17,290298	30	6,72
27	06/12/23	14:31	39,153891	17,298290	15:01	39,110132	17,366263	30	7,62
28	06/12/23	16:03	39,106477	17,393121	16:33	39,156652	17,468181	30	8,55
29	07/12/23	13:23	39,957639	17,860788	14:03	39,938462	17,911207	40	4,80
30	07/12/23	15:15	39,931358	17,910608	15:45	39,958550	17,886244	30	3,68

Table 9.1.1. Summary of the FML visual survey observation transects performed during the PIONEER cruise.

No challenges or recommendations are available for this activity.

11. Optical measurements

The GOS group at ISMAR Rome conducted a full set of optical measurements on board the Gaia Blu ship, with the main goals of (1) testing the ship's suitability for such sampling and identifying possible weak points, (2) expanding the group's optical database, that is being utilized for a variety of activities, from satellite validation until more scientific ones. These measurements are summarized in the paragraphs below.

11.1. Insights

- *In-water radiometry*

In-water radiometry stands for the passive measurement of sun radiation for different depths in the water. These measurements are made of light coming from several directions, and at different bands (wavelengths). To achieve these goals while minimizing the uncertainties, the procedure followed is the free-falling profiling. This consists of a profiler with a slightly lesser buoyancy with respect to water, so that it slowly sinks in the water column. A rocket-like shape helps to keep the profiler in a vertical position. To minimize the ship optical disturbance, the profiler is kept far away from stern, while keeping the ship's course away from the sun. The profiler is recovered by hand using the same data cable. Several consecutive profiles are used to derive the final measurement. These measurements include useful variables for satellite validation and algorithm development, such as the remote-sensing reflectance and the diffuse attenuation coefficient.

A	B
	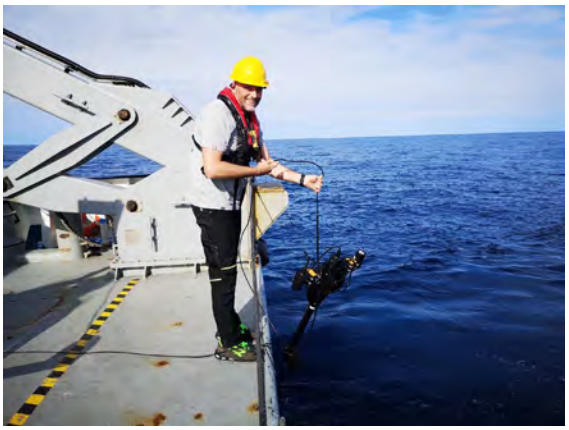
C	
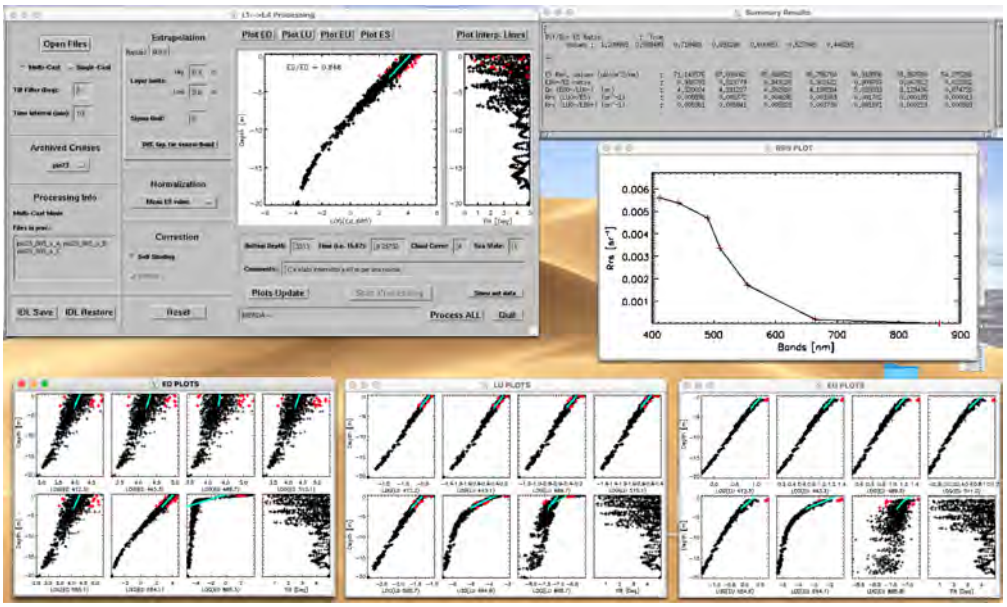	

Figure 10.1.1. A. SATLANTIC radiometer that measures the radiance and irradiance of sunlight in seawater. deployed at sea. B. Recovery of the radiometer. C. Data collected by the radiometer for a first quality check.

- *Inherent optical properties (IOPs)*

The importance of measuring seawater IOPs stands in its relationship with radiometry observations. Radiometry can more or less be interpreted as the total signal as perceived by the human eye or by a satellite remote sensor and the IOP measurements help disentangling the various contributors to that signal: phytoplankton biomass and its size distribution along with the coloured dissolved organic matter in the open ocean with the addition of suspended terrigenous materials in the coastal domain. Onboard Gaia Blu, GOS group performed IOP

measurements using one single instrumentation package implemented in two different setup configurations: profile mode and underway. In both configurations data acquisition and processing remain the same in which the measurements are made i) over the seawater as is and ii) after its filtration through a 0.2 µm high surface filter to allow the dissolved properties to be measured. By subtraction the particulate fraction of the signal is computed. During the underway measurements, the transition between total and filtered measurements is made automatically through an electrovalve operated via computer. In profile mode, two consecutive casts are performed, with and without the water passing through the 0.2 µm filter.

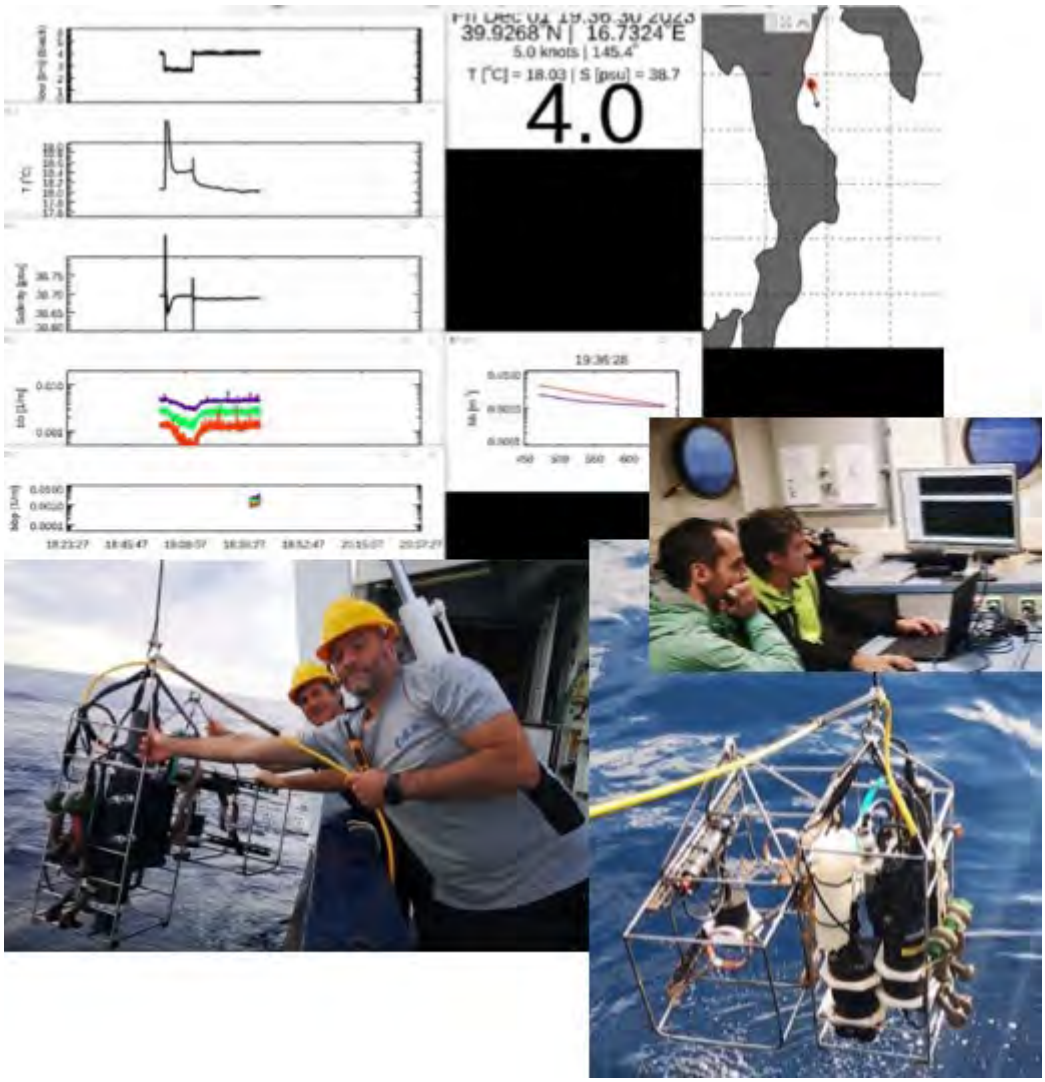

Figure 10.1.2. Kaleidoscope of images related to the deployment of the IOP instrument and processing of data.

11.2. Challenges

The deployment system of the instrument may be suitable, and the operations proceeded smoothly. However, it is noted that the winch and portal are poorly positioned as they are located near the stationary propeller. This causes the disruption of the water column in the first few meters (which may alter the water column structure) and the presence of air bubbles.

11.3. Recommendations

It is suggested to have greater maneuverability on the starboard side by using the CTD winch to deploy other instruments, with the need for enlarging the designated area. The addition of a seawater and freshwater inlet in the CTD compartment will be necessary.

Winch: A meter pulley and precise speed adjustment are required for the winch. It should be operable from both the stern and the control room. A cable with a minimum length of 3000 m and a load capacity of at least 100 kg is needed.

Stern deployment: For deployments from the stern, a controlled cable of at least 3000 m and a load capacity of at least 100 kg is necessary.

12. **Science Control Room**

12.1. Insights

The Science Control room allows to display, monitor and operate all the navigation system and control the geophysical equipment hull-mounted including: multibeam systems, CHIRP systems, ADCP systems, scientific echo sounders, USBL system. The Science Control Room also hosts the remote control for CDT/Rosette and sediment sampling winches (coring system at starboard and box coring system through the multipurpose winch) and it is therefore the neuralgic centre of the vessel.

Figure 11.1.1. Remote control of the CTD/Rosette winch from inside the Science Control Room.

12.2. Challenges

There has been a small number of technical failures of the screens, UPS and consoles, mainly due to the obsolescence of some monitors which have been already replaced and some electrical connectivity issues that are under consideration by the vessel technical crew.

12.3. Recommendations

It is suggested to always remind the bridge to switch to science mode navigation once DP operations or full speed operations are concluded. in order to reduce vibrations (400 RMPs instead of 600 RMPs or full engine) and enhance geophysical data quality, especially during multibeam and CHIRP acquisition. Radio communications should be the preferable way to keep the science control room informed about activities taking place on deck and on the bridge, to expedite related actions.

13. **Geophysical data acquisition**

Geophysical surveys consisted mainly of multibeam bathymetry and backscatter data acquisition using the intermediate (0-1500 m) and deep water (> 1500 m) EM712 and EM304 systems hull-mounted on the vessel; high-resolution seismic reflection data of the sub-bottom were acquired using the hull-mounted 3.5-12 kHz 3260 Knudsen CHIRP echosounder. Acquisitions of ADCP data using the 45 kHz Workhorse have been conducted to test the signal interference with EM304 data, as the synchronization software (Kongsberg K-sync) is currently unavailable for ADCP Teledyne's systems. The K-sync was instead used to deconflict multibeam and sub-bottom profiler acquisitions during transits.

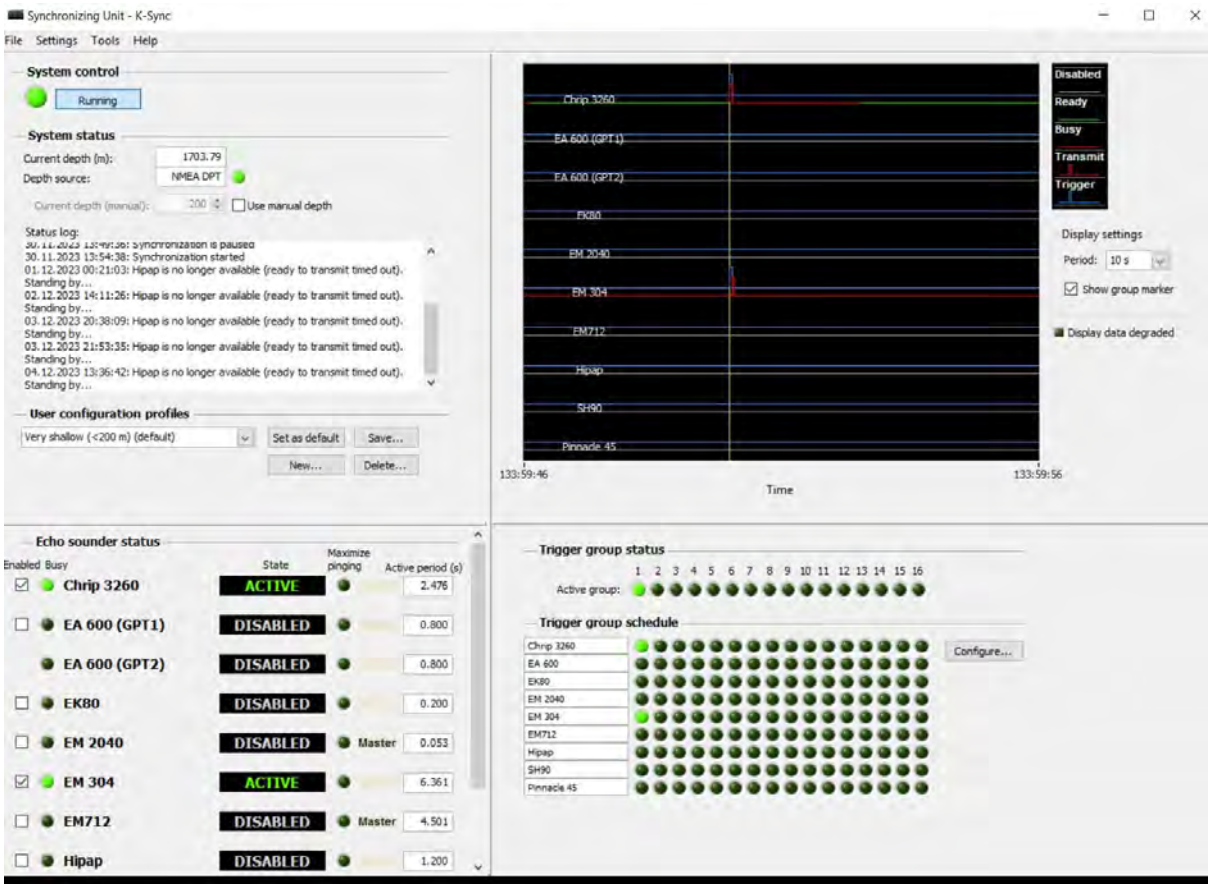

Figure 12.1.1. K-sync display, the system was mainly used to configure the timing of pinging of the

Knudsen echosunder and EM304 deep-water echosounder. The EM304 is the master unit as the longest transmitting-receiving system, the CHIRP is subordinated to the listening window of the EM304.

- *Positioning, Heading and Attitude*

The Seapath 380 system provides continuous information of: Global Satellite Positioning by 2 GNSS antenna, attitude information by 1 Motion Reference Unit MRU5. Heading information is computed from the 2 antennae position. The accuracy of positioning is achieved by differential satellite positioning DGNSS subscription (Fugro Marinestar GNSS G4, survey average accuracy 0.12 m). For instrumental offsets see file OFFSET/ GBL.SE.G.200.01-Offset Definition.pdf. The Seapath 380 system is used for ship positioning, supplied by a Fugro HP differential Global Positioning System (DGPS), accurate up to 0.2 m. The Kongsberg motion sensor MRU 5 and a Dual Antenna GPS integrated in the Seapath will correct pitch, roll, heave and yaw movements (reaching 0.02° roll and pitch accuracy, and 0.075° heading accuracy).

- *Vessel draft*

The vessel draft is derived using stability calculations provided by Intershalt Maritime System Stability Software -SEACOS MACS3, belonging to the bridge management system. The center of gravity of the boat (CoG) is calculated as of September 19, 2023, based on load distribution and navigation settings (longitudinal center of gravity, LcG 36.12; vertical center of gravity VcG 5.45).

- *Multibeam sensors*

Multibeam data (MBES) were collected d using three different multibeam echosounder systems: the Kongsberg EM2040-04 MKII 0.4°x0.7° suited for water depths between 50 and 1250 m, Kongsberg EM712 1°x0.5° for water depths between 1250 and 10500 m and Kongsberg EM304 MKII 1°x1° for water depth greater than 10500 m. The MBESs are hull-mounted on the R/V Gaia Blu's gondola with a T-configuration of linear transducer arrays. The Seapath 380 system was used for ship positioning, supplied by a Fugro HP differential Global Positioning System (DGPS), with Marinestar GNSS signal accuracy better than 5 cm. The Kongsberg motion sensor MRU (Motion Reference Unit) 5 and a Dual Antenna GPS integrated in the Seapath, were used to correct for the pitch, roll, heave and yaw movements (reaching 0.02° roll and pitch accuracy, and 0.075° heading accuracy).

A Valeport mini SVS sensor is attached close to the transducers to continuously measure the sound velocity for the beamforming.The multi bean coverage is about four times the water depth and a 20% overlap between lines is normally achieved. Data are logged, displayed and checked in real-time by the Kongsberg data acquisition and control software SIS 5 (Seafloor Information System). The multibeam systems were operated with average swath opening angles of about 60°/70° depending on signal/noise ratio. Sound velocity profiles were collected with a Valeport Midas SVP 45305.

Multibeam data collected during PIONEER are now part of the EMODnet Bathymetry data infrastructure under the CDI-record id 3680061 of the Pan-European Infrastructure for Ocean & Marine Data Management SeaDataNet and will be part of the 2024 release of the 1/16 * 1/16 arc minutes (ca. 115 m grid) EMODnet DTM and concur to the high resolution DTMs with

metadata described as Sextant entries. The EMODnet DTM is updated every 2 years and made available to everyone in the EMODnet Mapviewer, by OGC web services, and by downloading in multiple formats for use in GIS systems and as base layer for numerical hydraulic models. See https://emodnet.ec.europa.eu/geoviewer/

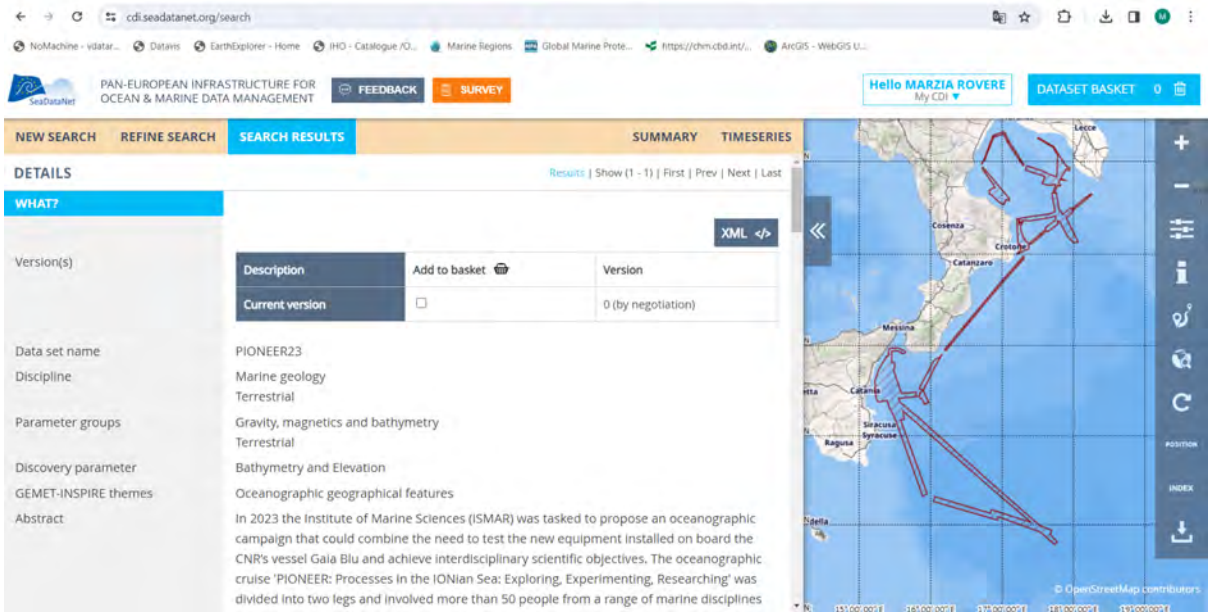

Figure 12.1.2. SeaDataNet visualization of metadata (CDI) of the PIONEER23 cruise.

1° leg	**19-28.11.2023**			
SVP	**LON DDMM.xxx**	**LAT DDMM.xxx**	**LON DD.xxx**	**LAT DD.xxx**
19112023_1240 - MIDAS SVP S/N 45305	15°25.5476009' E	37°26.3834793' N	15,4257933	37,4397247
20112023_1901 - MIDAS SVP S/N 45305	17°44.9200631'E	35°53.1772471' N	17,7486677	35,8862875
21112023_0830 - MIDAS SVP S/N 45305	16°56.6898362'E	36°06.9810179' N	16,9448306	36,1163503
22112023_0930 - MIDAS SVP S/N 45305	15°49.9123838'E	36°29.9393675' N	15,83187306	36,49898946
24112023_1522 - MIDAS SVP S/N 45305	15°35.5757062'E	37°13.9182489	15,59292844	37,23197082
26112023_1611 - MIDAS SVP S/N 45305	15°25.5688848'E	37°26.4380988' N	15,42614808	37,44063498
27112023_1008 - MIDAS SVP S/N 45305	15°52.6118968'E	37°29.1349113' N	15,87686495	37,48558186

2° leg	**28.11-09.12.2023**			
	LON DDMM.xxx	**LAT DDMM.xxx**	**LON DD.xxx**	**LAT DD.xxx**
29112023_0925 - MIDAS SVP S/N 45305	17°21,7859' E	39°04,1077'N	17,3630983	39,0684617
30112023_0553 - MIDAS SVP S/N 45305	17°17,9872	39°02,9904	17,2997867	39,0498400
01122023_2123 - MIDAS SVP S/N 45305	16°50,58052	39°49,03358	16,84300867	39,81722633
02122023_1027 - MIDAS SVP S/N 45305	16°56,41716	39°44,396217	16,940286	39,73993695
03122023_0823 - MIDAS SVP S/N 45305	16°57,682693	39°42,361969	16,96137821	39,70603282
05122023_0446 - MIDAS SVP S/N 45305	17°51,61219	39°24,01985	17,86020317	39,40033083
06122023_0729 - MIDAS SVP S/N 45305	17°12,44557	38°59,56986	17,20742617	38,992831
08122023_1113 - MIDAS SVP S/N 45305	17°46,36529	39°46,21357	39,77022617	17,77275483
08122023_2009 - MIDAS SVP S/N 45305	17°35,84574	39°49,22685	17,597429	39,8204475

Table 12.1.1. Coordinates of the SVP profiles collected together with CTD/Rosette deployment.

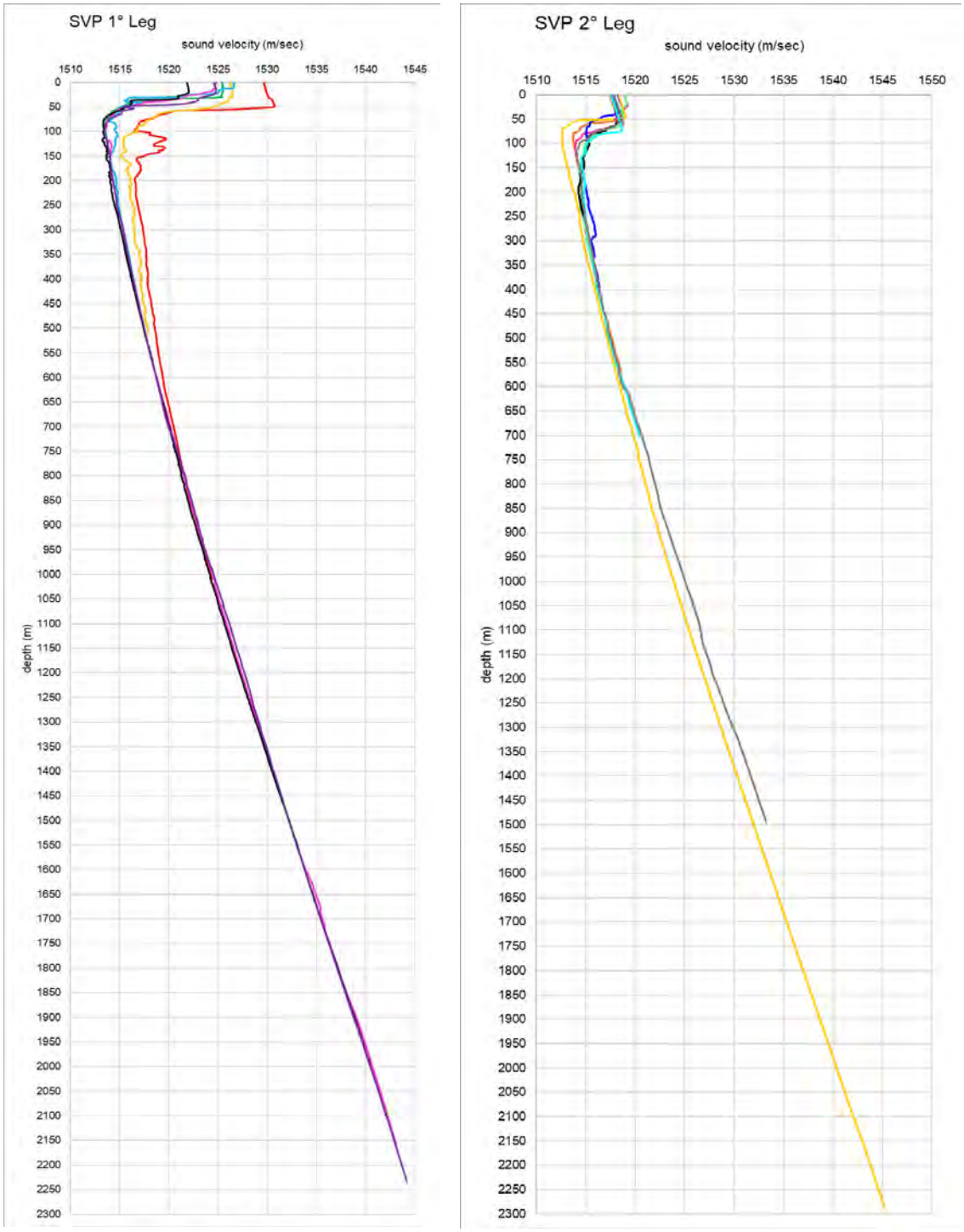

Figure 12.1.3. Sound velocity profiles collected during leg 1 and 2 of the PIONEER cruise to correct the sound propagation for multibeam data.

- *Navigation system*

The overall navigation and bridge communications system is supported by QPS-Qinsy 9.5.6. The Seapath 380 positioning system installed provides a common reference point (CRP) for all the systems on board, including the Kongsberg Multibeam Echosounders and the Knudsen Sub-Bottom profiler (SBP). The Kongsberg Multibeam software directly applies all the necessary software and positioning inertial corrections as well as offset computations to data

in both pinging and recording modes. The Qinsy navigation system stores all the offsets of the installed systems, and its positioning computations relative to each node are sent to the respective systems. The draft can be applied in post-processing to the Knudsen CHIRP data.

A few tests were conducted on the EM712 and EM2040 multibeam sensor calibration settings (yaw, pitch, roll and heave) which are stored in the proprietary Kongsberg SIS5 system in Attitude 1. A second configuration, named Attitude 2, does not contain calibration settings however is the active configuration, which is read by the processing software suite while importing the multibeam data. This configuration directly influences the vessel configuration created by the processing software leading to uncalibrated data. Different configurations were tested during the PIONEER cruise, such as copying calibration data in Attitude 2, setting manually Motion 1 and Motion 2 in the processing software; the best results were achieved using calibration data in Attitude 2, however, further investigation are necessary as this configuration has not been validated by Kongsberg during the sea trials and the commissioning phase.

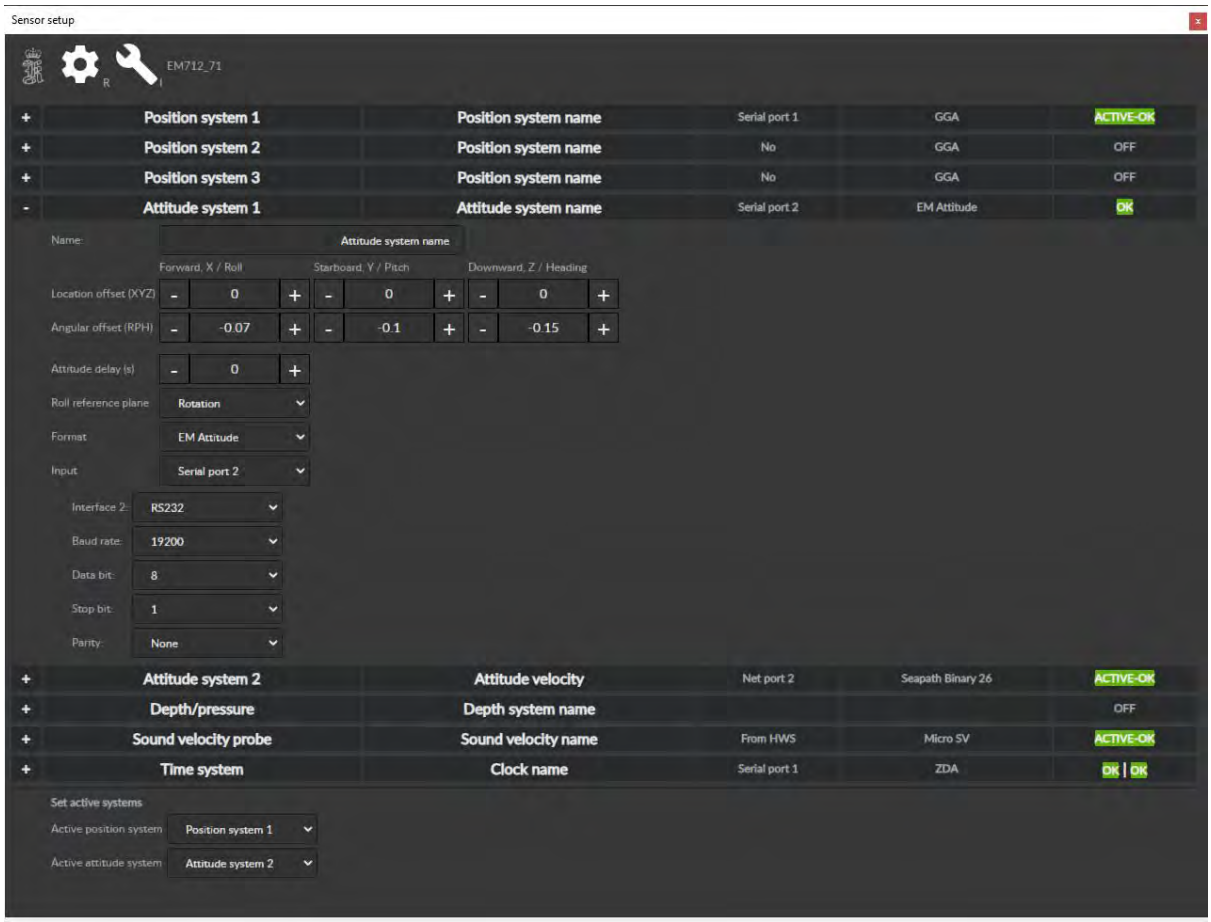

Figure 12.1.4. Display of the multibeam sensor setup divided into Attitude system 1 and 2.

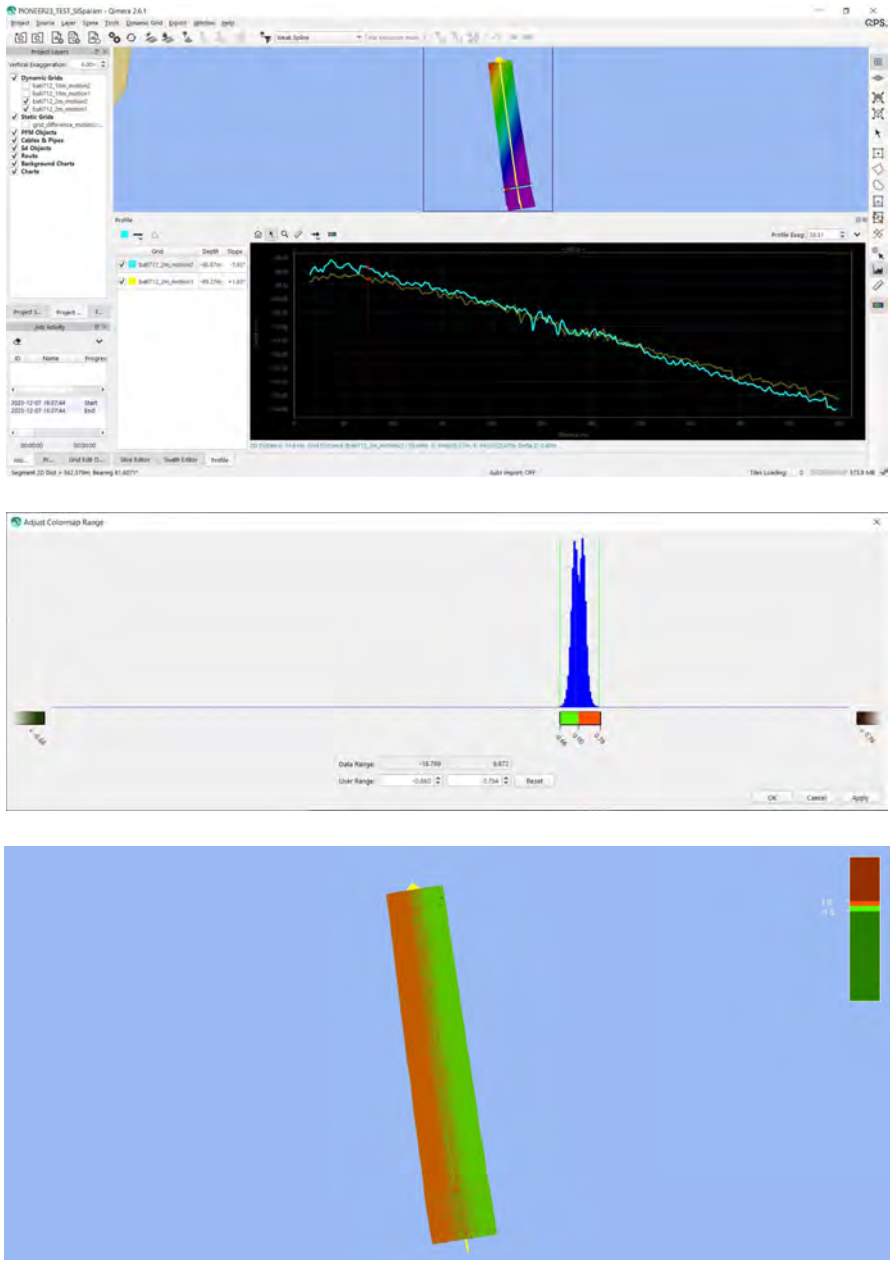

Figure 12.1.5. Results of the various tests made on the multibeam calibration settings.

- *CHIRP sensors*

While the acquisition of bathymetric data allowed the analysis of geomorphology and seafloor gradients, sub-bottom CHIRP (SBP) profiles return high-resolution stratigraphic information of the first 10 to 40 meters of sediment. Based on the seismic facies and a derived assessment of the grain size, piston or gravity coring was performed in that particular station.

The processing of the SBP data is divided into the following work phases: 1) Conversion of the files from the native digital format .KEB to SEG-Y and/or import of the native wires into commercial processing software (e.g. Geomarine Survey Systems Geo-suite AllWorks, Moga Software SeaView SBP) or academic ones for free use with the creation of a dedicated routine (Seispro). 2) Preliminary evaluation of the quality of the raw data, even uncorrelated data when necessary, for the creation of a customized processing sequence and the Hilbert transform,

where improved; 3) Application of the processing sequence, which basically includes the envelope of the amplitudes, filters and gains to improve the interpretation of the data, including e.g. time-windowing, time varying gain (TVG) with automatic and/or manual identification and picking of the reflector corresponding to the seabed; 4) Cross-checking the seabed depth using bathymetric DEMs and applying, where necessary, an offset using the speed of sound recorded at the head of the MBES during acquisition simultaneously with the SBP profile; 5) Muting of the water column; 6) Export of processed files in SEG-Y or XTF interchange format; 7) Import into 2D seismic interpretation suites (e.g. Schlumberger Petrel E&P, Geomarine Survey Systems Geo-suite AllWorks, Global S&P Kingdom Seismic and geological interpretation software).

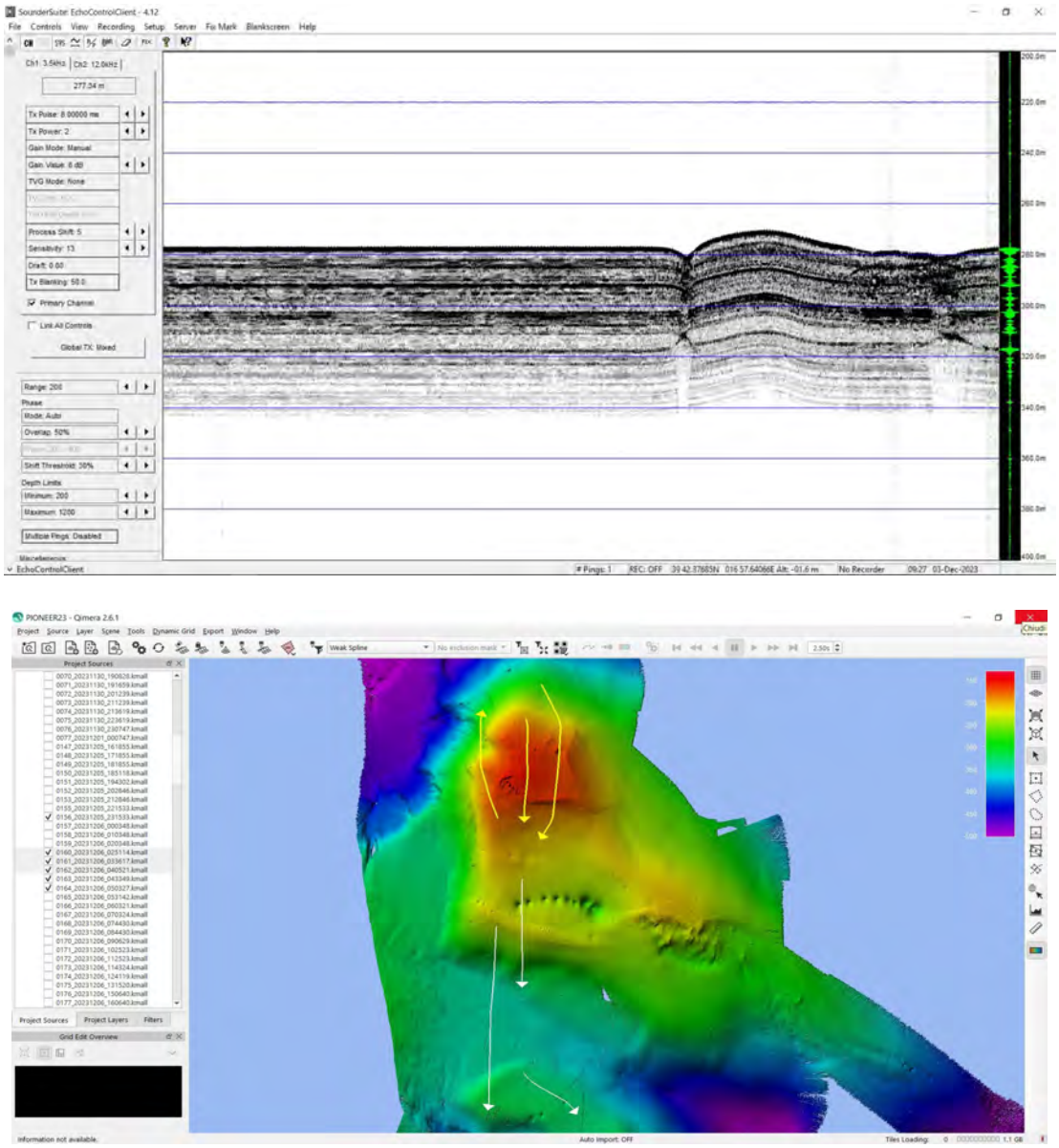

Figure 12.1.6. Display of CHIRP data showing the most common parameters used during acquisition (above). Multibeam bathymetric data post-processed using the software QPS-Qimera on pockmarks crossed by the CHIRP profile (below).

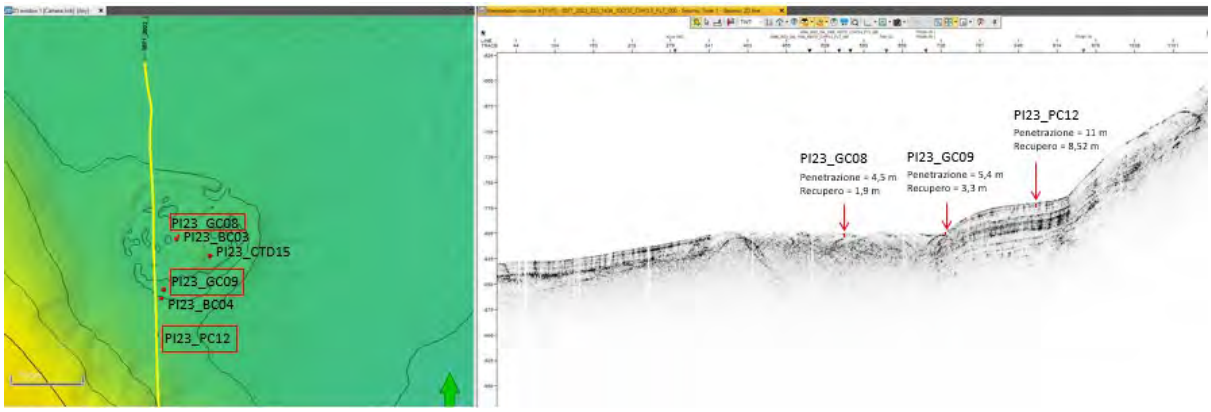

Figure 12.1.7. CHIRP profile as displayed in the AllWorks GeoSuite software, where functions such as Amplitude Envelope and Gain were applied to better highlight the seismic signal. The profile is ca. N-S oriented across a flat area at around 600 m water depth along three sediment cores (PI23_GC08, 09, 12).

14. Outreach activities

During the PIONEER campaign, photo video documentation was created with the aim of acquiring archive material and a 360° virtual tour of the ship, a video connection was also realized with two middle schools.

- *Video streaming*

During the second leg of the campaign, an interactive connection was created between the ship, two middle schools, the Tor Vergata research area and the CNR-ISMAR headquarters in Bologna. The interactive video conference and the use of a mobile video camera allowed the students to closely follow all the research activities occurring inside the scientific control room and at the Baltic Room. The connection lasted about an hour with the possibility of having a question and answer session with the pupils.

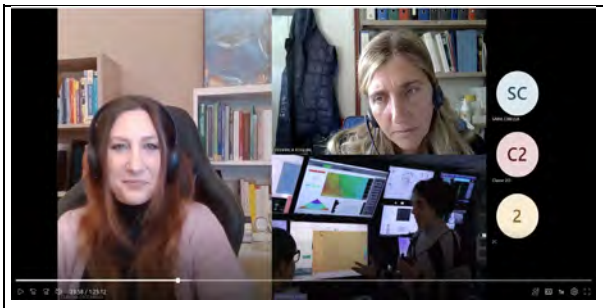

Figure 13.1.1. Video footage of the Teams connection with ashore middle schools.

- *360° virtual tour*

Navigable 360° photographic shots were taken with the aim of creating a website that allows navigation of the internal and external environments. Within this virtual tour you will be able to view technical data sheets relating to the ship. 360-degree documentation of the research activity was created.

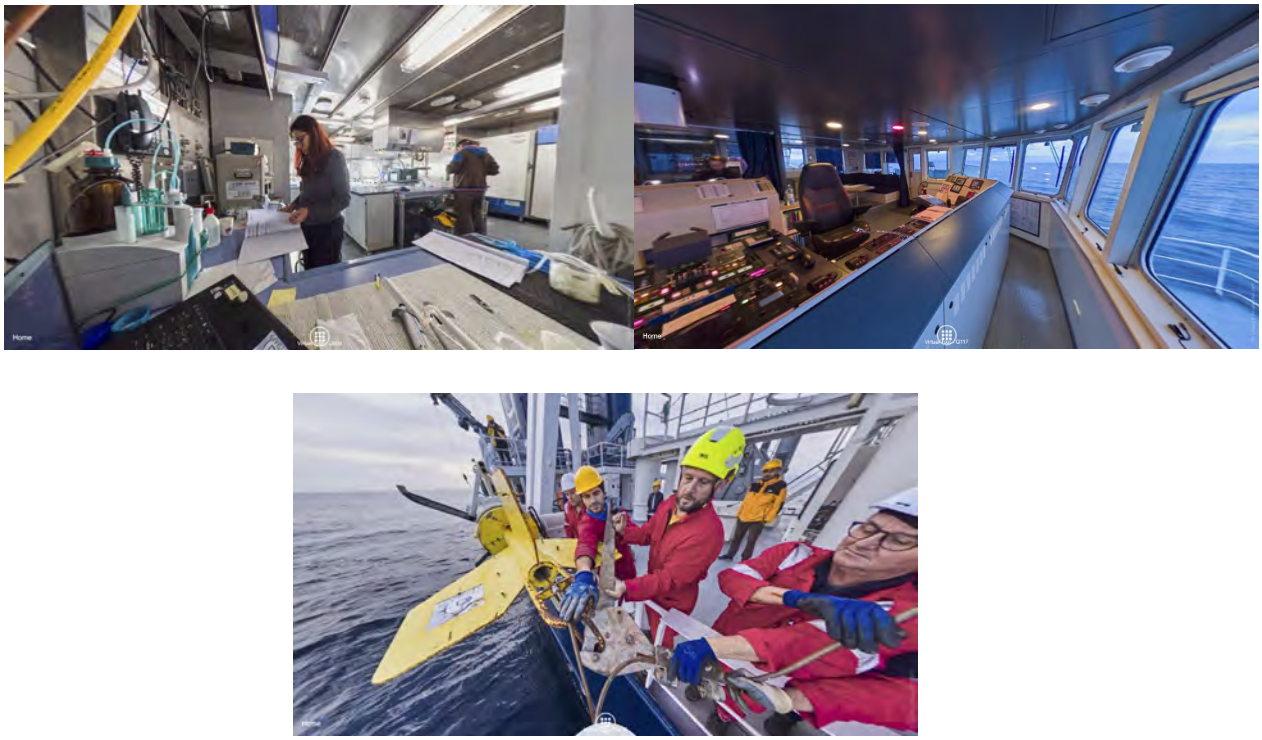

Figure 13.1.2. Examples of 360° visualization of different locations onboard the R/V Gaia Blu.

- *Foto and video documentation*

Photos and videos of the cruise were taken with the aim of creating an image repertoire to be made available to the Cnr scientific community and for carrying out communication activities via institutional websites and the press.

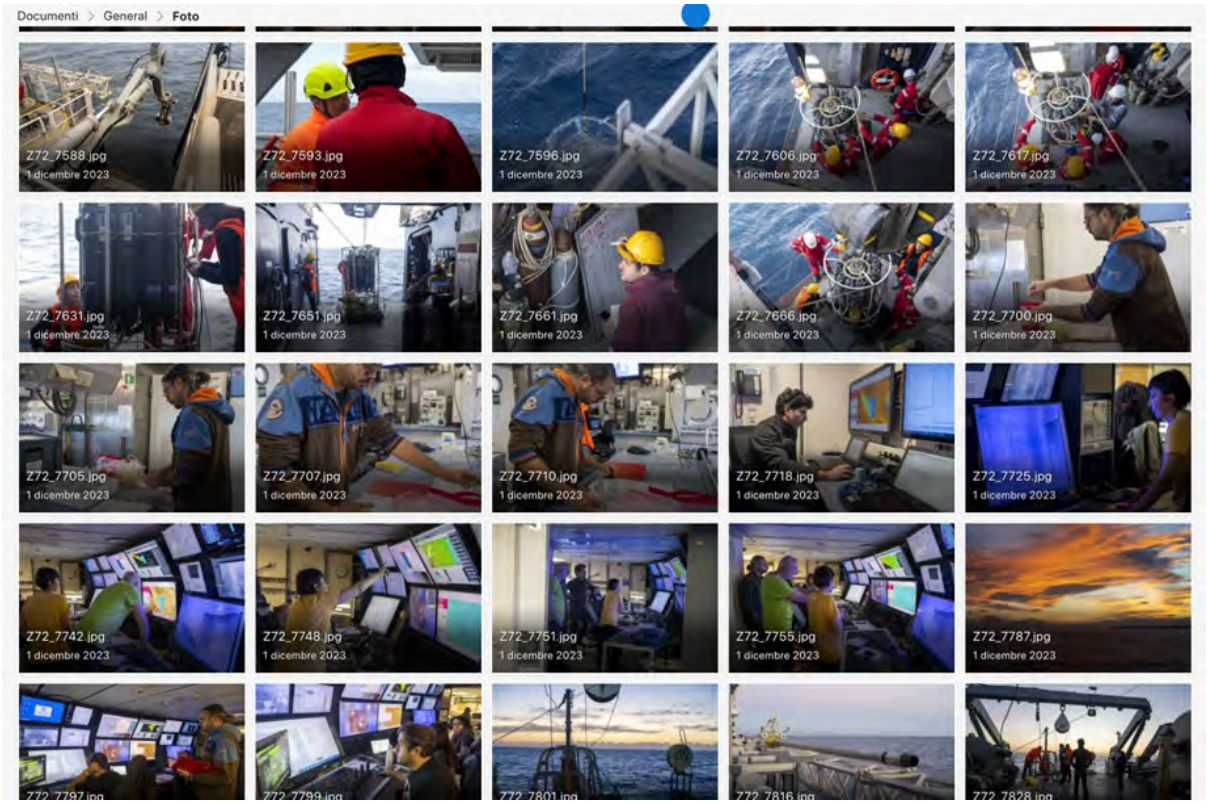

Figure 13.1.1. Overview of photos taken onboard during Leg 2 of the PIONEER cruise.

15. References

Argnani, A., Pellegrini, C., Rovere., M. (2023). Morphology and Fluid Expulsion Offshore Crotone (Calabrian Accretionary Prism). Marine Geology, submitted.

Argnani, A., 2020. Comment on “Geometry of the deep Calabrian subduction (Central Mediterranean Sea) from wide-angle seismic data and3-D gravity modeling ”by Dellong et al. Geochemistry, Geophysics, Geosystems,21, e2020GC009077.

Argnani, A., Favali, P., Frugoni, F., Gasperini, M., Ligi, M., Marani, M., & Mele, G. (1993). Foreland deformational pattern in the Southern Adriatic Sea. Annali di Geofisica.

Argnani, A., Frugoni, F., Cosi, R., Ligi, M., & Favali, P. (2001). Tectonics and seismicity of the Apulian Ridge south of Salento peninsula (Southern Italy).

Argnani, A., Bonazzi, C., 2005. Malta Escarpment fault zone offshore eastern Sicily: Plio-Quaternary tectonic evolution based on new multichannel seismic data, Tectonics, 24, TC4009.

Argnani, A., & Pino, N.A. (2023), The 1908 Messina Straits Earthquake: Cornerstones and the Need to Step Forward. Seismological Research Letters, doi:10.1785/0220220355.

Artale, V., Falcini, F., Marullo, S., Bensi, M., Kokoszka, F., Iudicone, D., & Rubino, A. (2018). Linking mixing processes and climate variability to the heat content distribution of the Eastern Mediterranean abyss. Scientific reports, 8(1), 1-10.

Bachi et al. (2023). DOM accumulation in oligotrophic surface waters: new insights from the Mediterranean Sea, EGU General Assembly 2023, Vienna, Austria, 24–28 Apr 2023, EGU23-14893.

Bellacicco, M., Anagnostou, C., Falcini, F., Rinaldi, E., Tripsanas, K., & Salusti, E. (2016). The 1987 Aegean dense water formation: A streamtube investigation by comparing theoretical model results, satellite, field, and numerical data with contourite distribution. Marine Geology, 375, 120-133.

Bensi, M., Cardin, V., Rubino, A., Notarstefano, G., & Poulain, P. M. (2013b). Effects of winter convection on the deep layer of the Southern Adriatic Sea in 2012. Journal of Geophysical Research: Oceans, 118(11), 6064-6075.

Bensi, M., Rubino, A., Cardin, V., Hainbucher, D., & Mancero-Mosquera, I. (2013a). Structure and variability of the abyssal water masses in the Ionian Sea in the period 2003-2010. Journal of Geophysical Research: Oceans, 118(2), 931-943.

Béranger, K., Mortier, L., Gasparini, G. P., Gervasio, L., Astraldi, M., & Crépon, M. (2004). The dynamics of the Sicily Strait: a comprehensive study from observations and models. Deep Sea Research Part II: Topical Studies in Oceanography, 51(4-5), 411-440.

Bergamasco, A., & Malanotte-Rizzoli, P. (2010). The circulation of the Mediterranean Sea: a historical review of experimental investigations. Advances in Oceanography and Limnology, 1(1), 11-28.

Billi et al. (2020). The SEISMOFAULTS project: first surveys and preliminary results for the Ionian Sea area, southern Italy. ANNALS OF GEOPHYSICS, 63, 3.

Bindoff, N. L., Willebrand, J., Artale, V., Cazenave, A., Gregory, J. M., Gulev, S. & Woodworth, P. (2007). Observations: oceanic climate change and sea level. Climate Change 2007: The Physical Science Basis, eds Solomon S, et al. (Cambridge Univ Press, Cambridge, UK), pp 747–845.

Bohrmann, G., Alvarez, R., Biller, T., Buchheister, S., Buttner, H., Canoni, O., et al. (2015). Report and preliminary results of R/V METEOR cruise M112, Dynamic of mud volcanoes and seeps in the Calabrian Accretionary Prism, Ionian Sea, Catania (Italy)—Catania (Italy), November 6 –December 15, 2014 (Rep. 306, p. 217). Bremen, Germany: Berichte, MARUM – Zentrum fur Marine Umweltwissenschaften, Fachbereich Geowissenschaften, Universit€at Bremen.

Boldrin, A., S. Miserocchi, S. Rabitti, M. M. Turchetto, V. Balboni, and G. Socal, Particulate matter in the southern Adriatic and Ionian Sea: Characterisation and downward fluxes, J. Mar. Syst., 33–34, 389–410, 2002.

Camerlenghi, A., Cita, M. B., Hieke, W., & Ricchiuto, T. (1992). Geological evidence for mud diapirism on the Mediterranean Ridge accretionary complex. Earth and Planetary Science Letters, 109(3–4), 493–504.

Casotti, R., Landolfi, A., Brunet, C., d'Ortenzio, F., Mangoni, O., Ribera d'Alcalà, M., & Denis, M. (2003). Composition and dynamics of the phytoplankton of the Ionian Sea (eastern Mediterranean). Journal of Geophysical Research: Oceans, 108(C9).

Catalano R., C. Doglioni and S. Merlini (2001), On the Mesozoic Ionian Basin, Geophysical Journal International, 144, 49-64.

Ceramicola, S., Praeg, D., Cova, A., Accettella, D., & Zecchin, M. (2014a). Seafloor distribution and last glacial to postglacial activity of mud volcanoes on the Calabrian accretionary prism, Ionian Sea. Geo-Marine Letters, 34, 111-129.

Ceramicola, S., Praeg, D., Cova, A., Accettella, D., & Zecchin, M. (2014b). Seafloor distribution and last glacial to postglacial activity of mud volcanoes on the Calabrian Accretionary Prism, Ionian Sea. Geo-Marine Letters, 34(2–3), 111–129.

Cernobori L., A. Hirn, J.H. McBride, R. Nicolich, L. Petronio and M. Romanelli, STREAMERS/PROFILES Working Groups (1996), Crustal image of the Ionian basin and its Calabrian margins, Tectonophysics, 264, 175-189.

Cita, M., Ryan, W., & Paggi, L., 1981. Prometheus mud breccia: An example of shale diapirism in the Western Mediterranean Ridge. Ann. Geol Pays Helleniques, 30, 543–557.

Civitarese, G., A. Crise, G. Crispi, and R. Mosetti, Circulation effects on nitrogen dynamics in the Ionian Sea, Oceanol. Acta, 19, 609–622, 1996.

Civitarese, G., Gačić, M., Lipizer, M., & Eusebi Borzelli, G. L. (2010). On the impact of the Bimodal Oscillating System (BiOS) on the biogeochemistry and biology of the Adriatic and Ionian Seas (Eastern Mediterranean). Biogeosciences, 7(12), 3987-3997.

Cuffaro, M., Billi, A., Bigi, S., Bosman, A., Caruso, C. G., Conti, A., Corbo, A., Costanza, A., D'Anna, G., Doglioni, C., Fertitta, G., Gasperini, L., Italiano, F., Lazzaro, G., Ligi, M., Longo, M., Martorelli, E., Petracchini, L., Petricca, P., Polonia, A., and Sgroi, T., 2018. The Bortoluzzi Mud Volcano (Ionian Sea, Italy) and its potential for tracking the seismic cycle of active faults, Solid Earth, 10, 1–23, 2019. https://doi.org/10.5194/se-10-1-2019

D' Agostino N., A. Avallone, D. Cheloni, E. D'Anastasio, S. Mantenuto, and G. Selvaggi (2008), Active tectonics of the Adriatic region from GPS and earthquake slip vectors, Journal of Geophysical Research, 113, B12413, doi:12410.11029/12008JB005860.

D'Ortenzio, F., & Ribera d'Alcalà, M. (2009). On the trophic regimes of the Mediterranean Sea: a satellite analysis. Biogeosciences, 6(2), 139-148.

D'Ortenzio, F., Ragni, M., Marullo, S., & Ribera d'Alcalà, M. (2003). Did biological activity in the Ionian Sea change after the Eastern Mediterranean Transient? Results from the analysis of remote sensing observations. Journal of Geophysical Research: Oceans, 108(C9).

Dannowski A., H. Kopp, F. Klingelhöfer, D. Klaeschen, M.-A. Gutscher, A. Krabbenhöft, D. Dellong, David, M. Rovere, D. Graindorge, C. Papenberg, I. Klaucke, 2019. Ionian Abyssal Plain: a window into the Tethys oceanic lithosphere. Solid Earth, 10(2), 447-462.

de Voogd B., C. Truffert, N. Chamot-Rooke, P. Huchon, S. Lallemant, and X. Le Pichon (1992), Two-ship deep seismic soundings in the basins of the Eastern Mediterranean Sea (Pasiphae cruise), Geophysical Journal International, 109, 536-552.

Dellong, D., Klingelhoefer, F., Dannowski, A., Kopp, H., Murphy, S., Graindorge, D., Margheriti L., Moretti M., Barreca G., Scarfì L., Polonia A., GUtscher M.-A. (2020). Geometry of the Deep Calabrian Subduction (Central Mediterranean Sea) From Wide - Angle Seismic Data and 3 - D Gravity Modeling. Geochemistry, Geophysics, Geosystems, 21.

Doglioni C., Ligi, M., Scrocca, D., Bigi, S., Bortoluzzi, G., Carminati, E., Cuffaro, M., D'Oriano, F., Forleo, V., Muccini, F., Riguzzi, F., 2012. The tectonic puzzle of the Messina area (Southern Italy): Insights from new seismic reflection data. Sci. Rep. 2, 970.

Doll, M., Römer, M., Pape, T., Kölling, M., Kaul, N., dos Santos Ferreira, C., Bohrmann, G. (submitted), Recent activity and surface structures of Sartori Mud Volcano in the Calabrian Arc, Mediterranean Sea, Frontiers in Earth Science.

Doglioni, C., Merlini, S., Cantarella, G., 1999. Foredeep geometries at the front of the Apennines in the Ionian Sea (central Mediterranean). Earth Planet. Sci. Lett. 168, 243–254. doi:10.1016/S0012-821X(99)00059-X.

Emeis, K. C., Schulz, H., Struck, U., Rossignol-Strick, M., Erlenkeuser, H., Howell, M. W., Kroon, D., Mackensen, A., Ishizuka, S., Oba, T., Sakamoto, T., & Koizumi, I. (2003). Eastern Mediterranean surface water temperatures and δ18O composition during deposition of sapropels in the late Quaternary. PaleOceanography, 18(1).

Faccenna, C., Molin, P., Orecchio, B., Olivetti, V., Bellier, O., Funiciello, F., Minelli, L., Piromallo, C., Billi, A., 2011. Topography of the Calabria subduction zone (southern Italy): Clues for the origin of Mt. Etna. Tectonics 30, TC1003. doi:10.1029/2010TC002694.

Faccenna, C., Piromallo, C., Crespo-Blanc, A., Jolivet, L., Rossetti, F., 2004. Lateral slab deformation and the origin of the western Mediterranean arcs. Tectonics 23, TC1012. doi:10.1029/2002TC001488.

Foucher, J. P., Westbrook, G., Boetius, A., Ceramicola, S., Dupre, S., Mascle, J., et al. (2009). Structure and drivers of cold seep ecosystems. Oceanography, 22(1), 92–109.

Franchi, F., Rovere, M., Gamberi, F., H. Rashed, O. Vasellli, F. Tassi, 2017. Authigenic minerals from the Paola Ridge (southern Tyrrhenian Sea): Evidences of episodic methane seepage. Marine and Petroleum Geology 86, 228-247.

Gauchery, T., Rovere, M., Pellegrini, C., Cattaneo C., Campiani,E., Trincardi, F., 2021a. Factors controlling margin instability during the Plio-Quaternary in the Gela Basin (Strait of Sicily, Mediterranean Sea). Marine and Petroleum Geology 123, 104767.

Gauchery, T., Rovere, M., Pellegrini, C., Asioli, A., Tesi, T., Cattaneo, A., Trincardi, F., 2021b. Post-LGM multi-proxy sedimentary record of bottom-current variability and downslope sedimentary processes in a contourite drift of the Gela Basin (Strait of Sicily). Marine Geology 439 (2021) 106564.

Gerkema, T., & Zimmerman, J. T. F. (2008). An introduction to internal waves. Lecture Notes, Royal NIOZ, Texel, 207.

Geological Society (2018). Report on Geology and the UN Sustainable Development Goals,, Lodon. www.geolsoc.org.uk/sustainabledevelopment.

Goudeau, M. L. S., Grauel, A. L., Tessarolo, C., Leider, A., Chen, L., Bernasconi, S. M., Versteegh, G. J. M., Zonneveld, K. A. F., Boer, W., Alonso-Hernandez, C. M., & de Lange, G. J. (2014). The Glacial-Interglacial transition and Holocene environmental changes in sediments from the Gulf of Taranto, central Mediterranean. Marine Geology, 348, 88–102.

Govers, R., Wortel, M. J. R., 2005. Lithosphere tearing at STEP faults: Response to edges of subduction zones. Earth Planet. Sci. Lett., 236, 505–523. doi:10.1016/j.epsl.2005.03.022.

Gutscher, M.-A., Dominguez, S., Mercier de Lepinay, B., Pinheiro, L., Gallais, F., Babonneau, N., Cattaneo, A., Le Faou, Y., Barreca, G., Micallet, A., Rovere, M., 2015. Tectonic expression of an active slab tear from high-ressolution seismic and bathymetric data offshore Sicily (Ionian Sea), Tectonics 34, doi:10.1002/2015TC003898.

Gutscher, M.- A., Kopp, H., Krastel, S., Bohrmann, G., Garlan, T., Zaragosi, S., Klaucke, I., Wintersteller, P., Loubrieu, B., le Faou, Y., San Pedro, L., Dominguez, S., Rovere, M., Mercier de Lepinay, B., Ranero, C., Sallares, V., 2017. Active tectonics of the Calabrian subduction revealed by new multi- beam bathymetric data and high-resolution seismic profiles in the Ionian Sea (Central Mediterranean). Earth and Planetary Science Letters, 461, 61– 72.

Hansell, D.A. (2005), Dissolved Organic Carbon Reference Material Program, Eos Trans. AGU, 86(35), 318–318.

Hensen C, Duarte JC, Vannucchi P, Mazzini A, Lever MA, Terrinha P, Géli L, Henry P, Villinger H, Morgan J, Schmidt M, Gutscher M-A, Bartolome R, Tomonaga Y, Polonia A, Gràcia

E, Tinivella U, Lupi M, Çagatay MN, Elvert M, Sakellariou D, Matias L, Kipfer R, Karageorgis AP, Ruffine L, Liebetrau V, Pierre C, Schmidt C, Batista L, Gasperini L, Burwicz E, Neres M, Nuzzo M. (2019) Marine Transform Faults and Fracture Zones: A Joint Perspective Integrating Seismicity, Fluid Flow and Life. Front. Earth Sci. 7:39. doi: 10.3389/feart.2019.00039

Holte, J., & Straneo, F. (2017). Seasonal overturning of the Labrador Sea as observed by Argo floats. Journal of Physical Oceanography, 47(10), 2531-2543.

Insinga, D.D., Tamburrino, S., Lirer, F., Vezzoli, L., Barra, M., De Lange, G.J., Tiepolo, M., Vallefuoco, M., Mazzola, S., Sprovieri, M., 2014. Tephrochronology of the astronomically-tuned KC01B deep-sea core, Ionian Sea: Insights into the explosive activity of the Central Mediterranean area during the last 200ka. Quat. Sci. Rev. 85, 63–84.

IOCCG Protocol Series (2018). Inherent Optical Property Measurements and Protocols: Absorption Coefficient, Neeley, A. R. and Mannino, A. (eds.), IOCCG Ocean Optics and Biogeochemistry Protocols for Satellite Ocean Colour Sensor Validation, Volume 1.0, IOCCG, Dartmouth, NS, Canada.

Klein, B., Roether, W., Kress, N., Manca, B. B., Ribera d'Alcala, M., Souvermezoglou, E., ... & Luchetta, A. (2003). Accelerated oxygen consumption in eastern Mediterranean deep waters following the recent changes in thermohaline circulation. Journal of Geophysical Research: Oceans, 108(C9).

Kunze, E., Firing, E., Hummon, J. M., Chereskin, T. K., & Thurnherr, A. M. (2006). Global abyssal mixing inferred from lowered ADCP shear and CTD strain profiles. Journal of Physical Oceanography, 36(8), 1553-1576.

Lawaetz A.J. & Stedmon C.A. (2009). Fluorescence Intensity Calibration Using the Raman Scatter Peak of Water. Applied Spectroscopy; 63(8):936-940.

La Ferla, R., Azzaro, M., Civitarese, G., & Ribera d'Alcalà, M. (2003). Distribution patterns of carbon oxidation in the eastern Mediterranean Sea: evidence of changes in the remineralization processes. Journal of Geophysical Research: Oceans, 108(C9).

Liubartseva, S., Federico, I., Coppini, G., Lecci, R. (2021). Stochastic oil spill modeling for environmental protection at the Port of Taranto (southern Italy). Mar. Pollut. Bull., 171,12744.

Loher, M., Ceramicola, S., Wintersteller, P., Meinecke, G., Sahling, H., & Bohrmann, G. (2018a). Mud volcanism in a canyon: Morphodynamic evolution of the active Venere mud volcano and its interplay with Squillace Canyon, Central Mediterranean. Geochemistry, Geophysics, Geosystems, 19, 356–378.

Loher, M., Pape, T., Marcon, Y., Römer, M., Wintersteller, P., Praeg, D., Torres, M., Sahling, H., & Bohrmann, G. (2018b). Mud extrusion and ring-fault gas seepage - Upward branching fluid discharge at a deep-sea mud volcano. Scientific Reports, 8(1).

Malanotte-Rizzoli, P., B.B. Manca, M. Ribera d'Alcalà, A. Theocharis, S. Brenner, G. Budillon and G.E. Ozsoy, The eastern Mediterranean in the 80's and in the 90's: The big transition in the intermediate and deep circulation, Dynam. Atmosph. Oceans 29 (1999), pp. 365–395.

Malinverno, A., Ryan, W. B. F., 1986. Extension in the Tyrrhenian Sea and shortening in the Apennines as result of arc migration driven by sinking of the lithosphere. Tectonics 5, 227–245. doi:10.1029/TC005i002p00227.

Marani, M., Argnani, A., Roveri, M., & Trincardi, F. (1993). Sediment drifts and erosional surfaces in the central Mediterranean: Seismic evidence of bottom- current activity. Sedimentary Geology, 82, 207– 220.

Mazzini, A., & Etiope, G. (2017). Mud volcanism: An updated review. Earth-Science Reviews, 168, 81–112.

Merlini, S., Cantarella, G., & Doglioni, C. (2000). On the seismic profile Crop M5 in the Ionian Sea. Bollettino della Società Geologica Italiana, 119(2), 227-236.

Micallef, A., Krastel, S., & Savini, A. (2022). Submarine geomorphology. Geological Society, London, Memoirs, 58, 379– 394.

Minelli, L., Faccenna, C., 2010. Evolution of the Calabrian accretionary wedge (central Mediterranean). Tectonics 29, TC4004. doi:10.1029/2009TC002562.
Morlotti, E., Sartori, R., Torelli, L., Barbieri, F., & Raffi, I. (1982). Chaotic deposits fromthe external Calabrian Arc (Ionian Sea, easternMediterranean). Memorie - Società Geologica Italiana, 24, 261–275.
Napolitano, E., Sannino, G., Artale, V., & Marullo, S. (2003). Modeling the baroclinic circulation in the area of the Sicily channel: The role of stratification and energy diagnostics. Journal of Geophysical Research: Oceans, 108(C7).
Narcisi, B., Vezzoli, L., 1999. Quaternary stratigraphy of distal tephra layers in the Mediterranean - An overview. Glob. Planet. Change 21, 31–50.
Negri, A., Capotondi, L., & Keller, J. (1999). Calcareous nannofossils, planktonic foraminifera and oxygen isotopes in the late Quaternary sapropels of the Ionian Sea. Marine Geology, 157(1-2), 89-103.
Omanović et al. (2019). An all-inclusive tool for analysis of UV–Vis spectra of colored dissolved organic matter (CDOM), Computers & Geosciences, 133, 104334.
Panieri G., Polonia A., Lucchi R. G., Zironi S., Capotondi L., Negri A., Torelli L., 2013. Mud volcanoes along the inner deformation front of the Calabrian Arc accretionary wedge (Ionian Sea). Marine Geology 336 (2013) 84–98.
Pape, T., Feseker, T., Kasten, S., Fischer, D., & Bohrmann, G. (2011). Distribution and abundance of gas hydrates in near-surface deposits of the Håkon Mosby Mud Volcano, SW Barents Sea. Geochemistry Geophysics Geosystems, 12, Q09009.
Pepe, F., di Donato, V., Insinga, D., Molisso, F., Faraci, C., Sacchi, M., Dera, R., Ferranti, L., & Passaro, S. (2018). Seismic stratigraphy of upper quaternary shallow- water contourite drifts in the Gulf of Taranto (Ionian Sea, southern Italy). Marine Geology, 397, 79– 92.
Placenti, F., Azzaro, M., Artale, V. et al. Biogeochemical patterns and microbial processes in the Eastern Mediterranean Deep Water of Ionian Sea. Hydrobiologia 815, 97–112 (2018).
Polonia A., Panieri G, Gasperini L, Gasparotto G, Bellucci L.G, Torelli L., 2013. Turbidite paleoseismology in the Calabrian Arc Subduction Complex (Ionian Sea). Geochemistry Geophysics Geosystems 01/2013; 14(1):112-140. doi:10.1029/2012GC004402
Polonia A., Gasperini L., Asioli A., Bonatti E., Hensen C., Lever M., Morgan J., Vanucchi P., Ruffine L., 2019. Serpentinite diapirs in the Calabrian Subduction sYstem return Lower plate mantLe from EArth's oldest ocean (SCYLLA). IODP 968-Pre.
Polonia A., Torelli L., Artoni A., M. Carlini, Faccenna C., Ferranti L., Gasperini L., Govers R., Klaeschen D., Monaco C., Neri G., Nijholt N., Orecchio B., Wortel R., 2016. The Ionian and Alfeo-Etna fault zones: new segments of an evolving plate boundary in the central Mediterranean Sea? Tectonophysics, 675, 69-90, 10.1016/j.tecto.2016.03.016.
Polonia A., Torelli L., Gasperini L., Cocchi L., Muccini F., Bonatti E., Hensen C., Schmidt M., S Romano, Artoni A., Carlini M., 2017. Lower plate serpentinite diapirism in the Calabrian Arc subduction complex. Nature Communications 8 (1), 2172.
Polonia A., Torelli L., Mussoni P., Gasperini L., Artoni A., Klaeschen D., 2011. The Calabrian Arc subduction complex in the Ionian Sea: Regional architecture, active deformation, and seismic hazard, Tectonics, 30 (5) , TC5018.
Polonia A., C. Bonetti, J. Bonetti, M.N. Çağatay, A. Gallerani, L. Gasperini, C. H. Nelson, S. Romano, 2021. Deciphering co-seismic sedimentary processes in the Mediterranean Sea using elemental, organic carbon and isotopic data. Geochemistry, Geophysics, Geosystems, 9446.
Powley, H. R., Krom, M. D., & Van Cappellen, P. (2017). Understanding the unique biogeochemistry of the Mediterranean Sea: Insights from a coupled phosphorus and nitrogen model. Global Biogeochemical Cycles, 31(6), 1010-1031.
Prandke et al. (2000). MITEC technology development: The microstructure/turbulence measuring system. Tech. Rep. EUR 19733 EN, European Commission, Joint Research Centre, Ispra, Italy.

Retelletti Brogi et al. (2021). DOM Biological Lability in an Estuarine System in Two Contrasting Periods. J. Mar. Sci. Eng. 2021, 9, 172.
Rovere, M., Gamberi, F., Mercorella, A., H. Rashed, A. Gallerani, E. Leidi, M. Marani, V. Funari, G.A. Pini, 2014. Venting and seepage systems associated with mud volcanoes and mud diapirs in the southern Tyrrhenian Sea. Marine Geology, 347, 153-171.
Rovere, M., Campiani, E., Leidi, E., Mercorella, A., 2017. Natural hydrocarbon seepage in the Italian offshore. Geoingegneria Ambientale e Mineraria, Anno LIV, 3, 35-40.
Rovere, M., Mercorella, A., Frapiccini, E., V. Funari, F. Spagnoli, C. Pellegrini, A. S. Bonetti, T. Veneruso, A. N. Tassetti, M. Dell'Orso, M. Mastroianni, G. Giuliani, R. De Marco, G. Fabi, F. Ciccone, I. Antoncecchi, 2020. Geochemical and Geophysical Monitoring of Hydrocarbon Seepage in the Adriatic Sea. Sensors, 20, 1504.
Rovere, M., Mercorella, A., Gamberi, F., Zgur, F., 2022. Hydrothermal vent complexes control seepage and hydrocarbon release on the overriding plate of the Tyrrhenian-Ionian subduction system (Paola Basin). Frontiers in Earth Science 10:852786.
Praeg, D., Ceramicola, S., Barbieri, R., Unnithan, V., & Wardell, N. (2009). Tectonically-driven mud volcanism since the late Pliocene on the Calabrian Accretionary Prism, Central Mediterranean Sea. Marine and Petroleum Geology, 26(9), 1849–1865.
Rebesco, M., Camerlenghi, A., Munari, V., Mosetti, R., Ford, J., Micallef, A., & Facchin, L. (2021). Bottom current- controlled Quaternary sedimentation at the foot of the Malta Escarpment (Ionian Basin, Mediterranean). Marine Geology, 441, 106596.
Roether, W., & Schlitzer, R. (1991). Eastern Mediterranean deep water renewal on the basis of chlorofluoromethane and tritium data. Dynamics of Atmospheres and Oceans, 15(3-5), 333-354.
Roether, W., B. Klein, B.B. Manca, A. Theocharis, S. Kioroglou , Progr. Ocean., 74 (2007) 540-571.
Roether, W., Manca, B. B., Klein, B., Bregant, D., Georgopoulos, D., Beitzel, V., ... & Luchetta, A. (1996). Recent changes in eastern Mediterranean deep waters. Science, 271(5247), 333-335.
Rosenbaum, G., Gasparon, M., Lucente, F. P., Peccerillo, A., Miller, M. S., 2008. Kinematics of slab tear faults during subduction segmentation and implications for Italian magmatism. Tectonics 27, TC2008. doi:10.1029/2007TC002143.
Rubino, A., Falcini, F., Zanchettin, D., Bouche, V., Salusti, E., Bensi, M., ... & Capone, A. (2012). Abyssal undular vortices in the Eastern Mediterranean basin. Nature communications, 3(1), 1-6.
Santinelli et al. (2015). Carbon isotope measurements reveal unexpected cycling of dissolved organic matter in the deep Mediterranean Sea, Marine Chemistry, 177, 2, 267-277.
Santinelli et al. (2021). Surface transport of DOC acts as a trophic link among Mediterranean sub-basins, Biogeosciences Discuss. https://doi.org/10.5194/bg-2018-418, 2018.Ribera d'Alcalà, M., Civitarese, G., Conversano, F., & Lavezza, R. (2003). Nutrient ratios and fluxes hint at overlooked processes in the Mediterranean Sea. Journal of Geophysical Research: Oceans, 108(C9).
Schellart, W. P. Mount Etna-Iblean volcanism caused by rollback-induced upper mantle upwelling around the Ionian slab edge: An alternative to the plume model. Geology 38, 691–694 (2010)Speranza, F., Minelli, L., Pignatelli, A. & Chiappini, M. The Ionian Sea: The oldest in situ ocean fragment of the world? J. Geophys. Res. Solid Earth 117, 1–13 (2012).
Schlitzer, R., Roether, W., Oster, H., Junghans, H. G., Hausmann, M., Johannsen, H., & Michelato, A. (1991). Chlorofluoromethane and oxygen in the Eastern Mediterranean. Deep Sea Research Part A. Oceanographic Research Papers, 38(12), 1531-1551.
Schroeder, K., Gasparini, G. P., Tangherlini, M., & Astraldi, M. (2006). Deep and intermediate water in the western Mediterranean under the influence of the Eastern Mediterranean Transient. Geophysical Research Letters, 33(21).
Selvaggi G. and C. Chiarabba, 1995. Seismicity and P-Wave Velocity Image of the Southern Tyrrhenian Subduction Zone. Geophysical Journal International, 121, 3, 818-826.

Send, U., & Testor, P. (2017). Direct observations reveal the deep circulation of the western Mediterranean Sea. Journal of Geophysical Research: Oceans, 122(12), 10091-10098.

Sparnocchia, S., Gasparini, G. P., Astraldi, M., Borghini, M., & Pistek, P. (1999). Dynamics and mixing of the Eastern Mediterranean outflow in the Tyrrhenian basin. Journal of Marine Systems, 20(1-4), 301-317.

Theocharis, A., B. Klein, K. Nittis, W. Roether, J. Mar. Syst., 33–34 (2002) 91–116.

Tugend, J., Chamot-Rooke, N., Arsenikos, S., Blanpied, C., & Frizon deLamotte, D. (2019). Geology of theIonian Basin and margins: A key to theEast Mediterranean geodynamics. Tectonics,38, 2668–2702.

van Haren, H., & Gostiaux, L. (2011). Large internal waves advection in very weakly stratified deep Mediterranean waters. Geophysical Research Letters, 38(22).

Van Heukelem L. & Thomas C.S. (2001). Computer-assisted high-performance liquid chromatography method development with applications to the isolation and analysis of phytoplankton pigments. Journal of Chromatography A, 910(1), 31-49.

Waldman, R., Brüggemann, N., Bosse, A., Spall, M., Somot, S., & Sevault, F. (2018). Overturning the Mediterranean thermohaline circulation. Geophysical Research Letters, 45(16), 8407-8415.

Wüst, G. (1961). On the vertical circulation of the Mediterranean Sea. Journal of Geophysical Research, 66(10), 3261-3271.

Zaccone, R., Caruso, G., Azzaro, M., Azzaro, F., Crisafi, E., Decembrini, F., De Domenico, E., De Domenico, M., La Ferla, R., Leonardi, M. , Lo Giudice, A., Maimone, G., Mancuso, M., Michaud, L. , Monticelli, L. S. , Raffa, F. , Ruggeri, G. and Bruni, V.(2010) 'Prokaryotic activities and abundance in pelagic areas of the Ionian Sea', Chemistry and Ecology, 26: 1, 169 — 197.

Zaccone, R., Monticelli, L. S., Seritti, A., Santinelli, C., Azzaro, M., Boldrin, A., ... & Ribera d'Alcalà, M. (2003). Bacterial processes in the intermediate and deep layers of the Ionian Sea in winter 1999: vertical profiles and their relationship to the different water masses. Journal of Geophysical Research: Oceans, 108(C9).

Zecchin, M., Civile, D., Caffau, M., Critelli, S., Muto, F., Mangano, G., & Ceramicola, S. (2020). Sedimentary evolution of the Neogene-Quaternary Crotone Basin (southern Italy) and relationships with large-scale tectonics: A sequence stratigraphic approach. Marine and Petroleum Geology, 117, 104381.

Appendix 1

Logbook of Activities

DIARIO DI BORDO PIONEER 2023 GAIA BLU - OPERAZIONI

DATA	ORARIO UTC	LONG DDMM.xxx	LAT DDMM.xxx	LONG DD.xxx	LAT DD.xxx	STAZIONE UNIVOCA	STAZIONE STRUMENTO	PROFONDITA' (m)	NOTE BREVI	FILE GEOFISICA	FILE LOG	ANNOTAZIONI	CONDIZIONI METEO
11/19/2023	6:40	15°05.5411' E	37°29.737' N									Partenza porto di Catania e trasferimento verso la stazione 22	mare leggermente mosso, poco vento
	8:57					22						raggiunta stazione 22. iniziano preparativi per carotaggio.	
11/19/2023	10:15	15°25.517037	37°26.383097	15.4252840	37.4397183	22	PI23_GR01	1980		012_323_0935_100737_CHT4.0_FLT_000.sgy (CHIRP);	191123_10.txt	Carotiere sul fondo. velocità di discesa 1 m/s; tiro max 4 t; penetrazione circa 4 m;	mare leggermente mosso,
11/19/2023	12:40	15°25.547600	37°26.383479	15.4257933	37.4397247	22	PI23_CTD01S		CTD + SVP		191123_12.txt	CTD e SVP. CTD in acqua. CTD calata da verricello di dritta.	
11/19/2023	12:44	15°25.547969	37°26.383790	15.4257995	37.4397298	22	PI23_CTD01B	200	CTD + SVP	svp_20231119_1240	191123_12.txt	STOP a 200 m; inizio recupero	
11/19/2023	12:53	15°25.523' E	37°26.387' N	15.4253833	37.4397833	22	PI23_CTD01E				191123_12.txt	CTD a bordo	
11/19/2023	13:05	15°25.520' E	37°26.397' N	15.4253333	37.4399500	22	PI23_RAD01				191123_13.txt	sonda per radiometria in acqua. Le calate vengono effettuate da poppa, lato dritta.	
11/19/2023	13:37									MB EM304 SOL 0001	191123_13.txt		
11/19/2023	13:50									MB EM304 SOL 0002	191123_13.txt		
11/19/2023	14:04									MB EM304 SOL 0003 con Water Column	191123_14.txt	acquisito MB con scopo di scouting su stazione 25	
11/19/2023	14:30											Carotiere in acqua, profondità presunta 2070 m	
11/19/2023	14:54	15°25.445300'	37°26.261400	15.4240883	37.4376900	25	PI23_GC02	2070		MB EM304 line 0003 con Water Column	191123_14.txt	carotiere sul fondo; velocità di discesa 1 m/s; tiro max 4,2 t; penetrazione circa 2 m; recupero 0 m	
11/19/2023	15:06									MB EM304 EOL 0003	191123_15.txt	insertia sonda SVP nel multibeam	
11/19/2023	15:40										191123_15.txt	Carotiere a bordo. Inizio test su motori	
11/19/2023	15:52									MB EM304 SOL 0004 no Water Column;	191123_15.txt	Inizio tersferimento verso stazione 3 passando per due punti con possibile presenza di relitti (Zona_7 e Zona_8).	
11/19/2023	16:08									SOL magnetometro	191123_16.txt	calato magnetometro da poppa. Circa 250 m di cavo fuori	
11/19/2023	18:36									MB EM304 line 0004, 0005	191123_18.txt		
11/20/2023	0:52									MB EM304 line 0007	201123_00.txt	transito su target relitto ZONA_7	
11/20/2023	0:54										201123_00.txt	transito verso target relitto ZONA_8	
11/20/2023	5:09									MB EM304 line 0008	201123_05.txt		mare da W-NW onda 0.8 m; swell N-NE 1 m di onda lunga; vento W-NW 10-11 nodi con raffiche da 12 nodi.
11/20/2023	7:11									MB EM304 line 0010	201123_07.txt	transito su target relitto ZONA_8	
11/20/2023	7:20										201123_07.txt	trasferimento verso stazione 3. ridotta velocità a 2 kn per recupero magnetometro	
11/20/2023	7:35										201123_07.txt	MAGNETOMETRO A BORDO	
11/20/2023	8:20					3				ADCP file POINEER 001	201123_08.txt	arrivo sulla stazione 3: acceso ADCP di bordo. Usata sia frequenza 45 kHz che 300 kHz	
11/20/2023	8:55	17°48.204306	35°51.473249	17.8034051	35.8578875	3	PI23_CTD02S	3968			201123_08.txt	CTD in acqua	
11/20/2023	9:00										201123_09.txt	CTD torna a pelo d'acqua e dopo un minuto ricomincia la calata	
11/20/2023	9:53										201123_09.txt	STOP a 2280 m per sistemare il verricello	
11/20/2023	9:56										201123_09.txt	riprende la discesa	
11/20/2023	10:14										201123_10.txt	STOP per controllo verricello	
11/20/2023	10:21										201123_10.txt	riprende la discesa	
11/20/2023	11:00	17°48.208581	35°51.557075	17.8034764	35.8592846	3	PI23_CTD02B	3950	CTD		201123_11.txt	STOP calata a 3950 m, inizio recupero	
11/20/2023	11:44	17°48.057306	35°51.860743	17.8009551	35.8643457	3	PI23_CTD02E				201123_11.txt	CTD a bordo	
11/20/2023	12:34	17°46.411729	35°52.527834	17.7735288	35.8754639	3	PI23_RAD02S	3969			201123_12.txt	sonda per radiometria in acqua	
11/20/2023	12:48	17°45.971453	35°52.988856	17.7661909	35.8831476	3	PI23_RAD02E				201123_12.txt	sonda per radiometria a bordo	
11/20/2023	13:05										201123_13.txt	tentativo di retinata. Operazione non conclusa a causa delle condizioni meteo. Si decide di effettuare lancio sonda ARGO e misure di turbolenza	
11/20/2023	13:08										201123_13.txt		vento da W con raffiche di 25 nodi; mare da W con onde di 1,5-2 m; swell da N-NE con 1,5 m di onda; corrente ver
11/20/2023	13:41									MB EM304 SOL 0012 no Water Column	201123_13.txt	MB di scouting nella stazione 3	
11/20/2023	14:10									MB EM304 EOL 0012	201123_14.txt		
11/20/2023	14:39	17°48.100920	35°51.429981	17.8016820	35.8571664	3	PI23_BGC-ARGO	3967			201123_14.txt	lancio BOA ARGO. Sonda calata con A-frame di poppa	
11/20/2023	14:50	17°47.87'E	35°51.407'N	17.7978333	35.8567833	3	PI23_TURB01S	3967 m bsl	1020 m fine calata		201123_14.txt	Sonda per misure di turbolenza in acqua. Fine calata 1020 m e poi recupero. La sonda viene calata con piccolo verricello posto a poppa lato di sinistra.	
11/20/2023	15:25	17°47.1540'E	35°51.8706'N	17.7859000	35.8645100	3	PI23_TURB02S	3967 m bsl	920 m fine calata		201123_15.txt	sonda per misure di turbolenza in acqua. Termine della calata 920 m di profondità, poi recupero	
11/20/2023	16:04	17°46.356902	35°52.352410	17.7726150	35.8725402	3	PI23_TURB02E				201123_16.txt	sonda a bordo	
11/20/2023	16:06	17°46.261799	35°52.352410	17.7710300	35.8725402	3	PI23_TURB03S				201123_16.txt	sonda per misure di turbolenza in acqua.	
11/20/2023	16:22	17°45.949497	35°52.575000	17.7658250	35.8762500	3	PI23_TURB03B				201123_16.txt	Stop calata circa 900 m, inizio recupero	
11/20/2023	16:25	17°45.870124	35°52.615458	17.7645021	35.8769243	3	PI23_TURB03E				201123_16.txt	sonda a bordo	
11/20/2023	16:27	17°45.847594	35°52.630056	17.7641266	35.8771676	3	PI23_TURB04S				201123_16.txt	sonda per mmisure di turbolenza in acqua	
11/20/2023	17:08	17°45.007493	35°53.093526	17.7501249	35.8848921	3	PI23_TURB04E				201123_17.txt	sonda a bordo	
11/20/2023	17:27	17°44.918287	35°53.178157	17.7486381	35.8863026	3	PI23_CTD03S	3954	CTD + IOP +SVP		201123_17.txt	CTD, IOP e SVP. CTD in acqua Non risultano salvati file SVP	
11/20/2023	17:39	17°44.920007	35°53.178386	17.7486668	35.8863064	3	PI23_CTD03B		circa 99 m fine calata		201123_17.txt	Stop calata circa 99 m. inizio recupero	
11/20/2023	17:43	17°44.918449	35°53.179780	17.7486408	35.8862996	3	PI23_CTD03E				201123_17.txt	CTD a bordo	
11/20/2023	17:57	17°44.920063	35°53.177247	17.7486677	35.8862875	3	PI23_CTD04S	3954 m bsl		svp_20231120_1901	201123_17.txt	CTD in acqua. Collegata sonda SVP per il profilo di velocità da inserire nel MB	
11/20/2023	18:17	17°44.921787	35°53.180317	17.7486965	35.8863386	3	PI23_CTD04B		stop discesa 1000 m		201123_18.txt	Stop discesa 1000 m. Inizio recupero.	
11/20/2023	18:44	17°44.927066	35°53.181499	17.7487844	35.8863583	3	PI23_CTD04E				201123_18.txt	CTD a bordo	
11/20/2023	19:12									MB EM304 SOL 0013	201123_19.txt	Inserito nuovo profilo di velocità. Trasferimento verso stazione 11	
11/21/2023	0:09					11				MB EM304 EOL 0014	211123_00.txt	preparazione per sonda di turbolenza. Previste 3 calate fino a circa 1000 m.	
11/21/2023	0:12	16°56.690728	36°06.929088	3N		11	PI23_TURB05S				211123_00.txt	sonda per misure di turbolenza in acqua	
11/21/2023	0:20					11					211123_00.txt	recupero sonda per problema tecnico	
11/21/2023	0:26					11					211123_00.txt	sonda a bordo, controllo strumento.	
11/21/2023	0:45	16°56.682984	36°07.073490	4N		11	PI23_TURB06S				211123_00.txt	sonda per misure di turbolenza in acqua	
11/21/2023	0:50					11					211123_00.txt	problema tecnico non risolto. Si recupera nuovamente lo strumento	
11/21/2023	1:08					11				MB EM304 SOL 0015	211123_01.txt	i problemi tecnici non sono attualmente risolvibili. Si decide di sospendere l'attività. Non potendo fare altre misurazioni o campionamenti si decide fi acquisire con il MB per aumentare la copertura batimetrica nell'area attorno alla stazione 11.	
11/21/2023	2:02					11				MB EM304 EOL 0015	211123_02.txt		
11/21/2023	2:30					11				MB EM304 SOL 0016	211123_02.txt		
11/21/2023	2:44					11				MB EM304 EOL 0016	211123_02.txt		
11/21/2023	3:18					11					211123_03.txt	preparazione per calata CTD deep	
11/21/2023	3:22	16°56.674609	36°06.969355	16.9445768	36.1161559	11	PI23_CTD05S	3412 m dbsl			211123_03.txt	CTD in acqua	
11/21/2023	4:20	16°56.678491	36°06.970837	16.9446415	36.1161806	11	PI23_CTD05B		stop discesa 3360 m		211123_04.txt	STOP calata 3360 m. Inizio recupero	
11/21/2023	5:14	16°56.684071	36°06.966184	16.9447345	36.1161031	11	PI23_CTD05E	3419 m bsl			211123_05.txt	sonda a bordo	
11/21/2023	5:19					11					211123_05.txt	Preparativi per calata retino. Sono previsti 3 campionamenti a diverse profondità: uno 0-100 m; uno a profondità 100-300 m; uno a profondità 300-500 m	CONDIZIONI METEO: vento W-SW con velocità 15 nodi e raffiche fino a 20 nodi; mare da W-SW con onda di 1 m;
11/21/2023	5:58	16°56.696553	36°06.964022	16.9449426	36.1160670	11	PI23_RET01S	3419 m bsl			211123_05.txt	retino in acqua. Il retino viene calato con verricello piccolo a poppa lato di simistra.	
11/21/2023	6:03	16°56.696523	36°06.962879	16.9449421	36.1160480	11	PI23_RET01B		stop discesa 100 m		211123_06.txt	STOP calata a 100 m. Inizio recupero	
11/21/2023	6:07	16°56.695771	36°06.962466	16.9449295	36.1160411	11	PI23_RET01E	3419 m bsl			211123_06.txt	retino a bordo.	
11/21/2023	6:22	16°56.696673	36°06.962612	16.9449446	36.1160435	11	PI23_RET02S	3419 m bsl			211123_06.txt	retino inacqua	
11/21/2023	6:35	16°56.695891	36°06.961835	16.9449315	36.1160306	11	PI23_RET02B		stop discesa 300 m		211123_06.txt	STOP calata 300 m, risalita a 100 m e chiusura. Recupero	
11/21/2023	6:51	16°56.698974	36°06.961835	16.9449829	36.1160306	11	PI23_RET02E	3419 m bsl			211123_06.txt	retino a bordo.	

11/21/2023	6:53					11					211123_06.txt		VENTO IN LEGGERO AUMENTO				
11/21/2023	7:13	16°56.700266	36°06.958665	16.9450044	36.1159778	11	PI23_RET03S	3419 m bsl			211123_07.txt	retino inacqua					
11/21/2023	7:26	16°56.701562	36°06.959623	16.9450260	36.1159937	11	PI23_RET03B		stop discesa 500 m		211123_07.txt	STOP calata a 500 m, risalita a 300 m e chiusura. Recupero					
11/21/2023	7:45	16°56.701414	36°06.957016	16.9450236	36.1159503	11	PI23_RET03E	3419 m bsl			211123_07.txt	retino in superficie					
11/21/2023	7:46					11					211123_07.txt	retino a bordo.					
11/21/2023	8:02	16°56.689836	36°06.981017	16.9448306	36.1163503	11	PI23_CTD06S	3420 m bsl	CTD + SVP	svp_20231121_0830	211123_08.txt	CTD e SVP. CTD in acqua.					
11/21/2023	8:14	16°56.690748	36°06.961737	16.9448458	36.1160290	11	PI23_CTD06B		stop discesa 500 m		211123_08.txt	STOP calata a 510 m. Inizio recupero					
11/21/2023	8:28	16°56.693616	36°06.960754	16.9448458	36.1160126	11	PI23_CTD06E	3420 m bsl			211123_08.txt	CTD a bordo					
11/21/2023	8:44	16°56.698178	36°06.958368	16.9449696	36.1159728	11	PI23_RAD03S				211123_08.txt	Sonda per radiometria in acqua					
11/21/2023	9:06	16°56.462745	36°06.909833	16.9410458	36.1151639	11	PI23_RAD03E				211123_09.txt	Sonda per radiometria a bordo					
11/21/2023	9:27	16°56.375502	36°06.895529	16.9395917	36.1149255	11	PI23_CTD07S		CTD +IOP		211123_09.txt	CTD e IOP. Calata CTD senza aprire le bottiglie. CTD in acqua.					
11/21/2023	9:39	16°56.379294	36°06.895363	16.9396549	36.1149227	11	PI23_CTD07B		stop discesa 98 m		211123_09.txt	STOP calata 100 m. Inizio recupero					
11/21/2023	9:45	16°56.375502	36°06.895084	16.9395917	36.1149181	11	PI23_CTD07E				211123_09.txt	CTD a bordo					
11/21/2023	9:46	16°56.379987	36°06.895948	16.9396665	36.1149325	11	PI23_CTD08S		CTD +IOP		211123_09.txt	CTD e IOP. Calata CTD senza aprire le bottiglie. CTD in acqua					
11/21/2023	9:56					11					211123_10.txt	inizio discesa					
11/21/2023	10:00	16°56.381308	36°06.894067	16.9396885	36.1149011	11	PI23_CTD08B		stop discesa 98 m		211123_10.txt	STOP calata a 98 m. Inizio recupero					
11/21/2023	10:06	16°56.381308	36°06.893101	16.9396885	36.1148850	11	PI23_CTD08E				211123_10.txt	CTD a bordo					
11/21/2023	10:43					11					211123_10.txt	Inizio operazioni per carotaggio profondo. Armato carotiere con 2 tubi da 5 m					
11/21/2023	11:08					11		3435 m bsl			211123_11.txt	carotiere in acqua					
11/21/2023	12:00	16°56.362655	36°06.895468	16.9393776	36.1149245	11	PI23_GC03	3434m bsl			211123_12.txt	carotiere sul fondo					
11/21/2023	12:02					11					211123_12.txt	recupero carotiere					
11/21/2023	13:06					11					211123_13.txt	carotiere a bordo. Penetrazione 1.70 m, recupero 1.70 m. Si decide di provare un nuovo carotaggio					
11/21/2023	13:50					11		3492 m bsl			211123_13.txt	carotiere in acqua					
11/21/2023	14:30	16°56.672482	36°06.650414	16.9445414	36.1108402	11	PI23_GC04	3492 m bsl			211123_14.txt	carotiere sul fondo; massimo tiro 5.7 t					
11/21/2023	15:44					11					211123_15.txt	carotiere a bordo. Penetrazione 10 m, recupero 5 m.					
11/21/2023	16:18	16°56.787023	36°06.387717	16.9464504	36.1064620	11	PI23_TURB07S	3375 m bsl			211123_16.txt	sonda per misure di turbolenza in acqua					
11/21/2023	16:25					11					211123_16.txt	inizio recupero sonda per problemi tecnici					
11/21/2023	16:32					11					211123_16.txt	sonda a bordo. Stand by per risolvere problemi tecnici sonda					
11/21/2023	16:42	16°56.289142	36°06.157855	16.9381524	36.1026309	11	PI23_TURB08S	3375 m bsl			211123_16.txt	sonda per misure di turbolenza in acqua.					
11/21/2023	16:52					11					211123_16.txt	inizio recupero sonda per problemi tecnici non risolti					
11/21/2023	16:57					11					211123_16.txt	sonda a bordo. Termine operazioni con sonda di turbolenza. Vengono pianificate due linee (L1 e L2) tra loro ortogonali che passano sopra il punto di carotaggio PI23_GC04. Durante le linee si acquisiranno dati chirp.					
11/21/2023	17:31			16.9159550	36.1044340	11				CHIRP SOL 0011_2023_325_1731	211123_17.txt	inizio linea L1 line bearing 73.43°; vessel speed 4.8 m					
11/21/2023	17:42					11					211123_17.txt	la nave passa vicino al punto PI23_GC04 con direzione 73°. Ch 3.5 kHz; Tx pulse 64 ms; Tx Power 3; Range 500; Sound speed 1519; Ping Rate 250 ms					
11/21/2023	18:01			16.9755500	36.1177710	11				CHIRP EOL 0011_2023_325_1731	211123_18.txt	fine linea accostata a sinistra per prendere la linea L2					
11/21/2023	18:02					11				CHIRP SOL 0012_2023_325_1803	211123_18.txt	inizio trasferimento tra L1 ed L2					
11/21/2023	18:46					11				CHIRP EOL 0012_2023_325_1803	211123_18.txt	fine trasferimento tra L1 ed L2					
11/21/2023	18:46			16.9382010	36.1299902	11				CHIRP SOL 0012_2023_325_1848	211123_18.txt	inizio linea L2, acquisizione CHIRP con bearing 163° circa					
11/21/2023	19:04					11					211123_19.txt	la nave passa vicino al punto PI23_GC04 con direzione 163°					
11/21/2023	19:31			16.9546360	36.0815450	11				CHIRP EOL 0012_2023_325_1848	211123_19.txt	fine linea L2.					
11/21/2023	19:40	16°57.421209	36°04.487997	16.9570202	36.0748000	11	PI23_TURB09S				211123_19.txt	sonda per misure di turbolenza in acqua					
11/21/2023	20:08	16°56.895926	36°04.577892	16.9482654	36.0762982	11	PI23_TURB10S				211123_20.txt	sonda per mmisure di turbolenza in acqua					
11/21/2023	20:18					11				MB EM304 SOL 0017	211123_20.txt	acquisizione MB EM304 fino a 3 miglia dall'inizio della zona di survey "chilometro cubo"					
11/21/2023	20:23					11					211123_20.txt	STOP calata. Inizio recupero strumento.					
11/21/2023	20:34					11					211123_20.txt	sondaper misure di turbolenza a bordo					
11/21/2023	20:35	16°56.385433	36°04.719267	16.9397572	36.0786545	11	PI23_TURB11S				211123_20.txt	sonda per misure di turbolenza in acqua					
11/21/2023	20:50										211123_20.txt	STOP calata. Inizio recupero					
11/21/2023	21:01										211123_21.txt	sonda per misure di turbolenza a bordo					
11/21/2023	21:05										211123_21.txt	inizio trasferimento verso area survey "chilometro cubo"					
11/22/2023	0:55									MB EM304 line 0018	221123_00.txt	acquisizione MB verso il target "Ctf_01_transit. L'acquisizione procederà fino a circa 3 migli da questo punto. Poi verrà aspento il MB ed acceso il CHIRP a 12 kHz. Verrà fatto in transetto mantenendosi ad una distanza di 2 miglia dal punto per verificare che la strumentazione sul fondo riceva il segnale acustico emesso.					
11/22/2023	1:43									MB EM304 line 0019	221123_01.txt	ridotta velocità di navigazione da 11 a 6 nodi ad una distanza di circa 4 miglia dal punto Ctf_01					
11/22/2023	1:49									MB EM304 EOL 0019	221123_01.txt	stop acquisizione MB a 3 miglia dal stop discesa					
11/22/2023	1:53									CHIRP SOL 0014_2023_356_0153	221123_01.txt	acceso il CHIRP. Trasduttore 12 kHz; Tx Pulse 32 ms; Tx Power 4; Range 500; Sound speed 1519; Ping Rate 250 ms; START RECORDING in Quincy					
11/22/2023	2:50									MB EM304 SOL 0020; CHIRP EOL 0014_2023_356_0153	221123_02.txt	discrepanza di orario tra il SIS e il CHIRP (EOL CHIRP 02:52)					
11/22/2023	4:21					KM3				MB EM304 EOL 0020	221123_04.txt	arrivo alla stazione KM3 ci si posiziona per calata CTD	CONDIZIONI METEO: vento da N-NW a 8 nodi; mare da N-NW con onda 0.8 m; swell da SW onda 1 m				
11/22/2023	4:41	15°50.018896	36°30.020251	15.8336483	36.5003375	KM3	PI23_CTD09S	3305 m bsl			221123_04.txt	CTD in acqua					
11/22/2023	5:37	15°50089168	36°30.015475	15.8334819	36.5002579	KM3	PI23_CTD09B	3305 m bsl	stop discesa 3260 m		221123_05.txt	STOP calata 3260 m. Inizio risalita con vari step per campionamento acque					
11/22/2023	6:34	15°50.013380	36°30.017719	15.8335563	36.5002953	KM3	PI23_CTD09E	3305 m bsl			221123_06.txt	CTD a bordo					
11/22/2023	7:07					KM3					221123_07.txt	inizio operazioni con retino (tre calate a profondità diversa).					
11/22/2023	7:08	15°50.030706	36°30.019454	15.8338451	36.5003242	KM3	PI23_RET04S				221123_07.txt	retino in acqua					
11/22/2023	7:16	15°50.029127	36°30.016392	15.8338188	36.5002732	KM3	PI23_RET04E				221123_07.txt	retino in superficie dopo calata a 130 m e risalita.					
11/22/2023	7:26	15°50.028337	36°30.017923	15.8338056	36.5002987	KM3	PI23_RET05S				221123_07.txt	retino in acqua					
11/22/2023	7:38	15°50.025271	36°30.019006	15.8337545	36.5003168	KM3	PI23_RET05E				221123_07.txt	retino in superficie dopo calata a 200 m e risalita a 130 m. Retino chiuso e recuperato					
11/22/2023	7:46	15°50.028151	36°30.016130	15.8338025	36.5002688	KM3	PI23_RET06S				221123_07.txt	retino in acqua					
11/22/2023	8:16	15°50.031692	36°30.015143	15.8338615	36.5002524	KM3	PI23_RET06E				221123_08.txt	retino in superficie dopo calata a 500 e risalita fino a 200 m (retino chiuso a 200 m, inizio recupero)					
11/22/2023	8:32	15°50.030017	36°30.015402	15.8338336	36.5002567	KM3	PI23_IOP01S				221123_08.txt	sonda IOP calata da poppa (stesso verricello dei retini). Ritirata su per un controllo e successivamente rimessa in acqua					
11/22/2023	8:34	15°50.031016	36°30.015715	15.8338503	36.5002619	KM3	PI23_IOP01rS				221123_08.txt	IOP in acqua. Replica della sonda precedente aborita per controllo					
11/22/2023	8:40	15°49.899996	36°29.929000	15.8316666	36.4988166	KM3	PI23_SE01				221123_08.txt	calata con disco Secchi per misure di visibilità e torbidità					
11/22/2023	8:59	15°50.033871	36°30.016254	15.8338979	36.5002709	KM3	PI23_IOP01rE				221123_08.txt	IOP a bordo					
11/22/2023	9:05	15°50.026104	36°30.014162	15.8337684	36.5002360	KM3	PI23_RAD04S				221123_09.txt	sonda per radiometria in acqua					
11/22/2023	9:20	15°49.928863	36°29.948559	15.8321477	36.4991427	KM3	PI23_RAD04E				221123_09.txt	sonda per radiometria a bordo					
11/22/2023	9:23					KM3					221123_09.txt	si staziona sul punto per preparare CTD					
11/22/2023	9:26	15°49.912383	36°29.939367	15.8318731	36.4989895	KM3	PI23_CTD10S	3312 m bsl	CTD + SVP	svp_20231122_0930	221123_09.txt	CTD in acqua					
11/22/2023	9:43	15°49.912755	36°29.940226	15.8318793	36.4990038	KM3	PI23_CTD10B		stop discesa 300 m		221123_09.txt	STOP calata a 300 m. Inizio recupero					
11/22/2023	9:53	15°49.912059	36°29.945811	15.8318676	36.4990969	KM3	PI23_CTD10E				221123_09.txt	CTD a bordo					
11/22/2023	10:16	15°49.878886	36°29.913168	15.8313148	36.4985528	KM3	PI23_TURB12S				221123_10.txt	sonda per mmisure di turbolenza in acqua					
11/22/2023	10:46	15°49.685740	36°29.783760	15.8280957	36.4963960	KM3	PI23_TURB12B				221123_10.txt	STOP calata ed inizio recupero.					
11/22/2023	11:00	15°49.591346	36°29.722618	15.8265224	36.4953770	KM3	PI23_TURB12E				221123_11.txt	sonda a bordo					
11/22/2023	11:01	15°49.582617	36°29.716222	15.8263770	36.4952704	KM3	PI23_TURB13S				221123_11.txt	sonda per misure di turbolenza in acqua					
11/22/2023	11:24	15°49.428656	36°29.616244	15.8238109	36.4936041	KM3	PI23_TURB13B				221123_11.txt	STOP calata ed inizio recupero.					
11/22/2023	11:38	15°49.334444	36°29.555765	15.8222407	36.4925961	KM3	PI23_TURB13E				221123_11.txt	sonda a bordo					

11/22/2023	11:56					KM3				MB EM304 SOL 0021	221123_11.txt	trasferimento verso la stazione KM3 per effettuare box corer				
11/22/2023	12:04					KM3				MB EM304 EOL 0021	221123_12.txt	arrivo sul punto KM3				
11/22/2023	12:17	15°50.029798	36°30.024815	3.8338300	36.5004136	KM3	PI23_BC01S	3330 m bsl			221123_12.txt	box corer in acqua. Il Box Corer viene calato da poppa con A-frame				
11/22/2023	13:15	15°50.030641	36°30.031357	0.8338440	36.5005226	KM3	PI23_BC01B	3330 m bsl			221123_13.txt	box corer sul fondo. Velocità di discesa 1m/s max tiro 3.7 tonnellate.	CONDIZIONI METEO in peggioramento con pioggia da lieve a moderata			
11/22/2023	14:16	15°49.942338	36°30.121776	7.8323723	36.5020296	KM3	PI23_BC01E				221123_14.txt	box corer a bordo.				
11/22/2023	14:30					to Taormina				MB EM304 SOL 0022	221123_14.txt	Inizio trasferimento verso Taormina per il peggioramento delle condizioni meteo.	CONDIZIONI METEO PEGGIORATE. Pioggia forte, lampi e fulmini			
11/22/2023	21:16									MB EM304 SOL 0025	221123_21.txt	continua acquisizione MB durante il trasferimento verso Taormina				
11/23/2023	4:59									MB EM304 SOL 0028	231123_04.txt	acquisizione MB a ridosso di Taormina. Velocità circa 3 nodi. NB linea MB 0027 rumorosa per moto ondoso				
11/23/2023	8:52									MB EM304 SOL 0029	231123_08.txt	acquisizione MB sotto lo stretto di Messina. Velocità 1.5- 2 nodi.				
11/23/2023	9:41									VMDAS 45 kHz SOL; MB line 0029	231123_09.txt	acceso il correntometro VMDAS 45 kHz per fare test di acquisizione in contemporanea MB. Il dato MB risulta molto rumoroso				
11/23/2023	9:58									CHRP SOL 0021_2023_327_1001; MB line 0029; VMDAS 45 kHz	231123_09.txt	Linee di test (CHIRP e MB) per vedere acquisizione simultanea di 3 strumenti: CHRP, ADCP e MB. NB: CHIRP line 0015-0016-0017 sonp brevissimi test da non considerare;				
11/23/2023	10:04									CHRP EOL 0021_2023_327_1001; MB EM304 EOL 0029	231123_10.txt	Si decide di interrompere l'acquisizione con il CHIRP.				
11/23/2023	10:05									MB EM304 SOL 0030	231123_10.txt	Continua acquisizione MB e VMDAS in contemporanea anche se consapevoli che il dato MB è deteriorato				
11/23/2023						to station 34					from 231123_10.txt	Per tutto il giorno si continua ad acquisire MB EM304 e VMDAS. Il stop discesa è raggiungere il punto di carotaggio 34 per le 05:30 UTC				
11/24/2023	4:21					to station 34				MB EM304 line 0037	241123_04.txt	l'acquisizione MB EM304 e VMDAS 45 kHz è proseguita tutta la notte con una velocità di navigazione di circa 2-2.5 nodi. Il stop discesa da raggiungere è il punto di carotaggio 34	CONDIZIONI METEO: vento da N a circa 5 nodi; swell 1,5 m; mare da N 0.8-0.9 m di onda			
11/24/2023	4:24					34				VMDAS 45 kHz EOL; MB EM304 EOL 0037	241123_04.txt	si decide di terminare acquisizione VMDAS 45 kHz per dare precedenza all'acquisizione MB in prossimità del punto di carotaggio				
11/24/2023	4:25					34				MB EM304 SOL 0038	241123_04.txt	vessel heading 167°; velocità 2.5 nodi				
11/24/2023	4:51					34				MB EM304 line 0038	241123_04.txt		AGGIORNAMENTO METEO; swell da SE 1.5 m; swell da E 1.5 m			
11/24/2023	5:07					34				MB EM304 line 0038	241123_05.txt	aumento velocità 4 nodi. Visto che le condizioni meteo non permettono di iniziare le operazioni di carotaggio si decide di effettuare un piccolo survey dell'area con acquisizione MB EM304 a copertura e poi CHIRP.				
11/24/2023	6:15					34				MB EM304 EOL 0038	241123_06.txt	si è passati sopra il punto di carotaggio 34 e si è proseguito con acquisizione MB lungo la direzione 167°. Inizio accostata per nuova linea MB. Si va a copertura.				
11/24/2023	6:22					34				MB EM304 SOL 0039	241123_06.txt	line bearing variabile da 337 a 320°; velocità 3.9 nodi. Si acquisisce a copertua				
11/24/2023	9:10					34				MB EM304 EOL 0040	241123_09.txt	preparazione ad un test per MB: la linea 0038 è stata acquisita con il settaggio ATTITUDE SYSTEM 2 -> ACTIVE in questo modo la velocità di variazione degli angoli di pitch, roll e heave viene inserita come informazione primaria nei dati acquisiti dal SIS che risultano più precisi. Si vuole vedere cosa succede se durante l'acquisizione di utilizza la configurazione ATTITUDE SYSTEM 1 -> ACTIVE in cui l'informazione primaria è relativa agli angoli di pitch, roll e heave sono quelli fissi determinatti durante la calibrazione dello strumento.				
11/24/2023	9:52					34				MB EM304 SOL 0041	241123_09.txt	linea di test da confrontare con la linea MB EM304 0038. Configurazione durante l'acquisizione ATTITUDE SYSTEM 1 -> ACTIVE				
11/24/2023	10:36					34				MB EM304 EOL 0041; CHIRP SOL 0023_2023_328_1040	241123_10.txt	stop acquisizione MB ed inizio acquisizione CHIRP				
11/24/2023	11:13					34				CHIRP EOL 0023_2023_328_1040	241123_11.txt					
11/24/2023	11:22					34				CHIRP SOL 0024_2023_328_1125	241123_11.txt					
11/24/2023	11:29					34				CHIRP line 0024_2023_328_1125	241123_11.txt	preparazione per misure di radiomentria				
11/24/2023	11:31	15°36.154651	37°12.275813	2.6025775	37.2045969	34	PI23_RAD05S				241123_11.txt	sonda per radiometria in acqua				
11/24/2023	11:47	15°36.220930	37°12.521547	1.6036822	37.2086925	34	PI23_RAD05E				241123_11.txt	sonda per radiometria a bordo				
11/24/2023	11:48					34				CHIRP EOL 0024_2023_328_1125; SOL 0025_2023_328_1151	241123_11.txt	trasferimento verso punto di carotaggio stazione 34				
11/24/2023	12:22					34		2200 m bsl		CHIRP EOL 0025_2023_328_1151	241123_12.txt	fine acquisizione CHIRP. Carotiere in acqua				
11/24/2023	13:05	15°35.569025	37°13.924622	5.5928171	37.2320770	34	PI23_GC05	2200 m bsl			241123_13.txt	carotiere sul fondo. Penetrazione 10 m; recupero 3.70 m.				
11/24/2023	13:06					34					241123_13.txt	inizio recupero				
11/24/2023	13:53					34					241123_13.txt	carotiere a bordo. Preparazione ad operazione con sonda CTD				
11/24/2023	14:22	15°35.575706	37°13.918248	9.5929284	37.2319708	34	PI23_CTD11S	2200 m bsl	CTD+SVP		241123_14.txt	CTD senza prelievo di acqua e con sonda SVP per tarare MB				
11/24/2023	14:58	15°35.565577	37°13.920713	9.5927596	37.2320119	34	PI23_CTD11B		stop discesa 2150 m	svp_20231124_1522	241123_14.txt	STOP calata a 2150 m. Inizio recupero.				
11/24/2023	15:22	15°35.572540	37°13.913018	1.4262090	37.2318836	34	PI23_CTD11E				241123_15.txt	CTD a bordo. Preparativi per sonda IOP. Scaricati dati sonda di velocità ed inseriti nel SIS				
11/24/2023	15:35	15°35.581665	37°13.901777	2.5930278	37.2316963	34	PI23_IOP02S		stop discesa circa 100 m		241123_15.txt	sonda IOP in acqua.				
11/24/2023	15:55	15°35.586484	37°13.902409	0.5931081	37.2317068	34	PI23_IOP02E				241123_15.txt	sonda IOP a bordo				
11/24/2023	15:57	15°35.586014	37°13.902689	7.5931002	37.2317115	34	PI23_IOP03S		stop discesa circa 100 m		241123_15.txt	sonda IOP in acqua per seconda calata				
11/24/2023	16:17	15°35.866770	37°13.904617	3.5977795	37.2317436	34	PI23_IOP03E			CHIRP SOL 0027_2023_328_1619	241123_16.txt	sonda IOP a bordo, si riprende acquisizione CHIRP				
11/24/2023	16:35					34				CHIRP EOL 0027_2023_328_1619; SOL 0028_2023_328_1635	241123_16.txt	linea con direzione 270 per passare sopra punto di carotaggio PI23_GC05				
11/24/2023	17:10					34				CHIRP EOL 0028_2023_328_1635	241123_17.txt					
11/24/2023	17:12					34				CHIRP SOL 0029_2023_328_1712	241123_17.txt					
11/24/2023	18:15					34				CHRP EOL 0029_2023_328_1712; SOL 0030_2023_328_1817	241123_18.txt					
11/24/2023	18:48					34				CHIRP EOL 0030_2023_328_1817	241123_18.txt					
11/24/2023	18:49					to station 26				MB EM304 SOL 0042	241123_18.txt	Start Quincy Recording. Inserita nuova sonda di velocità. Inizia survey MB con navigazione in copertura dei dati acquisiti.				
11/24/2023	21:18					26				MB EM304 line 0042	241123_21.txt	Stop Quincy Recording. Attivata stazione 26 come target per la navigazione				
11/24/2023	21:23					26					241123_21.txt	Start Quincy Recording				
11/24/2023	22:19					26				MB EM304 EOL 0043; SOL 0044	241123_22.txt	accostata verso est per completare copertura MB				
11/24/2023	22:42					26				MB EM304 EOL 0044	241123_22.txt					
11/24/2023	22:52					26				MB EM304 SOL 0045	241123_22.txt					
11/24/2023	22:56					26				MB EM304 EOL 0045; SOL 0046	241123_22.txt	trasferimento verso stazione 26				
11/25/2023	2:01					26				MB EM304 EOL 0048	from 241123_22.txt	Stop acquisizione MB (dato già acquisito); inizio acquisizione CHIRP				
11/25/2023	2:08					26				CHIRP SOL 0031_2023_329_0208	251123_02.txt					
11/25/2023	2:57					26				CHIRP EOL 0031_2023_329_0208; SOL 0032_2023_329_0257	251123_02.txt	cambio linea per cambio parametrid di registrazione chirp. Alle ore 03:07 il profilo passa sulla stazione 26)				
11/25/2023	3:12					26					251123_03.txt		CONDIZIONI METEO: vento da W-SW a 20 nodi; mare con 0.8 m di onda; swell da S-SE con 0.7 m di onda			
11/25/2023	3:46					26				CHIRP EOL 0032_2023_329_0257; MB EM304 SOL 0048	251123_03.txt	Stop acquisizione CHIRP, si riprende acquisizione MB con direzione 278° a 3.10 nodi per vento forte. Trasferimento dalla stazione 26 verso N per completare acquisizione MB nelle zone non coperte.				
11/25/2023	5:07					to station 26				MB EM304 line 0048	251123_05.txt	Viste le condizioni meteo in peggioramento, il rilievo MB a copertura viene interrotto per trasferirsi più vicino costa.	AGGIORNAMENTO METEO: aumento vento a 25 nodi con direzione S-SW; mare con onde apprezzabili di 1 m			
11/25/2023	5:48					26				MB EM304 EOL 0048; SOL 0049	251123_05.txt	cambio rotta da 270° a 340°				
11/25/2023	5:57					26				MB EM304 EOL0049	251123_05.txt					
11/25/2023	5:57					26				MB EM712 SOL 0000	251123_05.txt	Spento MB EM304 e acceso MB EM712 per acquisire in acque fino a profondità massime di 1500 m bsl. Alcuni minuti sono necessari per caricare sonda di velocità e settare alcuni parametri d acquisizione				
11/25/2023	6:10					26				MB EM712 EOL 0000; SOL 0001	251123_06.txt	sistemati i paramentri di acquisizione				
11/25/2023	8:30					26				MB EM712 line 0003	251123_08.txt					
11/25/2023	9:33					26				MB EM712 EOL 0004; SOL 0005	251123_09.txt	MB EM712 line 005 contiene accostata				

11/25/2023	9:42					26				MB EM712 EOL 0005; SOL 0006	251123_09.txt						
11/25/2023	11:04					26				MB EM712 EOL 0007	251123_11.txt						
11/25/2023	11:06					26				MB EM712 SOL 0008	251123_11.txt						
11/25/2023	11:14					26				MB EM712 EOL 0008	251123_11.txt						
11/25/2023	11:17					26				Start 20231125_111740-26-0001.qpd	251123_11.txt	Start Qynsi recording					
11/25/2023	11:24					26				MB EM712 SOL 0009	251123_11.txt						
11/25/2023	11:26					26				MB EM712 EOL 0009; SOL 0010	251123_11.txt	Line MB EM712 0010 verso NE a copertura					
11/25/2023	13:41					26				MB EM712 EOL 0012; SOL 0013	251123_13.txt	Line MB EM712 0013 accostata per andare verso S					
11/25/2023	13:45					26				MB EM712 EOL 0013	251123_13.txt						
11/25/2023	13:48					26				MB EM712 SOL 0014	251123_13.txt	inizio linea verso S con un po' di sovrapposizione con la batimetria acquisita com MB EM304					
11/25/2023	14:05					26				MB EM712 EOL 0014	251123_14.txt	STOP acquisizione MB per presenza di navi lungo la rotta. Inizio accostata a sinistra ma l'acquisizione non riprende perché dati già acquisiti. La registrazione del MB continua su Qynsi come qpd					
11/25/2023	15:08					26				MB EM712 SOL 0015	251123_15.txt						
11/25/2023	15:30					26				Start 20231125_153044-34-0001.qpd	251123_15.txt	Start Qynsi recording					
11/25/2023	15:42					26				MB EM712 EOL 0015	251123_15.txt						
11/25/2023	15:45					26				Start 20231125_154502-34-0001.qpd	251123_15.txt	Start Qynsi recording					
11/25/2023	15:55					26				MB EM712 SOL 0016; Stop 20231125_153044-34-0001.qpd	251123_15.txt	Stop Qynsi recording					
11/25/2023	17:05					26				MB EM712 EOL 0017	251123_17.txt						
11/25/2023	17:07					26				Start 2023_170735-L2-0001.qpd	251123_17.txt	Start Qynsi recording					
11/25/2023	17:28					26				MB EM712 SOL 0019	251123_17.txt						
11/25/2023	17:41					26				MB EM712 EOL 0019; SOL 0020	251123_17.txt	cambio rotta per 174°					
11/25/2023	18:41					26				MB EM712 EOL 0020; SOL 0021	251123_18.txt						
11/25/2023	19:00					26				MB EM712 EOL 0021; Stop 2023_170735-L2-0001.qpd	251123_19.txt	accostata verso N; Stop Qynsi recording					
11/25/2023	19:35					26				CHIRP SOL 0033_2023_329_1937	251123_19.txt	inizio acquisizione CHIRP					
11/25/2023	21:19					26				CHIRP EOL 0033_2023_329_1937; SOL 0034_2023_329_2122	251123_21.txt	modifica dei parametri di acquisizione CHIRP					
11/25/2023	21:46					26				CHIRP EOL 0034_2023_329_2122; MB712 SOL 0022	251123_21.txt	termine acquisizione CHIRP, riprende acquisizione MB					
11/25/2023	22:24					26				Start 20231125_222436-26-0001.qpd	251123_22.txt	Start Qynsi recording					
11/25/2023	22:28					26				MB EM712 EOL 0022	251123_22.txt	STOP acquisizione MB tramite SIS perché dataset già acquisito, continua il recording su Qynsi per ridondanza dati. Cambio rotta per presenza di navi .					
11/25/2023	23:01					26				Stop 20231125_222436-26-0001.qpd	251123_23.txt	Stop Qynsi recording. Copertura batimetrica totale dell'area.					
11/26/2023	0:27					26				MB EM712 SOL 0023	261123_00.txt	riprende acquisizione MB					
11/26/2023	0:28					26				Start 20231126_002847-26-0001.qpd	261123_00.txt	Start Qynsi recording					
11/26/2023	1:22					26				MB EM712 EOL 0023	261123_01.txt	area a copertura batimetrica completa					
11/26/2023	3:09					26				Stop 20231126_002847-26-0001.qpd	261123_03.txt	Stop Qynsi recording					
11/26/2023	3:14					26					261123_03.txt	TERMINA ACQUISIZIONE CON MB EM712 E RIPRENDE CON EM304. trasferimento verso la stazione 26					
11/26/2023	3:16					26				MB EM304 SOL 0049	261123_03.txt	trasferimento verso stazione 26					
11/26/2023	3:51					26				Start 20231126_035112-26-0001.qpd	261123_03.txt	Start Qynsi recording					
11/26/2023	4:00					26				Stop 20231126_035112-26-0001.qpd	261123_04.txt	Stop Qynsi recording per difficoltà nella gestione del Navigation Display. Il file PI23.grd ha raggiunto dimensioni > 120 GB. Acquisizione MB con il SIS continua					
11/26/2023	4:28					26					261123_04.txt		CONDIZIONI METEO: vento da NW con velocità di 16-17 nodi; mare da N-NW con 1.5 m di onda				
11/26/2023	5:10					26				MB EM304 EOL 0049	261123_05.txt	raggiunta stazione 26; in attesa che le condizioni meteo migliorino per effettuare carotaggio si eseguono alcune linee con CHIRP					
11/26/2023	5:33					26				CHIRP SOL 0038_2023_330_0335	261123_05.txt	linea CHIRP nella zona di carotaggio					
11/26/2023	5:45					26				CHIRP EOL 0038_2023_330_0335; SOL 0039_2023_330_0547	261123_05.txt	linea CHIRP nella zona di carotaggio					
11/26/2023	6:36					26				CHIRP EOL 0039_2023_330_0547	261123_05.txt	linea CHIRP nella zona di carotaggio					
11/26/2023	6:47					26				Start 20231126_064742-26-0001.qpd	261123_06.txt	Start Qynsi recording					
11/26/2023	6:50					26				Start 20231126_065039-26-0001.qpd	261123_06.txt	Stop Qynsi recording; Start Qynsi recording					
11/26/2023	7:01					26				MB EM304 SOL 0050		per andare ad una maggiore velocità l'acquisizione non è stata fatta in modalità "science mode"					
11/26/2023	8:11					26				Stop 20231126_065039-26-0001.qpd	261123_06.txt	Stop Qynsi recording					
11/26/2023	8:13					26				Start 20231126_081335-26-0001.qpd	261123_08.txt	Start Qynsi recording					
11/26/2023	8:28					26				MB EM304 EOL 0050		Attivato K-Synk per acquisire MB EM304 e EM712 in contemporanea					
11/26/2023	8:32					26				Stop 20231126_081335-26-0001.qpd; MB EM304 SOL 0051; MB EM712 SOL 0024	261123_08.txt	Stop Qynsi recording. Start MB EM304 and EM712 acquisition with K-Synk acctive.					
11/26/2023	8:33					26				Start 20231126_083310-34-0001.qpd	261123_08.txt	Start Qynsi recording					
11/26/2023	8:42					26				CHIRP SOL 0041_2023_330_0844		acquisizione MB EM304, EM712 e CHIRP sincronizzati con k-Synk					
11/26/2023	8:52					26				Stop 20231126_083310-34-0001.qpd	261123_08.txt	Stop Qynsi recording					
11/26/2023	8:52					26				Start 20231126_085527-34-0001.qpd	261123_08.txt	Start Qynsi recording					
11/26/2023	9:42					26				Stop 20231126_085527-34-0001.qpd	261123_09.txt	Stop Qynsi recording, Stop MB acquisition. Inizio accostata					
11/26/2023	9:50					26				CHIRP EOL 0041_2023_330_0844	261123_09.txt						
11/26/2023	9:52					26				MB EM304 SOL 0052; MB EM712 SOL 0026	261123_09.txt - 263	Riprende acquisizione di entrambi i MB in modalità sincronizzata					
11/26/2023	9:59					26				CHIRP SOL 0042_2023_330_0959	261123_09.txt	Termina acquisizione MB EM712. Continua acquisizione MB EM304 e CHIRP con K-Synk attivo					
11/26/2023	10:03					26				MB EM712 EOL 0026; Start 20231126_100305-26-0001.qpd	261123_10.txt	Start Qynsi recording; Stop MB EM712					
11/26/2023	10:07					26				MB EM304 EOL 0052; CHIRP EOL 0042_2023_330_0959; Stop 20231126_100305-26-0001.qpd	261123_10.txt	Stop Qynsi recording; Stop MB EM304 acquisition; Stop Chirp acquisition					
11/26/2023	10:13					26				MB EM304 SOL 0053; Start 20231126_101318-26-0001.qpd	261123_10.txt	Start Qynsi recording					
11/26/2023	10:43					26				MB EM304 EOL 0053; Stop 20231126_101318-26-0001.qpd	261123_10.txt	Stop Qynsi recording					
11/26/2023	10:45					26				Start 20231126_104526-26-0001.qpd	261123_10.txt	Start Qynsi recording					
11/26/2023	10:51					26				MB EM304 SOL 0054	261123_10.txt	ci si riavvicina alla stazione 26 per carotaggio					
11/26/2023	11:10					26				MB EM304 line 0054	261123_11.txt	si acquisisce la colonna d'acqua					
11/26/2023	11:27					26				MB EM304 EOL 0054	261123_11.txt	passati sopra il punto di carotaggio 26 a scopo esplorativo, dopo accostata ci si riposiziona sulla stazione.					
11/26/2023	11:35					26				Stop 20231126_104526-26-0001.qpd	261123_11.txt	Stop Qynsi recording					
11/26/2023	11:37					26				CHIRP SOL 0043_2023_330_1137	261123_11.txt	Profilo chirp sulla stazione di carotaggio 26. Ci si prepara per il carotaggio					
11/26/2023	11:50					26		2050 m bsl			261123_11.txt	Carotiere in acqua					
11/26/2023	12:00					26				MB EM304 SOL 0055	261123_12.txt	si acquisisce la colonna d'acqua					
11/26/2023	12:29	15°25.49876'E	37°26.32315'N	15.4249793	37.4387192	26	**PI23_GC07**	2050 m bsl			261123_12.txt	Carotiere sul fondo. Velocità di discesa 100-80 m/min.					
11/26/2023	12:31	15°25.49000'E	37°26.32000'N	15.4248333	37.4386667	26	**PI23_RAD06S**				261123_12.txt	Durante il carotaggio si effettuano le misure di radiometria. Sonda per radiometria in acqua					
11/26/2023	12:45	15°25.49071'E	37°26.32570'N	15.4248452	37.4387617	26	**PI23_RAD06E**				261123_12.txt	Sonda per misure di radiometria a bordo					
11/26/2023	13:03	15°25.51463'E	37°26.31686'N	15.4252438	37.4386143	26	**PI23_SE02**				261123_13.txt	Misure con disco Secchi per visibilità-torbidità. Visibilità 33 m					
11/26/2023	13:11					26					261123_13.txt	Carotiere a bordo. Penetrazione 1 m, recupero 1 m. Il carotiere è risalito piegato					
11/26/2023	13:35	15°25.50990'E	37°26.30770'N	15.4251650	37.4384617	26	**PI23_RET07S**				261123_13.txt	retino in acqua					
11/26/2023	13:37					26				MB EM304 EOL 0056	261123_13.txt	si acquisisce la colonna d'acqua					

11/26/2023	13:41	15°25.508320	37°26.308484	0	15.4251387	37.4384747	26	PI23_RET07E				261123_13.txt	retino in superficie dopo calata a 100 m e risalita.				
11/26/2023	13:46	15°25.513723	37°26.308837	8	15.4252287	37.4384806	26	PI23_RET08S				261123_13.txt	retino in acqua				
11/26/2023	13:58	15°25.510199	37°26.309564	4	15.4251700	37.4384927	26	PI23_RET08E				261123_13.txt	retino in superficie dopo calata a 200 m e risalita a 100 m. Retino chiuso e recuperato				
11/26/2023	14:06	15°25.514606	37°26.308783	0	15.4252434	37.4384797	26	PI23_RET09S				261123_14.txt	retino in acqua				
11/26/2023	14:36	15°25.513893	37°26.308745	8	15.4252316	37.4384791	26	PI23_RET09E				261123_14.txt	retino in superficie dopo calata a 500 m e risalita a 200 m. Retino chiuso e recuperato				
11/26/2023	14:39						26					261123_14.txt	trasferimento verso il punto dove fare il Box Corer				
11/26/2023	14:51	15°25.547504	37°26.430195	1	15.4257917	37.4405033	26	PI23_BC02S	1993 m bsl			261123_14.txt	Box Corer in acqua				
11/26/2023	15:17	15°25.551139	37°26.429639	9	15.4258523	37.4404940	26	PI23_BC02B	1990 m bsl			261123_15.txt	Box Corer su fondo. Velocità di discesa 100 -> 40 m/min				
11/26/2023	15:23						26				CHIRP SOL 0044_2023_330_1525	261123_15.txt	acquisito profilo chirp durante la risalita del Box Corer				
11/26/2023	15:48	15°25.541076	37°26.430009	0	15.4256846	37.4405002	26	PI23_BC02E				261123_15.txt	Durante la risalita il cavo si è imbandolato attorno alla leva di sgancio aprendo il Box Corer. Il campione non è stato recuperato				
11/26/2023	15:50						26				CHIRP EOL 0044_2023_330_1525	261123_15.txt					
11/26/2023	16:11	15°25.568884	37°26.438098	8	15.4261481	37.4406350	26	PI23_CTD12S	1990 m bsl	CTD + SVP		261123_16.txt	CTD con prelievo acqua. Fatta anche sonda SVP per Multibeam				
11/26/2023	16:45	15°25.568972	37°26.442787	4	15.4261495	37.4407131	26	PI23_CTD12B	1971 m bsl		svp_20231126_1611	261123_16.txt	STOP calata 1971 m e recupero.				
11/26/2023	17:15	15°25.566718	37°26.444736	2	15.4261120	37.4407456	26	PI23_CTD12E				261123_17.txt	CTD a bordo				
11/26/2023	17:26	15°25.553883	37°26.449720	0	15.4258981	37.4408287	26	PI23_IOP04S				261123_17.txt	sonda IOP in acqua.				
11/26/2023	17:40	15°25.551630	37°26.451029	8	15.4258605	37.4408505	26	PI23_IOP04E				261123_17.txt	sonda IOP a bordo				
11/26/2023	17:43	15°25.551482	37°26.450876	5	15.4258580	37.4408479	26	PI23_IOP05S				261123_17.txt	sonda IOP in acqua.				
11/26/2023	17:53	15°25.551590	37°26.449770	9	15.4258598	37.4408295	26	PI23_IOP05E				261123_17.txt	sonda IOP a bordo				
11/26/2023	18:07	15°25.560685	37°26.448202	7	15.4260114	37.4408034	26	PI23_CTD13S	1990 m bsl			261123_18.txt	CTD con prelievo acqua. Ripetizione calata per prelievo solo a 60 m				
11/26/2023	18:10	15°25.566860	37°26.449927	5	15.4261143	37.4408321	26	PI23_CTD13B	60 m bsl			261123_18.txt	STOP calata 60 m e recupero.				
11/26/2023	18:15	15°25.565502	37°26.450661	9	15.4260917	37.4408444	26	PI23_CTD13E				261123_18.txt	CTD a bordo				
11/26/2023	18:27	15°25.562471	37°26.456316	9	15.4260412	37.4409386	26	PI23_TURB14S				261123_18.txt	sonda per mmisure di turbolenza in acqua				
11/26/2023	18:52	15°26.022016	37°26.711192	0	15.4337003	37.4451865	26	PI23_TURB14B				261123_18.txt	STOP calata ed inizio recupero.				
11/26/2023	19:09	15°26.407524	37°26.872692	3	15.4401254	37.4478782	26	PI23_TURB14E				261123_19.txt	sonda a bordo				
11/26/2023	19:15						26				CHIRP SOL 0045_2023_330_1917	261123_19.txt					
11/26/2023	19:25	15°25.696114	37°26.480556	6	15.4282686	37.4413426	26	PI23_TURB15S				261123_19.txt	sonda per misure di turbolenza in acqua				
11/26/2023	19:49	15°25.223864	37°26.445455	8	15.4203977	37.4407576	26	PI23_TURB15B				261123_19.txt	STOP calata ed inizio recupero.				
11/26/2023	20:05	15°24.953395	37°26.493355	4	15.4158899	37.4415559	26	PI23_TURB15E				261123_20.txt	sonda a bordo				
11/26/2023	20:18	15°25.524268	37°26.463183	4	15.4254045	37.4410531	26	PI23_TURB16S				261123_20.txt	sonda per misure di turbolenza in acqua				
11/26/2023	20:40						26				CHIRP EOL 0045_2023_330_1917	261123_20.txt					
11/26/2023	20:42	15°26.074482	37°26.202082	4	15.4345747	37.4367014	26	PI23_TURB16B				261123_20.txt	STOP calata ed inizio recupero.				
11/26/2023	20:58	15°26.446645	37°26.064676	9	15.4407774	37.4344113	26	PI23_TURB16E				261123_20.txt	sonda a bordo				
11/26/2023	21:04						**to station 27**					261123_21.txt	trasferimento verso la stazione 27. Si acquisiscono MB e chirp a scopo di scouting. Inserita sonda SVP				
11/26/2023	21:16						27				MB EM304 SOL 0056; CHIRP SOL 0047_2023_330_2120	261123_21.txt	Acquisizione MB EM304 e CHIRP con K-Synk attivo. Velocità 8 nodi				
11/26/2023	23:15						27				MB EM304 EOL 0056	261123_23.txt					
11/26/2023	23:36						27				CHIRP SOL 0049_2023_330_2336	261123_23.txt					
11/26/2023	23:44						27				CHIRP EOL 0049_2023_330_2336	261123_23.txt					
11/27/2023	0:13						27				CHIRP SOL 0050_2023_331_0013	271123_00.txt	Velocità di acquisizione 3 nodi				
11/27/2023	1:01						27				CHIRP EOL 0050_2023_331_0013	271123_01.txt					
11/27/2023	1:07						27				CHIRP SOL 0051_2023_331_0107	271123_01.txt					
11/27/2023	1:18						27				CHIRP EOL 0051_2023_331_0107	271123_01.txt	Transito sulla stazione di carotaggio 27. Il chirp mostra che il punto non è adatto alle operazioni di carotaggio.				
11/27/2023	1:39						**to station 29**				MB EM304 SOL 0057; CHIRP SOL 0052_2023_331_0139	271123_01.txt	Trasferimento verso stazione 29. Si acquisiscono contemporaneamente MB e CHIRP (trigger external mode). Velocità 8 nodi				
11/27/2023	2:29						29				MB EM304 EOL 0057; CHIRP EOL 0052_2023_331_0139	271123_02.txt					
11/27/2023	2:36						29				CHIRP SOL 0053_2023_331_0236	271123_02.txt	Transsito sulla stazione di carotaggio 29. Inizia acquisizione transetti chirp a scopo di scouting				
11/27/2023	2:58						29				CHIRP EOL 0053_2023_331_0236	271123_02.txt					
11/27/2023	3:05						29				CHIRP SOL 0054_2023_331_0305	271123_03.txt					
11/27/2023	3:19						29				CHIRP EOL 0054_2023_331_0305	271123_03.txt					
11/27/2023	3:37						29				CHIRP SOL 0055_2023_331_0337	271123_03.txt					
11/27/2023	4:02						29				CHIRP EOL 0055_2023_331_0337	271123_04.txt					
11/27/2023	4:17						29				CHIRP SOL 0056_2023_331_0419	271123_04.txt					
11/27/2023	4:38						29				CHIRP EOL 0056_2023_331_0419	271123_04.txt					
11/27/2023	5:01						29				CHIRP SOL 0058_2023_331_0503	271123_05.txt					
11/27/2023	5:09						29				CHIRP EOL 0058_2023_331_0503	271123_05.txt					
11/27/2023	5:12						29				CHIRP SOL 0059_2023_331_0512	271123_05.txt	accostata				
11/27/2023	5:17						29				CHIRP EOL 0059_2023_331_0512	271123_05.txt					
11/27/2023	5:19						29				CHIRP SOL 0060_2023_331_0519	271123_05.txt					
11/27/2023	5:28						29				CHIRP EOL 0060_2023_331_0519	271123_05.txt					
11/27/2023	5:29						29				CHIRP SOL 0061_2023_331_0530	271123_05.txt					
11/27/2023	5:51						29				CHIRP EOL 0061_2023_331_0530	271123_05.txt					
11/27/2023	5:51						29				CHIRP SOL 0062_2023_331_0551	271123_05.txt					
11/27/2023	6:08						29				CHIRP EOL 0062_2023_331_0551	271123_06.txt					
11/27/2023	6:17						29					271123_06.txt	termine rilievo chirp, identificato punto di carotaggio.				
11/27/2023	6:24						29		2448 m bsl			271123_06.txt	carotiere in acqua				
11/27/2023	6:57	15°57.01399	E 37°21.02935	N	15.9502332	37.3504892	29	PI23_GC07	2448 m bsl			271123_06.txt	carotiere sul fondo. Tiro max 4.2 t; velocità di discesa 60 m/min				
11/27/2023	7:32						29					271123_07.txt	carotiere a bordo. Penetrazione maggiore di 5 m, recupero 5 m				
11/27/2023	7:44						**to station NK25**				MB EM304 SOL 0058	271123_07.txt	trasferimento verso stazione NK25				
11/27/2023	8:40						NK25				MB EM304 EOL 0058	271123_08.txt	arrivo stazione NK25				
11/27/2023	8:54	15°52.611896	37°29.134911	3	15.8768649	37.4855819	NK25	PI23_CTD14S	2051 m bsl	CTD +SVP		271123_08.txt	CTD con prelievo di acqua, sonda SVP per MB				
11/27/2023	9:33	15°52.615264	37°29.132553	1	15.8769211	37.4855426	NK25	PI23_CTD14B			svp_20231127_1008	271123_09.txt	Stop calata e inizio recupero				
11/27/2023	9:59	15°52.619497	37°29.136285	5	15.8769916	37.4856048	NK25	PI23_CTD14E				271123_09.txt	CTD a bordo				
11/27/2023	10:21	15°52.6'E	37°29.13'N		15.8766667	37.4855000	NK25	PI23_RET10S				271123_10.txt	retino in acqua				
11/27/2023	10:27	15°52.6'E	37°29.13'N		15.8766667	37.4855000	NK25	PI23_RET10E				271123_10.txt	retino in superficie dopo calata a 100 m. Retino chiuso e recuperato				
11/27/2023	10:31	15°52.6'E	37°29.13'N		15.8766667	37.4855000	NK25	PI23_RET11S				271123_10.txt	retino in acqua				
11/27/2023	10:48	15°52.6'E	37°29.13'N		15.8766667	37.4855000	NK25	PI23_RET11E				271123_10.txt	retino in superficie dopo calata a 300 m e risalita a 100 m. Retino chiuso e recuperato				
11/27/2023	10:53	15°52.629442	37°29.127487	6	15.8771574	37.4854581	NK25	PI23_RET12S				271123_10.txt	retino in acqua				
11/27/2023	11:24	15°52.630652	37°29.127754	2	15.8771775	37.4854626	NK25	PI23_RET12E				271123_11.txt	retino in superficie dopo calata a 500 m e risalita a 300 m. Retino chiuso e recuperato				
11/27/2023	11:39	15°52.634818	37°29.132713	0	15.8772470	37.4855452	NK25	PI23_RAD07S				271123_11.txt	Sonda per misure di radiometria in acqua				
11/27/2023	12:01	15°52.535704	37°29.184149	7	15.8755951	37.4864025	NK25	PI23_RAD07E				271123_12.txt	Sonda per misure di radiometria a bordo				
11/27/2023	12:18	15°52.536703	37°29.198485	5	15.8756117	37.4866414	NK25	PI23_IOP06S				271123_12.txt	Sonda IOP in acqua				
11/27/2023	12:24	15°52.542317	37°29.205642	6	15.8757053	37.4867607	NK25	PI23_IOP06E				271123_12.txt	Sonda IOP a bordo. Cavo di trasmissione finito tra le eliche del motore, recuperato ma tranciato.				
11/27/2023	12:57						**transit to Crotone**					271123_12.txt	trasferimento verso Crotone				
11/27/2023	13:02						**transit to Crotone**				MB EM304 SOL 0059	271123_13.txt	trasferimento verso Crotone				

11/27/2023	15:55					**transit to Crotone**				MB EM712 SOL 0027		trasferimento verso Crotone				
11/27/2023	23:46					**transit to Crotone**				MB EM712 EOL 0034		standby meteo				
11/28/2023						**Crotone port call**							Onda lunga 2 m	h. 00 - 12	Vento dir SW; Forza 4	Mare dir SW; Forza 3
														h. 00 - 12	Vento dir SE; Forza 3	Mare dir SE; Forza 2
11/29/2023	7:00					**transit to station 50**							Parzialmente nuvoloso	h. 00 - 12	Vento dir SE; Forza 3	Mare dir SE; Forza 2
11/29/2023	8:01					**transit to station 50**			mb+ water column acquisition + Qinsy acquisition	MB EM712 SOL 0035		MB-EM712 SIS Sensor Setup: Position System 1: ACTIVE-OK Attitude System 1: OK Attitude System 2: ACTIVE-OK	Parzialmente nuvoloso	h. 00 - 12	Vento dir SE; Forza 3	Mare dir SE; Forza 2
11/29/2023	8:09					**transit to station 50**				CHIRP SOL 0063_2023_333_0811			Parzialmente nuvoloso	h. 00 - 12	Vento dir SE; Forza 3	Mare dir SE; Forza 2
11/29/2023	8:35					**transit to station 50**							Parzialmente nuvoloso	h. 00 - 12	Vento dir SE; Forza 3	Mare dir SE; Forza 2
11/29/2023	8:50					**transit to station 50**				MB EM712 & CHIP EOL			Parzialmente nuvoloso	h. 00 - 12	Vento dir SE; Forza 3	Mare dir SE; Forza 2
11/29/2023	9:13	17°21,6933'E	39°04,1735'N	17.3615550	39.0695583	**50**	**PI23_CTD15_S**	605	CTD +SVP				Parzialmente nuvoloso	h. 00 - 12	Vento dir SE; Forza 3	Mare dir SE; Forza 2
11/29/2023	9:15					**50**			MB+WC+Qinsy	MB EM712 SOL 0036		WC acquisition con nave ferma sul punto della ctd	Parzialmente nuvoloso	h. 00 - 12	Vento dir SE; Forza 3	Mare dir SE; Forza 2
11/29/2023	9:25	17°21,7859'E	39°04,1077'N	17.3630983	39.0684617	**50**	**PI23_CTD15_B**	607	CTD +SVP	svp_20231129_0925		Il cavo della CTD è uscito dalla puleggia. Per precauzione sono state spente le eliche di destra	Parzialmente nuvoloso	h. 00 - 12	Vento dir SE; Forza 3	Mare dir SE; Forza 2
11/29/2023	9:51					**50**				MB EM712 EOL 0036			Parzialmente nuvoloso	h. 00 - 12	Vento dir SE; Forza 3	Mare dir SE; Forza 2
11/29/2023	10:14					**50**						Fine delle operazione con cavo riportato nella puleggia. Parte della copertura di plastica del cavo è saltato	Parzialmente nuvoloso	h. 00 - 12	Vento dir SE; Forza 3	Mare dir SE; Forza 2
11/29/2023	10:25	17°21,98447'	39°03,94469'	17.3664078	39.0657448	**50**	**PI23_CTD15_E**						Parzialmente nuvoloso	h. 00 - 12	Vento dir SE; Forza 3	Mare dir SE; Forza 2
11/29/2023	11:03					**50**				svp_20231129_0925		applicata sonda nel SIS dell'EM712	Parzialmente nuvoloso	h. 00 - 12	Vento dir SE; Forza 3	Mare dir SE; Forza 2
11/29/2023	11:05					**50**			MB+WC+Qinsy	MB EM712 SOL 37		Inizio survey geofisico sulla struttura del campionamento di acqua CTD15	Parzialmente nuvoloso	h. 00 - 12	Vento dir SE; Forza 3	Mare dir SE; Forza 2
11/29/2023	11:09					**50**				CHIRP SOL 0064_2023_333_1112			Parzialmente nuvoloso	h. 00 - 12	Vento dir SE; Forza 3	Mare dir SE; Forza 2
11/29/2023	11:17					**50**				MB EM712 EOL 37		Il MB ha problemi per cui interrompiamo la linea	Parzialmente nuvoloso	h. 00 - 12	Vento dir SE; Forza 3	Mare dir SE; Forza 2
11/29/2023	11:18					**50**			MB+WC+Qinsy	MB EM712 SOL 38			Parzialmente nuvoloso	h. 00 - 12	Vento dir SE; Forza 3	Mare dir SE; Forza 2
11/29/2023	11:38					**50**				MB EM712 EOL 38; CHIRP EOL 0064_2023_333_1112			Parzialmente nuvoloso	h. 00 - 12	Vento dir SE; Forza 3	Mare dir SE; Forza 2
11/29/2023	11:43					**50**			MB+WC+Qinsy	MB EM712 SOL 39; CHIRP SOL 0065_2023_333_1146			Parzialmente nuvoloso	h. 00 - 12	Vento dir SE; Forza 3	Mare dir SE; Forza 2
11/29/2023	12:20					**50**				MB EM712 EOL 39; CHIRP EOL 0065_2023_333_1146			Parzialmente nuvoloso	h. 12 - 24	Vento dir NW; Forza 3	Mare dir NW; Forza 2
11/29/2023	12:30					**50**			MB+WC+Qinsy	MB EM712 SOL 40; CHIRP SOL 0066_2023_333_1230		in K-Synk, cambiamo i settaggi per la sincronizzazione (chirp calculated invece di fixed)	Parzialmente nuvoloso	h. 12 - 24	Vento dir NW; Forza 3	Mare dir NW; Forza 2
11/29/2023	13:03					**50**				MB EM712 EOL 40; CHIRP EOL 0066_2023_333_1230		sulla water column della linea mb 0040, controllare possibile fuoriuscita di gas	Parzialmente nuvoloso	h. 12 - 24	Vento dir NW; Forza 3	Mare dir NW; Forza 2
11/29/2023	13:08					**50**			MB+WC+Qinsy	MB EM712 SOL 41; CHIRP SOL 0067_2023_333_1311			Parzialmente nuvoloso	h. 12 - 24	Vento dir NW; Forza 3	Mare dir NW; Forza 2
11/29/2023	13:43					**50**				MB EM712 EOL 41; CHIRP EOL 0067_2023_333_1311			Parzialmente nuvoloso	h. 12 - 24	Vento dir NW; Forza 3	Mare dir NW; Forza 2
11/29/2023	13:53					**50**			MB+WC+Qinsy	MB EM712 SOL 42; CHIRP SOL 0068_2023_333_1355			Parzialmente nuvoloso	h. 12 - 24	Vento dir NW; Forza 3	Mare dir NW; Forza 2
11/29/2023	14:24					**50**				MB EM712 EOL 42; CHIRP EOL			Parzialmente nuvoloso	h. 12 - 24	Vento dir NW; Forza 3	Mare dir NW; Forza 2
11/29/2023	14:34					**50**			MB+WC+Qinsy	MB EM712 SOL 43; CHIRP SOL 0071_2023_333_1434		in Knudsen, cambiamo i settaggi del chirp: Range:200 Phase:600 Depth: 400-1200m Aggiunto anche MULTIPING	Parzialmente nuvoloso	h. 12 - 24	Vento dir NW; Forza 3	Mare dir NW; Forza 2
11/29/2023	15:07					**50**				MB EM712 EOL 43; CHIRP EOL 0071_2023_333_1434			Parzialmente nuvoloso	h. 12 - 24	Vento dir NW; Forza 3	Mare dir NW; Forza 2
11/29/2023	15:18					**50**			MB+WC+Qinsy	MB EM712 SOL 44; CHIRP SOL 0072_2023_333_1521			Parzialmente nuvoloso	h. 12 - 24	Vento dir NW; Forza 3	Mare dir NW; Forza 2
11/29/2023	15:40					**50**						rottura della pompa del FLOW THROUGH	Parzialmente nuvoloso	h. 12 - 24	Vento dir NW; Forza 3	Mare dir NW; Forza 2
11/29/2023	15:50					**50**				MB EM712 EOL 44; CHIRP EOL 0072_2023_333_1521			Parzialmente nuvoloso	h. 12 - 24	Vento dir NW; Forza 3	Mare dir NW; Forza 2
11/29/2023	15:56					**50**			MB+WC+Qinsy	MB EM712 SOL 45; CHIRP SOL 0073_2023_333_1559			Parzialmente nuvoloso	h. 12 - 24	Vento dir NW; Forza 3	Mare dir NW; Forza 2
11/29/2023	16:28					**50**				MB EM712 EOL 45; CHIRP EOL 0073_2023_333_1559			Parzialmente nuvoloso	h. 12 - 24	Vento dir NW; Forza 3	Mare dir NW; Forza 2
11/29/2023	16:43					**50**			MB+WC+Qinsy	MB EM712 SOL 46; CHIRP SOL 0074_2023_333_1643			Parzialmente nuvoloso	h. 12 - 24	Vento dir NW; Forza 3	Mare dir NW; Forza 2
11/29/2023	17:19					**50**				MB EM712 EOL 46; CHIRP EOL 0074_2023_333_1643			Parzialmente nuvoloso	h. 12 - 24	Vento dir NW; Forza 3	Mare dir NW; Forza 2
11/29/2023	17:39					**campo Federica**			MB+WC+Qinsy	MB EM712 SOL 47; CHIRP SOL 0075_2023_333_1742			Parzialmente nuvoloso	h. 12 - 24	Vento dir NW; Forza 3	Mare dir NW; Forza 2
11/29/2023	18:12					**campo Federica**				CHIRP EOL 0075_2023_333_1742			Parzialmente nuvoloso	h. 12 - 24	Vento dir NW; Forza 3	Mare dir NW; Forza 2
11/29/2023	18:14					**campo Federica**				MB EM712 EOL 47			Parzialmente nuvoloso	h. 12 - 24	Vento dir NW; Forza 3	Mare dir NW; Forza 2
11/29/2023	18:19					**campo Federica**			MB+WC+Qinsy	MB EM712 SOL 48			Parzialmente nuvoloso	h. 12 - 24	Vento dir NW; Forza 3	Mare dir NW; Forza 2
11/29/2023	18:20					**campo Federica**				CHIRP SOL 0076_2023_333_1822			Parzialmente nuvoloso	h. 12 - 24	Vento dir NW; Forza 3	Mare dir NW; Forza 2
11/29/2023	18:45					**campo Federica**				MB EM712 EOL 48; CHIRP EOL 0076_2023_333_1822			Parzialmente nuvoloso	h. 12 - 24	Vento dir NW; Forza 3	Mare dir NW; Forza 2
11/29/2023	18:51					**campo Federica**			MB+WC+Qinsy	MB EM712 SOL 49; CHIRP SOL 0077_2023_333_1853			Parzialmente nuvoloso	h. 12 - 24	Vento dir NW; Forza 3	Mare dir NW; Forza 2
11/29/2023	19:31					**campo Federica**				MB EM712 EOL 49; CHIRP EOL 0077_2023_333_1853			Parzialmente nuvoloso	h. 12 - 24	Vento dir NW; Forza 3	Mare dir NW; Forza 2
11/29/2023	19:40					**campo Federica**			MB+WC+Qinsy	MB EM712 SOL 50; CHIRP SOL 0078_2023_333_1943			Parzialmente nuvoloso	h. 12 - 24	Vento dir NW; Forza 3	Mare dir NW; Forza 2
11/29/2023	20:14					**campo Federica**				MB EM712 EOL 50; CHIRP EOL 0078_2023_333_1943			Parzialmente nuvoloso	h. 12 - 24	Vento dir NW; Forza 3	Mare dir NW; Forza 2
11/29/2023	20:23					**campo Federica**			MB+WC+Qinsy	MB EM712 SOL 51; CHIRP SOL 0079_2023_333_2026			Parzialmente nuvoloso	h. 12 - 24	Vento dir NW; Forza 3	Mare dir NW; Forza 2
11/29/2023	21:02					**campo Federica**				MB EM712 EOL 51; CHIRP EOL 0079_2023_333_2026			Parzialmente nuvoloso	h. 12 - 24	Vento dir NW; Forza 3	Mare dir NW; Forza 2
11/29/2023	21:13					**campo Federica**			MB+WC+Qinsy	MB EM712 SOL 52			Parzialmente nuvoloso	h. 12 - 24	Vento dir NW; Forza 3	Mare dir NW; Forza 2
11/29/2023	21:14					**campo Federica**				CHIRP SOL 0080_2023_333_2117			Parzialmente nuvoloso	h. 12 - 24	Vento dir NW; Forza 3	Mare dir NW; Forza 2
11/29/2023	21:55					**campo Federica**				MB EM712 EOL 52; CHIRP EOL 0080_2023_333_2117			Parzialmente nuvoloso	h. 12 - 24	Vento dir NW; Forza 3	Mare dir NW; Forza 2
11/29/2023	22:02					**campo Federica/Fedra**			MB+WC+Qinsy	MB EM712 SOL 53			Parzialmente nuvoloso	h. 12 - 24	Vento dir NW; Forza 3	Mare dir NW; Forza 2
11/29/2023	22:06					**campo Federica/Fedra**				CHIRP SOL 0081_2023_333_2209		Nuovi settaggi chirp: overlap: 50%; Tx power: 2; Shift Threshold: 30%; Min-Max Depth: 200-1200 m	Parzialmente nuvoloso	h. 12 - 24	Vento dir NW; Forza 3	Mare dir NW; Forza 2
11/29/2023	22:42									QINSY SOL		Non si capisce quando e perché l'acquisizione qinsy è stata terminata e poi ripresa	Parzialmente nuvoloso	h. 12 - 24	Vento dir NW; Forza 3	Mare dir NW; Forza 2
11/29/2023	23:15					**campo Fedra**				MB EM712 EOL 54; CHIRP EOL 0081_2023_333_2209		sembra esserci un buco nell'acquisizione multibeam, da controllare!	Parzialmente nuvoloso	h. 12 - 24	Vento dir NW; Forza 3	Mare dir NW; Forza 2
11/29/2023	23:28					**campo Fedra**			MB+WC+Qinsy	MB EM712 SOL 55; CHIRP SOL 0082_2023_333_2331		acquisizione su linea Fedra4 su Qinsy	Parzialmente nuvoloso	h. 12 - 24	Vento dir NW; Forza 3	Mare dir NW; Forza 2
11/30/2023	0:14					**campo Fedra**				MB EM712 EOL 55; CHIRP EOL 0082_2023_333_2331			Parzialmente nuvoloso	h. 00 - 12	Vento dir W; Forza 4	Mare dir W; Forza 3
11/30/2023	0:28					**campo Fedra**			MB+WC+Qinsy	MB EM712 SOL 56; CHIRP SOL 0083_2023_334_0031		acquisizione su linea Fedra3 su Qinsy	Parzialmente nuvoloso	h. 00 - 12	Vento dir W; Forza 4	Mare dir W; Forza 3
11/30/2023	1:21					**campo Fedra**				MB EM712 EOL 56; CHIRP EOL 0083_2023_334_0031			Parzialmente nuvoloso	h. 00 - 12	Vento dir W; Forza 4	Mare dir W; Forza 3
11/30/2023	1:30					**campo Fedra**			MB+WC+Qinsy	MB EM712 SOL 57; CHIRP SOL 0084_2023_334_0133		acquisizione su linea Fedra2 su Qinsy	Parzialmente nuvoloso	h. 00 - 12	Vento dir W; Forza 4	Mare dir W; Forza 3
11/30/2023	2:12					**campo Fedra**				MB EM712 EOL 57; CHIRP EOL 0084_2023_334_0133			Parzialmente nuvoloso	h. 00 - 12	Vento dir W; Forza 4	Mare dir W; Forza 3
11/30/2023	2:26					**campo Fedra**			MB+WC+Qinsy	MB EM712 SOL 58; CHIRP SOL 0085_2023_334_0228		acquisizione su linea Fedra1 su Qinsy	Parzialmente nuvoloso	h. 00 - 12	Vento dir W; Forza 4	Mare dir W; Forza 3
11/30/2023	3:10					**campo Fedra**				MB EM712 EOL 58; CHIRP EOL 0085_2023_334_0228			Parzialmente nuvoloso	h. 00 - 12	Vento dir W; Forza 4	Mare dir W; Forza 3
11/30/2023	3:19					**campo Fedra**				CHIRP SOL 0086_2023_334_0321		acquisito solo chirp durante il trasferimento sulla linea Fedra6 di Qinsy	Parzialmente nuvoloso	h. 00 - 12	Vento dir W; Forza 4	Mare dir W; Forza 3
11/30/2023	3:26					**campo Fedra**				CHIRP EOL 0086_2023_334_0321			Parzialmente nuvoloso	h. 00 - 12	Vento dir W; Forza 4	Mare dir W; Forza 3
11/30/2023	3:27					**campo Fedra**			MB+WC+Qinsy	MB EM712 SOL 59; CHIRP SOL 0087_2023_334_0329		in SIS, riportata la coverage a 70/70 (fin'ora, dal 29 novembre) avevamo acquisito con fascio più stretto perché abbiamo dato priorità alla copertura chirp	Parzialmente nuvoloso	h. 00 - 12	Vento dir W; Forza 4	Mare dir W; Forza 3
11/30/2023	4:02					**campo Fedra**				MB EM712 EOL 59; CHIRP EOL 0087_2023_334_0329			Parzialmente nuvoloso	h. 00 - 12	Vento dir W; Forza 4	Mare dir W; Forza 3
11/30/2023	4:02								MB+WC	MB EM712 SOL 61; CHIRP SOL 0088_2023_334_0405		acquisizione durante il trasferimento sul punto CTD3 (velocità: 8 nodi circa) la linea mb 0060 è di pochi secondi	Parzialmente nuvoloso	h. 00 - 12	Vento dir W; Forza 4	Mare dir W; Forza 3
11/30/2023	4:04									QINSY SOL			Parzialmente nuvoloso	h. 00 - 12	Vento dir W; Forza 4	Mare dir W; Forza 3
11/30/2023	4:30									MB EM712 EOL 61; CHIRP EOL 0088_2023_334_0405			Parzialmente nuvoloso	h. 00 - 12	Vento dir W; Forza 4	Mare dir W; Forza 3
11/30/2023	4:36								MB+WC+Qinsy	MB EM712 SOL 62; CHIRP SOL 0089_2023_334_0438		ancora acquisizione durante il trasferimento sul punto CTD3 (velocità: 3 nodi)	Parzialmente nuvoloso	h. 00 - 12	Vento dir W; Forza 4	Mare dir W; Forza 3
11/30/2023	4:51									MB EM712 EOL 62; CHIRP EOL 0089_2023_334_0438			Parzialmente nuvoloso	h. 00 - 12	Vento dir W; Forza 4	Mare dir W; Forza 3
11/30/2023	5:18	1717.99210	3902.99360	17.2998683	39.0498933	**CTD3**	**PI23_CTD16_S**	415	CTD +SVP				Parzialmente nuvoloso	h. 00 - 12	Vento dir W; Forza 4	Mare dir W; Forza 3
11/30/2023	5:30											ctd ferma per operazioni di nastramento del cavo	Parzialmente nuvoloso	h. 00 - 12	Vento dir W; Forza 4	Mare dir W; Forza 3
11/30/2023	5:52											ricomincia la discesa della ctd	Parzialmente nuvoloso	h. 00 - 12	Vento dir W; Forza 4	Mare dir W; Forza 3
11/30/2023	5:53	1717.98720	3902.99040	17.2997867	39.0498400	**CTD3**	**PI23_CTD16_B**	416	CTD +SVP	svp_20231130_0553			Parzialmente nuvoloso	h. 00 - 12	Vento dir W; Forza 4	Mare dir W; Forza 3
11/30/2023	6:10	1717.98840	3902.97950	17.2998067	39.0496583	**CTD3**	**PI23_CTD16_E**	418	CTD +SVP				Parzialmente nuvoloso	h. 00 - 12	Vento dir W; Forza 4	Mare dir W; Forza 3
11/30/2023	6:30								MB+WC	MB EM712 SOL 63; CHIRP SOL 0090_2023_334_0633		trasferimento verso il punto 50	Parzialmente nuvoloso	h. 00 - 12	Vento dir W; Forza 4	Mare dir W; Forza 3

11/30/2023	6:33											il formato del logfile DROP-ALL viene modificato così da renderlo più semplice e chiaro. Questo file contiene i log delle posizioni di carotiere, ctd e a-frame registrate ogni 10 secondi. Anche questo file cambia automaticamente ogni ora	Parzialmente nuvoloso	h. 00 - 12	Vento dir W; Forza 4	Mare dir W; Forza 3
11/30/2023	6:34									QINSY SOL			Parzialmente nuvoloso	h. 00 - 12	Vento dir W; Forza 4	Mare dir W; Forza 3
11/30/2023	7:16									MB EM712 EOL 63; CHIRP EOL 0090_2023_334_0633			Parzialmente nuvoloso	h. 00 - 12	Vento dir W; Forza 4	Mare dir W; Forza 3
11/30/2023	7:28	1721.54890	3904.20550	17.3591483	39.0700917	**50**	**PI23_BC03_S**	609					Parzialmente nuvoloso	h. 00 - 12	Vento dir W; Forza 4	Mare dir W; Forza 3
11/30/2023	7:43	1721.55400	3904.20540	17.3592333	39.0700900	**50**	**PI23_BC03_B**	609					Parzialmente nuvoloso	h. 00 - 12	Vento dir W; Forza 4	Mare dir W; Forza 3
11/30/2023	7:55	1721.55780	3904.20350	17.3592967	39.0700583	**50**	**PI23_BC03_E**						Parzialmente nuvoloso	h. 00 - 12	Vento dir W; Forza 4	Mare dir W; Forza 3
11/30/2023	8:36									CHIRP SOL 0091_2023_334_0839		chirp registrato sopra il punto GC08	Parzialmente nuvoloso	h. 00 - 12	Vento dir W; Forza 4	Mare dir W; Forza 3
11/30/2023	8:56	1721.56580	3904.21780	17.3594300	39.0702967		**PI23_GC08**	607				carotiere al fondo	Parzialmente nuvoloso	h. 00 - 12	Vento dir W; Forza 4	Mare dir W; Forza 3
11/30/2023	8:57									CHIRP EOL 0091_2023_334_0839		siamo ancora sul punto GC08	Parzialmente nuvoloso	h. 00 - 12	Vento dir W; Forza 4	Mare dir W; Forza 3
11/30/2023	9:53											trasferimento verso stazione 69	Parzialmente nuvoloso	h. 00 - 12	Vento dir W; Forza 4	Mare dir W; Forza 3
11/30/2023	10:10					**69**				CHIRP SOL 0092_2023_334_1013		nave a 0 nodi, ci mette un po' per posizionarsi sul punto 69	Parzialmente nuvoloso	h. 00 - 12	Vento dir W; Forza 4	Mare dir W; Forza 3
11/30/2023	10:18	1721.43378	3903.87657	17.3572297	39.0646094	**69**	**PI23_BC04_S**					fix mark su chirp per indicare il punto di campionamento	Parzialmente nuvoloso	h. 00 - 12	Vento dir W; Forza 4	Mare dir W; Forza 3
11/30/2023	10:32	1721.43495	3903.87610	17.3572492	39.0646017	**69**	**PI23_BC04_B**	615					Parzialmente nuvoloso	h. 00 - 12	Vento dir W; Forza 4	Mare dir W; Forza 3
11/30/2023	10:44	1721.43613	3903.87509	17.3572688	39.0645848	**69**	**PI23_BC04_E**						Parzialmente nuvoloso	h. 00 - 12	Vento dir W; Forza 4	Mare dir W; Forza 3
11/30/2023	12:46	1721.45314	3903.92916	17.3575523	39.0654860		**PI23_GC09**	612				chirp 0093_2023_334_1241 MARVI 199-GC sul fondo (??????) GC 5m su stazione 69 RECUPERO CAROTAGGIO: 3,3 metri	Parzialmente nuvoloso	h. 00 - 12	Vento dir W; Forza 4	Mare dir W; Forza 3
11/30/2023	13:55									CHIRP SOL 0094_2023_334_1558		linea 8	Parzialmente nuvoloso	h. 12 - 24	Vento dir S; Forza 5	Mare dir S; Forza 4
11/30/2023	14:21									CHIRP EOL 0094_2023_334_1558			Parzialmente nuvoloso	h. 12 - 24	Vento dir S; Forza 5	Mare dir S; Forza 4
11/30/2023	14:33									CHIRP SOL 0095_2023_334_1435		linea 9 sul chirp, GAIN aumentato da 10 a 12	Parzialmente nuvoloso	h. 12 - 24	Vento dir S; Forza 5	Mare dir S; Forza 4
11/30/2023	15:01									CHIRP EOL 0095_2023_334_1435			Parzialmente nuvoloso	h. 12 - 24	Vento dir S; Forza 5	Mare dir S; Forza 4
11/30/2023	15:17									CHIRP SOL 0096_2023_334_1519			Parzialmente nuvoloso	h. 12 - 24	Vento dir S; Forza 5	Mare dir S; Forza 4
11/30/2023	15:18								MB+WC	MB EM712 SOL 64		linea per coprire un buco nell'acquisizione multibeam	Parzialmente nuvoloso	h. 12 - 24	Vento dir S; Forza 5	Mare dir S; Forza 4
11/30/2023	15:20									QINSY SOL			Parzialmente nuvoloso	h. 12 - 24	Vento dir S; Forza 5	Mare dir S; Forza 4
11/30/2023	15:46									QINSY EOL			Parzialmente nuvoloso	h. 12 - 24	Vento dir S; Forza 5	Mare dir S; Forza 4
11/30/2023	15:47									QINSY SOL			Parzialmente nuvoloso	h. 12 - 24	Vento dir S; Forza 5	Mare dir S; Forza 4
11/30/2023	15:49									MB EM712 EOL 64; CHIRP EOL 0096_2023_334_1519			Parzialmente nuvoloso	h. 12 - 24	Vento dir S; Forza 5	Mare dir S; Forza 4
11/30/2023	15:56					**campo Federica**			MB+WC+Qinsy	MB EM712 SOL 65; CHIRP SOL 0097_2023_334_1559		acquisizione sulla linea trasversale Fede6 di Qinsy	Parzialmente nuvoloso	h. 12 - 24	Vento dir S; Forza 5	Mare dir S; Forza 4
11/30/2023	16:20					**campo Federica**						CHIRP: il gain passa da 12dB a 10dB	Parzialmente nuvoloso	h. 12 - 24	Vento dir S; Forza 5	Mare dir S; Forza 4
11/30/2023	16:25					**campo Federica**				MB EM712 EOL 65; CHIRP EOL 0097_2023_334_1559			Parzialmente nuvoloso	h. 12 - 24	Vento dir S; Forza 5	Mare dir S; Forza 4
11/30/2023	16:30					**campo Federica/Fedra**			MB+WC+Qinsy	MB EM712 SOL 66; CHIRP SOL 0098_2023_334_1632		linea di trasferimento da campo Federica a campo Fedra	Parzialmente nuvoloso	h. 12 - 24	Vento dir S; Forza 5	Mare dir S; Forza 4
11/30/2023	16:45					**campo Federica/Fedra**				MB EM712 EOL 66; CHIRP EOL 0098_2023_334_1632			Parzialmente nuvoloso	h. 12 - 24	Vento dir S; Forza 5	Mare dir S; Forza 4
11/30/2023	16:48					**campo Fedra**			MB+WC+Qinsy	MB EM712 SOL 67; CHIRP SOL 0099_2023_334_1650		acquisizione su linea fedra7 di Qinsy, direzione sud-nord	Parzialmente nuvoloso	h. 12 - 24	Vento dir S; Forza 5	Mare dir S; Forza 4
11/30/2023	17:29					**campo Fedra**				MB EM712 EOL 67; CHIRP EOL 0099_2023_334_1650			Parzialmente nuvoloso	h. 12 - 24	Vento dir S; Forza 5	Mare dir S; Forza 4
11/30/2023	17:32					**campo Fedra**			MB+WC+Qinsy	MB EM712 SOL 68; CHIRP SOL 0100_2023_334_1735		acquisizione su linea fedra8 di Qinsy, direzione nord-sud	Parzialmente nuvoloso	h. 12 - 24	Vento dir S; Forza 5	Mare dir S; Forza 4
11/30/2023	18:17					**campo Fedra**				MB EM712 EOL 68; CHIRP EOL 0100_2023_334_1735			Parzialmente nuvoloso	h. 12 - 24	Vento dir S; Forza 5	Mare dir S; Forza 4
11/30/2023	18:24					**campo Fedra**			MB+WC+Qinsy	MB EM712 SOL 69; CHIRP SOL 0101_2023_334_1827		acquisizione su linea fedra9 di Qinsy	Parzialmente nuvoloso	h. 12 - 24	Vento dir S; Forza 5	Mare dir S; Forza 4
11/30/2023	19:07					**campo Fedra**				MB EM712 EOL 69; CHIRP EOL 0101_2023_334_1827			Parzialmente nuvoloso	h. 12 - 24	Vento dir S; Forza 5	Mare dir S; Forza 4
11/30/2023	19:09					**campo Fedra**			MB+WC+Qinsy	MB EM712 SOL 70; CHIRP SOL 0102_2023_334_1912			Parzialmente nuvoloso	h. 12 - 24	Vento dir S; Forza 5	Mare dir S; Forza 4
11/30/2023	19:11					**campo Fedra**				MB EM712 EOL 70; CHIRP EOL 0102_2023_334_1912			Parzialmente nuvoloso	h. 12 - 24	Vento dir S; Forza 5	Mare dir S; Forza 4
11/30/2023	19:17					**campo Fedra**			MB+WC+Qinsy	MB EM712 SOL 71; CHIRP SOL 0103_2023_334_1920		acquisizione su linea fedra10 di Qinsy	Parzialmente nuvoloso	h. 12 - 24	Vento dir S; Forza 5	Mare dir S; Forza 4
11/30/2023	19:48	3907.87000	1719.07900	39.1311667	17.3179833	**campo Fedra**						su linea CHIRP, possibile fuoriuscita di fluidi (taglia?)	Parzialmente nuvoloso	h. 12 - 24	Vento dir S; Forza 5	Mare dir S; Forza 4
11/30/2023	20:07					**campo Fedra**				QINSY EOL		continua l'acquisizione mb solo con il SIS fino alla fine dell'accostata	Parzialmente nuvoloso	h. 12 - 24	Vento dir S; Forza 5	Mare dir S; Forza 4
11/30/2023	20:09					**campo Fedra**				MB EM712 EOL 71; CHIRP EOL 0103_2023_334_1920			Parzialmente nuvoloso	h. 12 - 24	Vento dir S; Forza 5	Mare dir S; Forza 4
11/30/2023	20:13								MB+WC+Qinsy	MB EM712 SOL 72; CHIRP SOL 0104_2023_334_2016		inizio del trasferimento verso il ridosso per maltempo	Parzialmente nuvoloso	h. 12 - 24	Vento dir S; Forza 5	Mare dir S; Forza 4
11/30/2023	21:37									MB EM712 EOL 72			Parzialmente nuvoloso	h. 12 - 24	Vento dir S; Forza 5	Mare dir S; Forza 4
11/30/2023	21:37								MB noWC	MB EM712 SOL 73			Parzialmente nuvoloso	h. 12 - 24	Vento dir S; Forza 5	Mare dir S; Forza 4
11/30/2023	23:07									MB EM712 EOL; CHIRP EOL			Parzialmente nuvoloso	h. 12 - 24	Vento dir S; Forza 5	Mare dir S; Forza 4
11/30/2023	23:08									MB EM712 SOL 76		continuazione della linea di transito. Da ora e fino al punto di ridosso acquisiamo solo mb	Parzialmente nuvoloso	h. 12 - 24	Vento dir S; Forza 5	Mare dir S; Forza 4
12/1/2023	0:21											stand-by meteo	Parzialmente nuvoloso	h. 00 - 12	Vento dir SE; Forza 6	Mare dir SE; Forza 4
12/1/2023	10:59	1707.36740	3935.11110	17.1227900	39.5851850	**44**	**PI23_CTD17_S**	677	CTD +SVP				Parzialmente nuvoloso	h. 00 - 12	Vento dir SE; Forza 6	Mare dir SE; Forza 4
12/1/2023	11:12	1707.36900	3935.11105	17.1228167	39.5851842	**44**	**PI23_CTD17_B**	676	CTD +SVP	svp_20231201_1112			Parzialmente nuvoloso	h. 00 - 12	Vento dir SE; Forza 6	Mare dir SE; Forza 4
12/1/2023	11:28	1707.36968	3935.11323	17.1228280	39.5852205	**44**	**PI23_CTD17_E**	675	CTD +SVP				Parzialmente nuvoloso	h. 00 - 12	Vento dir SE; Forza 6	Mare dir SE; Forza 4
12/1/2023	11:56					**44**			MB+WC+Qinsy	MB EM712 SOL 78; CHIRP SOL 0001_2023_335_1159		parametri chirp: Tx pulse: 8m; Tx power: 2; Gain value: 13dB; Range: 200; Mode: auto; Overlap: 50%; Shift Threshold: 30%; Depth limits: 0-1000m	Parzialmente nuvoloso	h. 00 - 12	Vento dir SE; Forza 6	Mare dir SE; Forza 4
12/1/2023	13:07					**44**			MB noWC	MB EM712 SOL 80		Interrotto solo mb mentre il chirp prosegue senza interruzioni	Parzialmente nuvoloso	h. 12 - 24	Vento dir SE; Forza 5	Mare dir SE; Forza 4
12/1/2023	14:06					**44**			MB noWC	MB EM712 SOL 81			Parzialmente nuvoloso	h. 12 - 24	Vento dir SE; Forza 5	Mare dir SE; Forza 4
12/1/2023	15:06					**44**			MB noWC	MB EM712 SOL 82			Parzialmente nuvoloso	h. 12 - 24	Vento dir SE; Forza 5	Mare dir SE; Forza 4
12/1/2023	16:00					**44**						momento foto in control room con luci rosse accese e tutto in ordine	Parzialmente nuvoloso	h. 12 - 24	Vento dir SE; Forza 5	Mare dir SE; Forza 4
12/1/2023	18:24					**44**						CHIRP fuori scala, modifichiamo i depth limits in 0-1000	Parzialmente nuvoloso	h. 12 - 24	Vento dir SE; Forza 5	Mare dir SE; Forza 4
12/1/2023	19:14					**44**				MB EM712 EOL 86			Parzialmente nuvoloso	h. 12 - 24	Vento dir SE; Forza 5	Mare dir SE; Forza 4
12/1/2023	19:17					**44**				CHIRP EOL 0001_2023_335_1159			Parzialmente nuvoloso	h. 12 - 24	Vento dir SE; Forza 5	Mare dir SE; Forza 4
12/1/2023	19:26					**44**			MB noWC+Qinsy	MB EM712 SOL 87; CHIRP SOL 0002_2023_335_1928			Parzialmente nuvoloso	h. 12 - 24	Vento dir SE; Forza 5	Mare dir SE; Forza 4
12/1/2023	20:20					**44**						crash SIS	Parzialmente nuvoloso	h. 12 - 24	Vento dir SE; Forza 5	Mare dir SE; Forza 4
12/1/2023	20:21					**44**				MB EM712 SOL 87			Parzialmente nuvoloso	h. 12 - 24	Vento dir SE; Forza 5	Mare dir SE; Forza 4
12/1/2023	21:44					**44**				MB EM712 EOL 88			Parzialmente nuvoloso	h. 12 - 24	Vento dir SE; Forza 5	Mare dir SE; Forza 4
12/1/2023	21:54					**44**				CHIRP EOL 0002_2023_335_1928			Parzialmente nuvoloso	h. 12 - 24	Vento dir SE; Forza 5	Mare dir SE; Forza 4
12/1/2023	22:02	1650.57630	3949.03437	16.8429383	39.8172395	**44**	**PI23_CTD18_S**		CTD +SVP				Parzialmente nuvoloso	h. 12 - 24	Vento dir SE; Forza 5	Mare dir SE; Forza 4
12/1/2023	22:13	1650.58052	3949.03358	16.8430087	39.8172263	**44**	**PI23_CTD18_B**	420	CTD +SVP	svp_20231201_2123			Parzialmente nuvoloso	h. 12 - 24	Vento dir SE; Forza 5	Mare dir SE; Forza 4
12/1/2023	22:23	1650.58260	3949.03455	16.8430433	39.8172425	**44**	**PI23_CTD18_E**		CTD +SVP				Parzialmente nuvoloso	h. 12 - 24	Vento dir SE; Forza 5	Mare dir SE; Forza 4
12/1/2023	22:50					**44**				CHIRP SOL 0003_2023_335_2153			Parzialmente nuvoloso	h. 12 - 24	Vento dir SE; Forza 5	Mare dir SE; Forza 4
12/1/2023	22:55					**44**			MB noWC+Qinsy	MB EM712 SOL 90			Parzialmente nuvoloso	h. 12 - 24	Vento dir SE; Forza 5	Mare dir SE; Forza 4
12/2/2023	4:21					**44**				MB EM712 EOL 95, CHIRP EOL 0003_2023_335_2153			Mezzo coperto	h. 00 - 12	Vento dir S; Forza 4	Mare dir S; Forza 4
12/2/2023	4:36					**44**				CHIRP SOL 0004_2023_336_0438			Mezzo coperto	h. 00 - 12	Vento dir S; Forza 4	Mare dir S; Forza 4
12/2/2023	4:39					**44**			MB noWC+Qinsy	MB EM712 SOL 96			Mezzo coperto	h. 00 - 12	Vento dir S; Forza 4	Mare dir S; Forza 4
12/2/2023	5:51					**44**				MB EM712 EOL 97, CHIRP EOL 0004_2023_336_0438			Mezzo coperto	h. 00 - 12	Vento dir S; Forza 4	Mare dir S; Forza 4
12/2/2023	6:12					**44**			MB noWC+Qinsy	MB EM712 SOL 98; CHIRP SOL 0005_2023_336_0616			Mezzo coperto	h. 00 - 12	Vento dir S; Forza 4	Mare dir S; Forza 4
12/2/2023	6:36					**44**				QINSY EOL		Interrotta solo l'acquisizione in Qinsy per correggere, nel setup, i valori di Tx assegnati al mb EM712 (erano stati erroneamente assegnati al Tx gli stessi valori dell'RX)	Mezzo coperto	h. 00 - 12	Vento dir S; Forza 4	Mare dir S; Forza 4
12/2/2023	6:37					**44**				QINSY SOL			Mezzo coperto	h. 00 - 12	Vento dir S; Forza 4	Mare dir S; Forza 4
12/2/2023	6:57					**44**			MB noWC+Qinsy	MB EM712 SOL 99; CHIRP SOL 0006_2023_336_0700		accostata per andare verso il punto di campionamento 44	Mezzo coperto	h. 00 - 12	Vento dir S; Forza 4	Mare dir S; Forza 4
12/2/2023	7:29					**44**						arrivo sul punto di campionamento 44	Mezzo coperto	h. 00 - 12	Vento dir S; Forza 4	Mare dir S; Forza 4

12/2/2023	9:35	1656.41077	3944.40254	16.9401796	39.7400423	44	PI23_PC10	370				Carotiere sul fondo. velocità di discesa xx m/s; tiro max x t; penetrazione xx m; recupero 8,36 m Il carotiere risulta infangato fino in testa, sembra che sia penetrato tutto nel sedimento ma sono state perse le masse a causa della rottura di un cavo in kevlar	Mezzo coperto	h. 00 - 12	Vento dir S; Forza 4	Mare dir S; Forza 4
12/2/2023	9:42					44				CHIRP EOL 0006_2023_336_0700			Mezzo coperto	h. 00 - 12	Vento dir S; Forza 4	Mare dir S; Forza 4
12/2/2023	10:18					44	PI23_CTD19_S						Mezzo coperto	h. 00 - 12	Vento dir S; Forza 4	Mare dir S; Forza 4
12/2/2023	10:27	1656.41716	3944.39622	16.9402860	39.7399369	44	PI23_CTD19_B	370	CTD +SVP	svp_20231202_1027			Mezzo coperto	h. 00 - 12	Vento dir S; Forza 4	Mare dir S; Forza 4
12/2/2023	10:42	1656.41769	3944.39651	16.9402948	39.7399418	44	PI23_CTD19_E					coordinate dei pockmarl dell'Amendolara: 39°42,3659'N 16°57,67189'E	Mezzo coperto	h. 00 - 12	Vento dir S; Forza 4	Mare dir S; Forza 4
12/2/2023	11:58	1656.43514	3944.37248	16.9405857	39.7395413	44	PI23_BC05_S	367					Mezzo coperto	h. 00 - 12	Vento dir S; Forza 4	Mare dir S; Forza 4
12/2/2023	12:00					44				CHIRP SOL 0007_2023_336_1203			Mezzo coperto	h. 00 - 12	Vento dir S; Forza 4	Mare dir S; Forza 4
12/2/2023	12:05	1656.43582	3944.37521	16.9405970	39.7395868	44	PI23_BC05_B	368					Mezzo coperto	h. 12 - 24	Vento dir S; Forza 6	Mare dir S; Forza 5
12/2/2023	12:14	1656.43396	3944.38542	16.9405660	39.7397570	44	PI23_BC05_E	369					Mezzo coperto	h. 12 - 24	Vento dir S; Forza 6	Mare dir S; Forza 5
12/2/2023	12:34	1656.44380	3944.38210	16.9407300	39.7397017	44	PI23_BC06_S	368				replica di PI23_BC05	Mezzo coperto	h. 12 - 24	Vento dir S; Forza 6	Mare dir S; Forza 5
12/2/2023	12:40	1656.45150	3944.38064	16.9408583	39.7396773	44	PI23_BC06_B	368					Mezzo coperto	h. 12 - 24	Vento dir S; Forza 6	Mare dir S; Forza 5
12/2/2023	12:52	1656.45918	3944.37877	16.9409863	39.7396462	44	PI23_BC06_E	368				alla fine del box corer ci trasferiamo verso costa a causa del mare mosso	Mezzo coperto	h. 12 - 24	Vento dir S; Forza 6	Mare dir S; Forza 5
12/2/2023	13:35					44				QINSY SOL			Mezzo coperto	h. 12 - 24	Vento dir S; Forza 6	Mare dir S; Forza 5
12/2/2023	14:14					44			MB noWC+Qinsy	MB EM712 SOL 100			Mezzo coperto	h. 12 - 24	Vento dir S; Forza 6	Mare dir S; Forza 5
12/2/2023	14:19					44				CHIRP SOL 0009_2023_336_1422			Mezzo coperto	h. 12 - 24	Vento dir S; Forza 6	Mare dir S; Forza 5
12/2/2023	15:03					44				CHIRP EOL 0009_2023_336_1422			Mezzo coperto	h. 12 - 24	Vento dir S; Forza 6	Mare dir S; Forza 5
12/2/2023	15:03					44				CHIRP SOL 0010_2023_336_1505		CHIRP: NO multiping. Proviamo a togliere il multiping perché il chirp continua a saltare da una profondità falsa (480m) ad una profondità vera (reale). Nonostante questa modifica, il problema persiste Altri parametri del chirp: Tx pulse: 8ms; Tx power: 2; Gain value: 9dB; Range: 200; Overlap: 50%; Shift Threshold: 50%; Depth min-max: 200-1200m	Mezzo coperto	h. 12 - 24	Vento dir S; Forza 6	Mare dir S; Forza 5
12/2/2023	16:32					44				MB EM712 EOL 102, CHIRP EOL 0010_2023_336_1505			Mezzo coperto	h. 12 - 24	Vento dir S; Forza 6	Mare dir S; Forza 5
12/2/2023	16:47					44			MB noWC+Qinsy	MB EM712 SOL 103, CHIRP SOL 0011_2023_336_1650		CHIRP: dopo vari test vediamo che con Shift Threshold: 30% sembra che l'acquisizione di stabilizzi	Mezzo coperto	h. 12 - 24	Vento dir S; Forza 6	Mare dir S; Forza 5
12/2/2023	19:28					44				MB EM712 EOL 105, CHIRP EOL 0011_2023_336_1650			Mezzo coperto	h. 12 - 24	Vento dir S; Forza 6	Mare dir S; Forza 5
12/2/2023	19:38					44			MB noWC+Qinsy	MB EM712 SOL 106, CHIRP SOL 0012_2023_336_1941			Mezzo coperto	h. 12 - 24	Vento dir S; Forza 6	Mare dir S; Forza 5
12/2/2023	20:02					44				MB EM712 EOL 106, CHIRP EOL 0012_2023_336_1941			Mezzo coperto	h. 12 - 24	Vento dir S; Forza 6	Mare dir S; Forza 5
12/2/2023	20:13					44			MB noWC+Qinsy	MB EM712 SOL 107, CHIRP SOL 0013_2023_336_2016			Mezzo coperto	h. 12 - 24	Vento dir S; Forza 6	Mare dir S; Forza 5
12/2/2023	23:07					44				MB EM712 EOL 107, CHIRP EOL 0013_2023_336_2016			Mezzo coperto	h. 12 - 24	Vento dir S; Forza 6	Mare dir S; Forza 5
12/2/2023	23:07					44			MB noWC+Qinsy	MB EM712 SOL 110/111, CHIRP SOL 0014_2023_336_2309/0015_2023_336_2338			Mezzo coperto	h. 12 - 24	Vento dir S; Forza 6	Mare dir S; Forza 5
12/2/2023	23:52					44				MB EM712 EOL 111, CHIRP EOL 0015_2023_336_2338			Mezzo coperto	h. 12 - 24	Vento dir S; Forza 6	Mare dir S; Forza 5
12/2/2023	23:52					44			MB noWC+Qinsy	MB EM712 SOL 112, CHIRP SOL 0016_2023_336_2355		alle ore 00:45 il mb registra un po' di rumore sul fondale. Velocità 3,2Kn; Direzione: 333°. Anche il chirp registra un po' di disturbo	Mezzo coperto	h. 12 - 24	Vento dir S; Forza 6	Mare dir S; Forza 5
12/3/2023	3:43					44				MB EM712 EOL 115, CHIRP EOL 0016_2023_336_2355			Mezzo coperto	h. 00 - 12	Vento dir W/NW; Forza 5	Mare dir W/NW; Forza 4
12/3/2023	3:54					44			MB noWC+Qinsy	MB EM712 SOL 116, CHIRP SOL 0017_2023_337_0357			Mezzo coperto	h. 00 - 12	Vento dir W/NW; Forza 5	Mare dir W/NW; Forza 4
12/3/2023	5:42					44				MB EM712 EOL 117, CHIRP EOL 0017_2023_337_0357			Mezzo coperto	h. 00 - 12	Vento dir W/NW; Forza 5	Mare dir W/NW; Forza 4
12/3/2023	6:10					44				CHIRP SOL 0018_2023_337_0612			Mezzo coperto	h. 00 - 12	Vento dir W/NW; Forza 5	Mare dir W/NW; Forza 4
12/3/2023	6:17					44			MB noWC+Qinsy	MB EM712 SOL 118			Mezzo coperto	h. 00 - 12	Vento dir W/NW; Forza 5	Mare dir W/NW; Forza 4
12/3/2023	7:50					44				CHIRP EOL 0018_2023_337_0612			Mezzo coperto	h. 00 - 12	Vento dir W/NW; Forza 5	Mare dir W/NW; Forza 4
12/3/2023	8:03					44				MB EM712 EOL 119			Mezzo coperto	h. 00 - 12	Vento dir W/NW; Forza 5	Mare dir W/NW; Forza 4
12/3/2023	8:15	1657.67551	3942.36297	16.9612585	39.7060494	44	PI23_CTD20_S					stazione sopra un pockmark	Mezzo coperto	h. 00 - 12	Vento dir W/NW; Forza 5	Mare dir W/NW; Forza 4
12/3/2023	8:23	1657.68269	3942.36197	16.9613782	39.7060328	44	PI23_CTD20_B	287		svp_20231203_0823		manca velocità e tiro	Mezzo coperto	h. 00 - 12	Vento dir W/NW; Forza 5	Mare dir W/NW; Forza 4
12/3/2023	8:32	1657.66823	3942.36335	16.9611372	39.7060558	44	PI23_CTD20_E						Mezzo coperto	h. 00 - 12	Vento dir W/NW; Forza 5	Mare dir W/NW; Forza 4
12/3/2023	8:48	1657.66470	3942.36020	16.9610783	39.7060033	44	PI23_BC07_S	281					Mezzo coperto	h. 00 - 12	Vento dir W/NW; Forza 5	Mare dir W/NW; Forza 4
12/3/2023	8:55	1657.66250	3942.36010	16.9610417	39.7060017	44	PI23_BC07_B	281					Mezzo coperto	h. 00 - 12	Vento dir W/NW; Forza 5	Mare dir W/NW; Forza 4
12/3/2023	9:04	1657.65620	3942.35930	16.9609367	39.7059883	44	PI23_BC07_E	281				box corer fallito perché ha penetrato troppo. Si decide quindi di togliere delle masse così da renderlo più leggero	Mezzo coperto	h. 00 - 12	Vento dir W/NW; Forza 5	Mare dir W/NW; Forza 4
12/3/2023	9:38					44				CHIRP SOL 0020_2023_337_0941		acquisizione a nave ferma sul pockmark	Mezzo coperto	h. 00 - 12	Vento dir W/NW; Forza 5	Mare dir W/NW; Forza 4
12/3/2023	9:38	1657.65928	3942.37131	16.9609880	39.7061885	44	PI23_BC08_S						Mezzo coperto	h. 00 - 12	Vento dir W/NW; Forza 5	Mare dir W/NW; Forza 4
12/3/2023	9:47	1657.66471	3942.37022	16.9610785	39.7061703	44	PI23_BC08_B	281					Mezzo coperto	h. 00 - 12	Vento dir W/NW; Forza 5	Mare dir W/NW; Forza 4
12/3/2023	9:56					44				CHIRP EOL 0020_2023_337_0941			Mezzo coperto	h. 00 - 12	Vento dir W/NW; Forza 5	Mare dir W/NW; Forza 4
12/3/2023	9:59	1657.66088	3942.37221	16.9610147	39.7062035	44	PI23_BC08_E					box corer fallito per lo stesso motivo	Mezzo coperto	h. 00 - 12	Vento dir W/NW; Forza 5	Mare dir W/NW; Forza 4
12/3/2023	10:43	1657.66630	3942.36671	16.9611050	39.7061118	44	PI23_BC09_S					riduciamo la corsa di caduta del box corer e togliamo tutte le masse	Mezzo coperto	h. 00 - 12	Vento dir W/NW; Forza 5	Mare dir W/NW; Forza 4
12/3/2023	10:51	1657.66325	3942.36741	16.9610541	39.7061235	44	PI23_BC09_B	281					Mezzo coperto	h. 00 - 12	Vento dir W/NW; Forza 5	Mare dir W/NW; Forza 4
12/3/2023	11:00	1657.66001	3942.36793	16.9610002	39.7061322	44	PI23_BC09_E						Mezzo coperto	h. 00 - 12	Vento dir W/NW; Forza 5	Mare dir W/NW; Forza 4
12/3/2023	13:09	1656.39890	3944.40000	16.9399817	39.7400000	44	PI23_SW11_S	361					Mezzo coperto	h. 12 - 24	Vento dir N; Forza 5	Mare dir N; Forza 3
12/3/2023	13:27					44				CHIRP SOL 0021_2023_337_1329			Mezzo coperto	h. 12 - 24	Vento dir N; Forza 5	Mare dir N; Forza 3
12/3/2023	13:28	1656.40290	3944.40000	16.9400483	39.7400000	44	PI23_SW11_B	369					Mezzo coperto	h. 12 - 24	Vento dir N; Forza 5	Mare dir N; Forza 3
12/3/2023	13:38	1656.39670	3944.40060	16.9399450	39.7400100	44	PI23_SW11_E	369					Mezzo coperto	h. 12 - 24	Vento dir N; Forza 5	Mare dir N; Forza 3
12/3/2023	14:37	1656.83420	3941.56910	16.9472367	39.6928183	44	PI23_CTD21_S	386					Mezzo coperto	h. 12 - 24	Vento dir N; Forza 5	Mare dir N; Forza 3
12/3/2023	14:49	1656.83220	3941.57000	16.9472033	39.6928333	44	PI23_CTD21_B	387	CTD +SVP	svp_20231203_1437			Mezzo coperto	h. 12 - 24	Vento dir N; Forza 5	Mare dir N; Forza 3
12/3/2023	15:58	1656.84110	3941.56430	16.9473517	39.6927383	44	PI23_CTD21_E	387					Mezzo coperto	h. 12 - 24	Vento dir N; Forza 5	Mare dir N; Forza 3
12/3/2023	15:17					44			MB noWC+Qinsy	MB EM712 SOL 120, CHIRP SOL 0022_2023_337_1519			Mezzo coperto	h. 12 - 24	Vento dir N; Forza 5	Mare dir N; Forza 3
12/3/2023	20:01					44				MB EM712 EOL 124, CHIRP EOL 0022_2023_337_1519			Mezzo coperto	h. 12 - 24	Vento dir N; Forza 5	Mare dir N; Forza 3
12/3/2023	20:03					44				CHIRP SOL 0023_2023_337_2006		CHIRP: depth limits 0-1200m	Mezzo coperto	h. 12 - 24	Vento dir N; Forza 5	Mare dir N; Forza 3
12/3/2023	20:14					44			TEST SIS parameters	MB EM712 SOL 125		Attitude System 1: OK Attitude System 2: ACTIVE OK Line heading: 353°; Vel: 4Kn	Mezzo coperto	h. 12 - 24	Vento dir N; Forza 5	Mare dir N; Forza 3
12/3/2023	20:37					44			TEST SIS parameters	MB EM712 EOL 125			Mezzo coperto	h. 12 - 24	Vento dir N; Forza 5	Mare dir N; Forza 3
12/3/2023	20:51					44			TEST SIS parameters	MB EM712 SOL 126		Attitude System 1: ACTIVE OK Attitude System 2: OK Line heading: 173°; Vel: 4Kn	Mezzo coperto	h. 12 - 24	Vento dir N; Forza 5	Mare dir N; Forza 3
12/3/2023	21:14					44			TEST SIS parameters	MB EM712 EOL 126			Mezzo coperto	h. 12 - 24	Vento dir N; Forza 5	Mare dir N; Forza 3
12/3/2023	21:27					44			TEST SIS parameters	MB EM712 SOL 127		Attitude System 1: ACTIVE OK Attitude System 2: OK Line heading: 353°; Vel: 4Kn	Mezzo coperto	h. 12 - 24	Vento dir N; Forza 5	Mare dir N; Forza 3
	21:51					44			TEST SIS parameters	MB EM712 EOL 127			Mezzo coperto	h. 12 - 24	Vento dir N; Forza 5	Mare dir N; Forza 3
12/3/2023	20:52					44				CHIRP EOL 0023_2023_337_2006		dalle 20:40 in poi il CHIRP ha acquisito anche il loop che ha fatto la nave per tornare sulla linea di test	Mezzo coperto	h. 12 - 24	Vento dir N; Forza 5	Mare dir N; Forza 3

12/3/2023	21:58					44			MB noWC+Qinsy	MB EM712 SOL 128, CHIRP SOL 0024_2023_337_2200		parametri del SIS riportati allo stato originale, ovvero: Attitude System 1: OK Attitude System 2: ACTIVE OK	Mezzo coperto	h. 12 - 24	Vento dir N; Forza 5	Mare dir N; Forza 3
12/4/2023	5:40					44/75				MB EM712 EOL 128, CHIRP EOL 0024_2023_337_2200			Mezzo coperto	h. 00 - 12	Vento dir N; Forza 3	Mare dir N; Forza 3
12/4/2023	5:43					75				CHIRP SOL 0025_2023_338_0545		acquisizione solo CHIRP sul punto di campionamento	Mezzo coperto	h. 00 - 12	Vento dir N; Forza 3	Mare dir N; Forza 3
12/4/2023	6:00	1701.65391	4018.06601	17.0275652	40.3011002	75	PI23_BC10_S	1008					Mezzo coperto	h. 00 - 12	Vento dir N; Forza 3	Mare dir N; Forza 3
12/4/2023	6:16	1701.65637	4018.06339	17.0276062	40.3010565	75	PI23_BC10_B	1008				vel. di caduta: 20min/m; tiro: 1,87ton; prof. cavo: 994m	Mezzo coperto	h. 00 - 12	Vento dir N; Forza 3	Mare dir N; Forza 3
12/4/2023	6:36	1701.65642	4018.06496	17.0276070	40.3010827	75	PI23_BC10_E					box corer FALLITO (non si è chiuso)	Mezzo coperto	h. 00 - 12	Vento dir N; Forza 3	Mare dir N; Forza 3
12/4/2023	6:39					75				CHIRP EOL 0025_2023_338_0545			Mezzo coperto	h. 00 - 12	Vento dir N; Forza 3	Mare dir N; Forza 3
12/4/2023	6:40	1701.66239	4018.06511	17.0277065	40.3010852	75	PI23_BC11_S	1007					Mezzo coperto	h. 00 - 12	Vento dir N; Forza 3	Mare dir N; Forza 3
12/4/2023	6:58	1701.67411	4018.06229	17.0279018	40.3010382	75	PI23_BC11_B	1007				vel. di caduta: 20min/m; tiro: 1,61ton; prof. cavo: 994m	Mezzo coperto	h. 00 - 12	Vento dir N; Forza 3	Mare dir N; Forza 3
12/4/2023	7:15	1701.67763	4018.05985	17.0279606	40.3009976	75	PI23_BC11_E					box corer ok	Mezzo coperto	h. 00 - 12	Vento dir N; Forza 3	Mare dir N; Forza 3
12/4/2023	7:31	1701.67973	4018.05599	17.0279956	40.3009332	75	PI23_BC12_S					box REPLICA di PI23_BC_11	Mezzo coperto	h. 00 - 12	Vento dir N; Forza 3	Mare dir N; Forza 3
12/4/2023	7:47	1701.67853	4018.05857	17.0279755	40.3009762	75	PI23_BC12_B	1008				vel. di caduta: 20min/m; tiro: 2,61ton; prof. cavo: 992m Box corer stabilizzato a 20 metri dal fondo invece che a 30 metri come i precedenti	Mezzo coperto	h. 00 - 12	Vento dir N; Forza 3	Mare dir N; Forza 3
12/4/2023	8:06	1701.68090	4018.06050	17.0280150	40.3010083	75	PI23_BC12_E					box corer ok	Mezzo coperto	h. 00 - 12	Vento dir N; Forza 3	Mare dir N; Forza 3
12/4/2023	8:15					75						inizio trasferimento verso stazione 76	Mezzo coperto	h. 00 - 12	Vento dir N; Forza 3	Mare dir N; Forza 3
12/4/2023	8:19					75			MB noWC+Qinsy	MB EM712 SOL 136; CHIRP SOL 0026_2023_338_0824		velocità: 8Kn, quindi l'acquisizione è un po' rumorosa	Mezzo coperto	h. 00 - 12	Vento dir N; Forza 3	Mare dir N; Forza 3
12/4/2023	9:08					76				MB EM712 EOL 136; CHIRP EOL 0026_2023_338_0824			Mezzo coperto	h. 00 - 12	Vento dir N; Forza 3	Mare dir N; Forza 3
12/4/2023	9:15	1705.32926	4012.31868	17.0888210	40.2053113	76	PI23_BC13_S						Mezzo coperto	h. 00 - 12	Vento dir N; Forza 3	Mare dir N; Forza 3
12/4/2023	9:17					76				CHIRP SOL 0027_2023_338_0920			Mezzo coperto	h. 00 - 12	Vento dir N; Forza 3	Mare dir N; Forza 3
12/4/2023	9:30	1705.32892	4012.31565	17.0888153	40.2052608	76	PI23_BC13_B	1209				vel. di caduta: 20min/m; tiro: 0,85ton; prof. cavo: 1201m	Mezzo coperto	h. 00 - 12	Vento dir N; Forza 3	Mare dir N; Forza 3
12/4/2023	9:45					76				CHIRP EOL 0027_2023_338_0920			Mezzo coperto	h. 00 - 12	Vento dir N; Forza 3	Mare dir N; Forza 3
12/4/2023	9:57	1705.32847	4012.31964	17.0888078	40.2053273	76	PI23_BC13_E					risalita lenta (60m/min) perché cavo vibra tra la puleggia e il verricello. Sostituiamo la puleggia durante il transito	Mezzo coperto	h. 00 - 12	Vento dir N; Forza 3	Mare dir N; Forza 3
12/4/2023	10:09	1705.32847	4012.31964	17.0888078	40.2053273	76	PI23_BC14_S					box REPLICA di stazione 76	Mezzo coperto	h. 00 - 12	Vento dir N; Forza 3	Mare dir N; Forza 3
12/4/2023	10:30	1705.33072	4012.31502	17.0888453	40.2052503	76	PI23_BC14_B	1208				vel. di caduta: 20min/m; tiro: 0,88ton; prof. cavo: 1200m	Mezzo coperto	h. 00 - 12	Vento dir N; Forza 3	Mare dir N; Forza 3
12/4/2023	10:57	1705.33105	4012.31710	17.0888508	40.2052850	76	PI23_BC14_E					box corer FALLITO	Mezzo coperto	h. 00 - 12	Vento dir N; Forza 3	Mare dir N; Forza 3
12/4/2023	11:04	1705.33094	4012.31707	17.0888490	40.2052845	76	PI23_BC15_S	1207				box seconda REPLICA di PI23_BC_13	Mezzo coperto	h. 00 - 12	Vento dir N; Forza 3	Mare dir N; Forza 3
12/4/2023	11:23	1705.32960	4012.31917	17.0888267	40.2053195	76	PI23_BC15_B	1205				vel. di caduta: 20min/m; tiro: 24ton; prof. cavo: 1200m la puleggia salta durante la risalita	Mezzo coperto	h. 00 - 12	Vento dir N; Forza 3	Mare dir N; Forza 3
12/4/2023	11:50	1705.33090	4012.33320	17.0888483	40.2055533	76	PI23_BC15_E						Mezzo coperto	h. 00 - 12	Vento dir N; Forza 3	Mare dir N; Forza 3
12/4/2023	11:58					76/77			MB noWC+Qinsy	MB EM712 SOL 137, CHIRP SOL 0028_2023_338_1201			Mezzo coperto	h. 00 - 12	Vento dir N; Forza 3	Mare dir N; Forza 3
12/4/2023	13:08					76/77						in Qinsy, il grid non è più visibile quindi aumentiamo la depth massima dell'EM712 portandola a 2000m (il SIS invece è settato bene)	Mezzo coperto	h. 12 - 24	Vento dir N; Forza 3	Mare dir N; Forza 3
12/4/2023	13:36					76/77				MB EM712 EOL 128		spegniamo EM712 e accendiamo EM304 perché il fondale è diventato molto profondo	Mezzo coperto	h. 12 - 24	Vento dir N; Forza 3	Mare dir N; Forza 3
12/4/2023	13:40					76/77				MB EM304 SOL 61			Mezzo coperto	h. 12 - 24	Vento dir N; Forza 3	Mare dir N; Forza 3
12/4/2023	13:44					76/77				SOL Qinsy			Mezzo coperto	h. 12 - 24	Vento dir N; Forza 3	Mare dir N; Forza 3
12/4/2023	13:55					77				MB EM304 EOL 61, CHIRP EOL 0028_2023_338_1201			Mezzo coperto	h. 12 - 24	Vento dir N; Forza 3	Mare dir N; Forza 3
12/4/2023	14:01	1719.39270	3955.70650	17.3232117	39.9284417	77	PI23_BC16_S	1708					Mezzo coperto	h. 12 - 24	Vento dir N; Forza 3	Mare dir N; Forza 3
12/4/2023	14:28	1719.38496	3955.70090	17.3230827	39.9283483	77	PI23_BC16_B	1708				vel. di caduta: 20min/m; tiro: 277ton; prof. cavo: 1686m	Mezzo coperto	h. 12 - 24	Vento dir N; Forza 3	Mare dir N; Forza 3
12/4/2023	14:59	1719.38830	3955.70840	17.3231383	39.9284733	77	PI23_BC16_E	1711				cambio puleggia per il prossimo box corer	Mezzo coperto	h. 12 - 24	Vento dir N; Forza 3	Mare dir N; Forza 3
12/4/2023	15:18	1719.38820	3955.70470	17.3231367	39.9284117	77	PI23_BC17_S	1708				box REPLICA di stazione 77	Mezzo coperto	h. 12 - 24	Vento dir N; Forza 3	Mare dir N; Forza 3
12/4/2023	15:38	1719.38685	3955.70775	17.3231142	39.9284625	77	PI23_BC17_B	1708				vel. di caduta: 20min/m; tiro: 2,36ton; prof. cavo: 1690m	Mezzo coperto	h. 12 - 24	Vento dir N; Forza 3	Mare dir N; Forza 3
12/4/2023	16:00	1719.38672	3955.70969	17.3231120	39.9284948	77	PI23_BC17_E						Mezzo coperto	h. 12 - 24	Vento dir N; Forza 3	Mare dir N; Forza 3
12/4/2023	16:14					77/CTD16			MB noWC+Qinsy	MB EM304 SOL 62, CHIRP SOL 0029_2023_338_1617		linea di trasferimento verso CTD16, vel. 10 nodi CHIRP: Tx power: 4; Tx pulse: 8ms	Mezzo coperto	h. 12 - 24	Vento dir N; Forza 3	Mare dir N; Forza 3
12/4/2023	17:42									CHIRP EOL 0029_2023_338_1617			Mezzo coperto	h. 12 - 24	Vento dir N; Forza 3	Mare dir N; Forza 3
12/4/2023	17:42									CHIRP SOL 0030_2023_338_1745		CHIRP: Tx power: 3; Depth limits: 50/2000m	Mezzo coperto	h. 12 - 24	Vento dir N; Forza 3	Mare dir N; Forza 3
12/4/2023	17:50									MB EM304 EOL 62		Cambio multibeam di acquisizione (quindi cambiamo impostazioni su k-sync e qinsy)	Mezzo coperto	h. 12 - 24	Vento dir N; Forza 3	Mare dir N; Forza 3
12/4/2023	17:52									MB EM712 SOL 0140			Mezzo coperto	h. 12 - 24	Vento dir N; Forza 3	Mare dir N; Forza 3
12/4/2023	18:29											mark su linea chirp 0030_2023_338_1745 in corrispondenza del punto (ma ad 1 Nm di distanza	Mezzo coperto	h. 12 - 24	Vento dir N; Forza 3	Mare dir N; Forza 3
12/4/2023	19:21									MB EM712 EOL 0142, CHIRP EOL 0030_2023_338_1745			Mezzo coperto	h. 12 - 24	Vento dir N; Forza 3	Mare dir N; Forza 3
12/4/2023	19:32									MB EM2040 SOL 001		Cambio multibeam di acquisizione. New survey nel SIS del 2040 (nome: PI23_em2040)	Mezzo coperto	h. 12 - 24	Vento dir N; Forza 3	Mare dir N; Forza 3
12/4/2023	19:49									QINSY SOL			Mezzo coperto	h. 12 - 24	Vento dir N; Forza 3	Mare dir N; Forza 3
12/4/2023	20:14									CHIRP SOL 0031_2023_338_2014			Mezzo coperto	h. 12 - 24	Vento dir N; Forza 3	Mare dir N; Forza 3
12/4/2023	21:29									MB EM2040 EOL 004, CHIRP EOL 0031_2023_338_2014			Mezzo coperto	h. 12 - 24	Vento dir N; Forza 3	Mare dir N; Forza 3
12/4/2023	21:38	1820.38569	3942.00499	18.3397615	39.7000832	CTD16	PI23_CTD22_S	121					Mezzo coperto	h. 12 - 24	Vento dir N; Forza 3	Mare dir N; Forza 3
12/4/2023	21:43	1820.38547	3942.00545	18.3397578	39.7000908	CTD16	PI23_CTD22_B	121	CTD				Mezzo coperto	h. 12 - 24	Vento dir N; Forza 3	Mare dir N; Forza 3
12/4/2023	21:52	1820.38330	3942.00522	18.3397217	39.7000870	CTD16	PI23_CTD22_E						Mezzo coperto	h. 12 - 24	Vento dir N; Forza 3	Mare dir N; Forza 3
12/4/2023	22:04								MB noWC+Qinsy	MB EM2040 SOL 005, CHIRP SOL 0032_2023_338_2207			Mezzo coperto	h. 12 - 24	Vento dir N; Forza 3	Mare dir N; Forza 3
12/4/2023	22:38									MB EM2040 EOL 006, CHIRP EOL 0032_2023_338_2207			Mezzo coperto	h. 12 - 24	Vento dir N; Forza 3	Mare dir N; Forza 3
12/4/2023	22:54	1815.58171	3939.01118	18.2596952	39.6501863	CTD15	PI23_CTD23_S						Mezzo coperto	h. 12 - 24	Vento dir N; Forza 3	Mare dir N; Forza 3
12/4/2023	23:02	1815.58156	3939.01158	18.2596927	39.6501930	CTD15	PI23_CTD23_B	196	CTD				Mezzo coperto	h. 12 - 24	Vento dir N; Forza 3	Mare dir N; Forza 3
12/4/2023	23:13	1815.58217	3939.01201	18.2597028	39.6502002	CTD15	PI23_CTD23_E						Mezzo coperto	h. 12 - 24	Vento dir N; Forza 3	Mare dir N; Forza 3
12/4/2023	23:21								MB noWC+Qinsy	MB EM712 SOL 143, CHIRP SOL 0033_2023_338_2324		Cambio multibeam di acquisizione da EM2040 a EM712	Mezzo coperto	h. 12 - 24	Vento dir N; Forza 3	Mare dir N; Forza 3
12/4/2023	23:51									MB EM712 EOL 143, CHIRP EOL 0033_2023_338_2324			Mezzo coperto	h. 12 - 24	Vento dir N; Forza 3	Mare dir N; Forza 3
12/5/2023	0:03	1810.79239	3936.01392	18.1798732	39.6002320	CTD14	PI23_CTD24_S	414					Parzialmente nuvoloso	h. 00 - 12	Vento dir S; Forza 4	Mare dir S; Forza 3
12/5/2023	0:13	1810.79794	3936.02145	18.1799657	39.6003575	CTD14	PI23_CTD24_B	412	CTD				Parzialmente nuvoloso	h. 00 - 12	Vento dir S; Forza 4	Mare dir S; Forza 3
12/5/2023	0:28	1810.79551	3936.02270	18.1799252	39.6003783	CTD14	PI23_CTD24_E	413					Parzialmente nuvoloso	h. 00 - 12	Vento dir S; Forza 4	Mare dir S; Forza 3
12/5/2023	0:33								MB noWC+Qinsy	MB EM712 SOL 144, CHIRP SOL 0034_2023_339_0036			Parzialmente nuvoloso	h. 00 - 12	Vento dir S; Forza 4	Mare dir S; Forza 3
12/5/2023	1:39									MB EM712 EOL 145, CHIRP EOL 0034_2023_339_0036			Parzialmente nuvoloso	h. 00 - 12	Vento dir S; Forza 4	Mare dir S; Forza 3
12/5/2023	1:48	1801.19306	3930.00421	18.0198843	39.5000702	CTD12	PI23_CTD25_S	1355					Parzialmente nuvoloso	h. 00 - 12	Vento dir S; Forza 4	Mare dir S; Forza 3
12/5/2023	2:16	1801.19248	3930.00427	18.0198747	39.5000712	CTD12	PI23_CTD25_B	1356	CTD				Parzialmente nuvoloso	h. 00 - 12	Vento dir S; Forza 4	Mare dir S; Forza 3
12/5/2023	2:40	1801.19187	3930.00631	18.0198645	39.5001052	CTD12	PI23_CTD25_E	1356					Parzialmente nuvoloso	h. 00 - 12	Vento dir S; Forza 4	Mare dir S; Forza 3
12/5/2023	2:48								MB noWC+Qinsy	MB EM712 SOL 146, CHIRP SOL 0035_2023_339_0251			Parzialmente nuvoloso	h. 00 - 12	Vento dir S; Forza 4	Mare dir S; Forza 3
12/5/2023	2:59									MB EM712 EOL 146		Cambio multibeam di acquisizione da EM712 a EM304	Parzialmente nuvoloso	h. 00 - 12	Vento dir S; Forza 4	Mare dir S; Forza 3
12/5/2023	3:03									MB EM304 SOL 063			Parzialmente nuvoloso	h. 00 - 12	Vento dir S; Forza 4	Mare dir S; Forza 3
12/5/2023	3:09											CRASH QINSY	Parzialmente nuvoloso	h. 00 - 12	Vento dir S; Forza 4	Mare dir S; Forza 3

12/5/2023	3:12									QINSY SOL			Parzialmente nuvoloso	h. 00 - 12	Vento dir S; Forza 4	Mare dir S; Forza 3
12/5/2023	3:53									MB EM304 EOL 064, CHIRP EOL 0035_2023_339_0251			Parzialmente nuvoloso	h. 00 - 12	Vento dir S; Forza 4	Mare dir S; Forza 3
12/5/2023	4:08	1751.61078	3924.61855	17.8601797	39.4103092	**CTD10**	**PI23_CTD26_S**	2275					Parzialmente nuvoloso	h. 00 - 12	Vento dir S; Forza 4	Mare dir S; Forza 3
12/5/2023	4:46	1751.61219	3924.01985	17.8602032	39.4003308	**CTD10**	**PI23_CTD26_B**	2274	CTD+SVP	svp_20231205_0446			Parzialmente nuvoloso	h. 00 - 12	Vento dir S; Forza 4	Mare dir S; Forza 3
12/5/2023	5:17	1751.61182	3924.01694	17.8601970	39.4002823	**CTD10**	**PI23_CTD26_E**						Parzialmente nuvoloso	h. 00 - 12	Vento dir S; Forza 4	Mare dir S; Forza 3
12/5/2023	5:21											Riaccendiamo e spegnamo software SIS dell'EM2040. In questo modo, e non so perché, il K-Sync smette di ricevere un segnale di input dal 2040 che c'era da quando è stato spento e che non si riusciva a mandare via pur avendo deselezionato il 2040 sia in trigger group status che in echo sounder status (notare però che il 2040 non ha external trigger nei runtime parameters). L'active period dell'em304 resta di 6,7 secondi (sembrava tanto ma facendo il calcolo velocità del suono e profondità risulta essere un tempo ragionevole)	Parzialmente nuvoloso	h. 00 - 12	Vento dir S; Forza 4	Mare dir S; Forza 3
12/5/2023	5:32									CHIRP SOL 0036_2023_339_0534		CHIRP: Tx power: 4, Tx pulse: 8ms; Gain: 8dB; Depth limits: 300-2500m	Parzialmente nuvoloso	h. 00 - 12	Vento dir S; Forza 4	Mare dir S; Forza 3
12/5/2023	5:34									MB EM304 SOL 065			Parzialmente nuvoloso	h. 00 - 12	Vento dir S; Forza 4	Mare dir S; Forza 3
12/5/2023	5:52											CHIRP: Depth limits: 500-3000m	Parzialmente nuvoloso	h. 00 - 12	Vento dir S; Forza 4	Mare dir S; Forza 3
12/5/2023	7:28									MB EM304 EOL 065, CHIRP EOL 0036_2023_339_0534			Parzialmente nuvoloso	h. 00 - 12	Vento dir S; Forza 4	Mare dir S; Forza 3
12/5/2023	7:33	1802.50720	3907.26940	18.0417867	39.1211567	**80**	**PI23_BC18_S**						Parzialmente nuvoloso	h. 00 - 12	Vento dir S; Forza 4	Mare dir S; Forza 3
12/5/2023	7:34									CHIRP SOL 0037_2023_339_0737		acquisizione chirp su stazione 80	Parzialmente nuvoloso	h. 00 - 12	Vento dir S; Forza 4	Mare dir S; Forza 3
12/5/2023	8:01	1802.50958	3907.27283	18.0418263	39.1212138	**80**	**PI23_BC18_B**	2594				vel. di caduta: 20min/m; tiro: 2,83ton; prof. cavo: 2555m A 2520 metri stabilizziamo il cavo e facciamo gli utlimi metri più lentamente (prima siamo scesi tra 60 e 100 m/min)	Parzialmente nuvoloso	h. 00 - 12	Vento dir S; Forza 4	Mare dir S; Forza 3
12/5/2023	8:32	1802.51391	3907.27369	18.0418985	39.1212282	**80**	**PI23_BC18_E**						Parzialmente nuvoloso	h. 00 - 12	Vento dir S; Forza 4	Mare dir S; Forza 3
12/5/2023	8:36									CHIRP EOL 0037_2023_339_0737			Parzialmente nuvoloso	h. 00 - 12	Vento dir S; Forza 4	Mare dir S; Forza 3
12/5/2023	8:45	1802.51786	3907.27448	18.0419643	39.1212413	**80**	**PI23_BC19_S**					box REPLICA di stazione 80 Discesa 100-120 m/min. A 2535 metri il cavo viene stabilizzato e continua la discesa a 20 m/min	Parzialmente nuvoloso	h. 00 - 12	Vento dir S; Forza 4	Mare dir S; Forza 3
12/5/2023	9:10	1802.51714	3907.27038	18.0419523	39.1211730	**80**	**PI23_BC19_B**	2592				vel. di caduta: 20min/m; tiro: 2,77ton; prof. cavo: 2554m Risalita a 120 m/min	Parzialmente nuvoloso	h. 00 - 12	Vento dir S; Forza 4	Mare dir S; Forza 3
12/5/2023	9:30											Problema al motore del verricello del box corer. Si risale a 25 m/min	Parzialmente nuvoloso	h. 00 - 12	Vento dir S; Forza 4	Mare dir S; Forza 3
12/5/2023	10:07	1802.51676	3907.26151	18.0419460	39.1210252	**80**	**PI23_BC19_E**					Sia per problema al verricello che per meteo avverso si abbandona il transetto di box corer	Parzialmente nuvoloso	h. 00 - 12	Vento dir S; Forza 4	Mare dir S; Forza 3
12/5/2023	10:18								MB noWC+Qinsy	MB EM304 SOL 066			Parzialmente nuvoloso	h. 00 - 12	Vento dir S; Forza 4	Mare dir S; Forza 3
12/5/2023	10:20									QINSY EOL			Parzialmente nuvoloso	h. 00 - 12	Vento dir S; Forza 4	Mare dir S; Forza 3
12/5/2023	10:29									QINSY SOL			Parzialmente nuvoloso	h. 00 - 12	Vento dir S; Forza 4	Mare dir S; Forza 3
12/5/2023	10:31									QINSY EOL			Parzialmente nuvoloso	h. 00 - 12	Vento dir S; Forza 4	Mare dir S; Forza 3
12/5/2023	11:50									CHIRP SOL 0038_2023_339_1150			Parzialmente nuvoloso	h. 00 - 12	Vento dir S; Forza 4	Mare dir S; Forza 3
12/5/2023	12:04											Cambio direzione di navigazione delle linee, da se-nw mettiamo la prua a 360° a causa del mare mosso	MARE MOSSO	h. 00 - 12	Vento dir S; Forza 4	Mare dir S; Forza 3
12/5/2023	12:16									CHIRP EOL 0038_2023_339_1150			Parzialmente nuvoloso	h. 12 - 24	Vento dir SW; Forza 7	Mare dir SW; Forza 4
12/5/2023	12:16									CHIRP SOL 0039_2023_339_1216			Parzialmente nuvoloso	h. 12 - 24	Vento dir SW; Forza 7	Mare dir SW; Forza 4
12/5/2023	12:59									MB EM304 EOL 067, CHIRP EOL 0039_2023_339_1216			Parzialmente nuvoloso	h. 12 - 24	Vento dir SW; Forza 7	Mare dir SW; Forza 4
12/5/2023	13:02								MB noWC+Qinsy	MB EM304 SOL 068, CHIRP SOL 0040_2023_339_1303			Parzialmente nuvoloso	h. 12 - 24	Vento dir SW; Forza 7	Mare dir SW; Forza 4
12/5/2023	16:00								MB noWC+Qinsy	MB EM304 SOL 070, CHIRP SOL 0041_2023_339_1605		Cambio direzione, navigazione con heading a 180°	Parzialmente nuvoloso	h. 12 - 24	Vento dir SW; Forza 7	Mare dir SW; Forza 4
12/5/2023	16:15									MB EM304 EOL 070			Parzialmente nuvoloso	h. 12 - 24	Vento dir SW; Forza 7	Mare dir SW; Forza 4
12/5/2023	16:20									MB EM712 SOL 147		Cambio multibeam di acquisizione da EM304 a EM712	Parzialmente nuvoloso	h. 12 - 24	Vento dir SW; Forza 7	Mare dir SW; Forza 4
12/5/2023	18:50									MB EM712 EOL 149			Parzialmente nuvoloso	h. 12 - 24	Vento dir SW; Forza 7	Mare dir SW; Forza 4
12/5/2023	18:52									MB EM712 SOL 150			Parzialmente nuvoloso	h. 12 - 24	Vento dir SW; Forza 7	Mare dir SW; Forza 4
12/5/2023	19:41									MB EM712 EOL 150, CHIRP EOL 0041_2023_339_1605			Parzialmente nuvoloso	h. 12 - 24	Vento dir SW; Forza 7	Mare dir SW; Forza 4
12/5/2023	19:43									MB EM712 SOL 151, CHIRP SOL 0042_2023_339_1946			Parzialmente nuvoloso	h. 12 - 24	Vento dir SW; Forza 7	Mare dir SW; Forza 4
12/5/2023	20:24									MB EM712 EOL 151, CHIRP EOL 0042_2023_339_1946			Parzialmente nuvoloso	h. 12 - 24	Vento dir SW; Forza 7	Mare dir SW; Forza 4
12/5/2023	20:29									MB EM712 SOL 152, CHIRP SOL 0043_2023_339_2032			Parzialmente nuvoloso	h. 12 - 24	Vento dir SW; Forza 7	Mare dir SW; Forza 4
12/5/2023	21:57									MB EM712 EOL 153, CHIRP EOL 0043_2023_339_2032			Parzialmente nuvoloso	h. 12 - 24	Vento dir SW; Forza 7	Mare dir SW; Forza 4
12/5/2023	22:15									MB EM712 SOL 155, CHIRP SOL 0044_2023_339_2218			Parzialmente nuvoloso	h. 12 - 24	Vento dir SW; Forza 7	Mare dir SW; Forza 4
12/5/2023	22:46	3910.69765	1715.55194	39.1782942	17.2591990							Possibili biocostruzioni (o, meno probabilmente, vulcani di fango)	Parzialmente nuvoloso	h. 12 - 24	Vento dir SW; Forza 7	Mare dir SW; Forza 4
12/5/2023	23:00	3910.75739	1715.52230	39.1792898	17.2587050							Fix e screenshot su linea chirp 0044 per possibili biocostruzioni	Parzialmente nuvoloso	h. 12 - 24	Vento dir SW; Forza 7	Mare dir SW; Forza 4
12/5/2023	23:05								MB+WC	MB EM712 SOL 156		Inizio acquisizione della colonna d'acqua nel multibeam	Parzialmente nuvoloso	h. 12 - 24	Vento dir SW; Forza 7	Mare dir SW; Forza 4
12/5/2023	23:44											Fine acquisizione colonna d'acqua	Parzialmente nuvoloso	h. 12 - 24	Vento dir SW; Forza 7	Mare dir SW; Forza 4
12/5/2023	23:54									MB EM712 EOL 156, CHIRP EOL 0044_2023_339_2218			Parzialmente nuvoloso	h. 12 - 24	Vento dir SW; Forza 7	Mare dir SW; Forza 4
12/6/2023	0:04								MB noWC+Qinsy	MB EM712 SOL 157, CHIRP SOL 0045_2023_340_0008			Mezzo coperto	h. 00 - 12	Vento dir SW; Forza 5	Mare dir SW; Forza 4
12/6/2023	2:13					**campo Fedra**				MB EM712 EOL 159, CHIRP EOL 0045_2023_340_0008			Mezzo coperto	h. 00 - 12	Vento dir SW; Forza 5	Mare dir SW; Forza 4
12/6/2023	2:28					**campo Fedra**				CHIRP SOL 0046_2023_340_0228			Mezzo coperto	h. 00 - 12	Vento dir SW; Forza 5	Mare dir SW; Forza 4
12/6/2023	2:52					**campo Fedra**				CHIRP EOL 0046_2023_340_0228			Mezzo coperto	h. 00 - 12	Vento dir SW; Forza 5	Mare dir SW; Forza 4
12/6/2023	2:52					**campo Fedra**			MB+WC+Qinsy	MB EM712 SOL 160, CHIRP SOL 0047_2023_340_0255			Mezzo coperto	h. 00 - 12	Vento dir SW; Forza 5	Mare dir SW; Forza 4
12/6/2023	2:53					**campo Fedra**				CHIRP SOL 0046_2023_340_0228			Mezzo coperto	h. 00 - 12	Vento dir SW; Forza 5	Mare dir SW; Forza 4
12/6/2023	3:22					**campo Fedra**				MB EM712 EOL 161, CHIRP EOL 0046_2023_340_0228			Mezzo coperto	h. 00 - 12	Vento dir SW; Forza 5	Mare dir SW; Forza 4
12/6/2023	3:37					**campo Fedra**			MB+WC+Qinsy	MB EM712 SOL 161, CHIRP SOL 0048_2023_340_0339			Mezzo coperto	h. 00 - 12	Vento dir SW; Forza 5	Mare dir SW; Forza 4
12/6/2023	3:58					**campo Fedra**				MB EM712 EOL 161, CHIRP EOL 0048_2023_340_0339			Mezzo coperto	h. 00 - 12	Vento dir SW; Forza 5	Mare dir SW; Forza 4
12/6/2023	4:05					**campo Fedra**			MB+WC+Qinsy	MB EM712 SOL 162, CHIRP SOL 0049_2023_340_0408			Mezzo coperto	h. 00 - 12	Vento dir SW; Forza 5	Mare dir SW; Forza 4
12/6/2023	4:24					**campo Fedra**				MB EM712 EOL 162			Mezzo coperto	h. 00 - 12	Vento dir SW; Forza 5	Mare dir SW; Forza 4
12/6/2023	4:35					**campo Fedra**			MB+WC+Qinsy	MB EM712 SOL 163			Mezzo coperto	h. 00 - 12	Vento dir SW; Forza 5	Mare dir SW; Forza 4
12/6/2023	4:51					**campo Fedra**				MB EM712 EOL 163			Mezzo coperto	h. 00 - 12	Vento dir SW; Forza 5	Mare dir SW; Forza 4
12/6/2023	5:03					**campo Federica**			MB+WC+Qinsy	MB EM712 SOL 164, CHIRP SOL 0050_2023_340_0507		acquisizione per coprire un buco nella copertura multibeam	Mezzo coperto	h. 00 - 12	Vento dir SW; Forza 5	Mare dir SW; Forza 4
12/6/2023	5:17					**campo Federica**				MB EM712 EOL 164, CHIRP EOL 0050_2023_340_0507			Mezzo coperto	h. 00 - 12	Vento dir SW; Forza 5	Mare dir SW; Forza 4
12/6/2023	5:21					**campo Federica**				CHIRP SOL 0051_2023_340_0524		acquisizione solo chirp perché il multibeam è già stato acquisito	Mezzo coperto	h. 00 - 12	Vento dir SW; Forza 5	Mare dir SW; Forza 4
12/6/2023	5:23					**campo Federica**				MB EM712 SOL 165			Mezzo coperto	h. 00 - 12	Vento dir SW; Forza 5	Mare dir SW; Forza 4
12/6/2023	6:39					**campo Federica**				CHIRP EOL 0051_2023_340_0524, CHIRP SOL 0052_2023_340_0641		CHIRP: Tx Pulse: 4ms; Gain: 3dB; Depth Limits: 15-800m	Mezzo coperto	h. 00 - 12	Vento dir SW; Forza 5	Mare dir SW; Forza 4
12/6/2023	6:42									MB EM712 EOL 166			Mezzo coperto	h. 00 - 12	Vento dir SW; Forza 5	Mare dir SW; Forza 4

12/6/2023	6:45										CHIRP EOL 0052_2023_340_0641						
12/6/2023	6:52	1713.21327	3859.99442	17.2202212	38.9999070	**CTD02**	**PI23_CTD27_S**	62	CTD+SVP					mare calmo	h. 00 - 12	Vento dir SW; Forza 5	Mare dir SW; Forza 4
12/6/2023	6:54	1713.21080	3859.99381	17.2201800	38.9998968	**CTD02**	**PI23_CTD27_B**	62	CTD+SVP	svp_20231206_0654		AMP di Capo Rizzuto Strano profilo di velocità del suono (svp)		Mezzo coperto	h. 00 - 12	Vento dir SW; Forza 5	Mare dir SW; Forza 4
12/6/2023	7:01	1713.20940	3859.99712	17.2201567	38.9999520	**CTD02**	**PI23_CTD27_E**							Mezzo coperto	h. 00 - 12	Vento dir SW; Forza 5	Mare dir SW; Forza 4
12/6/2023	7:04								MB noWC+Qinsy	MB EM712 SOL 167				Mezzo coperto	h. 00 - 12	Vento dir SW; Forza 5	Mare dir SW; Forza 4
12/6/2023	7:13									CHIRP SOL 0053_2023_340_0715				Mezzo coperto	h. 00 - 12	Vento dir SW; Forza 5	Mare dir SW; Forza 4
12/6/2023	7:20									MB EM712 EOL 167; CHIRP EOL 0053_2023_340_0715				Mezzo coperto	h. 00 - 12	Vento dir SW; Forza 5	Mare dir SW; Forza 4
12/6/2023	7:26	1712.44751	3859.57261	17.2074585	38.9928768	**CTD01**	**PI23_CTD28_S**							Mezzo coperto	h. 00 - 12	Vento dir SW; Forza 5	Mare dir SW; Forza 4
12/6/2023	7:29	1712.44557	3859.56986	17.2074262	38.9928310	**CTD01**	**PI23_CTD28_B**	40	CTD+SVP	svp_20231206_0729		AMP di Capo Rizzuto Strano profilo di velocità del suono (svp)		Mezzo coperto	h. 00 - 12	Vento dir SW; Forza 5	Mare dir SW; Forza 4
12/6/2023	7:36	1712.44291	3859.56978	17.2073818	38.9928297	**CTD01**	**PI23_CTD28_E**							Mezzo coperto	h. 00 - 12	Vento dir SW; Forza 5	Mare dir SW; Forza 4
12/6/2023	7:41									QINSY EOL				Mezzo coperto	h. 00 - 12	Vento dir SW; Forza 5	Mare dir SW; Forza 4
12/6/2023	7:44									MB EM712 SOL 168, CHIRP SOL 0054_2023_340_0749		CHIRP: Tx Power:2; Gain: 0dB		Mezzo coperto	h. 00 - 12	Vento dir SW; Forza 5	Mare dir SW; Forza 4
12/6/2023	8:57									MB EM712 EOL 169, CHIRP EOL 0054_2023_340_0749				Mezzo coperto	h. 00 - 12	Vento dir SW; Forza 5	Mare dir SW; Forza 4
12/6/2023	9:06								MB+WC	MB EM712 SOL 170, CHIRP SOL 0055_2023_340_0909		Acquisizione statica		Mezzo coperto	h. 00 - 12	Vento dir SW; Forza 5	Mare dir SW; Forza 4
12/6/2023	9:28									MB EM712 EOL 170, CHIRP EOL 0055_2023_340_0909				Mezzo coperto	h. 00 - 12	Vento dir SW; Forza 5	Mare dir SW; Forza 4
12/6/2023	9:38	1721.39349	3903.68433	17.3565582	39.0614055	**69bis**	**PI23_PC12**	590	Piston Core			carotiere sul fondo; velocità di discesa 20 m/min; tiro max 2,07 t; penetrazione 11 m; recupero 8,52 m		Mezzo coperto	h. 00 - 12	Vento dir SW; Forza 5	Mare dir SW; Forza 4
12/6/2023	10:00											In seguito a collequi con IBERCISA, si decide che le condizioni di operatività del verricello multipurpose non sono sicure		Mezzo coperto	h. 00 - 12	Vento dir SW; Forza 5	Mare dir SW; Forza 4
12/6/2023	10:20											Inizio del trasferimento verso PI23_GC13_bio		Mezzo coperto	h. 00 - 12	Vento dir SW; Forza 5	Mare dir SW; Forza 4
12/6/2023	10:25								MB+WC+Qinsy	MB EM712 SOL 171, CHIRP SOL 0056_2023_340_1029				Mezzo coperto	h. 00 - 12	Vento dir SW; Forza 5	Mare dir SW; Forza 4
12/6/2023	11:58	1715.54870	3910.80273	17.2591450	39.1800455	**Biocostru**	**PI23_CTD29_S**	160		QINSY EOL				Mezzo coperto	h. 00 - 12	Vento dir SW; Forza 5	Mare dir SW; Forza 4
12/6/2023	12:02	1715.54870	3910.80200	17.2591450	39.1800333	**Biocostru**	**PI23_CTD29_B**	160	CTD+SVP	svp_20231206_1202		calata CTD fino a 134		Mezzo coperto	h. 00 - 12	Vento dir SW; Forza 5	Mare dir SW; Forza 4
12/6/2023	12:10	1715.54910	3910.79970	17.2591517	39.1799950	**Biocostru**	**PI23_CTD29_E**	160						Mezzo coperto	h. 12 - 24	Vento dir SW; Forza 3	Mare dir SW; Forza 2
12/6/2023	12:46	1715.55940	3910.78183	17.2593233	39.1796972	**Biocostru**	**PI23_GC13**	160	Gravity Core			carotiere sul fondo; velocità di discesa 60 m/min; tiro max 3,8 t; penetrazione 3,0 m; recupero 2,8 m		Mezzo coperto	h. 12 - 24	Vento dir SW; Forza 3	Mare dir SW; Forza 2
12/6/2023	13:05								MB+WC	MB EM712 EOL 174				Mezzo coperto	h. 12 - 24	Vento dir SW; Forza 3	Mare dir SW; Forza 2
12/6/2023	13:16									MB EM712 SOL 175, CHIRP SOL 0057_2023_340_1319		inserita svp_20231206_1202 in EM712		Mezzo coperto	h. 12 - 24	Vento dir SW; Forza 3	Mare dir SW; Forza 2
12/6/2023	14:12									MB EM712 EOL 175, CHIRP EOL 0057_2023_340_1319				Mezzo coperto	h. 12 - 24	Vento dir SW; Forza 3	Mare dir SW; Forza 2
12/6/2023	14:20	1722.81061	3906.01041	17.3801768	39.1001735	**CTD04**	**PI23_CTD30_S**	591						Mezzo coperto	h. 12 - 24	Vento dir SW; Forza 3	Mare dir SW; Forza 2
12/6/2023	14:33	1722.80942	3906.01101	17.3801570	39.1001835	**CTD04**	**PI23_CTD30_B**	588	CTD+SVP	svp_20231206_1433				Mezzo coperto	h. 12 - 24	Vento dir SW; Forza 3	Mare dir SW; Forza 2
12/6/2023	14:50	1722.80657	3906.01445	17.3801095	39.1002408	**CTD04**	**PI23_CTD30_E**	588						Mezzo coperto	h. 12 - 24	Vento dir SW; Forza 3	Mare dir SW; Forza 2
12/6/2023	15:05									CHIRP SOL 0058_2023_340_1507				Mezzo coperto	h. 12 - 24	Vento dir SW; Forza 3	Mare dir SW; Forza 2
12/6/2023	15:07								MB noWC+Qinsy	MB EM712 SOL 176				Mezzo coperto	h. 12 - 24	Vento dir SW; Forza 3	Mare dir SW; Forza 2
12/6/2023	16:09									MB EM712 EOL 177, CHIRP EOL 0058_2023_340_1507				Mezzo coperto	h. 12 - 24	Vento dir SW; Forza 3	Mare dir SW; Forza 2
12/6/2023	16:24	1732.40005	3912.00488	17.5400008	39.2000813	**CTD06**	**PI23_CTD31_S**							Mezzo coperto	h. 12 - 24	Vento dir SW; Forza 3	Mare dir SW; Forza 2
12/6/2023	16:44	1732.39846	3912.00465	17.5399743	39.2000775	**CTD06**	**PI23_CTD31_B**	1129	CTD+SVP	svp_20231206_1644		calata CTD fino a 1050		Mezzo coperto	h. 12 - 24	Vento dir SW; Forza 3	Mare dir SW; Forza 2
12/6/2023	17:04	1732.39899	3912.00626	17.5399832	39.2001043	**CTD06**	**PI23_CTD31_E**							Mezzo coperto	h. 12 - 24	Vento dir SW; Forza 3	Mare dir SW; Forza 2
12/6/2023	17:22								MB noWC+Qinsy	MB EM712 SOL 178, CHIRP SOL 0059_2023_340_1723				Mezzo coperto	h. 12 - 24	Vento dir SW; Forza 3	Mare dir SW; Forza 2
12/6/2023	17:56									MB EM304 SOL 071		Acquisizione sia con EM712 che con EM304		Mezzo coperto	h. 12 - 24	Vento dir SW; Forza 3	Mare dir SW; Forza 2
12/6/2023	18:31									MB EM712 EOL 179				Mezzo coperto	h. 12 - 24	Vento dir SW; Forza 3	Mare dir SW; Forza 2
12/6/2023	18:34									MB EM304 EOL 072, CHIRP EOL 0059_2023_340_1723				Mezzo coperto	h. 12 - 24	Vento dir SW; Forza 3	Mare dir SW; Forza 2
12/6/2023	18:51	1742.01892	3918.01394	17.7003153	39.3002323	**CTD08**	**PI23_CTD32_S**							Mezzo coperto	h. 12 - 24	Vento dir SW; Forza 3	Mare dir SW; Forza 2
12/6/2023	19:19	1742.02321	3918.01449	17.7003868	39.3002415	**CTD08**	**PI23_CTD32_B**	1662	CTD					Mezzo coperto	h. 12 - 24	Vento dir SW; Forza 3	Mare dir SW; Forza 2
12/6/2023	19:45	1742.00283	3918.01605	17.7000472	39.3002675	**CTD08**	**PI23_CTD32_E**							Mezzo coperto	h. 12 - 24	Vento dir SW; Forza 3	Mare dir SW; Forza 2
12/6/2023	19:47								MB noWC+Qinsy	MB EM304 SOL 073, CHIRP SOL 0060_2023_340_1947				Mezzo coperto	h. 12 - 24	Vento dir SW; Forza 3	Mare dir SW; Forza 2
12/6/2023	20:45					**CTD09**				MB EM304 EOL 073, CHIRP EOL 0060_2023_340_1947				Mezzo coperto	h. 12 - 24	Vento dir SW; Forza 3	Mare dir SW; Forza 2
12/6/2023	20:54	1746.78099	3921.01258	17.7796832	39.3502097	**CTD09**	**PI23_CTD33_S**							Mezzo coperto	h. 12 - 24	Vento dir SW; Forza 3	Mare dir SW; Forza 2
12/6/2023	21:26	1746.77478	3921.01488	17.7795797	39.3502480	**CTD09**	**PI23_CTD33_B**	1893				calata CTD fino a 1876 metri		Mezzo coperto	h. 12 - 24	Vento dir SW; Forza 3	Mare dir SW; Forza 2
12/6/2023	21:52	1746.77352	3921.01289	17.7795587	39.3502148	**CTD09**	**PI23_CTD33_E**							Mezzo coperto	h. 12 - 24	Vento dir SW; Forza 3	Mare dir SW; Forza 2
12/6/2023	22:12									MB EM304 SOL 074				Mezzo coperto	h. 12 - 24	Vento dir SW; Forza 3	Mare dir SW; Forza 2
12/6/2023	22:30									MB EM304 EOL 074				Mezzo coperto	h. 12 - 24	Vento dir SW; Forza 3	Mare dir SW; Forza 2
12/6/2023	22:35									MB EM304 SOL-EOL 075-076				Mezzo coperto	h. 12 - 24	Vento dir SW; Forza 3	Mare dir SW; Forza 2
12/6/2023	22:57									MB EM304 EOL 076				Mezzo coperto	h. 12 - 24	Vento dir SW; Forza 3	Mare dir SW; Forza 2
12/6/2023	22:58									MB EM304 SOL 077		inserita svp_20231206_R_2126 in EM712		Mezzo coperto	h. 12 - 24	Vento dir SW; Forza 3	Mare dir SW; Forza 2
12/6/2023	23:08									QINSY SOL-EOL-SOL				Mezzo coperto	h. 12 - 24	Vento dir SW; Forza 3	Mare dir SW; Forza 2
12/6/2023	23:35									CHIRP SOL 0061_2023_340_2338		disturbo del CHIRP su EM304 con pulse lenght 16 ms		Mezzo coperto	h. 12 - 24	Vento dir SW; Forza 3	Mare dir SW; Forza 2
12/7/2023	0:05									MB EM304 EOL 077 MB EM712 SOL 180		trasferimento verso piattaforma off Gallipoli		Parzialmente nuvoloso	h. 00 - 12	Vento dir NW; Forza 4	Mare dir NW; Forza 3
12/7/2023	0:27									CHIRP SOL 0062_2023_341_0027				Parzialmente nuvoloso	h. 00 - 12	Vento dir NW; Forza 4	Mare dir NW; Forza 3
12/7/2023	0:40									SOL QINSY EM712				Parzialmente nuvoloso	h. 00 - 12	Vento dir NW; Forza 4	Mare dir NW; Forza 3
12/7/2023	4:59								MB noWC+Qinsy	CHIRP EOL 0062_2023_341_0027 MB EM712 EOL 184				Parzialmente nuvoloso	h. 00 - 12	Vento dir NW; Forza 4	Mare dir NW; Forza 3
12/7/2023	5:34									MB EM712 SOL 185, CHIRP SOL 0063_2023_341_0533				Parzialmente nuvoloso	h. 00 - 12	Vento dir NW; Forza 4	Mare dir NW; Forza 3
12/7/2023	5:35									CHIRP EOL 0063_2023_341_0533		acquisizione MB sembra disturbata perché tolto science moe, dovendo raggiungere		Parzialmente nuvoloso	h. 00 - 12	Vento dir NW; Forza 4	Mare dir NW; Forza 3
12/7/2023	5:39									CHIRP SOL 0064_2023_341_0533				Parzialmente nuvoloso	h. 00 - 12	Vento dir NW; Forza 4	Mare dir NW; Forza 3
12/7/2023	6:57					**48**				EOL CHIRP, MB, QINSY		carotaggio abortito per condizio meteo		Parzialmente nuvoloso	h. 00 - 12	Vento dir NW; Forza 4	Mare dir NW; Forza 3
12/7/2023	7:12									CHIRP SOL 0065_2023_341_0715				Parzialmente nuvoloso	h. 00 - 12	Vento dir NW; Forza 4	Mare dir NW; Forza 3
12/7/2023	7:13								MB noWC+Qinsy	MB EM712 SOL 187		trasferimento stazione 45		Parzialmente nuvoloso	h. 00 - 12	Vento dir NW; Forza 4	Mare dir NW; Forza 3
12/7/2023	8:39									CHIRP EOL 0065_2023_341_0715				Parzialmente nuvoloso	h. 00 - 12	Vento dir NW; Forza 4	Mare dir NW; Forza 3
12/7/2023	8:53					**45**				CHIRP SOL 0066_2023_341_0856				Parzialmente nuvoloso	h. 00 - 12	Vento dir NW; Forza 4	Mare dir NW; Forza 3
12/7/2023	9:14	1752.63496	3957.22098	17.8772493	39.9536830	**45**	**PI23_PC14**	200				velocità caduta 20 m/min tiro 4,08 t, penetrazione 11 m, recupero 8,49 m		Parzialmente nuvoloso	h. 00 - 12	Vento dir NW; Forza 4	Mare dir NW; Forza 3
12/7/2023	9:25									CHIRP EOL 0066_2023_341_0856				Parzialmente nuvoloso	h. 00 - 12	Vento dir NW; Forza 4	Mare dir NW; Forza 3
12/7/2023	10:19								MB noWC+Qinsy	MB EM712 SOL 189, CHIRP SOL 0067_2023_341_1019				Parzialmente nuvoloso	h. 00 - 12	Vento dir NW; Forza 4	Mare dir NW; Forza 3
12/7/2023	10:53									EOL CHIRP, MB, QINSY				Parzialmente nuvoloso	h. 00 - 12	Vento dir NW; Forza 4	Mare dir NW; Forza 3
12/7/2023	11:00									MB EM712 SOL 190				Parzialmente nuvoloso	h. 00 - 12	Vento dir NW; Forza 4	Mare dir NW; Forza 3
12/7/2023	11:23									MB EM712 EOL 190, CHIRP, QINSY				Parzialmente nuvoloso	h. 00 - 12	Vento dir NW; Forza 4	Mare dir NW; Forza 3
12/7/2023	11:41									MB EM712 SOL 192, CHIRP SOL 0068_2023_341_1144				Parzialmente nuvoloso	h. 00 - 12	Vento dir NW; Forza 4	Mare dir NW; Forza 3

12/7/2023	13:35									MB EM712 EOL 192, CHIRP EOL 0068_2023_341_1144			Parzialmente nuvoloso	h. 12 - 24	Vento dir NW; Forza 6	Mare dir NW; Forza 5
12/7/2023	13:36								MB noWC+Qinsy	MB EM712 SOL 193, CHIRP SOL 0069_2023_341_1339			Parzialmente nuvoloso	h. 12 - 24	Vento dir NW; Forza 6	Mare dir NW; Forza 5
12/7/2023	13:53									MB EM712 SOL 194, CHIRP SOL 0070_2023_341_1353		trasferimento verso porto Cesareo per condizioni meteo	Parzialmente nuvoloso	h. 12 - 24	Vento dir NW; Forza 6	Mare dir NW; Forza 5
12/7/2023	22:20									MB EM712 EOL 202, CHIRP EOL 0070_2023_341_1353						
12/7/2023	22:23									MB EM712 SOL 203, CHIRP SOL 0071_2023_341_2227						
12/8/2023	4:00									MB EM712 EOL 208, CHIRP EOL 0071_2023_341_2227		fine accostata, inizio trasferimento verso punto 48.				
12/8/2023	4:00									MB EM712 SOL 209, CHIRP SOL 0072_2023_342_0403		Direzione di navigazione: nord-sud				
12/8/2023	6:36									CHIRP EOL 0072_2023_3412_0403, CHIRP SOL 0073_2023_342_0639		CHIRP: Tx power da 1 a 2				
12/8/2023	6:50									MB EM712 EOL 211, CHIRP EOL 0073_2023_342_0639						
12/8/2023	6:59									CHIRP SOL 0074_2023_342_0659						
12/8/2023	7:03									MB EM712 SOL 212+QINSY						
12/8/2023	7:24									MB EM712 EOL 212, CHIRP EOL 0074_2023_342_0659						
12/8/2023	7:30					**48**				MB EM712 SOL 213, CHIRP SOL 0075_2023_342_0734		acquisizione su stazione 48				
12/8/2023	8:27									crash survey manager QINSY						
12/8/2023	8:40									QINSY EOL						
12/8/2023	8:41									QINSY SOL						
12/8/2023	8:45									MB EM712 EOL 214, CHIRP EOL 0075_2023_342_0734						
12/8/2023	8:53									MB EM712 SOL 216, CHIRP SOL 0076_2023_342_0856		navighiamo attorno alla stazione 48 aspettando che il mare si calmi e ci consenta di mettere a mare il carotiere				
12/8/2023	9:36											CHIRP: inserito fix mark per segnare la proiezione della stazione	mare calmo			
12/8/2023	9:59									MB EM712 EOL 216, CHIRP EOL 0076_2023_342_0856						
12/8/2023	10:07									MB EM712 SOL 217, CHIRP SOL 0077_2023_342_1010						
12/8/2023	10:25									MB EM712 EOL 217, CHIRP EOL 0077_2023_342_1010		finalmente ci dirigiamo verso la stazione 48				
12/8/2023	10:38					**48**				CHIRP SOL 0078_2023_342_1041						
12/8/2023	10:42	1746.36357	3946.21394	39.7702323	17.7727262	**48**	**PI23_CTD34_S**									
12/8/2023	10:54	1746.36529	3946.21357	39.7702262	17.7727548	**48**	**PI23_CTD34_B**	710	CTD+SVP	svp_20231208_1113		calata CTD fino a 696m				
12/8/2023	11:00					**48**				CHIRP EOL 0078_2023_342_1041						
12/8/2023	11:13	1746.36672	3946.21607	39.7702678	17.7727787	**48**	**PI23_CTD34_E**	709								
12/8/2023	11:57									CHIRP SOL 0079_2023_342_1159						
12/8/2023	12:23	1746.36489	3946.23066	39.7705110	17.7727482	**48**	**PI23_PC15**	712				velocità caduta 20 m/min tiro 3,78 t, penetrazione 11 m, recupero 8,57 m				
12/8/2023	12:27									CHIRP EOL 0079_2023_342_1159						
12/8/2023	13:41									CHIRP SOL 0080_2023_342_1344						
12/8/2023	13:42									MB EM712 SOL 219, QINSY SOL						
12/8/2023	14:52									CHIRP EOL 0080_2023_342_1344		mb e qinsy continuano ad acquisire in accostata				
12/8/2023	15:06									CHIRP SOL 0081_2023_342_1509						
12/8/2023	16:22									MB EM712 EOL 223						
12/8/2023	16:24									CHIRP EOL 0081_2023_342_1509						
12/8/2023	16:30									CHIRP SOL 0082_2023_342_1633		non acquisiamo il MB perché è già tutto abbastanza coperto				
12/8/2023	16:47									CHIRP EOL 0082_2023_342_1633						
12/8/2023	16:54	1746.61491	3947.72201	17.77692	39.7953668		**PI23_CTD35_S**									
12/8/2023	17:06	1746.62140	3947.72362	17.77702	39.7953937		**PI23_CTD35_B**	538				calata CTD fino a 506 metri				
12/8/2023	17:16	1746.61940	3947.72295	17.77699	39.7953825		**PI23_CTD35_E**									
12/8/2023	17:27									MB EM712 SOL 224, CHIRP SOL 0083_2023_342_1731						
12/8/2023	18:50								MB noWC+Qinsy	MB EM712 SOL 225, CHIRP SOL 0084_2023_342_1854						
12/8/2023	19:36									CHIRP EOL 0084_2023_342_1854						
12/8/2023	19:43	1735.84580	3949.22740	17.59743	39.8204567		**PI23_CTD36_S**									
12/8/2023	20:09	1735.84574	3949.22685	17.59743	39.8204475		**PI23_CTD36_B**	1492	CTD+SVP	svp_20231208_2029						
12/8/2023	20:30	1735.84745	3949.22523	17.59746	39.8204205		**PI23_CTD36_E**									
12/8/2023	20:51									MB EM304 SOL 78, CHIRP SOL 0085_2023_342_2054						
12/8/2023	22:16									CHIRP EOL 0085_2023_342_2054						
12/8/2023	22:23									MB EM304 EOL 78						
12/8/2023	22:35									CHIRP SOL 0086_2023_342_2235						
12/8/2023	23:40															
12/8/2023	23:50								MB noWC+Qinsy	CHIRP SOL 0087_2023_342_2352						